Bottom-up Development of Urea Sorbents for Dialysate Regeneration

Jacobus Adrianus Wilhelmus Jong

Bottom-up Development of Urea Sorbents for Dialysate Regeneration

Thesis with a summary in Dutch, Department of Pharmaceutics, Utrecht University and Department of Nephrology and Hypertension, University Medical Centre Utrecht, Utrecht, the Netherlands

ISBN:	978-90-393-7197-8
Author:	J.A.W. Jong
Cover:	Jasper Bleeker
Lay-Out:	www.proefschriftmaken.nl
Printed by:	www.proefschriftmaken.nl

The research presented in this thesis was financially supported by the Dutch organization for Scientific Research (NWO-TTW, project 14433) and the Dutch Kidney Foundation/ NeoKidney.

Printing of this thesis was kindly supported by : Utrecht Institute of Pharmaceutical Sciences (UIPS) and the Dutch Kidney Foundation.

Bottom-up Development of Urea Sorbents for Dialysate Regeneration

Bottom-up Ontwikkeling van Ureum Absorbentia voor Dialysaat Regeneratie

(met samenvatting in het Nederlands)

Proefschrift

ter verkrijging van de graad van doctor aan de
Universiteit Utrecht
op gezag van de
rector magnificus prof. dr. H.R.B.M. Kummeling,
ingevolge het besluit van het college van promoties
in het openbaar te verdedigen op

maandag 16 december 2019 des middags te 2.30 uur

door

Jacobus Adrianus Wilhelmus Jong

geboren op 14 juli 1992
te Alkmaar

Promotoren:	Prof. Dr. Ir. W.E. Hennink Prof. Dr. M.C. Verhaar
Copromotoren:	Dr. C.F. van Nostrum Dr. K.G.F. Gerritsen

Table of Contents

1

Chapter 1

General Introduction

1.1 Kidney Function

The kidneys have the function to continuously remove waste compounds (so called uremic toxins) and excess fluid from the blood and maintain body homeostasis by regulating electrolyte, water and acid base balance.[1] An important measure for kidney function is the glomerular filtration rate (GFR). This is the amount of blood plasma that is filtered per minute, which is > 90 mL/min/1.73 m^2 of body-surface for healthy subjects. Loss of kidney function, due to damage to the kidneys, is indicated by a lowered GFR and as a consequence may lead to accumulation of uremic toxins in the body. The state when the GFR drops below 15 mL/min/1.73 m^2 is called end-stage kidney disease (ESKD)[2]. Renal replacement therapy is often required in ESKD to correct metabolic disturbances, fluid overload and/or reduce 'uremic symptoms', such as nausea and vomiting, loss of appetite, fatigue, itching and sleep disturbances. In the European Union, approximately ~0.12% of the population suffers from ESKD.[3] In the Netherlands every year ~2000 people are diagnosed with ESKD.[4]

Uremic toxins can be divided in three categories: small and freely water-soluble molecules (MW < 0.5 kDa), middle molecules (MW 0.6 – 60 kDa) and protein bound uremic toxins. Examples of uremic toxins of the small water soluble molecule class are urea, uric acid and creatinine. Small proteins like cytokines and β-2-microglobulin are examples of uremic toxins of the middle class. Protein-bound uremic toxins are small molecules like *p*-cresyl sulfate and indoxyl sulfate that bind predominantly to albumin.[5] The structures of some uremic toxins are shown in figure 1.[6-7]

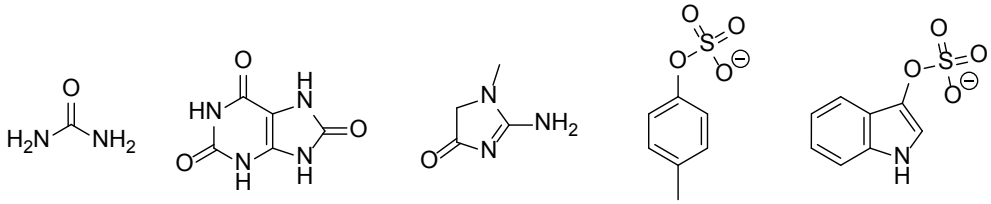

Figure 1: Structures of small, freely water soluble uremic toxins (urea, uric acid and creatinine) and that of the protein bound uremic toxins (*p*-cresyl sulfate and indoxyl sulfate).

1.2 Dialysis

Ideally, ESKD-patients should receive kidney transplantation from either a deceased or living donor. However, not all patients are eligible for kidney transplantation and there is a lack of viable kidneys available for transplantation. Therefore, many ESKD-patients have to undergo dialysis to replace kidney function, either by hemodialysis or peritoneal dialysis. In 2010 over 2.5 million patients depended on dialysis worldwide, in 2018 3.4 million and it is expected to be over 5 million by 2030.[8,9]

With standard hemodialysis, patients are treated 3 times per week for 3-4 hours in a hospital to remove the accumulated uremic toxins and excess water from their body and to adjust their electrolyte concentrations.[10] A schematic overview of hemodialysis is shown in figure 1. Blood is pumped from the patient's body into a dialyzer, in which small solutes can move (via diffusion and/or convection) across a semi-permeable membrane (made of *e.g.* polysulfone or cellulose triacetate) to an aqueous solution called dialysate, after which the blood is returned to the body.[11] Removal of excess water from the blood occurs via a pressure gradient across the membrane (i.e. ultrafiltration). The dialysate is an aqueous buffered electrolyte solution (composition is selected by the nephrologist and can vary per patient) which, after passing the dialyzer and exchanging waste solutes and water with the patient's body, is discarded into the sewage system after a single pass. For a single standard dialysis session ~120 L of dialysate is used.

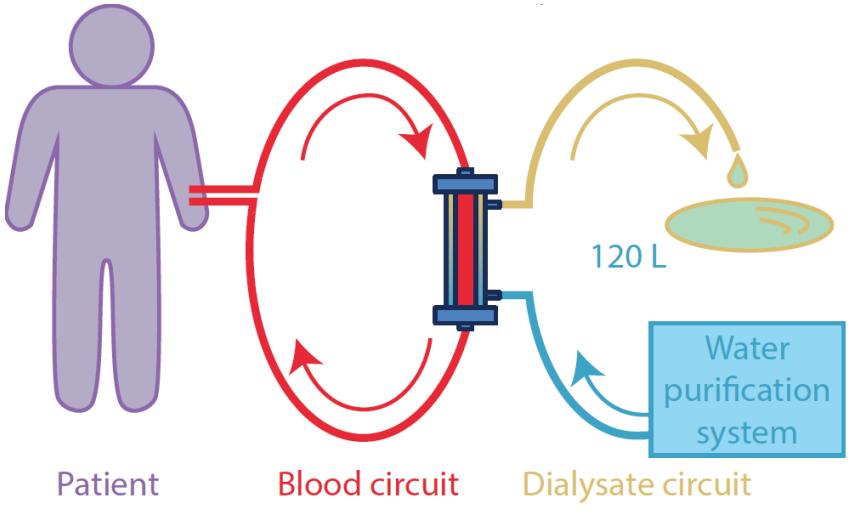

Figure 2: Schematic overview of hemodialysis (from Chapter 2).

With peritoneal dialysis the membrane that lines the abdominal cavity, the peritoneum, is used as semi-permeable membrane. Dialysate is instilled into the abdominal cavity via a single lumen PD catheter. Waste solutes move across the peritoneal membrane into the dialysate via diffusion and convection. Excess water is extracted via osmosis by applying dialysate with high osmolarity by using glucose (76 – 214 mM) as osmotic agent or icodextrin (75 g/L), a starch-derived glucose polymer, as osmotic agent. Because the majority of the ESKD patients undergoes hemodialysis we further focus on this technique. Peritoneal dialysis is further discussed in **Chapter 2**.

1.3 Wearable Artificial Kidney

The removal of uremic toxins and excess fluid with conventional dialysis is inadequate as compared to healthy kidneys, which results in an overall poor well-being and high mortality among ESKD-patients. Prolonged and more frequent dialysis sessions would improve the adequacy of the treatment,[12-13] however this would also limit the autonomy and flexibility of the patient. A wearable dialysis device, which the patient can operate unaccompanied, that is independent of a fixed water supply and can be used at home or elsewhere, would improve autonomy and flexibility of the patient and would facilitate more frequent and prolonged dialysis sessions. Key for the realization of such a dialysis device is the elimination of the large volume of dialysate (~120 L) needed for a single treatment. The amount of dialysate could be reduced to wearable proportions (ideally < 0.5 L) if the dialysate is re-used in a closed-loop system, instead of being discarded after a single pass through the dialyzer. To enable this, the dialysate has to be regenerated by a purification unit that removes waste solutes and corrects for electrolyte changes. A schematic overview of such a wearable dialysis device is shown in figure 3.

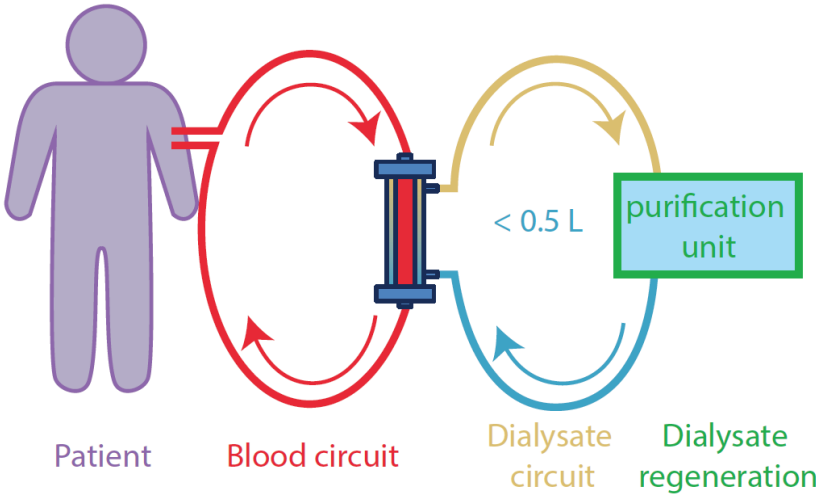

Figure 3: Schematic overview of a wearable dialysis device (from Chapter 2).

Although most uremic toxins and waste electrolytes can effectively be removed from spent dialysate (dialysate that has passed the dialyzer) by activated carbon and ion-exchangers, respectively, removal of urea (scheme 1, compound **1**) is a major challenge in the realization of a wearable dialysis device.[14-15] Urea is the uremic toxin with the highest daily production (240-470 mmol/day).[16-17] The uremic concentration of urea is higher than that of other uremic toxins and toxic effects have been described at concentrations representative for ESKD (~20-30 mM).[18-19]

1.4 Urea Sorbents

As discussed in **Chapter 2**, one strategy to remove urea from spent dialysate is by chemisorption with a sorbent. In this case the sorbent has functional groups that form covalent bonds with urea. The sorbent may be placed in a replaceable cartridge in the purification unit. Although several urea sorbents have been reported in literature,[20-22] (also discussed in more detail in **Chapter 2**) the main problem of these materials is that the kinetics of urea removal are generally slow, and therefore unsuitable for application in a wearable dialysis device. Therefore a urea sorbent suitable for the regeneration of dialysate should have the following requirements:

1) The sorbent needs to be stable during storage and operation and should not leach potentially toxic components into the dialysate.[23]
2) The sorbent needs to have sufficiently fast urea removal kinetics to remove the daily urea production (around 400 mmol or 24 g) in one dialysis session. Ideally, a sorbent removes at least 2.0 mmol/g/8h; thereby maximum 200 grams will be sufficient to remove the daily urea production in a dialysis session of 8 hours (i.e. a typical duration of a nocturnal hemodialysis session).
3) It should be possible to immobilize the sorbent in the purification unit with only limited pressure building up at the high dialysate flow rate used in dialysis (300 - 500 mL/min).
4) The sorbent selectively reacts with urea, and not with other nucleophilic solutes that are present in the dialysate (e.g. amino acids and creatinine) that will occupy the binding sites, thereby lowering the urea binding capacity.
5) The sorbent needs to withstand sterilization conditions, for instance gamma radiation, dry heating (160-170 °C for 1-2 hour), steam sterilization or autoclaving.
6) The reaction between the sorbent and urea is irreversible under dialysis conditions, but ideally the sorbent beads can be regenerated, *e.g.* under acid or basic conditions. Regeneration of the sorbent would allow the possibility of re-use of the sorbent, thereby potentially reducing the cost of the sorbent and making the sorbent more cost-effective.

A sorbent with fast urea removal kinetics logically contains functional chemical groups that are 1) highly reactive towards urea and 2) accessible for dialysate. To maximize the amount of urea that can be removed by the sorbent, the functional groups should be present at a highest possible density in a certain matrix, such as a polymer network. Leaching of residual compounds used in the preparation of the sorbent (i.e. monomers, solvents) can be prevented by proper washing of the sorbent, however, degradation of the sorbents due to *e.g.* hydrolytic reactions during dialysis can still lead to leaching of potentially toxic components and should therefore be prevented. Polymers with **carbon-carbon bond** backbones are considered a suitable basis for a urea sorbent, as these bonds are very stable

under physiological conditions, making leaching due to degradation of the sorbent matrix unlikely. A polymer with carbon-carbon backbone can be obtained by radical polymerization of monomers with a carbon-carbon double bond. The structural design of such a sorbent is shown in figure 1.

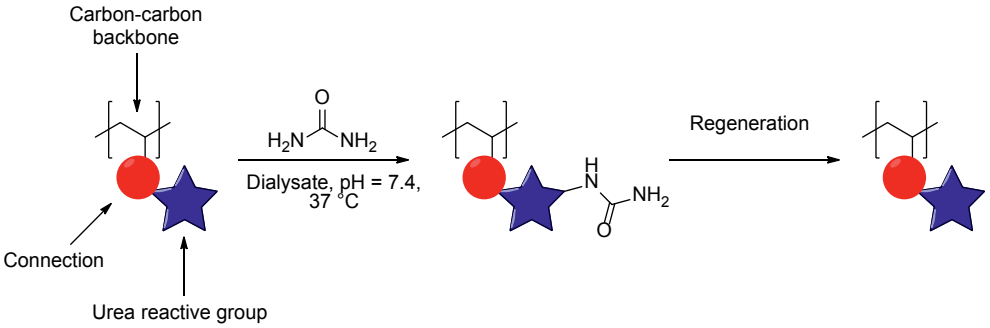

Scheme 1: Structural design of a urea sorbent.

Polymeric beads are considered as a suitable morphology of the sorbent as they are easily immobilized in a column by a filter. However, dialysate flowing with a certain flow rate through a bed of spherical beads in a column will result in a pressure drop which can be calculated using the Kozeny-Carman equation (equation 1), in which Δp is the pressure drop, L is the height of the sorbent bed, Q is the flow rate, μ is the viscosity of the fluid, ϕ is the sphericity of the beads, D_p is the average diameter of the beads and ε is the porosity of the sorbent bed.[24]

$$(1) \quad \Delta p = \frac{180LQ\ \mu(1-\varepsilon)^2}{\phi^2 D_p^2 \varepsilon^3}$$

For spherical and non-porous beads and at a fixed viscosity of the dialysate, the pressure drop scales with the length of the column in which the beads are packed and inversely with the diameter of the beads to the power two. For regeneration of dialysate it has been reported that sorbent particles with a size <50 μm resulted in a pressure drop of 45-48 kPa. This pressure drop strongly decreases with an increased particle size to only 2.6-4.0 kPa for particles with a size of 150-200 μm.[25] Therefore, we estimated that the sorbent beads should also have a diameter of ~200 μm. However this pressure drop needs to be determined experimentally and can be tailored to an acceptable level by a combination the geometry of the column and the size of the beads. Aim is to keep the pressure drop across the cartridge below ~100 kPa (= 1 bar = 750 mmHg) to keep the system requirements manageable and limit the risk of leakage. It should be mentioned that the kinetics decrease with in increasing diameter due to longer diffusion distances inside the beads. We hypothesized that loss of accessibility might be overcome by increasing the porosity of the beads (and thereby the surface area), and/or by increasing hydrophilicity (and thus the swelling capacity) of the sorbent.[26-27]

Among the best urea sorbents reported in literature are polystyrene beads in which the aromatic group has been modified in ninhydrin or phenylglyoxaldehyde groups.[20, 26, 28] Both of these functional groups contain carbonyl groups that are in equilibrium with the corresponding hydrate (scheme 2), and have been reported to form covalent bonds with urea in dialysate. These sorbents are used as a starting point for the work described in this thesis and are further discussed in **Chapters 2-6**.

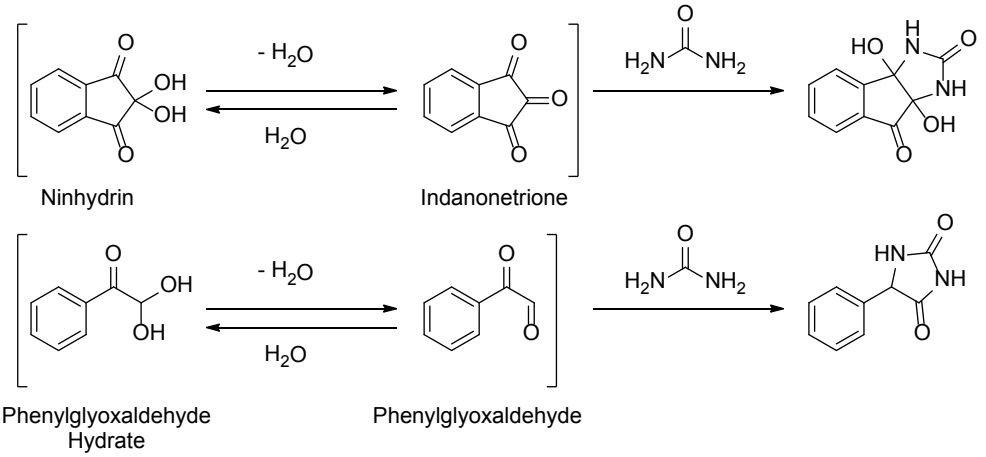

Scheme 2: The structures of ninhydrin and phenylglyoxaldehyde and their carbonyl-hydrate equilibrium and the subsequent reaction with urea.

1.5 Aim and outline of this thesis

The research described in this thesis was financially supported by TTW (project 14433) and NeoKidney, aided by expertise from DSM and Cabot. The aim of the research described in this thesis is to develop novel urea sorbents with efficient, selective and fast urea removal (at least 2.0 mmol/g in 8 hours at 37 °C) for the regeneration of dialysate in a wearable dialysis device. The physico-chemical properties of urea, the concept of dialysis and the state of the art of several urea removal strategies are reviewed in **Chapter 2**, along with the drawbacks and possibilities to overcome these.

As ninhydrin-type sorbents have been reported to remove urea from dialysate, it was investigated whether ninhydrin derivatives have better urea binding characteristics. Thus, the influence of electron donating and electron withdrawing substituents on the reactivity of ninhydrin with urea was studied in **Chapter 3**. In addition, this would also determine how the ninhydrin-group is best connected to the carbon-carbon backbone of a sorbent and would give further into insights in the reaction mechanism.

To identify carbonyl compounds (other than ninhydrin and phenylglyoxaldehyde)

which can form covalent bond with urea in dialysate, the reaction of urea with various carbonyl compounds is studied in **Chapter 4**. The kinetic rate constants of these reactions and the reaction products were determined and established, thereby providing important insights into the reaction mechanism of urea with those carbonyl groups. This knowledge was used to select the most suitable urea-reactive groups which should be incorporated in a urea sorbent.

Based on the knowledge obtained in **Chapter 3** and **Chapter 4** we designed and synthesized new monomers that, after a polymerization and oxidation step, resulted in urea-reactive sorbents with a high urea binding capacity. Thus, in **Chapter 5**, sorbents containing phenylglyoxaldehyde groups were synthesized, and the reactivity and sorption kinetics towards urea were studied in simulated dialysate.

Similarly, in **Chapter 6**, sorbents containing ninhydrin groups were synthesized. The kinetics of urea removal by this sorbent was studied in simulated dialysate (30 mM urea solution in phosphate buffered saline) and how this is influenced by temperature and the ninhydrin : urea ratio.

In **Chapter 7**, the findings of this thesis are summarized. The potential use of the sorbents developed in this thesis is put in perspective of the development of a future wearable dialysis device.

References

1. Legallais, C.; Kim, D.; Mihaila, S. M.; Mihajlovic, M.; Figliuzzi, M.; Bonandrini, B.; Salerno, S.; Yousef Yengej, F. A.; Rookmaaker, M. B.; Sanchez Romero, N.; Sainz-Arnal, P.; Pereira, U.; Pasqua, M.; Gerritsen, K. G. F.; Verhaar, M. C.; Remuzzi, A.; Baptista, P. M.; De Bartolo, L.; Masereeuw, R.; Stamatialis, D., Bioengineering organs for blood detoxification. *Adv. Healthc. Mater.* **2018,** *7* (21), e1800430.
2. Stevens, L. A.; Coresh, J.; Greene, T.; Levey, A. S., Assessing kidney function — Measured and estimated glomerular filtration rate. *N. Engl. J. Med.* **2006,** *354* (23), 2473-2483.
3. Facts & figures, European Renal care providers Association, Retrieved from: https://ercpa.eu/index.php/facts-figures/ [Accessed Auguest 23rd 2019).
4. Feiten en cijfers, Nierstichting [Online], Retrieved from : https://www.nierstichting.nl/leven-met-een-nierziekte/feiten-en-cijfers/, [accessed August 23rd 2019].
5. Itoh, Y.; Ezawa, A.; Kikuchi, K.; Tsuruta, Y.; Niwa, T., Protein-bound uremic toxins in hemodialysis patients measured by liquid chromatography/tandem mass spectrometry and their effects on endothelial ROS production. *Anal. Bioanal. Chem.* **2012,** *403* (7), 1841-1850.
6. Wernert, V.; Schaf, O.; Ghobarkar, H.; Denoyel, R., Adsorption properties of zeolites for artificial kidney applications. *Micropor. Mesopor. Mat.* **2005,** *83* (1-3), 101-113.
7. Gryp, T.; Vanholder, R.; Vaneechoutte, M.; Glorieux, G., p-Cresyl sulfate. *Toxins (Basel)* **2017,** *9* (2), 52.
8. V.A. Luyckx; M. Tonelli; Stanifer, J. W., The global burden of kidney disease and the sustainable development goals. *Bull. World Health Organ.* **2018,** *96*, 414-422.
9. Fresenius Medical Care (FMC) Annual Report, **2018**. [Online] Retrieved from: https://www.freseniusmedicalcare.com/fileadmin/data/com/pdf/Media_Center/Publications/Annual_Reports/FME_Annual-Report_2018.pdf. [Accessed 11 July 2019]
10. Saha, M.; Allon, M., Diagnosis, treatment, and prevention of hemodialysis emergencies. *Clin. J. Am. Soc. Nephrol.* **2017,** *12* (2), 357-369.
11. van Gelder, M. K.; Mihaila, S. M.; Jansen, J.; Wester, M.; Verhaar, M. C.; Joles, J. A.; Stamatialis, D.; Masereeuw, R.; Gerritsen, K. G. F., From portable dialysis to a bioengineered kidney. *Expert Rev. Med. Devices* **2018,** *15* (5), 323-336.
12. Culleton, B. F.; Walsh, M.; Klarenbach, S. W.; Mortis, G.; Scott-Douglas, N.; Quinn, R. R.; Tonelli, M.; Donnelly, S.; Friedrich, M. G.; Kumar, A.; Mahallati, H.; Hemmelgarn, B. R.; Manns, B. J., Effect of frequent nocturnal hemodialysis vs conventional hemodialysis on left ventricular mass and quality of life: a randomized controlled trial. *JAMA,* **2007,** *298* (11), 1291-9.
13. Chertow, G. M.; Levin, N. W.; Beck, G. J.; Depner, T. A.; Eggers, P. W.; Gassman, J. J.; Gorodetskaya, I.; Greene, T.; James, S.; Larive, B.; Lindsay, R. M.; Mehta, R. L.; Miller, B.; Ornt, D. B.; Rajagopalan, S.; Rastogi, A.; Rocco, M. V.; Schiller, B.; Sergeyeva, O.; Schulman, G.; Ting, G. O.; Unruh, M. L.; Star, R. A.; Kliger, A. S., In-center hemodialysis six times per week versus three times per week. *N. Engl. J. Med.* **2010,** *363* (24), 2287-300.
14. Agar, J. W., Review: understanding sorbent dialysis systems. *Nephrology (Carlton)* **2010,** *15* (4), 406-11.
15. Ash, S. R., Sorbents in treatment of uremia: a short history and a great future.

Semin. Dial. **2009,** *22* (6), 615-22.
16. Weiner, I. D.; Mitch, W. E.; Sands, J. M., Urea and ammonia metabolism and the control of renal nitrogen excretion. *Clin. J. Am. Soc. Nephrol.* **2015,** *10* (8), 1444-58.
17. Shinaberger, C. S.; Kilpatrick, R. D.; Regidor, D. L.; McAllister, C. J.; Greenland, S.; Kopple, J. D.; Kalantar-Zadeh, K., Longitudinal associations between dietary protein intake and survival in hemodialysis patients. *Am. J. Kidney. Dis.* **2006,** *48* (1), 37-49.
18. Singh, L. R.; Dar, T. A.; Ahmad, F., Living with urea stress. *J. Biosci.* **2009,** *34* (2), 321-31.
19. Vanholder, R.; Gryp, T.; Glorieux, G., Urea and chronic kidney disease: the comeback of the century? (in uraemia research). *Nephrol. Dial. Transplant.* **2018,** *33* (1), 4-12.
20. Smakman, R.; van Doorn, A. W., Urea removal by means of direct binding. *Clin. Nephrol.* **1986,** *26 Suppl 1*, S58-62.
21. Shimizu, T.; Fujishige, S., A newly prepared surface-treated oxystarch for removal of urea. *J. Biomed. Mater. Res.* **1983,** *17* (4), 597-612.
22. Deepak, D., Evaluation of adsorbents for the removal of metabolic wastes from blood. *Med. Biol. Eng. Comput.* **1981,** *19* (6), 701-6.
23. van Doorn, A. W., Regeneration of dialysate. *Artif. Organs* **1979,** *3* (2), 190-2.
24. Kruczek, B., Carman–Kozeny Equation. In *Encyclopedia of Membranes*, 2014; pp 1-3.
25. Bluchel, C. G.; Wang, Y.; Tan, K.C., Sorbent for a dialysis device., **2011**., U.S. Patent 0171713 A1.
26. Poss, M. J.; Blom, H.; Odufu, A.; Smakman, R., Macromolecular ketoaldehydes. U.S. Patent 6,861,473 B2: 2005.
27. Gokmen, M. T.; Du Prez, F. E., Porous polymer particles—A comprehensive guide to synthesis, characterization, functionalization and applications. *Prog. Polym. Sci.* **2012,** *37* (3), 365-405.
28. Smakman, R., Macromolecular carbonyl groups containing material suitable for use as sorbent for nitrogen compounds., **1990**, U.S. Patent 4,897,200.

2

Chapter 2

Urea Removal Strategies for Dialysate Regeneration in a Wearable Artificial Kidney

Maaike K. van Gelder[a]*, Jacobus A.W. Jong[a,b]*, Laura Folkertsma[a,c], Yong Guo[b], Christian Blüchel[d], Marianne C. Verhaar[a], Mathieu Odijk[c], Cornelus F. Van Nostrum[b], Wim E. Hennink[b] and Karin G.F. Gerritsen[a]**

[a] Department of Nephrology and Hypertension, University Medical Centre Utrecht, Heidelberglaan 100, 3584 CX Utrecht, the Netherlands.
[b] Department of Pharmaceutics, Utrecht Institute for Pharmaceutical Sciences (UIPS), Utrecht University, Universiteitsweg 99, 3584 CG Utrecht, the Netherlands.
[c] BIOS-Lab on a Chip Group, MESA+ Institute of Nanotechnology, Technical Medical Centre, Max Planck Center for Complex Fluid Dynamics, University of Twente, 7522 NH Enschede, the Netherlands.
[d] Dialyss Pte Ltd, 21 Tampines Avenue 1, 529757 Singapore, Singapore.
* Both authors contributed equally

Submitted

Abstract

The availability of a wearable artificial kidney (WAK) that provides dialysis outside the hospital would be an important advancement for dialysis patients. The concept of a WAK is based on regeneration of a small volume of dialysate in a closed-loop. Removal of urea, the primary waste product of nitrogen metabolism, is the major challenge for the realization of a WAK since it is a molecule with low reactivity that is difficult to adsorb while it is the waste solute with the highest daily molar production. Currently, no efficient urea removal technology is available that allows for miniaturization of the WAK to a size and weight that is acceptable for patients to carry. Several urea removal strategies have been explored, including enzymatic hydrolysis by urease, electro-oxidation and sorbent systems. However, thus far, these methods have toxic side effects, limited removal capacity or slow removal kinetics. This review discusses different urea removal strategies for application in a wearable dialysis device, from both a chemical and a medical perspective.

1. Introduction

Patients with end stage kidney disease (ESKD) may undergo hemodialysis (HD) (figure 1) or peritoneal dialysis (PD) (figure 2) to replace kidney function. The quality of life of dialysis patients is poor due to a high morbidity and high treatment burden.[1] The vast majority of patients (88%[2]) is treated with intermittent in-center hemodialysis (3 × 4 h per week), resulting in inadequate removal of waste solutes and excess water, which are normally excreted continuously by the healthy kidneys *via* the urine. Accumulation of waste solutes causes uremic symptoms, such as nausea and pruritus (itchy skin) that markedly decrease patients' well-being. Importantly, retained waste solutes exert toxic effects to multiple organs, particularly those of the cardiovascular system.[3-4] Fluid overload is associated with hypertension, heart failure and mortality.[5] To limit accumulation of water and waste solutes, dialysis patients have to adhere to strict fluid and dietary restrictions, which further compromise their quality of life.[6-7] In addition, the time spent travelling to the dialysis center and dialysis procedure, significantly limits patients' freedom and autonomy. PD provides more continuous renal replacement therapy outside the hospital. However, the level of blood purification (or clearance, *i.e.* the volume of body water that is cleared of a solute per time unit) is relatively low for patients that undergo this treatment.[8] Moreover, most patients can be treated with PD for only a limited period of time due to functional decline of the peritoneal membrane, primarily caused by exposure to toxic high glucose concentrations in PD solutions, and recurrent infection of the peritoneal membrane. As a consequence, patients that are treated with PD have to switch to HD after a median of 3.7 years.[9]

A wearable artificial kidney (WAK) that could provide more frequent (up to permanent) high toxin clearance outside the hospital would be a considerable improvement for both HD and PD patients. In other words, a small dialysis device, preferably less than 2.0 kg when worn on the body[10] or less than 11 kg when used as a table device (*i.e.* the advised maximum weight to lift for PD patients[11]), will substantially increase patients' mobility, freedom and ability to engage in social and economic life. Importantly, more frequent or continuous treatment with a WAK will possibly reduce waste solute concentrations and fluctuations of patients' internal environment and may therefore improve clinical outcomes, including quality of life, as observed with more frequent and prolonged HD.[12-14]

The key for the development of a WAK is efficient regeneration of spent dialysate in a closed-loop system (figures 1-2). Regeneration of spent dialysate will allow for the use of a small volume of dialysate (ideally less than 0.5 L), whereas conventional single-pass HD uses a large volume of dialysate (approximately 120 L per 4-h HD session) typically produced by a stationary water treatment system. Traditional PD requires a considerable volume of bagged dialysis fluids (8 - 12 L per day) to be stored at the patients' home. Dialysate regeneration entails removal of uremic

solutes from spent dialysate and maintenance of stable dialysate pH and electrolyte concentrations. The solutes that need to be removed to regenerate the dialysate are uremic waste solutes that are normally excreted by the healthy kidneys. This includes ions, such as phosphate and potassium which accumulation leads to vascular calcification and (lethal) arrhythmia, respectively, and organic solutes, such as small nitrogenous waste products (*e.g.* urea, creatinine) and low molecular weight proteins (*e.g.* β2-microglobulin, a protein associated with dialysis related amyloidosis). Phosphate and potassium ions are removed by ion-exchangers and most organic waste solutes can efficiently be removed by activated carbon (AC).[15-16] Importantly, the affinity of AC for urea is relatively low (0.1-0.2 mmol/g, see paragraph 5.1)[17-18] while daily molar production of urea is higher than that of other waste solutes (240-470 mmol per day).[19-20] As a consequence, the greatest challenge for efficient dialysate regeneration is urea removal.[21] The aim of this review is to discuss strategies to remove urea from dialysate that can be applied in a WAK (*i.e.* enzymatic hydrolysis, electro-chemical oxidation (EO), chemisorption and physisorption) and the advantages, disadvantages and possible improvements of these methods both from a chemical and clinical perspective.

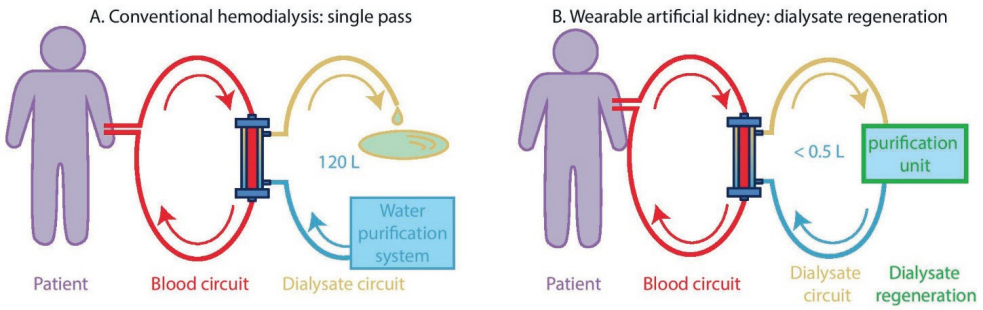

Figure 1. A) Schematic representation of conventional single-pass hemodialysis. During hemodialysis, the patient's blood is circulated through a dialyzer, in which solutes pass across a semi-permeable membrane by diffusion and convection into an aqueous solution called dialysate. This dialysate in turn flows in counter-current direction to maximize the diffusive mass transport across the membrane, and is discarded into the sewage system after a single pass through the dialyzer. B) Schematic representation of a wearable artificial kidney with dialysate regeneration. Spent dialysate is continuously regenerated by a purification unit and reused.

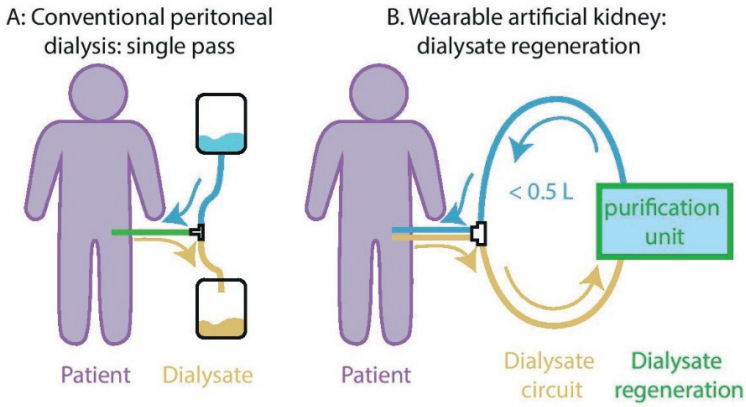

Figure 2. A) Schematic representation of conventional PD. During PD, hypertonic dialysate is instilled into the peritoneal cavity *via* a catheter to allow for diffusive and convective removal of waste solutes and osmotic removal of excess water across the peritoneal membrane. After a certain period of time, the dialysate (containing waste solutes and excess water) is drained and discarded. B) Schematic representation for peritoneal dialysate regeneration by a wearable artificial kidney. Peritoneal effluent is continuously regenerated by a purification unit and reused.

2. Urea

In the human body, proteins and other nitrogen-containing nutrients are metabolized into ammonium, which is converted in the liver into urea *via* the urea cycle.[22] Urea is transported to the kidneys through the bloodstream, where it is excreted into the urine.[23] Urea is the main circulating non-protein nitrogen compound and accounts for approximately 90% of renal nitrogen excretion.[19] It is the waste solute with the highest daily molar production of 240 to 470 mmol, depending on protein intake.[19-20] Since elevated plasma urea concentrations (20 - 30 mM), representative for ESKD, are associated with toxicity, effective urea removal is crucial for successful dialysate regeneration.

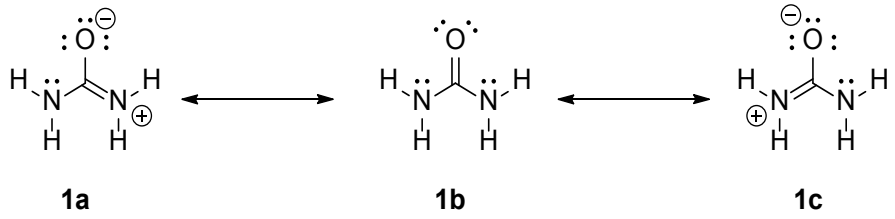

Scheme 1: Resonance structures of urea.

Urea is usually depicted as resonance structure **1b** as shown in scheme 1.[24] However, as in amide bonds, the lone electron pairs on both nitrogen atoms are delocalized in the C-N bonds (structures **1a** and **1c**). Therefore the C-N bonds also have a double bond character and the C-O bond also has single bond character, which makes the chemical reactivity of urea very low. In aqueous solution urea is in equilibrium with traces of the fragmentation products, ammonium and cyanate (0.1-0.8%) (scheme

2A)[25] Cyanate can further react with H_2O under acidic conditions to form CO_2 and NH_3 (scheme 2B).

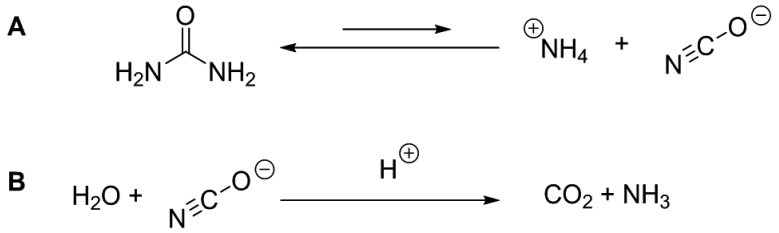

Scheme 2: A) Equilibrium of urea with ammonium and cyanate in water. B) Reaction of cyanate with water in the presence of acid.

Urea is a chaotropic agent that can disrupt the globular structure of proteins at supraphysiological concentrations by breaking hydrogen bonds, thereby altering protein and enzyme function.[26] Although mildly elevated urea concentrations in the range of 10 to 20 mM are well tolerated, uremic concentrations above 20 mM have been associated with toxicity, including insulin resistance, disruption of the gastrointestinal barrier which may result in leakage of pro-inflammatory mediators from the gut into the bloodstream, production of radical oxygen species, induction of apoptosis and cell death of smooth muscle cells, and endothelial changes promoting atherosclerosis.[27] These effects are either caused by urea directly, by cyanate or ammonium (scheme 2A), or as a result of the reaction of isocyanic acid (conjugated acid of cyanate) with arginine or lysine residues in proteins (carbamylation),[28] as shown in reaction 1.

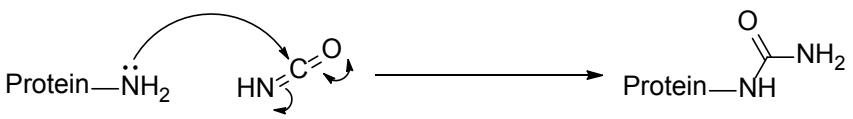

(1)

Carbamylated proteins cause a variety of biochemical alterations, including transition of mesangial cells into a profibrogenic cell type, altered leukocyte response (caused by carbamylated collagen), vascular damage (caused by carbamylated low-density lipoprotein) and abnormal erythropoietin response (caused by carbamylated erythropoietin). Therefore, high urea concentrations should be avoided.[27] To remove the daily urea production of 240 to 470 mmol[19-20] while keeping the urea concentration below 20 mM with a daily 8-h dialysis regime, urea clearance during dialysis should be at least 25-49 mL/min, respectively, resulting in a 24-h time-averaged clearance of 8-16 mL/min.

3. Enzymatic hydrolysis of urea

3.1 Ureases

Krajewska published extensive reviews on ureases, their binding pockets, catalytic properties and their inhibitors.[29-30] Most ureases found in plants and fungi are present as a trimer or hexamer of subunits with a molecular weight of ca. 90 kDa per subunit and have a hydrodynamic diameter of ca. 14 nm.[29, 31] Ureases use a zinc-ion to coordinate the carbonyl group of urea, making the carbonyl group more electrophilic. While urea is very stable in physiological aqueous solutions towards chemical hydrolysis (pH 7.4 and 37 °C)[29]), urease-catalyzed hydrolysis of urea into ammonium and bicarbonate (reaction 2) is very efficient. Urease derived from jack beans (*canavalia ensiformis*) is one of the most active ureases. This enzyme follows Michaelis-Menten kinetics, has a relatively low K_M of 2.9 to 3.6 mM, *i.e.* the substrate concentration at which urease activity is 50% of the maximum activity, and is most active at a pH of 7.0 to 7.5.[29] The turnover rate of urease is up to 5.9 × 10^3 s^{-1},[32-34] while the rate of uncatalyzed urea hydrolysis is too slow to determine experimentally and independent of the pH in the range of 4-10.[35-36] Since the dialysate urea concentration is ~10 to 30 mM (thus, far above the K_M) and pH of the dialysate is around 7.4, the activity of urease is close to V_{max} in dialysate. Based on these values, in theory, only ~3-5 milligrams of active urease is sufficient for complete removal of urea from dialysate during a 4-h dialysis session at dialysate flow rates up to 300 mL/min and urea concentrations ranging from 2 to 40 mM. However, it was found empirically that ~30-50 grams of immobilized urease (including matrix) is needed to accomplish this (unpublished data). Therefore, from that point of view, enzymatic urea hydrolysis would be a very attractive approach to remove urea from dialysate.[37-38] However, the formed ammonium is much more toxic than urea itself. Therefore, a urea removal strategy based on urease should be complemented with a strategy to remove ammonium, as discussed in the "the REDY sorbent system" section.

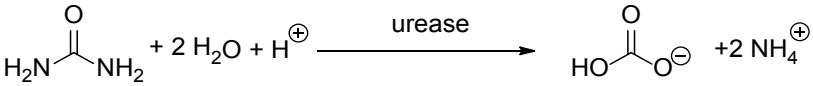

(2)

3.2 Urease immobilization

Immobilization of urease onto a solid support is essential for the development of a urease-based WAK. Urease immobilization has been reviewed by Krajewska[30] and can be achieved by chemical (covalent bonding) or physical immobilization (non-covalent bonding). In general, immobilization reduces V_{max} and increases K_M. A higher urease activity level is usually maintained by physical immobilization as compared to chemical linkage to a carrier. Urease has been chemically immobilized on porous chitosan/glutaraldehyde beads,[39] poly(*N*-isopropylacrylamide-*co*-

N-acryloxysuccinimide-*co*-2-hydroxyethyl methacrylate) hydrogels,[40] poly-acrylonitrile hollow fibers,[41-42] beads based on poly(acrylamide-*co*-acrylic acid,[43] poly-vinylalcohol,[44] gelatin,[45] microporous epoxy-functionalized methacrylamide copolymer (Eupergit®)[46] and cellulose.[47] Beyond that, it has been physically immobilized on AC, Al_2O_3 and zirconium phosphate.[48-49] The different immobilization methods are associated with varying strengths of the bond between support material and enzyme. Physical immobilization is weakest, and is considered easily reversible. Chemical immobilization is generally better, although certain functional groups used for binding, such as e.g. the imine-linkages created by glutaraldehyde immobilization, may be hydrolysable (i.e. reversible) under the conditions found in dialysate. The preferred option for application in a wearable artificial kidney is therefore immobilization through non-hydrolysable chemical linkers, for example through amine or ether linkages derived from epoxy-substituted support materials. Depending on the reaction conditions, epoxy-substituted support materials can form covalent bonds with carboxylic acid-, thiol-, amino- or phenolic groups of the enzyme. Bortone *et al*. reported that single-point immobilization of urease on Eupergit® by epoxy coupling slightly reduced the enzyme□s binding constant (Michaelis constant) K_M for urea from 3 mM to 5 mM,[29, 46] while the constant for the conversion of urea to ammonium (k_{cat}) remained approximately unchanged. The activity of the enzyme was reduced by factor 2 upon immobilization as a result of limited diffusion of urea (and therefore a local urea concentration lower than K_M in the sorbent).

3.3 The REDY sorbent system

Until now, the REcirculation DialYsis (REDY) sorbent system,[50] which contains urease (derived from jack beans and immobilized on aluminium oxide (Al_2O_3)) for enzymatic conversion of urea, is the only dialysate regeneration system that has been marketed. From 1973 to 1994, more than six million treatments were successfully performed with this transportable (approximately 20 kg) dialysis system, demonstrating the clinical feasibility of HD with dialysate regeneration.[51] [25]However, manufacturing of the REDY sorbent system was discontinued in 1994. The relatively high costs of the sorbent cartridges, inferior treatment adequacy compared to single-pass dialysis as a result of limited dialysate flow rates (max. 250 mL/min) and concerns about aluminium-induced osteomalacia (bone softening) and dementia may have contributed to this.[52-56]

Dialysate regeneration with the REDY sorbent system has been described in detail by Agar[15] and Ash[16] and others.[57-59] In brief, dialysate passes several sorbent layers, starting with AC which adsorbs non-urea organic compounds. Next, urea is hydrolyzed by immobilized urease into ammonium and (bi)carbonate. Subsequently, ammonium is exchanged for sodium or hydrogen cations by a zirconium phosphate ion-exchanger.[60] Finally, zirconium oxide and zirconium carbonate adsorb

phosphate in exchange for hydroxide, bicarbonate and acetate. Even though urease (hydrodynamic diameter ca. 14 nm[29, 31]) cannot pass the dialysis membrane (cut off 5-8 nm[61]), it is important that urease is immobilized upstream of the zirconium phosphate layer to prevent ammonium release into the patient. A schematic overview of the REDY sorbent system is shown in the review by Roberts.[37]

The REDY system, however, has several drawbacks. First, following equation 1, for every equivalent of urea, two equivalents of ammonium are formed. Thus, the daily urea production of 240 to 470 mmol[19-20, 62] would be converted into 480 to 940 mmol of ammonium. Moreover, ammonium is more toxic than urea,[63] and a relatively large amount of zirconium phosphate (~1.5 kg) is required to (almost) completely bind ammonium. Second, zirconium phosphate does not only bind ammonium, but also calcium, magnesium and (too much) potassium ions, resulting in the necessity to re-infuse these adsorbed cations from a separate reservoir.[64] Although this allows for a personalized dialysate prescription by adjustment of the calcium, magnesium and potassium ion concentrations to the patients' need, the re-infusion reservoir further increases the size and weight of the device. Third, the adsorbed cations are exchanged for hydrogen and sodium cations. The released protons may (partially) react with bicarbonate generated during urea hydrolysis to form water and carbon dioxide, which can be effectively removed from the dialysate circuit *via* a degasser.[65] Bicarbonate release into the spent dialysate is in fact favorable as it may correct for metabolic acidosis, a common complication of kidney failure due to impaired excretion of non-volatile acid. However, sodium release is a major concern as higher dialysate sodium concentrations are associated with weight gain between dialysis sessions and related complications such as hypertension.[66] To prevent a rise in dialysate sodium concentration, a sodium-free dialysate reservoir could be used to dilute the released sodium ions, although this would be at the expense of miniaturization.

In addition to the miniaturization issues, long-term treatment with the REDY system has been associated with a severe form of fracturing osteomalacia and encephalopathy (brain injury) due to leaching of aluminium ions from AC that was often contaminated with aluminium.[53-54, 56, 67-68] In 1982, cartridges became available with reduced aluminium content that did not show aluminium release above the maximum allowable level of 0.37 µM in water for dialysate preparation according to the Association for the Advancement of Medical Instrumentation (AAMI).[69-70] Still, urease immobilization onto Al_2O_3 is considered a potential hazard for chronic dialysis patients. These drawbacks and non-cost competitiveness with single-pass HD, resulted in the disappearance of the REDY system from clinical practice in 1994.[37]

3.4 'Second generation' REDY-based wearable artificial kidney devices

Several research groups are currently working on REDY-like sorbent system for the development of miniature dialysis systems for both HD and PD.[71] Best known is the WAK as developed by Gura *et al*., which has been evaluated during two pilot clinical trials.[64, 72] In the most recent trial in 2016, seven HD patients were treated with the WAK up to 24 h while being mobile.[64] The device weighed approximately 5 kg, including dialysate and sorbents (65 g immobilized urease on Al_2O_3, 600 g zirconium phosphate, 51 g hydrous zirconium oxide and 153 g AC). Mean plasma clearances of urea, creatinine, phosphate and β2-microglobulin per 24-h treatment compared favorably to time-averaged plasma clearances of intermittent HD.[8, 73]

Importantly, no serious adverse events were observed. However, several urease related technical problems were reported. In one patient after 11 h of treatment, dialysate ammonium concentration exceeded 2.9 mM, which was set as the maximum allowable concentration, indicating zirconium phosphate saturation. Plasma sodium concentration remained stable during the first 16 h of treatment (~130 mM) and tended to increase to 135±4 mM (p=0.13) after 24 h of treatment (sodium balance was not reported). Other encountered problems were excessive carbon dioxide bubbles in the dialysate circuit exceeding degassing capacity, formation of blood clots in the blood circuit and technical issues such as tubing kinking and early battery failure, which prompted early termination of the trial.[8, 73]

Most other miniature dialysis systems that are currently under development make use of a modified REDY-type sorbent system for dialysate regeneration.[71] AWAK Pte Ltd (Singapore and Burbank, CA) recently evaluated an automated wearable artificial kidney (AWAK PD™, <2 kg[74]) for PD during a First-In-Human clinical trial in 14 PD patients.[75] AWAK treatment for >10.5 h per day up to three days resulted in a significant decrease in urea, creatinine and phosphate plasma concentrations from 20.8 to 14.9 mM (p=0.001), 976 to 668 µM (p=0.001) and 1.7 to 1.5 mM (p=0.03), respectively. A weekly peritoneal K_t/V_{urea} (the volume cleared of urea over the total urea distribution volume) of >1.7 was achieved, which is the minimum Kt/V_{urea} in anuric patients recommended by the International Society of Peritoneal Dialysis guidelines.[76] Although no serious adverse events occurred, 73% of subjects experienced temporary abdominal discomfort, which resolved spontaneously after dialysate drainage or bowel movement. Importantly, plasma sodium, potassium and bicarbonate concentrations were stable, although systemic ammonium concentrations were not reported. The company Diality (formerly named Easydial) evaluated a portable (~10 kg) HD device (Dharma) and reported a mean urea reduction ratio (URR) of 78% at a plasma urea concentration of 40 mM, which is higher than the recommended minimum URR of 65%.[77-80] However, mean plasma sodium concentrations increased by 7.3 mM which is unacceptable for patients.[81] A schematic overview of a urease-based sorbent purification system is shown in figure 3.

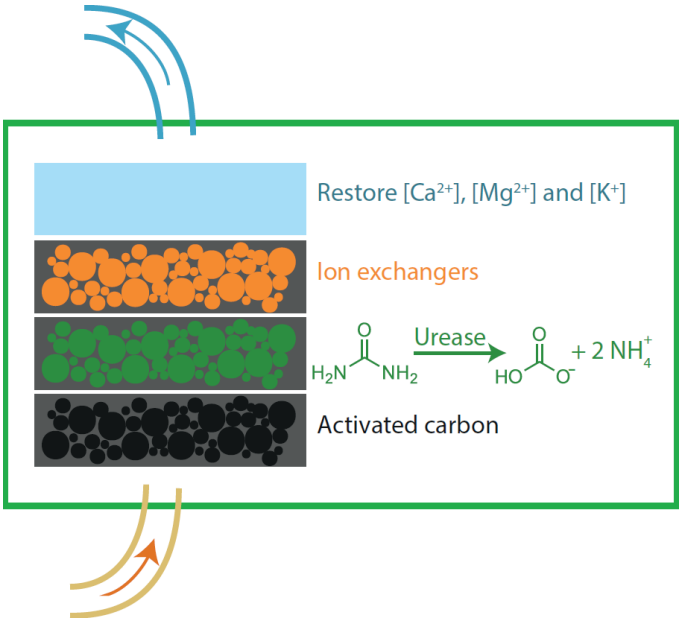

Figure 3. Schematic overview of a urease-based sorbent system purification unit.

4. Electrochemical decomposition of urea

In 1966, Tuwiner published a report on a water reclamation system for manned space vehicles that used electrochemical treatment to remove urea from urine.[82] This report initiated research on electro-oxidation (EO) of urea for dialysate regeneration (see table 1 for an overview of studies). A schematic representation of an EO-based purification unit is shown in figure 4, in which AC is placed upstream of the EO-unit to remove most organic waste solutes. EO is in principle an attractive technique for a WAK because it converts urea into gaseous products (nitrogen, hydrogen and carbon dioxide) that can easily be removed from dialysate by a bubble trap, and, importantly, EO-modules are small in size, lightweight, have a long life time and are relatively inexpensive. However, the challenge for EO is control of the exact reactions and formed products, because besides the mentioned gasses also other, mainly toxic, compounds are generated, such as active chlorine species and chloramines that need to be removed by placing AC downstream of the EO-unit (figure 4).

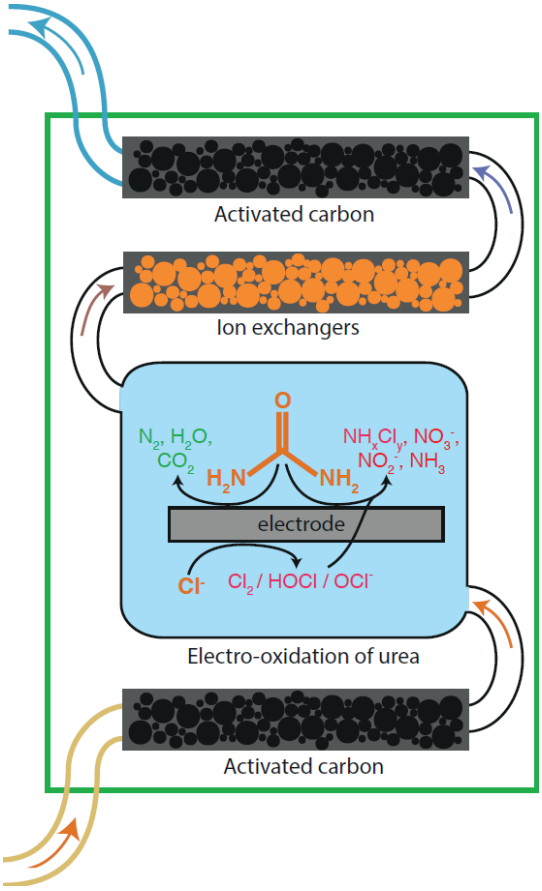

Figure 4. Schematic representation of an EO-based WAK. Products of complete urea oxidation are presented in green, unwanted toxic by-products of urea oxidation are presented in red.

4.1 Reactions and products

Direct EO of urea converts urea into nitrogen gas (N_2), carbon dioxide gas (CO_2) and hydrogen gas (H_2) (reaction 3). This reaction is the net result of urea oxidation at the anode and simultaneous reduction of water at the cathode. When chloride ions (Cl^-) are present in the solution, as is the case in dialysate, the oxidation of urea can occur *via* a second indirect route, mediated by anodically generated active chlorine species such as hypochlorite (OCl^-).[83-84]

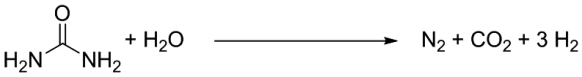

(3)

$$6\ Cl^- \rightarrow 3\ Cl_2 + 6\ e^- \quad (4)$$

$$3\ Cl_2 + 3\ H_2O \rightarrow 3\ HOCl + 3\ H^+ + 3\ Cl^- \quad (5)$$

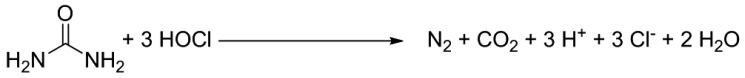

$$H_2N(C{=}O)NH_2 + 3\,HOCl \longrightarrow N_2 + CO_2 + 3\,H^+ + 3\,Cl^- + 2\,H_2O \quad (6)$$

Ideally, the indirect reactions 4-6 result in the same products as the direct route, i.e. nitrogen, carbon dioxide and hydrogen gas. However, in most cases, at least trace amounts of toxic side products such as nitrate (NO_3^-), nitrite (NO_2^-), ammonia (NH_3), chloramines (NH_xCl_y) and active chlorine species are formed. Nitrate may cause gastric cancer in adults and methemoglobinemia in infants.[85-86] Ammonia is toxic for many organs, particularly the brain.[63] Chloramines, which are derivatives of ammonia by substitution of hydrogen with chlorine atoms, may cause oxidative damage to red blood cells and shorten their survival resulting in anemia.[87] Furthermore, active chlorine species have strong oxidizing properties and can react with proteins[88] and other components of the dialysate to form toxic chlorine products. Most of these products can be removed with AC, but considering their reactivity and toxicity, it is preferable to prevent their formation.

Another factor to consider is undesired oxidation of other dialysate components, which may also result in the formation of potentially hazardous products. An example is oxidation of glucose into aldehydes, which occurs more readily than oxidation of urea, as observed in a number of studies.[89-95] For PD, aldehydes are associated with pathological changes of the peritoneal membrane.[96-97] Consequently, to render EO suitable for dialysate regeneration, control over reactions and their products is paramount. Key parameters which can be used to control the reactions and products are the electrode material, applied potential, and applied current density. In the following paragraphs we will discuss these parameters and how they affect the formation of unwanted products. Subsequently, the efficacy of urea removal and the current efficiency will be discussed.

4.2 Electrode material

The electrode material has to meet several requirements. First, it needs to be chemically stable to ensure its continuous operation for at least several days. Hence, corrosion or degradation is highly undesired. Second, the material should not leach toxic metals, as has been observed for platinum and ruthenium electrodes.[83, 92, 98] Third, the ideal electrode material should be selective, favoring the desired reaction and hardly catalyze undesired reactions. The electrode material determines to some extent which reactions can take place. Often, reagents need to bind to the electrode surface in a specific configuration before electron transfer between the reagent and electrode can take place. Furthermore, the potential at which reactions occur is electrode material dependent which means that the order in which reagents react can vary with the electrode material. For example, platinum is a known catalyst for many reactions, among which chloride and water oxidation which occur at lower potentials on platinum electrodes than on non-catalytic materials. Water oxidation in the WAK is undesired, because this will greatly reduce the current efficiency

(see below) and results in formation of oxygen bubbles that can block the anode. Conversely, boron-doped diamond electrodes do not catalyze water oxidation, but generate hydroxyl radicals with high efficiency.[99] Hydroxyl radicals in turn can act as mediator in the indirect oxidation of urea, just like active chlorine species.[100]

Wester *et al.* compared platinum, ruthenium and graphite electrodes and found graphite to be the most favorable because of its acceptable urea removal rate with limited chlorine formation.[83] Researchers from Lockheed Inc. investigated over 50 anode materials for their corrosion resistance in electrochemical treatment of urine. They found that 10% rhodium-containing platinum was the optimal electrode material based on corrosion resistance and current efficiency.[98] In addition, various cathode materials were studied for urine pretreatment and platinum was selected as the best, because of its low overpotential for hydrogen evolution.[98] This means that closing the current loop by reactions at the counter electrode will readily occur through hydrogen evolution from water reduction, making it possible for this electrode to sustain large current densities without undesired side reactions taking place. Other materials that have been investigated for their applicability as anode for EO of urea, for either dialysate regeneration or waste water treatment, are listed in table 1. Publications on waste water regeneration under physiological conditions are included, since urea removal from urine is comparable to dialysate regeneration. Recently, nickel-based electrodes have received a lot of attention in waste water treatment due to their efficient urea oxidation capacity.[101] However, these electrodes only function at or above pH 9, and are therefore unsuitable for dialysate regeneration at physiological conditions (pH 7.4 – 8.0). Besides the electrode material, functionalization of the electrode surface with catalytic groups or incorporation of selective membranes may increase selectivity of the reaction at the electrode.

Table 1. Publications reporting electro-oxidation of urea

Anode material	[Urea] (mM)	Applied current density (mA cm^{-2}) or potential (V)	Urea removal per unit area (mmol/h/m^2)	In vitro (S,D, sD, U, aU[a]), or in vivo (V)	Ref.
Pt	8.7	0.5 mA cm^{-2}	2.4 – 5.3	S	93
Pt	8.3	6 – 18 V	$4.2 \cdot 10^3$ – $7.3 \cdot 10^3$	D	102
Pt	10	a) 0.11 mA cm^{-2} b) 0.22 mA cm^{-2}; c) 0.8 V d) 1.0 V e) none	a) 7.4 b) 4.6 c) 8.3 d) 9.1 e) 2.9	S	92
Pt	3.3	Not specified	$1.1 \cdot 10^2$ – $1.9 \cdot 10^2$	D	94
Pt	33	7-20 mA cm^{-2}	$5.1 \cdot 10^3$	D	91
C foil	42	25.2 – 39.1 mA cm^{-2} / 8.5-11.5 V	$1.4 \cdot 10^3$ – $1.7 \cdot 10^3$	–	103
Pt	a) 9-33; b) 43	0.88 mA cm^{-2}, ≤1.2 V; 0.64 mA cm^{-2}, ≥-1.0 V	a) 17 – 37 b) 1.4 – 1.5	a) S b) sD	90
Ru-Ti-Sn-O (RTTO)	0- 500	4 – 61 mA cm^{-2}	$7.0 \cdot 10^2$	S	84
Pt	12.9	10; 20; 30; 39; 49; 59 mA cm^{-2}	11 – 79	D	89
Pt	29	5 mA cm^{-2}	$1.9 \cdot 10^2$ – $5.1 \cdot 10^2$	U	104
a) PtIr b) Fe and PtIr	a) 71.4 b) NaN	40 mA cm^{-2}	a) $6.0 \cdot 10^2$ b) 16 – $5.3 \cdot 10^2$	a) aU b) U	85
a) $(Pt\text{-}Ir)_{70:30}$ b) $(Ta_2O_2\text{-}IrO_2)_{70:30}$	0- 167	20 – 100 mA cm^{-2}	a) $1.4 \cdot 10^3$ – $3.4 \cdot 10^3$ b) 78 – $3.1 \cdot 10^3$	S	105
a) Pt b)$(RuO_2\text{-}TiO_2)_{40:60}$	17- 167	2 – 10 mA cm^{-2}	a) $1.4 \cdot 10^3$ – $4.8 \cdot 10^3$ b) $1.1 \cdot 10^3$ – $3.3 \cdot 10^3$	S	106
Ti/IrO_2	266	15 ± 0.3 mA cm^{-2}	$4.4 \cdot 10^2$ – $7.1 \cdot 10^2$	U	107
BiO_x/TiO_2	41.6	a) 2.0 V b) 2.8 V	a) 0.53 b) 4.7 – 8.9	S	108
a) Pt b) RuO_2 c) Graphite d) Graphite	a) 20 b) 20 c) 5 – 30 d) ~20	a) 10 mA cm^{-2} b) 10 mA cm^{-2} c) 6.8 – 17 mA cm^{-2} d) 10 mA cm^{-2}	a) $7.3 \cdot 10^2$ b) $4.5 \cdot 10^2$ c) $1.7 \cdot 10^2$ – $4.8 \cdot 10^2$ d) $3.2 \cdot 10^2$	a) S b) S c) S d) sD	83
a) Pt b) Ti-RuO_2 c) SnO_2–Sb_2O_5 c) BDD	0.03	5 – 20 mA cm^{-2}	a) 32 – $4.2 \cdot 10^2$ b) – c) 61 – $1.0 \cdot 10^3$ d) $1.7 \cdot 10^2$– $1.5 \cdot 10^3$	S	100
a) BDD b) IrO_2	200	40 mA cm^{-2}	a) 700 b) –	aU	109
a) Graphite b) BDD c) MoDD d) Si/C e) Si/C/Fe f) Si/C/Mo g) Pt	30	5 mA cm^{-2}	a) $2.5 \cdot 10^2$ b) $2.5 \cdot 10^2$ c) $2.5 \cdot 10^2$ d) $2.5 \cdot 10^2$ e) – f) $3.2 \cdot 10^2$ g) $1.2 \cdot 10^2$	S	110
Graphite	7-14	10 mA cm^{-2}	96 – $1.8 \cdot 10^2$	V	95

a) S, salt solution; D, unused dialysate with added urea; sD, spent dialysate; U, urine; aU, artificial urine.

4.3 Oxidation potential of urea

Whether or not a species such as urea can be oxidized at the anode is primarily dependent on the applied potential, which has to be high enough to overcome the oxidation potential of urea. However, the exact oxidation potential is unknown, as discussed below. Cyclic voltammetry (CV) is routinely used to determine the oxidation potential of compounds. During CV a potential scan is performed and the resulting current is measured. When the oxidation potential is approached, oxidation of the tested compound occurs, which in turn results in an increase of the current. At higher potentials, all available molecules of the oxidizable species near the electrode surface are instantly depleted and oxidation becomes diffusion limited resulting in a decrease of the current. CV diagrams therefore often have distinctive shapes, with clear oxidation peaks, see figure 5A. Unfortunately, urea does not give such a sharp oxidation peak in the CV diagram, but a small increase in current over a wide range of potentials is observed, see figure 5B for an example.[83, 85, 93, 105-106]

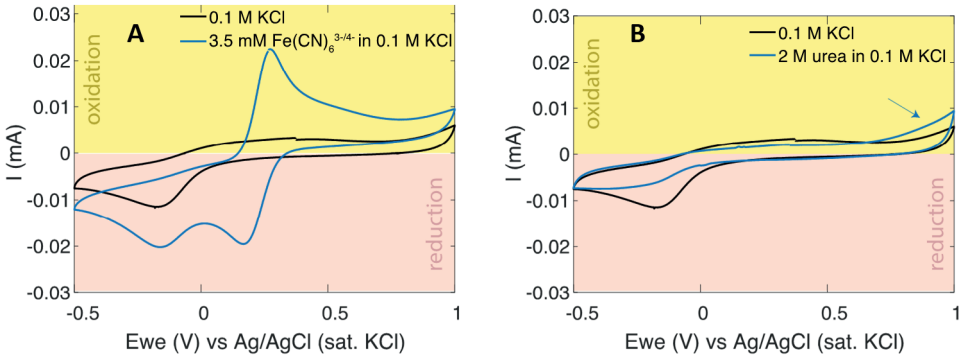

Figure 5. Cyclic voltammograms of A) 0.1 M KCl and 3.5 mM ferro/ferricyanide in 0.1 M KCl; and B) 0.1 M KCl and 2 M urea in 0.1 M KCl (unpublished data). The arrow indicates a slight increased oxidation current at potentials >0.7 V in the presence of urea, likely due to increased chloride oxidation. Ewe: potential applied (E) to the Pt working electrode (we). Scan rate was 100 mV/s.

For platinum electrodes, changes in currents for urea were reported between 0.5 and 0.9 V *vs* Ag/AgCl.[90, 92, 105, 111-112] Since chloride was present in the urea solutions and the standard potential of chloride oxidation is in the same range (0.6-1.2 V),[113] the increased currents could be due to oxidation of chloride, resulting in indirect oxidation of urea (reaction scheme 6). Formation of hypochlorite was not detected below 1.2 V, but this may be due to complete consumption of hypochlorite by (indirect) urea oxidation at lower potentials. Reports of CV in the absence of chloride are rare, likely because chloride is unavoidable in reported applications of EO for urea removal such as dialysis regeneration and waste water treatment. Hernandez *et al.* performed CV in a sodium perchlorate solution and reported increased currents on platinum electrodes between 0.7 and 1.2 V, suggesting that

the oxidation potential of urea lies within this range for platinum electrodes.[100] On the other hand, using Ti-RuO_2-electrodes at the same voltages, only urea adsorption and no urea oxidation was observed.[100] On boron doped diamond (BDD) and SnO_2-SbO_5 electrodes neither direct urea oxidation, nor adsorption of urea was observed, but water oxidation occurred, suggesting indirect oxidation of urea by the formed hydroxyl radicals.[100] The observation that urea can be oxidized by active chlorine and hydroxyl radicals suggests that the oxidation potential of urea is lower than that of chloride (0.6 – 1.2 V) and water (1.0 V). Nevertheless, direct oxidation of urea does not readily occur on the investigated materials under physiological conditions. This may be due to blocking of the electrode surface by strongly adsorbed urea on materials such as platinum, and lack of adsorption of urea and therefore lack of interaction with the electrode surface for other materials. Taken together, due to the presence of chloride in the dialysate and no or minimal direct oxidation of urea below chloride oxidation potentials with the electrode materials tested thus far, the best strategy for electrochemical dialysate regeneration needs to be focused on indirect urea oxidation. However, if a material would be found, which enables direct oxidation of urea, this could theoretically increase the efficiency and safety of the process. Unfortunately, such a material has not been identified so far.

4.4 Current driven and potential driven mode

Electro-oxidation can be performed in a current or a potential driven mode. This means that either the current or the potential at the anode can be set, and the other follows as a result of the setting and therefore cannot be independently selected. The magnitude of the potential difference between anode and cathode determines which reactions take place and only (combinations of) reactions with an oxidation potential lower than the potential difference between the electrodes occur.

4.4.1 Current driven mode and current density

In most publications a current driven mode is used, probably because this is the easiest to implement. At the electrode-electrolyte interface electrons have to be transferred to molecules or ions through a redox reaction resulting in oxidation of molecules at the anode and simultaneous reduction at the cathode. First, the most reactive species, i.e. the species with the lowest oxidation potentials, will participate in this reaction. When these species are depleted, the potential difference between the electrodes increases resulting in oxidation of less reactive species. This gives little control over the exact reactions and carries a high risk of undesired side reactions such as electrolysis of water.

Since electron transfer occurs at the electrode surface, the surface area of the electrode is an important determinant of the reactions. When the same current can be divided over twice the surface area, twice as many molecules of the reactive

species are available for reaction. The applied current is therefore normally expressed as *current density*: the current per unit electrode area. Thus, there are two ways to decrease undesired side reactions: (1) increasing the concentration of the desired reagent, or (2) decreasing the current density. Of note, increasing the concentration at or in the vicinity of the electrode surface can also be achieved by active convection such as stirring or application of flow over the electrode surface. In the case of indirect oxidation of urea by active chlorine species, the oxidation of chloride is desired yielding active chlorine species which in turn decompose urea, but also result in the formation of unwanted by-products such as chloramines. Controlling the ratio of urea supply *vs* current density is therefore of utmost importance. When the current density is too low, insufficient amounts of active chlorine will be formed, which leads to incomplete urea oxidation and accumulation of intermediate products such as chloramines. When the current density is too high, this results in excess formation of active chlorine, which increases the concentration of undesired active chlorine in the effluent. Thus, there is a delicate balance between incomplete oxidation, complete oxidation and over-chlorination. The challenge is to determine the point at which chlorine levels exceed the oxidant demand and free chlorine starts to build up in the dialysate, which is called break-point chlorination.

4.4.2. Potential driven mode and pulsed-potential techniques

In the potential driven mode, a fixed potential is applied at the anode which is in contrast with the current driven mode where there is no control over the potential difference that develops between the electrodes. The potential driven mode has been less widely used in literature, likely because it depends on a three electrode system, in which besides a cathode and anode also a reference electrode is used. In potential driven oxidation, the potential at the anode relative to the reference electrode can be used to tailor which reactions occur, since no reaction with an oxidation potential higher than the applied potential will take place. The potential at the cathode changes to accommodate the current needed to sustain the anodic potential but the potential at the cathode is otherwise not controlled. For removal of urea, the anode potential should be set at such a value that urea oxidation occurs, but not higher to prevent side reactions such as water oxidation. However, the potential at which urea oxidation occurs is relatively high (>0.7 V), which implies that not all side reactions can be avoided.

An alternative method, which may improve the selectivity of EO for urea in dialysate is the application of pulsed potentials.[114-115] For lidocaine it was found that oxidation by potential pulses (of 3.0 V *vs* Ag pseudo-reference electrode) considerably enhanced the yield of the reaction products as compared to a continuous potential (of 3.0 V *vs* Ag). Tuning of the cycle time modulated the selectivity of the oxidation reaction (more 4-hydroxylation product at cycle times of 0.2-12 s and more N-dealkylation product at cycle times <0.2 s).[114] The increased selectivity for certain

reaction paths is likely a result of a more active electrode surface, since the surface is rapidly passivated under oxidative conditions during the pulse, but recovers between the pulses at the lower potential. The same may hold for urea oxidation, where adsorption and deactivation of the platinum electrode surface is a known phenomenon.[79] In an attempt to overcome this, Yao *et al.* switched the potentials of anode and cathode every 20 s to repel adsorbed species from the anode, while limiting the anode potential to maximum 1.2 V and the cathode potential to minimum -1.0 V to prevent side-reactions. However, although they mention that switching "provides a certain degree of selectivity", unwanted oxidation of glucose, creatinine and uric acid still occurred.[90] Optimization of the pulse time and applied potentials may further improve selectivity.

4.5 Urea removal efficacy

Besides urea removal with minimal formation of unwanted toxic side products, effective urea removal is important to enable miniaturization of the WAK device. A large range of urea removal rates has been reported in literature ranging from 0.53 to $7.3 \cdot 10^3$ mmol/h/m^2 (median $3.8 \cdot 10^2$ mmol/h/m^2, interquartile range $1.3 \cdot 10^2$ to $1.1 \cdot 10^3$ mmol/h/m^2), see table 1. Therefore, to remove a daily urea production of 240 to 470 mmol with a daily 8-h dialysis scheme, 0.2 – 3.6 m^2 of electrode surface is required. By using mesh or nano-structured electrodes, or by folding, dividing or stacking the electrodes, such electrode areas can be easily incorporated into a WAK. Moreover, nano-structuring the electrodes may even improve the catalytic activity of the electrodes.[116]

The urea removal rate depends on various parameters. First, it increases with increasing current density since more species in the solution are activated.[83, 100, 105-106] Second, it increases with increasing urea concentration which results in a faster supply of urea to the electrodes. However, a maximum urea removal rate is reached when urea removal is limited by generation of active chlorine.[83, 95, 105-106] Third, urea removal is higher at higher temperature, possibly as a result of faster diffusion and thereby faster mixing of urea and active chlorine[103] or due to the increased number of molecules with a kinetic energy higher than the activation energy of the reaction. Keller *et al.* report 22% lower urea removal at 25°C *vs* 37°C[92, 94] and others found complete urea removal only above 55°C.[103] Finally, the cell configuration (electrode pairs in parallel or in series) affects urea removal rates. Koster *et al.* reported higher removal rates for a parallel configuration of four EO units than for a series configuration with equal net flow, suggesting that a longer residence time within a single EO unit is more efficient than multiple short residences on the same electrodes.[92]

4.6 Current efficiency

For application of EO in a WAK, it is important to consider the current efficiency of urea oxidation, because it determines the size and weight of the battery. Current efficiency is defined as the ratio of the current used for urea removal to the total current through the cell. Simka *et al.*[105-106] observed that higher current densities resulted in lower current efficiencies, probably because at high current density supply of reagents cannot keep up with the current which is consequently wasted on side-reactions. On the other hand, higher urea concentrations led to more efficient use of the active chlorine due to a higher probability to react with urea resulting in an higher current efficiency. In principle, there is an optimum current density, where supply of reagent and current are in balance. Because supply of reagents to the electrode is an important factor determining the current efficiency, it can be increased by forced convection near the electrode surface, such as through stirring or increased flow rates.

5. Urea sorbents

A sorbent that can specifically and efficiently bind urea would be an attractive material for a WAK because, unlike with enzymatic- and electrochemical degradation, no potentially harmful side-products are generated. The need of the sorbent to be specific can be circumvented by placing AC upstream of the urea sorbent, as AC can remove most competing solutes such as amino acid and creatinine from dialysate. Recent developments have shown potential of sorbents for effective removal of urea from dialysate, among which AC, silica, zeolites, chitosan, synthetic molecular imprinted polymers (MIPs) and (multi)carbonyl-containing compounds, as discussed in the following sections. A schematic representation of a proposed sorbent-based urea purification unit is shown in figure 6.

Sorbents can remove urea from dialysate either by forming covalent or coordination bonds (chemisorption) or by non-covalent bonds (Van der Waals forces, dipole interactions and hydrogen bonds, *i.e.* physisorption). Since urea is uncharged under physiological conditions it is unable to form ionic bonds. In order to remove the daily urea production (240 to 470 mmol/day) during a 4- to 8-h dialysis session with a reasonable amount of sorbent (<500 g), both high binding capacity and fast sorption kinetics are required. However, urea sorption from dialysate is difficult because urea and water are both small, polar and weakly nucleophilic molecules.[21] Therefore, a sorbent with affinity for urea based on hydrogen bonds, dipole interactions or electrophilicity, most likely also has affinity for water which is present in the dialysate in a huge molar excess (55 M versus 60 mM for urea at most).

In general, chemisorption is an exothermic and thermally activated process in which non-reversible covalent or coordination bonds are formed with specific functional

groups or metal ions present in e.g. a polymeric matrix. However, the kinetics of urea binding to such matrices are relatively slow. In contrast to chemisorption, physisorption is very fast and reversible[117] Because urea is a very polar molecule, physisorption primarily occurs *via* hydrogen bonding and dipole interactions, resulting in mono- or multilayers on the sorbent's surface.[118] A disadvantage of non-covalent bonding is that sorbent-bound urea is in equilibrium with urea dissolved in the dialysate. The relation between the adsorbed amount and the concentration of urea in solution can be described by the so-called Langmuir isotherm. Since the urea concentration of the dialysate decreases during dialysis, the amount of urea bound per time unit (and thus removed from dialysate) decreases in time.

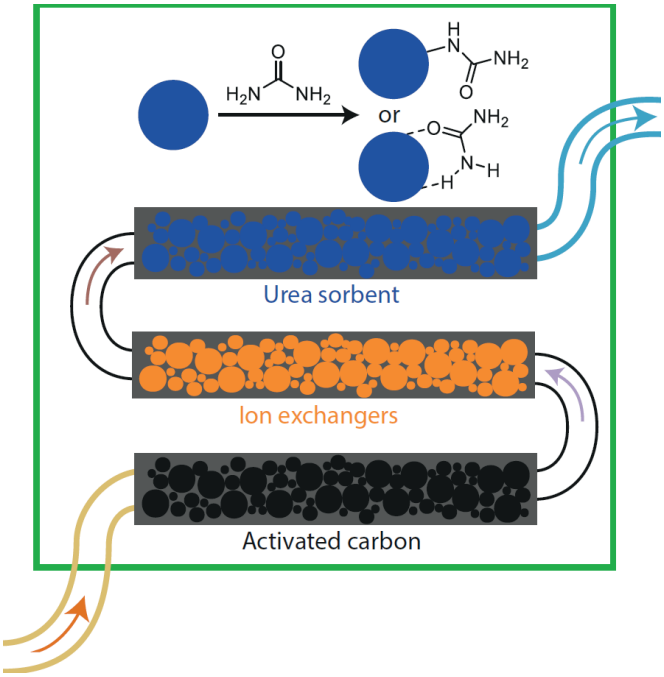

Figure 6. Schematic representation of a proposed urea sorbent-based WAK.

5.1 Activated carbon, silica, zeolites and MXenes

A frequently studied sorbent for urea is activated carbon (AC), a carbonized and chemically activated material with a surface area commonly in the range of 500-1500 m^2/g.[119] Its urea binding capacity has been evaluated under both static (sorbent suspended in an aqueous urea solution) and dynamic (urea solution pumped through a sorbent cartridge) conditions, as summarized in table 2. To compare binding capacities of different materials, we calculated the amount of urea adsorbed per gram of sorbent ($q_{adsorbed}$, mmol/g) at a dialysate urea concentration of 20 mM (table 2), a concentration representative for dialysis patients.[120] The amount of urea adsorbed per gram of sorbent was calculated based on the Langmuir

adsorption model (equation 1)[121] or linear correlation,[122-124] as appropriate. Studies were excluded if $q_{adsorbed}$ at 20 mM could not be estimated from the available data.[17, 118, 125-129] Of note, urea binding capacity of sorbents is presented per gram of dry material. However, when used for dialysis, the sorbents are hydrated and thus heavier.

$$q_{adsorbed} = q_{max} \frac{K_L[urea]}{1 + K_L[urea]} \quad \text{(Eq. 1)}$$

Equation 1. K_L = Langmuir constant , q_{max} = maximum binding capacity.

Table 2. Binding capacity of activated carbon (AC), silicas, zeolites and MXenes calculated at a urea concentration of 20 mM ($q_{adsorbed}$).

Material	S_{BET} Surface area (m^2/g)	Conditions	Maximum binding capacity q_{max} (mmol/g)	K_L (L/mmol)	$q_{adsorbed}$ at 20 mM urea in mmol/g and (μmol/m^2)	Ref.
Commercial AC (Sigma-Aldrich Co. St. Louis)	978.5	RT*	0.41	0.057	0.22[a] (0.22)	117
AC from palm empty fruit bunch	654	RT*	>14.6			127
Commercial AC (I-Chem Solution Sdn Bhd)	576	RT*	5.8	0.36[b]	5.1[a] (8.85)	130
Commercial AC (Norit A SUPRA EUR)	n.a.	RT*			0.19[c]	131
Commercial AC (Union Carbide Corporation)	n.a.	1 °C **			0.24[d]	123-124
Commercial AC (Calgon Carbon 207C)	n.a.	5 °C**			0.18[d]	122
Commercial AC (Calgon Carbon 207C)	n.a.	37 °C **			0.10[e]	122
Commercial AC (Chemviron type 400)	1050-1200	37 °C *			1.2[f] (1.00-1.14)	126
Graphene Oxide	74.8	RT*	0.45	0.040	0.20[a] (2.67)	117
Silica (SBA-15)	488	RT*	8.31	0.51[b]	7.6[a] (15.6)	130
Silica (Amine-functionalized SBA-15)	158	RT*	9.04	0.67[b]	8.4[a] (53.2)	130
Silicalite (SiO_2, NH_4F and tetrapropylammonium)	n.a.	37 °C *			1.0[f]	126
Zeolite ZSM-5 with SiO_2:Al_2O_3 = 23:400	361.3	RT*	0.70	0.019	0.19[a] (0.52)	117
Zeolite (Stilbite treated with NaCl)	n.a.	37 °C *			1.1-1.2[f]	126
$Ti_3C_2T_x$ MXenes nanosheets	-	37 °C *	0.27	0.040	0.12[a]	132

K_L = Langmuir constant. RT = room temperature. n.a. = not available. q_{max} = maximum binding capacity. $q_{adsorbed}$ = amount of urea adsorbed per gram of sorbent at a certain urea concentration. S_{BET} = surface area per gram

of sorbent in m^2/g . *Static conditions. ** Dynamic conditions. a) Calculated based on equation 7, b) $q_{adsorbed}$ for calculation of K_L was estimated based on figure 5 presented in,[130] c) initial dialysate urea concentration not reported, but it is assumed to be 20 mM, d) estimation based on the concentration dependent formula provided by the authors, e) estimation based on a comparison with $q_{absorbed}$ at 5°C, f) $q_{adsorbed}$ at 8 and 41 mM was reported in[126] and linearly interpolated to $q_{adsorbed}$ at 20 mM.

As shown in table 2, most types of AC have a urea binding capacity of approximately 0.2 mmol/g at equilibrium urea concentration of 20 mM.[117, 122, 131] Equilibrium is reached within 2 h.[117, 127, 130] Kim, Lehmann and Giordano showed that urea adsorption by AC increased during "cold dialysis", when the dialysate was cooled to 0-5 °C.[122-124, 128] Since adsorption of urea onto AC is exothermic, the desorption of urea from AC is endothermic. Therefore, at lower temperatures the adsorption-desorption equilibrium shifts towards adsorption and $q_{adsorbed}$ thus increased. Another strategy to increase the affinity of AC for urea is to increase the number of oxide functional groups which has been shown to increase the affinity for urea due to H-bonding with the NH_2 group of urea (~0.20 mmol/g versus ~0.07 mmol/g for the un-oxidized AC tested at an equilibrium urea concentration of 40 mM).[133] However, the urea binding capacity reported was still low (0.20 mmol/g).

Silicon dioxide (SiO_2), also known as silica, has been used as a sorbent for both organic and inorganic compounds. Some forms of silica such as mesoporous SBA-15 (Santa Barbara Amorphous-15) and MCM-41 (Mobil Composition Matter-41) have a high surface area (generally 400-900 m^2/g[134]) and small pores (±10 nm) which make them attractive materials for applications such as waste water treatment and drug delivery.[135-136] Cheah *et al*. reported a very high $q_{adsorbed}$ for SBA-15 and amine-functionalized SBA-15 (38 mM urea solution in distilled water) of 7.9 and 8.7 mmol/g, respectively.[130] However, the reported $q_{adsorbed}$ for commercial AC that they used as a reference (*i.e.* 5.4 mmol/g at 38 mM urea in distilled water) was much higher than found in other publications, which might be explained by the use of an unvalidated method for urea concentration determination. Although the authors found that functionalization of the mesoporous silica with amines reduced the surface area, q_{max} and $q_{adsorbed}$ increased, possibly because the introduced (protonated) amino groups allowed a better packing of urea molecules on the silica surface *via* hydrogen bonding and/or dipole interactions.

Zeolites are nano porous and crystalline materials mainly consisting of silicium and aluminium oxides. These aluminosilicate networks have an overall negative charge, which is counterbalanced by cations such as Na^+ and K^+ in the lattice. Zeolites are widely used as sorbents and ion exchangers.[137-139] Cheng *et al*. investigated Zeolite ZSM-5 for urea sorption and found that q_{max} (0.70 mmol/g) was higher than that of AC (0.41 mmol/g) and graphene oxide (0.45 mmol/g) while $q_{adsorbed}$ was comparable with that of AC and graphene oxide because of the relatively low K_L (0.019 L/mmol compared to 0.057 L/mmol for AC) for ZSM-5.[117] Wernert *et al.* tested uremic toxin binding of several zeolites (Linde type A, stilbite, silicalite, mordenite and faujasite) with different physical and chemical properties, among which pore sizes

and counter cations.[126] It was found that a smaller pore size did not increase the affinity for urea, but decreased the affinity for other (bigger) solutes instead. Stilbite ($X_n(Si_{27}Al_9)O_{72}\cdot 28(H_2O)$) with Na^+ counter ions ($X_n = Na_9$) showed higher affinity for urea than for other solutes than stilbite with K^+ or Ca^{2+} as counter ions although urea binding capacity of STI-Na (1.1-1.2 mmol/g) was comparable to the binding capacity of AC (1.2 mmol/g) reported in this study. Importantly, aluminium leaching from aluminium-containing zeolites is a potential hazard.[117] The aluminium-free silicalite would therefore be a safer option for application in a WAK, but its urea binding capacity was slightly lower than the binding capacity of AC (1.0 *vs* 1.1-1.2 mmol/g) reported in this study.[126] Overall, mesoporous silicas and zeolites seem to be attractive urea sorbents, although two studies also reported an unlikely high urea sorption capacity for AC (1.0-5.1 mmol/g at a urea concentration of 20 mM),[126, 130] putting the reported high values for these sorbents into question.

Recently, two-dimensional (single layer) transition metal carbides with O-, OH- and F- surface terminations (MXenes) have been reported as novel urea sorbents for dialysate regeneration.[132] MXenes are stacked nanosheets with a thickness of ~1 nm per layer and have a size of 1 – 4 µm. The general formula of these materials is $Ti_3C_2T_x$ in which T_x represents surface groups such as O-, OH- or F- that bind urea *via* hydrogen bonds and dipole interactions. Even though the binding capacity of the reported MXenes for urea is low at 37 °C ($q_{adsorbed}$ = 0.12 mmol/g) the authors state that the fact that these materials bind urea is very promising because MXenes represent a large family of materials with different compositions which can be further explored to identify the best urea sorbent.

5.2 Chitosan-based urea sorbents

Chitosan (CS, figure 7), a partially deacetylated polymer of chitin (deacetylation > 50%), is a linear polysaccharide composed of randomly distributed β-1,4-linked D-glucosamine and *N*-acetyl-D-glucosamine units.[140-142] The amino groups in CS accounts for its sorption capacity due to hydrogen bonds and dipole-interactions with various biomolecules including urea, proteins,[143] nucleic acids[144] and cholesterol.[145] CS and its derivatives have many pharmaceutical and biomedical applications, including use in drug delivery systems, tissue engineering, wound dressings and vaccine delivery.[146-147]

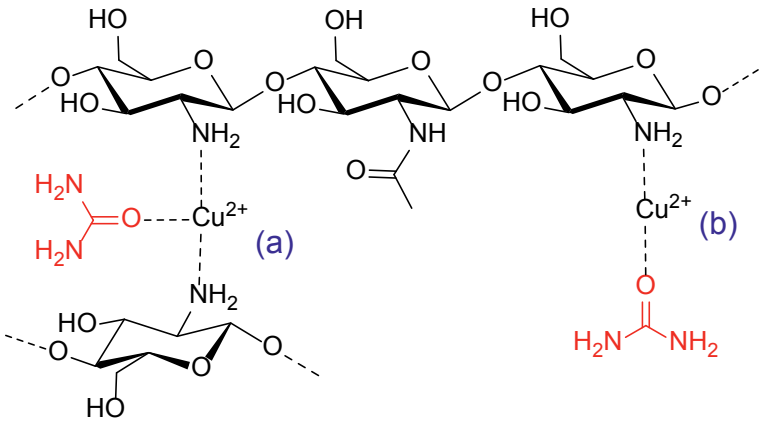

Figure 7: Coordination model for CS/Cu^{2+}/urea complex, (a) the "bridge model" and (b) the "pendant model".

Table 3. Chitosan (CS) based urea sorbents.

Material	[Urea] (mM) in simulated dialysate	Experimental conditions	Urea binding capacity (mmol/g)	Ref.
CS coated dialdehyde cellulose membrane	18.8	pH 7.5 buffer solution, 37 °C, 24 h	0.14	148
CS-silk fibroin/Cu^{2+} dense membrane	21.7	pH 7 buffer solution, RT, 8 h	0.3	149
CS/Cu^{2+} macroporous membrane	21.7	pH 7 buffer solution, RT, 12 h	1.3	150
CS/Cu^{2+} macroporous particles	21.7	pH 6 buffer solution, 37 °C, 8 h	2.0	151
CS/Cu^{2+} membrane and particles	20	Physiological fluid, 37 °C, 4 h	0.3 - 0.4	152
CS-magnetite nanocomposites	16.7	Blood serum, 4 h	0.5	153
Cross-linked CS/Cu^{2+} copolymer	30	pH 7, RT, 12 h	4.4	154-155
Cross-linked CS/ Zn^{2+}particle	34.2	Deionized water, RT, 12 h	0.8	156

Table 3 shows the urea binding capacity of CS based urea sorbents. Jing *et al.* utilized CS to stabilize oxycellulose based urea sorbents and developed a membrane consisting of a 90% oxycellulose core and a 10% CS coating with urea binding capacity of 0.14 mmol/g.[148] Even though CS is capable of binding urea *via* hydrogen bonds, the binding capacity is too low for application in a WAK. Therefore, several attempts have been made to improve its binding efficiency.[150-154, 157-158] The most frequently studied approach is complexation of CS with metal ions *via* coordinate bonds with the amino groups of CS. It has been shown that urea binds to the unoccupied *d*-orbital of metal ions, among which Cu^{2+} and Zn^{2+},[156] *via* its oxygen atom (Figure 7).[159-160] The coordinate bond is generally an order of magnitude stronger than the

hydrogen bond with water, and therefore urea preferentially binds to metal ions. Cu^{2+} has been studied most extensively for urea binding, because it has a relatively high affinity for CS compared with other metal ions (Cu^{2+} >> Hg^{2+} > Zn^{2+} > Cd^{2+} > Ni^{2+} >Co^{2+} ~ Ca^{2+}) and, importantly, fabrication of CS/metal ion complexes is a simple process which can be achieved by immersing CS into aqueous solution containing metal ions.[141] Key to obtain a high binding capacity of CS/Cu^{2+} complexes for urea is to increase the Cu^{2+} loading content of CS, which can be achieved by improving accessibility (by applying macroporosity or smaller particles) or by increasing availability of amino groups (by using a crosslinker, see next paragraph). Chen *et al*. prepared Cu^{2+} loaded CS-silk fibroin blend membranes and observed a urea binding capacity of 0.3 mmol/g at a urea concentration of 22 mM.[149] The fibroin blend membrane was rather dense, which limited the accessibility of amino groups for Cu^{2+} binding. When the accessibility of amino groups was improved by fabricating a macroporous CS membrane with pores of 25-35 µm, the amount of Cu^{2+} loaded in CS increased as compared to the fibroin blend membranes, which resulted in a substantial increase of urea binding capacity from 0.3 to 1.3 mmol/g.[150] In addition to CS/Cu^{2+} complex membranes, CS/Cu^{2+} sorbent particles have also been explored for urea binding.[151-153, 157] Zhou *et al*. synthesized CS/Cu^{2+} particles (size not reported) with a pore size of 200 nm and observed a urea binding capacity of 2.0 mmol/g at a urea concentration of 22 mM.[151, 157] Pathak *et al*. compared urea binding capacities of CS/Cu^{2+} membranes and particles, and found that the urea binding capacities of membranes was slightly lower than that of particles.[152] Furthermore, urea sorption increased with decreasing particle size (0.1, 0.2 and 0.4 mmol/g for particles with diameters of 710, 320 and 297 µm, respectively), which is likely due to the increased surface area and therefore the accessibility of the functional groups in the smaller particles. In another paper, Pathak *et al*. prepared CS-magnetite (CS-Fe_3O_4) nanocomposite particles with a size of 12 - 33 nm, by coprecipitation of Fe^{2+} and Fe^{3+} with NaOH in the presence of CS, followed by hydrothermal treatment of the aqueous dispersion from 30 °C to 80 °C for 2 hours. The urea binding capacity of the CS-Fe_3O_4 nanoparticles only slightly increased as compared to the larger CS/Cu^{2+} particles (size 297 µm) (0.5 mmol/g *vs* 0.4 mmol/g), probably because the advantage of the larger surface area of the nanoparticles hardly outweighed that of the stronger interaction between Cu^{2+} and urea (than that between Fe^{2+} and Fe^{3+} and urea).[153]

Although the aforementioned studies show that urea binding capacity of CS can be increased by complexation with metal ions, the ability of CS to form complexes with metal ions in water is limited, since most of the amino groups and hydroxyl groups of CS form hydrogen bonds with each other and water molecules, thereby decreasing the number of amino groups available for metal ion complex formation and thus for urea adsorption.[149, 161] Chen *et al.* showed that the capacity to form CS-metal ion complexes increased by partially cross-linking the amino groups of CS with glutaraldehyde.[162] Even though part of the amino groups is consumed by

the reaction with glutaraldehyde, the cross-linking process prevents remaining amino groups from forming hydrogen bonds with hydroxyl groups, resulting in an overall higher number of available amino groups for CS-metal ion complex formation.[154, 156] Wilson *et al.* hypothesized that, in addition to the unreacted amino groups of CS,[154] the aldehyde groups originating from glutaraldehyde can also complex Cu^{2+} ions, and they prepared CS/Cu^{2+} complexes by incubating Cu^{2+} ions with glutaraldehyde cross-linked CS. A high urea binding capacity of 4.4 mmol/g was found at a urea concentration of 1-30 mM, however the CS:urea ratio was not specified.[154] This material showed fast urea sorption kinetics at 10 mM urea concentration as equilibrium was reached within 20 minutes.[155] Of note, the molar ratio of amino groups of CS and aldehydes of glutaraldehyde was 1:2, which means that theoretically all amino groups can be converted into imines.

In conclusion, CS/Cu^{2+} complex sorbents demonstrate high urea binding capacities, especially when glutaraldehyde cross-linking is performed. However, for application in a WAK, potential copper leaching is a major concern. In addition, glutaraldehyde leaching is another safety concern since the imine formed in the reaction between the amino group of CS and glutaraldehyde can be hydrolyzed depending on the pH. Acute and/or chronic toxicity due to Cu^{2+} release may manifest as gastrointestinal symptoms, hemolytic anemia and/ or hepato-, neuro- and renal toxicity.[163] Although Zhou *et al.*[151] and Pathak and Bajpai[152] did not detect Cu^{2+} desorption from CS/Cu^{2+} complex sorbents, safety concerns are an issue for copper ion based urea sorbents.

5.3 Molecular imprinting-based urea sorbents

Molecular imprinting is a relatively novel technique to create a polymer matrix with binding sites complementary to the template molecule (e.g. urea) in terms of shape, size and location of binding units.[164-166] Scheme 3 shows a schematic preparation procedure of a Molecularly Imprinted Polymer (MIP) with specific recognition for the template molecule. Technically, MIP production is rather simple and easy to modulate. Neither complex organic synthesis nor molecule design are required. In general, MIPs show excellent chemical and thermal stability, regenerability, and solvent resistance compared with natural counterparts that also possess specific recognition abilities, such as antibodies.[167] Specific urea recognition is advantageous for a urea sorbent in a WAK to avoid competition by other nitrogenous solutes and prevent adsorption of other beneficial molecules such as amino acids. MIPs are widely used for various applications, such as chromatographic separation,[168] sensing,[169] drug delivery[170] and catalysis.[171]

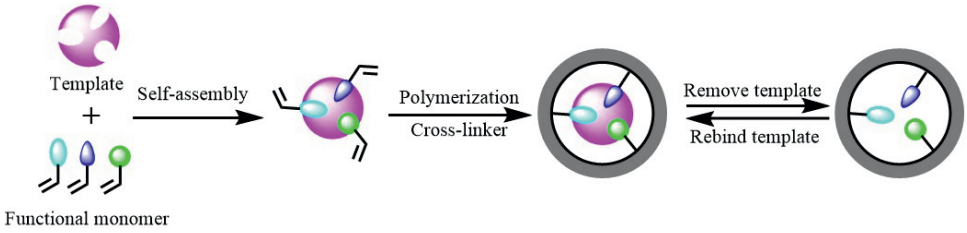

Scheme 3: The formation of template-specific gaps in the polymeric matrix of a molecularly imprinted polymer (MIP).

For the preparation of a MIP (figure 8), a reversible complex is first formed between the template and complementary functional monomers *via* covalent and/or non-covalent binding. Subsequently, the complex is co-polymerized with an excess amount of cross-linker, resulting in fixation of the complex in a solid polymer matrix. When the template is removed from the polymerized complex, the geometry and position of the remaining functional groups will be complementary to the template. The imprinting factor is a measure of the imprinting quality, and is defined as the ratio of the binding capacity of imprinted polymer to that of control (non-imprinted) polymer.

Several attempts have been made to synthesize a urea-imprinted MIP for urea detection or removal,[172-180] in which the template recognition is based on hydrogen bonding. Alizadeh *et al*. synthesized a urea-imprinted MIP using methacrylic acid as functional monomer and ethylene glycol di-methacrylate as cross-linker, all dissolved in acetonitrile. The authors reported a urea binding capacity of 6.3 mmol/g and an imprinting factor of 12.6 in aqueous solution at an unspecified urea concentration.[178] This is a remarkable but questionable finding because the theoretical maximum urea binding capacity of this MIP is only 0.28 mmol/g (assuming that each template molecule added to the mixture provides one imprinting site). Additionally, the carboxylic acid groups, which imprint the sorbent in acetonitrile during the synthesis, are likely protonated during the binding experiment in unbuffered water, but will be deprotonated in a buffered solution (such as dialysate), thereby changing the specific binding. The authors do not comment on both issues, which questions the credibility of this paper.

Macromolecules with suitable functional groups have also been employed to prepare MIPs for urea, even without the addition of a cross-linker.[172-177, 180] Huang *et al*.[180] and Lee *et al*.[176] evaporated DMSO in which poly(ethylene-co-vinyl alcohol) and urea were dissolved, followed by removal of urea by extraction with ethanol and water, which resulted in the formation of a urea-imprinted MIP membrane. Despite the absence of a cross-linker which normally maintains imprinting site integrity during processing, the MIP membrane demonstrated good imprinting quality with an imprinting factor of 2.3 and a urea binding capacity of 0.4 mmol/g at a urea

concentration of 16.7 mM. Also chitosan has been used for the design of a urea-imprinted MIP.[172, 174-175] For example, an electrochemical urea sensor was constructed based on MIP films which were prepared by potentiostatic electrodeposition of chitosan onto an Au disk electrode in the presence of urea, followed by removal of urea.[175] The sensor works in a urea concentration range of 10 nM - 40 µM but has a very limited urea binding capacity.

5.4 Carbonyl-type sorbents

Carbonyl-type sorbents lack the selectivity of MIPs and zeolites, but they possess high urea binding capacities and have the ability to form one or two irreversible covalent bonds between their electrophilic carbonyl groups and weakly nucleophilic urea molecules. The electron pair on the nitrogen atom can undergo a nucleophilic attack on the carbonyl group, resulting in a hemi-aminal or imine group (Scheme 4).[181-182]

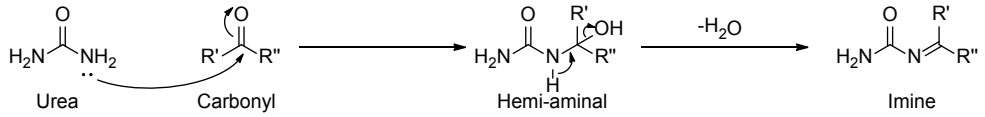

Scheme 4: General reaction mechanism of urea nitrogen with a carbonyl group.

Several urea sorbents that are composed of (crosslinked) polymers with urea-reactive carbonyl groups have been reported in literature such as aldehydes, glyoxaldehydes, ketoesters and ninhydrins (figure 8). Carbonyl-based urea sorbents and their binding capacity are shown in table 4.

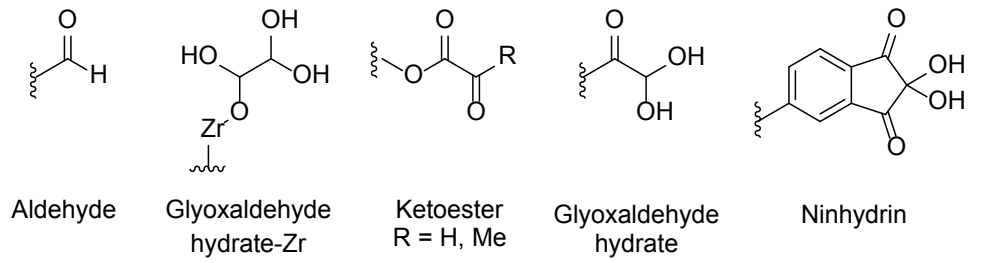

Figure 8: Structures of urea-reactive carbonyl groups.

Table 4. Covalent urea sorbents reported in literature.

Polymer matrix	Appearance	Urea-reactive group	Urea-reactive groups available (mmol/g)	Reported urea binding capacity (mmol/g)	Ref.
Oxystarch	Gel	Aldehyde	0.62-4.2	0.14-0.20[a]	[183]
Oxycellulose	Gel	Aldehyde	n.a.	0.13-0.22	[125]
Oxystarch	Particles	Aldehyde	n.a.	3.0	[184]
Oxidized crosslinked cyclodextran	Particles	Aldehyde	4.5	1.1	[185]
Glyoxylic ester-PVA	Gum	Ketoester	n.a.	0.01 – 4.2	[186]
Zr/glyoxal complex	Immobilized on AC or on Zirconium sorbent	Glyoxaldehyde (hydrate)	0.52-1.1	0.20-0.45	[187]
Modified PS	Linear polymer	Glyoxaldehyde (hydrate)	3.8-4.0	0.52	[188-189]
Modified PS-DVB copolymer	Macroporous beads	Glyoxaldehyde (hydrate)	3.1-3.6	1.5	[190]
Modified PS-DVB copolymer	Macroporous beads	Indanetrione (ninhydrin)	>2.7 [191]	1.1-2.0	[192]

[a]Over the first 24 h.

Oxidation of alcohol groups in biopolymers such as starch and cellulose using oxidizing agents such as hydrogen peroxide,[184] results in aldehyde-containing sorbents with a theoretical maximum aldehyde content and thus urea binding capacity of 4.2 mmol/g if all alcohol groups were oxidized and the aldehyde and urea react in a 1:1 ratio.[183] However, as shown in table 4, the observed binding capacities of these materials are relatively low: 0.14-0.22 mmol/g.[125, 183] This might be due to the fact that urea does not react with the aldehyde, as was observed in a study with ^{14}C-labeled urea[193] and in our own study on the kinetics of urea with a variety of carbonyl groups including aldehydes.[194] In this study, the authors propose that the urea-ammonium/cyanate equilibrium (scheme 2) shifts when ammonia is bound by the aldehydes in the sorbent and thus urea in fact decomposes.[193] In this case, two aldehyde groups are needed to remove one urea molecule. Moreover, the low urea binding capacities can also be attributed to the slow kinetics of the spontaneous formation of ammonium from urea (scheme 2). Besides, some oxycelluloses are reported to be unstable in dialysate, as small fragments of the sorbent were formed, which carries the risk of passage through the dialysis membrane into the bloodstream.[195] The low binding capacity and poor stability in dialysate, render these aldehyde-based materials unsuitable as sorbents in a WAK. Recently, Abidin *et al*. reported oxidized starch nanoparticles containing aldehyde groups with a urea binding capacity of 3.0 mmol/g.[184] The authors proposed that urea forms covalent bonds with the aldehyde groups, but according to the IR spectrum presented and carbonyl content determination assay, the number of

carbonyl groups on the oxystarch is too low (0.068 carbonyl groups per 100 glucose units) to remove urea based on covalent binding alone. Similarly, Bing-Lin *et al.* reported that oxidized epichlorohydrin-crosslinked cyclodextrin reported covalent bonds with urea.[185] They reported a urea binding capacity of 1.1 mmol/g from aqueous solution of pH 7 at 37 °C. However the materials were not characterized with any spectroscopic method. The reported urea removal kinetics of both the work of Abidin *et al*.[184] and Bing-Lin *et al*.[185] do not match the typical rate of covalent adsorption and Bing-Lin *et al.* reported that the urea binding capacity increased with an increasing urea concentration. Therefore, we conclude that urea is most likely bound by physisorption.[184] Finally, Eisen filed a patent in which modified polyvinylalcohol sorbents are claimed containing ketoester moieties with very high and fast urea binding (4.2 mmol/g in 1h) in a concentrated urea solution (420 mM) at room temperature. However urea binding is not reported at concentrations more relevant to dialysate purification.[186]

5.4.1 Carbonyl-hydrate sorbents

A sorbent with high reactivity towards urea should favorably be very electrophilic. However, highly electrophilic carbonyl groups tend to react with water as a competing nucleophile to form a hydrate. Usually, the carbonyl and its hydrate are in equilibrium in an aqueous environment. However, water has only one nucleophilic site (its oxygen atom), while urea has two (its nitrogen atoms). Therefore, if two or three carbonyl groups are adjacent, for example in indanetrione (**11**) that is in equilibrium with its hydrate ninhydrin (**10**), urea reacts first with the central carbonyl of the triketone (to form intermediate **12**), and then the second nitrogen will form a second intramolecular covalent bond with one of the adjacent carbonyl groups. This results in the formation of a favorable 5-membered ring (**13**), completing the reaction (scheme 5).[196] In short, the reaction between water and the carbonyl groups is an equilibrium, whereas the reaction between urea and the carbonyl groups is not and therefore urea will be effectively removed from dialysate.

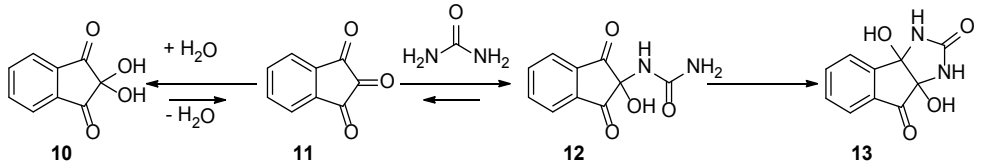

Scheme 5: The reaction of urea with vicinal ketones.

In a recent publication we reported rate constants (k_2) of urea with low molecular weight hydrated carbonyl compounds under physiological conditions. We found that phenyl glyoxaldehyde and ninhydrin are among the compounds that react fastest with urea (k_2 = 4.1 and 6.8 $M^{-1}h^{-1}$, respectively). Triformylmethane reacted even faster (factor ~23 faster than ninhydrin). Therefore a sorbent in which triformylmethane is incorporated may be very interesting for urea removal from

spent dialysate.[194]

A drawback of carbonyl-hydrate based sorbents is their relative complex synthesis. Nevertheless, several carbonyl-hydrate sorbents have been reported. Wong reported a zirconium-glyoxaldehyde complex with a urea binding capacity of 0.45 mmol/g.[187] Kuntz *et al*. reported a three-step modification of polystyrene to obtain ketoaldehyde hydrate groups.[188-189] Similarly, Poss *et al.* chemically modified polystyrene to form ketoaldehyde hydrate groups in only two reaction steps, and they reported higher urea binding than the material described by Kuntz (1.5 *vs* 0.52 mmol/g) (scheme 6).[190] Under physiological conditions, ketoaldehyde hydrates are in equilibrium with water and the dehydrated ketoaldehyde group that can form covalent bonds with urea.[190]

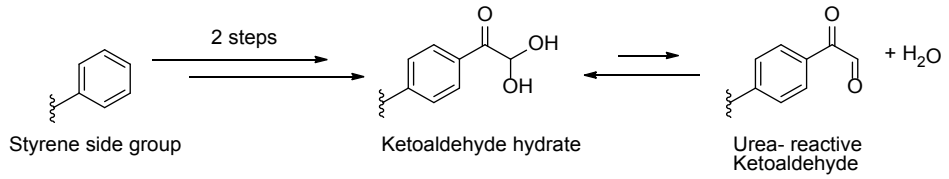

Scheme 6: Synthetic route towards ketoaldehyde-hydrate-type sorbent and its equilibrium with water.

Similarly, Smakman and Van Doorn modified polystyrene in five steps to form a resin with ninhydrin groups (scheme 7).[192] Analogous to the ketoaldehyde-type sorbent presented above, the urea reactive group, indanetrione, is in equilibrium with the ninhydrin group.[196] This ninhydrin-type sorbent showed a maximum binding capacity of 2.0 mmol/g. They also reported that this sorbent bound 1.2 mmol/g from simulated dialysate with a urea concentration of 25-33 mM at 37 °C in 8 h. Furthermore, the material could be sterilized by γ-radiation and did not leach any compounds into the dialysate.[191]

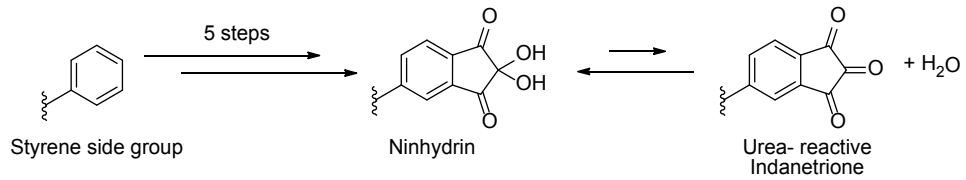

Scheme 7: Synthetic route towards ninhydrin-type sorbent and its equilibrium with water.

5.4.2. Kinetics of carbonyl-type urea sorbents

Carbonyl-type urea sorbents are characterized by relatively slow urea sorption.[183] For this reason, it usually takes several days before the maximum binding capacity is reached at 37°C. As the covalent binding of urea is a thermally activated process, the reaction rate increases at higher temperatures. Smakman and Van Doorn monitored urea sorption at several temperatures over time and found that at 37°C 0.75 mmol of urea per gram sorbent was bound after 4 h, after which the rate

of urea sorption decreased but sorption continued beyond 20 h. This implies that ~300-600 g of this material is needed to remove the daily production of urea (240-470 mmol) in a 4 hour dialysis session at 37 °C. Interestingly at 80°C, the maximum binding capacity (2.0 mmol/g) was almost reached after 4 h, but unfortunately this is not an option in a WAK.[191] In addition, carbonyl-based sorbents are not selective towards urea because they will react faster with more nucleophilic compounds present in the dialysate (such as creatinine and amino acids). These solutes can be prevented from entering the urea-sorbent column by placing AC upstream of the urea sorbent column.

6. Conclusions and perspectives

The greatest challenge in the development of a WAK is the development of an efficient urea removal technology. Enzymatic hydrolysis, electrochemical decomposition, physisorption and chemisorption have been explored, but all of these methods have disadvantages. A summary of the urea removal strategies and their advantages and disadvantages is given in table 5.

Table 5. Overview of urea removal strategies.

Method	Selectivity	Toxic by-product	Urea removal capacity	Urea removal rate	Remarks
Enzymatic hydrolysis	+++	Ammonium	+++	+++	Large amount of cation exchanger, strategy for limiting sodium release and specific storage conditions needed.
Electrochemical decomposition	--	Oxidation products	+	+	Biocompatibility issues, AC required to remove oxidation products.
Physisorption	-	None*	--	++	Competition with water.
Chemisorption	-	None*	+	--	Complex syntheses of sorbent

*Leaching of substances should be excluded. AC = activated carbon.

Urease for enzymatic hydrolysis of urea followed by ammonium adsorption by a cation-exchanger is currently the most efficient and effective method to remove urea from dialysate. A relatively small amount of enzyme immobilized on a substrate (30-50 grams) is required to convert the daily urea production into ammonium and bicarbonate. Even though bicarbonate formation is an advantage as it may correct for metabolic acidosis, a urease-based urea removal system is associated with some major disadvantages: (1) the need for a relatively large amount of zirconium phosphate to remove ammonium ions, (2) risk of early sorbent exhaustion resulting in release of toxic ammonium into the patient, (3) binding of other cations (i.e. calcium, magnesium and potassium) requiring replenishment of these cations from

a separate reservoir, and (4) sodium release which complicates fluid management. Overall, urea removal by enzymatic hydrolysis is effective and offers prospects for a portable artificial kidney, but all elements required to overcome the existing disadvantages of this method make it very difficult to reduce the size of the device to wearable proportions without the need for frequent change of disposables.

Urea removal by electro-oxidation seems promising, but significant challenges remain. First of all, the selectivity has to be ensured to minimize generation of harmful side-products and undesired oxidation of important dialysate components. Options for improving selectivity include optimization of the electrode material, functionalization of the electrode with catalytic groups or selective membranes and pulsed-potential techniques. Furthermore, a trade-off between efficacy and current efficiency (the fraction of the current used for urea removal) will have to be made. Increasing the electrode area and/or area to volume ratio will have positive effects on both the efficacy and the efficiency. Moreover, forced convection may further improve both. Increased current density to improve efficacy is not a good approach, as this increases formation of toxic side-products and reduces efficiency. Alternatively, a potential driven approach can be implemented, which should reduce side-products and increase efficiency. However, complete avoidance of side-products will be challenging due to the relatively high oxidation potential of urea and primary dependence on indirect oxidation. This will require strategies to reduce the supply of other readily oxidizable substances to the electrodes and to remove side-products downstream of the electrodes (e.g. by applying activated carbon up- and downstream of the electrodes, respectively).

An applicable urea sorbent with high specificity, high binding capacity and fast kinetics that does not release toxic side products, is not yet available. The affinity for urea of AC and zeolites is still too low to allow for application in a wearable device. Future studies might yield urea-specific zeolites or modified AC with high affinity and binding capacity. Urea sorption on silica shows high urea binding capacities, but needs to be validated to evaluate the true potential of this material for incorporation in a WAK.

(Glutaraldehyde-crosslinked) CS/Cu^{2+} complex sorbents show high urea binding capacity. However, potential copper leaching is a substantial concern for application in a WAK.

A urea-imprinted MIP seems appealing because of its potential specificity for urea. However, molecular imprinting technology for the synthesis of a urea sorbent is still at a very early stage. MIP-based urea sorbents have been developed for urea detection, but only a few studies focused on urea binding for dialysate regeneration. Furthermore, available urea-imprinted MIPs are based on hydrogen bond interaction, which poses the problem of competitive binding by water. Another possible drawback of MIP based urea sorbents is that a substantial amount

of “nonfunctional” cross-linker is required to maintain the MIP structure, which decreases the maximum binding capacity. Alternative imprinting strategies such as covalent or coordination imprinting are potentially suitable and need further exploration.

Carbonyl-hydrate urea sorbents seem promising for application in a WAK as (1) they are capable of removing urea from dialysate without releasing potentially harmful side-products and (2) a relatively small amount of sorbent (300-600 g of ninhydrin-type sorbents) would suffice to remove the daily urea production of 240-470 mmol. However, a limitation of carbonyl-type sorbents is the slow adsorption kinetics under physiological conditions. Urea sorption is fastest within the first hours but insufficient (max. 0.75 mmol/g in 4 h), which would significantly increase the amount of sorbent beyond the acceptable limit for a wearable device. Further research should focus on a covalent urea sorbent with a higher binding capacity and faster kinetics. Another issue of the carbonyl-hydrate sorbent is the low specificity for urea. Urea is a very weak nucleophile, so stronger nucleophiles such as amino acids and creatinine would most likely also react with these sorbents, thereby reducing the number of potential binding sites for urea. This might be circumvented by placing AC upstream of the sorbent to remove these components before they pass the urea sorbent.

In conclusion, none of the available urea removal methods are ideal to make a WAK feasible at present. However, several technological developments in the different urea removal strategies may enable realization of a light-weight WAK in the future.

7. Acknowledgement

The Dutch Kidney Foundation (grant NT 12.05) and the European Commission (WEAKID, Horizon 2020 research and innovation program, grant agreement no. 733169) supported the work of M.K. van Gelder and K.G.F. Gerritsen. J.A.W. Jong and Y. Guo are supported by the Dutch organization for Scientific Research (NWO-TTW, project 14433) and the Dutch Kidney Foundation. All authors acknowledge the financial support of the strategic alliance of the University of Twente, University of Utrecht and University Medical Center Utrecht. J.A.W. Jong, Y. Guo, W.E. Hennink, C.F. van Nostrum and K.G.F. Gerritsen are currently working on new covalent urea sorbents and have recently filed a patent on this topic (WO2019110557). M.K. van Gelder, K.G.F. Gerritsen and C. Blüchel are involved in the development of urease-based portable artificial kidney devices supported by NeoKidney – an initiative of the Dutch Kidney Foundation. M.K. van Gelder, L. Folkertsma, M. Odijk and K.G.F. Gerritsen are working on an electro-oxidation based urea removal system.

8. Data availability

The data reported in this review can be retrieved from the original papers as cited in the text.

9. References

1. Broers, N. J. H.; Martens, R. J. H.; Canaud, B.; Cornelis, T.; Dejagere, T.; Diederen, N. M. P.; Hermans, M. M. H.; Konings, C.; Stifft, F.; Wirtz, J.; Leunissen, K. M. L.; van der Sande, F. M.; Kooman, J. P., Health-related quality of life in end-stage renal disease patients: the effects of starting dialysis in the first year after the transition period. *Int. Urol. Nephrol.* **2018,** *50* (6), 1131-1142.
2. Fresenius Medical Care (FMC). Annual Report 2018. [ONLINE] Retrieved from: https://www.freseniusmedicalcare.com/fileadmin/data/com/pdf/Media_Center/Publications/Annual_Reports/FME_Annual-Report_2018.pdf. [Accessed 11 July 2019].
3. Vanholder, R.; Pletinck, A.; Schepers, E.; Glorieux, G., Biochemical and clinical impact of organic uremic retention solutes: a comprehensive update. *Toxins* **2018,** *10* (1).
4. Susel, J.; Batycka-Baran, A.; Reich, A.; Szepietowski, J. C., Uraemic pruritus markedly affects the quality of life and depressive symptoms in haemodialysis patients with end-stage renal disease. *Acta Derm. Venereol.* **2014,** *94* (3), 276-81.
5. Zoccali, C.; Moissl, U.; Chazot, C.; Mallamaci, F.; Tripepi, G.; Arkossy, O.; Wabel, P.; Stuard, S., Chronic fluid overload and mortality in ESRD. *J. Am. Soc. Nephrol.* **2017,** *28* (8), 2491-2497.
6. Kalantar-Zadeh, K.; Tortorici, A. R.; Chen, J. L.; Kamgar, M.; Lau, W. L.; Moradi, H.; Rhee, C. M.; Streja, E.; Kovesdy, C. P., Dietary restrictions in dialysis patients: is there anything left to eat? *Semin. Dial.* **2015,** *28* (2), 159-68.
7. Silva, L. F.; Lopes, G. B.; Cunha, T. O.; Protasio, B. M.; Pisoni, R. L.; James, S. A.; Lopes, A. A., Coping with fluid restriction and the quality of life in hemodialysis patients with very low or no daily urine output. *Int. J. Artif. Organs* **2014,** *37* (6), 427-35.
8. Evenepoel, P.; Meijers, B. K.; Bammens, B.; Viaene, L.; Claes, K.; Sprangers, B.; Naesens, M.; Hoekstra, T.; Schlieper, G.; Vanderschueren, D.; Kuypers, D., Phosphorus metabolism in peritoneal dialysis- and haemodialysis-treated patients. *Nephrol. Dial. Transplant* **2016,** *31* (9), 1508-14.
9. Mujais, S.; Story, K., Peritoneal dialysis in the US: evaluation of outcomes in contemporary cohorts. *Kidney Int. Suppl.* **2006,** (103), S21-6.
10. Kotsokalis, C., FP7-248261 Periodic Report Nephron+. *Unpublished* **2011**.
11. International Society of Peritoneal Dialysis (ISPD). Questions about PD. (2013). [ONLINE]. Retrieved from: https://ispd.org/question/what-is-the-rule-of-thumb-when-advising-a-patient-about-lifting-restrictions/. [Accessed 19 June 2019].
12. Rocco, M. V.; Lockridge, R. S., Jr.; Beck, G. J.; Eggers, P. W.; Gassman, J. J.; Greene, T.; Larive, B.; Chan, C. T.; Chertow, G. M.; Copland, M.; Hoy, C. D.; Lindsay, R. M.; Levin, N. W.; Ornt, D. B.; Pierratos, A.; Pipkin, M. F.; Rajagopalan, S.; Stokes, J. B.; Unruh, M. L.; Star, R. A.; Kliger, A. S.; Frequent Hemodialysis Network Trial, G.; Kliger, A.; Eggers, P.; Briggs, J.; Hostetter, T.; Narva, A.; Star, R.; Augustine, B.; Mohr, P.; Beck, G.; Fu, Z.; Gassman, J.; Greene, T.; Daugirdas, J.; Hunsicker, L.; Larive, B.; Li, M.; Mackrell, J.; Wiggins, K.; Sherer, S.; Weiss, B.; Rajagopalan, S.; Sanz, J.; Dellagrottaglie, S.; Kariisa, M.; Tran, T.; West, J.; Unruh, M.; Keene, R.; Schlarb, J.; Chan, C.; McGrath-Chong, M.; Frome, R.; Higgins, H.; Ke, S.; Mandaci, O.; Owens, C.; Snell, C.; Eknoyan, G.; Appel, L.; Cheung, A.; Derse, A.; Kramer, C.; Geller, N.; Grimm, R.; Henderson, L.; Prichard, S.; Roecker, E.; Rocco, M.; Miller, B.; Riley, J.; Schuessler, R.; Lockridge, R.;

Pipkin, M.; Peterson, C.; Hoy, C.; Fensterer, A.; Steigerwald, D.; Stokes, J.; Somers, D.; Hilkin, A.; Lilli, K.; Wallace, W.; Franzwa, B.; Waterman, E.; Chan, C.; McGrath-Chong, M.; Copland, M.; Levin, A.; Sioson, L.; Cabezon, E.; Kwan, S.; Roger, D.; Lindsay, R.; Suri, R.; Champagne, J.; Bullas, R.; Garg, A.; Mazzorato, A.; Spanner, E.; Rocco, M.; Burkart, J.; Moossavi, S.; Mauck, V.; Kaufman, T.; Pierratos, A.; Chan, W.; Regozo, K.; Kwok, S., The effects of frequent nocturnal home hemodialysis: the frequent hemodialysis network nocturnal trial. *Kidney Int.* **2011,** *80* (10), 1080-91.

13. Chertow, G. M.; Levin, N. W.; Beck, G. J.; Depner, T. A.; Eggers, P. W.; Gassman, J. J.; Gorodetskaya, I.; Greene, T.; James, S.; Larive, B.; Lindsay, R. M.; Mehta, R. L.; Miller, B.; Ornt, D. B.; Rajagopalan, S.; Rastogi, A.; Rocco, M. V.; Schiller, B.; Sergeyeva, O.; Schulman, G.; Ting, G. O.; Unruh, M. L.; Star, R. A.; Kliger, A. S., In-center hemodialysis six times per week versus three times per week. *N. Engl. J. Med.* **2010,** *363* (24), 2287-300.
14. Culleton, B. F.; Walsh, M.; Klarenbach, S. W.; Mortis, G.; Scott-Douglas, N.; Quinn, R. R.; Tonelli, M.; Donnelly, S.; Friedrich, M. G.; Kumar, A.; Mahallati, H.; Hemmelgarn, B. R.; Manns, B. J., Effect of frequent nocturnal hemodialysis vs conventional hemodialysis on left ventricular mass and quality of life: a randomized controlled trial. *Jama* **2007,** *298* (11), 1291-9.
15. Agar, J. W., Review: understanding sorbent dialysis systems. *Nephrology (Carlton)* **2010,** *15* (4), 406-11.
16. Ash, S. R., Sorbents in treatment of uremia: a short history and a great future. *Semin. Dial.* **2009,** *22* (6), 615-22.
17. Yatzidis, H., A convenient haemoperfusion micro-apparatus for treatment of endegeneous and exogenous intoxicatons; its use as an effective artificial kidney. *Proc. Eur. Dial. Transplant. Assoc. 1* **1964**, 83-87.
18. Bock, J. C., A study of a decolorizing carbon. *J. Am. Chem. Soc.* **1920,** *42*, 1564-1569.
19. Weiner, I. D.; Mitch, W. E.; Sands, J. M., Urea and ammonia metabolism and the control of renal nitrogen excretion. *Clin. J. Am. Soc. Nephrol.* **2015,** *10* (8), 1444-58.
20. Shinaberger, C. S.; Kilpatrick, R. D.; Regidor, D. L.; McAllister, C. J.; Greenland, S.; Kopple, J. D.; Kalantar-Zadeh, K., Longitudinal associations between dietary protein intake and survival in hemodialysis patients. *Am. J. Kidney. Dis.* **2006,** *48* (1), 37-49.
21. Lehmann, H. D.; Marten, R.; Gullberg, C. A., How to catch urea? Considerations on urea removal from hemofiltrate. *Artif. Organs* **1981,** *5* (3), 278-85.
22. Deignan, J. L.; Cederbaum, S. D.; Grody, W. W., Contrasting features of urea cycle disorders in human patients and knockout mouse models. *Mol. Genet. Metab.* **2008,** *93* (1), 7-14.
23. Francis, P. S.; Lewis, S. W.; Lim, K. F., Analytical methodology for the determination of urea: current practice and future trends. *Trac-Trend Anal Chem* **2002,** *21* (5), 389-400.
24. Vaughan, P.; Donohue, J., The structure of urea - interatomic distances and resonance in urea and related compounds. *Acta Crystallogr* **1952,** *5* (4), 530-535.
25. Dirnhuber, P.; Schutz, F., The isomeric transformation of urea into ammonium cyanate in aqueous solutions. *Biochem. J.* **1948,** *42* (4), 628-32.
26. Singh, L. R.; Dar, T. A.; Ahmad, F., Living with urea stress. *J. Biosci.* **2009,** *34* (2), 321-31.
27. Vanholder, R.; Gryp, T.; Glorieux, G., Urea and chronic kidney disease: the comeback of the century? (in uraemia research). *Nephrol. Dial. Transplant.* **2018,** *33* (1), 4-12.

28. Sun, S.; Zhou, J. Y.; Yang, W.; Zhang, H., Inhibition of protein carbamylation in urea solution using ammonium-containing buffers. *Anal. Biochem.* **2014,** *446*, 76-81.
29. Krajewska, B., Ureases I. Functional, catalytic and kinetic properties: A review. *J Mol Catal B-Enzym* **2009,** *59* (1-3), 9-21.
30. Krajewska, B., Ureases. II. Properties and their customizing by enzyme immobilizations: A review. *J Mol Catal B-Enzym* **2009,** *59* (1-3), 22-40.
31. Follmer, C.; Pereira, F. V.; Da Silveira, N. P.; Carlini, C. R., Jack bean urease (EC 3.5.1.5) aggregation monitored by dynamic and static light scattering. *Biophys. Chem.* **2004,** *111* (1), 79-87.
32. Shaw, W. H. R.; Walker, D. G., Kinetic studies of thiourea derivatives. IV. The methylated thioureas. Conclusions. *J. Am. Chem. Soc.* **1958,** *80* (20), 5337-5342.
33. Shaw, W. H. R.; Bordeaux, J. J., The decomposition of urea in aqueous media. *J. Am. Chem. Soc.* **1955,** *77* (18), 4729-4733.
34. Callahan, B. P.; Yuan, Y.; Wolfenden, R., The burden borne by urease. *J. Am. Chem. Soc.* **2005,** *127* (31), 10828-9.
35. Yao, M.; Chen, X.; Zhan, C. G., Reaction pathway and free energy barrier for urea elimination in aqueous solution. *Chem. Phys. Lett.* **2015,** *625*, 143-146.
36. Yao, M.; Tu, W.; Chen, X.; Zhan, C. G., Reaction pathways and free energy profiles for spontaneous hydrolysis of urea and tetramethylurea: unexpected substituent effects. *Org. Biomol. Chem.* **2013,** *11* (43), 7595-605.
37. Roberts, M., The regenerative dialysis (REDY) sorbent system. *Nephrology* **1998,** *4* (4), 275-278.
38. M. Gordon; M. Popovtzer; M. Greenbaum; M. McArthur; J. R. De Palma; Maxwell, H., Zirconium phosphate-A potentially useful adsorbent in the treatment of chronic uremia. *Proc. Eur. Dialysis Transplant Assoc.* **1968,** *5*, 86.
39. Chen, J. P.; Chiu, S. H., Preparation and characterization of urease immobilized onto porous c hitosan beads for urea hydrolysis. *Bioprocess Eng* **1999,** *21* (4), 323-330.
40. Chen, J.; Chiu, S., A poly(N-isopropylacrylamide-co-N-acryloxysuccinimide-co-2-hydroxyethyl methacrylate) composite hydrogel membrane for urease immobilization to enhance urea hydrolysis rate by temperature swing. *Enzyme Microb. Technol.* **2000,** *26* (5-6), 359-367.
41. Lin, C. C.; Yang, M. C., Urea permeation and hydrolysis through hollow fiber dialyzer immobilized with urease: storage and operation properties. *Biomaterials* **2003,** *24* (11), 1989-1994.
42. Yang, M. C.; Lin, C. C., Urea permeation and hydrolysis through hollow fiber dialyzer immobilized with urease. *Biomaterials* **2001,** *22* (9), 891-896.
43. Kara, F.; Demirel, G.; Tumturk, H., Immobilization of urease by using chitosan-alginate and poly(acrylamide-co-acrylic acid)/kappa-carrageenan supports. *Bioprocess Biosyst. Eng.* **2006,** *29* (3), 207-11.
44. Rejikumar, S.; Devi, S., Preparation and characterization of urease bound on crosslinked poly(vinyl alcohol). *J Mol Catal B-Enzym* **1998,** *4* (1-2), 61-66.
45. Srivastava, P. K.; Kayastha, A. M.; Srinivasan, R., Characterization of gelatin-immobilized pigeonpea urease and preparation of a new urea biosensor. *Biotechnol. Appl. Biochem.* **2001,** *34* (Pt 1), 55-62.
46. Bortone, N.; Fidaleo, M.; Moresi, M., Immobilization/stabilization of acid urease on Eupergit(R) supports. *Biotechnol. Prog.* **2012,** *28* (5), 1232-44.
47. Monier, M.; El-Sokkary, A. M., Modification and characterization of cellulosic cotton

fibers for efficient immobilization of urease. *Int. J. Biol. Macromol.* **2012,** *51* (1-2), 18-24.
48. Wang, L.; Wang, S.; Deng, X. Y.; Zhang, Y. C.; Xiong, C. R., Development of coconut shell activated carbon-tethered urease for degradation of urea in a packed bed. *Acs Sustain Chem Eng* **2014,** *2* (3), 433-439.
49. Kibarer, G. D.; Akovali, G., Optimization studies on the features of an activated charcoal-supported urease system. *Biomaterials* **1996,** *17* (15), 1473-9.
50. Blumenkrantz, M. J.; Gordon, A.; Roberts, M.; Lewin, A. J.; Pecker, E. A.; Moran, J. K.; Coburn, J. W.; Maxwell, M. H., Applications of the Redy sorbent system to hemodialysis and peritoneal dialysis. *Artif. Organs* **1979,** *3* (3), 230-6.
51. Association for the Advancement of Medical Instrumentation (AAMI). Sorbent-Based Regenerative Hemodialysis Systems. AAMI TIR77:**2018**.
52. L.H. Lameire, C. Ronco (eds.). Dialysis, Dialyzers and Sorbents. Where are we going? *Basel: Karger Medical and Scientific Publishers*; **2001**. p. 140-53.
53. Mion, C.; Branger, B.; Issautier, R.; Ellis, H. A.; Rodier, M.; Shaldon, S., Dialysis fracturing osteomalacia without hyperparathyroidism in patients treated with HCO3 rinsed Redy cartridge. *Trans. Am. Soc. Artif. Intern. Organs* **1981,** *27*, 634-8.
54. Pierides, A. M.; Frohnert, P. P., Aluminum related dialysis osteomalacia and dementia after prolonged use of the Redy cartridge. *Trans. Am. Soc. Artif. Intern. Organs* **1981,** *27*, 629-33.
55. Pierides, A. M.; Myli, M. P., Iron and aluminum osteomalacia in hemodialysis patients. *The New England journal of medicine* **1984,** *310* (5), 323.
56. Drury, P. J.; Harston, G. A.; Ineson, P. R.; Smith, S.; Stoves, J. L.; Bray, C. S.; Black, M. M., Aluminium release from the Sorbsystem D-3160 and D-3260 cartridges. *Life Support Syst.* **1986,** *4* (3), 211-9.
57. McGill, R. L.; Bakos, J. R.; Ko, T.; Sandroni, S. E.; Marcus, R. J., Sorbent hemodialysis: clinical experience with new sorbent cartridges and hemodialyzers. *Am. Soc. Artif. Intern. Organs J.* **2008,** *54* (6), 618-21.
58. Shapiro, W. B., The current status of sorbent hemodialysis. *Semin. Dial.* **1991,** *4* (1), 40-45.
59. W. Drukker; F.M. Parsons; Gordon, A., *Practical application of dialysate regeneration: The Redy system*. Springer: **1979**.
60. Sherman, J. D.; Bem, D. S.; Lewis, G. J. Process for removing toxins from bodily fluids using zirconium or titanium microporous compositions. US6332985B1, **2001**.
61. De Vriese, A. S.; Langlois, M.; Bernard, D.; Geerolf, I.; Stevens, L.; Boelaert, J. R.; Schurgers, M.; Matthys, E., Effect of dialyser membrane pore size on plasma homocysteine levels in haemodialysis patients. *Nephrol. Dial. Transplant* **2003,** *18* (12), 2596-600.
62. Ikizler, T. A.; Greene, J. H.; Yenicesu, M.; Schulman, G.; Wingard, R. L.; Hakim, R. M., Nitrogen balance in hospitalized chronic hemodialysis patients. *Kidney Int. Suppl.* **1996,** *57*, S53-6.
63. Dasarathy, S.; Mookerjee, R. P.; Rackayova, V.; Rangroo Thrane, V.; Vairappan, B.; Ott, P.; Rose, C. F., Ammonia toxicity: from head to toe? *Metab. Brain Dis.* **2017,** *32* (2), 529-538.
64. Gura, V.; Rivara, M. B.; Bieber, S.; Munshi, R.; Smith, N. C.; Linke, L.; Kundzins, J.; Beizai, M.; Ezon, C.; Kessler, L.; Himmelfarb, J., A wearable artificial kidney for patients with end-stage renal disease. *JCI Insight* **2016,** *1* (8), 15.

65. Davenport, A., Dialysis: A wearable dialysis device: the first step to continuous therapy. *Nat. Rev. Nephrol.* **2016,** *12* (9), 512-4.
66. Munoz Mendoza, J.; Arramreddy, R.; Schiller, B., Dialysate sodium: Choosing the optimal hemodialysis bath. *Am. J. Kidney Dis.* **2015,** *66* (4), 710-20.
67. Pierides, A. M.; Edwards, W. G., Jr.; Cullum, U. X., Jr.; McCall, J. T.; Ellis, H. A., Hemodialysis encephalopathy with osteomalacic fractures and muscle weakness. *Kidney Int.* **1980,** *18* (1), 115-24.
68. Ward, M. K.; Pierides, A. M.; Fawcett, P.; Shaw, D. A.; Perry, R. H.; Tomlinson, B. E.; Kerr, D. N. S., Dialysis encephalopathy syndrome. *Proc. Eur. Dial. Transplant Assoc.* **1976,** *13*, 348.
69. Llach, F.; Gardner, P. W.; George, C. R.; Cairoli, O., Aluminum kinetics using bicarbonate dialysate with the sorbent system. *Kidney international* **1993,** *43* (4), 899-902.
70. Association for the Advancement of Medical Instrumentation (AAMI). Hemodialysis systems, ANSI/AAMI RD 5:**1981**.
71. van Gelder, M. K.; Mihaila, S. M.; Jansen, J.; Wester, M.; Verhaar, M. C.; Joles, J. A.; Stamatialis, D.; Masereeuw, R.; Gerritsen, K. G. F., From portable dialysis to a bioengineered kidney. *Expert Rev. Med. Devices* **2018,** *15* (5), 323-336.
72. Davenport, A.; Gura, V.; Ronco, C.; Beizai, M.; Ezon, C.; Rambod, E., A wearable haemodialysis device for patients with end-stage renal failure: a pilot study. *Lancet* **2007,** *370* (9604), 2005-10.
73. Lornoy, W.; Becaus, I.; Billiouw, J. M.; Sierens, L.; Van Malderen, P.; D'Haenens, P., On-line haemodiafiltration. Remarkable removal of beta2-microglobulin. Long-term clinical observations. *Nephrol. Dial. Transplant* **2000,** *15 Suppl 1*, 49-54.
74. Automated Wearable Artificial Kidney (AWAK). [ONLINE]. Retrieved from: http://awak.com/product/. [Accessed 30 December 2018].
75. H., H., Evaluation of safety of automated wearable artificial kidney (AWAK) device in PD patients. ISN WCN Melbourne, Australia, **2019**.
76. Lo, W. K.; Bargman, J. M.; Burkart, J.; Krediet, R. T.; Pollock, C.; Kawanishi, H.; Blake, P. G., Guideline on targets for solute and fluid removal in adult patients on chronic peritoneal dialysis. *Perit. Dial. Int.* **2006,** *26* (5), 520-2.
77. EasyDial. [ONLINE]. Retrieved from: http://easydialhdbs.com/. [Accessed 11 July 2019].
78. McNamara, T.; Khawar, O.; Foster, S., In-vitro dialysis clearances uing darma, the EasyDial portable hemodialysis machine [abstract]. *ASN* **2017,** *FR-PO825*.
79. National Institute of Diabetes and Kidney Diseases (NIH). Hemodialysis Dose & Adequacy. [ONLINE]. Retrieved from: https://www.niddk.nih.gov/health-information/kidney-disease/kidney-failure/hemodialysis/dose-adequacy. [Accessed 11 July 2019].
80. Diality. [ONLINE]. Retrieved from: https://www.diality.com/. [Accessed 11 July 2019].
81. Khawar, O.; McNamara, T.; Foster, S., In-vitro dialysate regeneration using dharma, the EasyDial portable hemodialysis machine [abstract]. *ASN* **2017,** *SA-PO758*.
82. Tuwiner, S. B. *Research, design, and development of an improved water reclamation system for manned space vehicles*; RAI Research Corp. Report 364 for NASA Contract NASA-4373, **1966**.
83. Wester, M.; Simonis, F.; Lachkar, N.; Wodzig, W. K.; Meuwissen, F. J.; Kooman, J.

P.; Boer, W. H.; Joles, J. A.; Gerritsen, K. G., Removal of urea in a wearable dialysis device: a reappraisal of electro-oxidation. *Artif. Organs* **2014,** *38* (12), 998-1006.
84. Wright, J. C.; Michaels, A. S.; Appleby, A. J., Electrooxidation of urea at the ruthenium titanium-oxide electrode. *Aiche J.* **1986,** *32* (9), 1450-1458.
85. Ikematsu, M.; Kaneda, K.; Iseki, M.; Matsuura, H.; Yasuda, M., Electrolytic treatment of human urine to remove nitrogen and phosphorus. *Chem Lett* **2006,** *35* (6), 576-577.
86. Till, B. A.; Weathers, L. J.; Alvarez, P. J. J., Fe(0)-supported autotrophic denitrification. *Environ Sci Technol* **1998,** *32* (5), 634-639.
87. Tipple, M. A.; Shusterman, N.; Bland, L. A.; McCarthy, M. A.; Favero, M. S.; Arduino, M. J.; Reid, M. H.; Jarvis, W. R., Illness in hemodialysis patients after exposure to chloramine contaminated dialysate. *ASAIO transactions* **1991,** *37* (4), 588-91.
88. Peck, B.; Workeneh, B.; Kadikoy, H.; Patel, S. J.; Abdellatif, A., Spectrum of sodium hypochlorite toxicity in man-also a concern for nephrologists. *NDT plus* **2011,** *4* (4), 231-5.
89. Patzer, J. F.; Wolfson, S. K.; Yao, S. J., Reactor control and reaction-kinetics for electrochemical urea oxidation. *Chem Eng Sci* **1990,** *45* (8), 2777-2784.
90. Yao, S. J.; Wolfson, S. K.; Krupper, M. A.; Wu, K. J., Controlled-potential controlled-current electrolysis: In vitro and in vivo electrolysis of urea. *Bioelectrochem. Bioenerg.* **1984,** *13* (1-3), 15-24.
91. Schuenemann, B.; Quellhorst, E.; Kaiser, H.; Richter, G.; Mundt, K.; Weidlich, E.; Loeffler, G.; Zachariae, M.; Schunk, O., Regeneration of filtrate and dialysis fluid by electro-oxidation and absorption. *Trans. Am. Soc. Artif. Inter. Organs* **1982,** *28* (1), 49-53.
92. Keller, R. W.; Yao, S. J.; Brown, J. M.; Wolfson, S. K.; Zeller, M. V., Electrochemical removal of urea from physiological buffer as the basis for a regenerative dialysis system. *Bioelectrochem. Bioenerg.* **1980,** *7* (3), 469-485.
93. Yao, S. J.; Wolfson, S. K.; Tokarsky, J. M.; Ahn, B. K., De-ureation by electrochemical oxidation. *Bioelectrochem. Bioenerg.* **1974,** *1* (1-2), 180-186.
94. Fels, M., Recycle of dialysate from the artificial kidney by electrochemical degradation of waste metabolites: continuous reactor investigations. *Med. Biol. Eng. Comput.* **1982,** *20* (3), 257-63.
95. Wester, M.; van Gelder, M. K.; Joles, J. A.; Simonis, F.; Hazenbrink, D. H. M.; van Berkel, T. W. M.; Vaessen, K. R. D.; Boer, W. H.; Verhaar, M. C.; Gerritsen, K. G. F., Removal of urea by electro-oxidation in a miniature dialysis device: a study in awake goats. *Am. J. Physiol. Renal. Physiol.* **2018,** *315* (5), F1385-F1397.
96. Tuncer, M.; Sarikaya, M.; Sezer, T.; Ozcan, S.; Suleymanlar, G.; Yakupoglu, G.; Ersoy, F. F., Chemical peritonitis associated with high dialysate acetaldehyde concentrations. *Nephrol. Dial. Transplant* **2000,** *15* (12), 2037-40.
97. Schwenger, V.; Morath, C.; Salava, A.; Amann, K.; Seregin, Y.; Deppisch, R.; Ritz, E.; Bierhaus, A.; Nawroth, P. P.; Zeier, M., Damage to the peritoneal membrane by glucose degradation products is mediated by the receptor for advanced glycation end-products. *J. Am. Soc. Nephrol.* **2006,** *17* (1), 199-207.
98. Inc., L. M. S. C. *Electrolytic pretreatment of urine*; National Aeronautics & Space Administration: 1977.
99. Kraft, A., Doped diamond: A compact review on a new, versatile electrode material. *Int. J. Electrochem. Sci.* **2007,** *2* (5), 355-385.

100. Hernández, M. C.; Russo, N.; Panizza, M.; Spinelli, P.; Fino, D., Electrochemical oxidation of urea in aqueous solutions using a boron-doped thin-film diamond electrode. *Diam. Relat. Mater.* **2014,** *44*, 109-116.
101. Urbanczyk, E.; Sowa, M.; Simka, W., Urea removal from aqueous solutions-a review. *J Appl Electrochem* **2016,** *46* (10), 1011-1029.
102. Fels, M., Recycle of dialysate from the artificial kidney by electrochemical degradatian of waste metabolites: Small-scale laboratory investigations. *Med. Biol. Eng. Comput.* **1978,** *16* (1), 25-30.
103. Koster, K.; Wendt, H.; Gallus, J.; Krisam, G.; Lehmann, H. D., Regeneration of hemofiltrate by anodic-oxidation of urea. *Artif. Organs* **1983,** *7* (2), 163-168.
104. Grinval'd, V. M.; Leshchinskii, G. M.; Rodin, V. V.; Strelkov, S. I.; Iakovleva, A. A., Unit of electrochemical oxidation of hemodialysis products--development and research. *Med. Tekh.* **2003,** (2), 3-7.
105. Simka, W.; Piotrowski, J.; Nawrat, G., Influence of anode material on electrochemical decomposition of urea. *Electrochim. Acta* **2007,** *52*, 5696-5703.
106. Simka, W.; Piotrowski, J.; Robak, A.; Nawrat, G., Electrochemical treatment of aqueous solutions containing urea. *J Appl Electrochem* **2009,** *39* (7), 1137-1143.
107. Amstutz, V.; Katsaounis, A.; Kapalka, A.; Comninellis, C.; Udert, K. M., Effects of carbonate on the electrolytic removal of ammonia and urea from urine with thermally prepared IrO2 electrodes. *J Appl Electrochem* **2012,** *42* (9), 787-795.
108. Cho, K.; Hoffmann, M. R., Urea degradation by electrochemically generated reactive chlorine species: products and reaction pathways. *Environ Sci Technol* **2014,** *48* (19), 11504-11.
109. Li, H.; Yu, Q.; Yang, B.; Li, Z.; Lei, L., Electro-catalytic oxidation of artificial human urine by using BDD and IrO2 electrodes. *J. Electroanal. Chem.* **2015,** *738*, 14-19.
110. Bazaev, N., Investigation of carbon materials for urea degradation via electrolysis for systems with dialysis regeneration unit. *Nephrol Dial Transpl* **2018,** *33* (suppl_1), i511.
111. Patzer, J. F.; Yao, S. J.; Wolfson, S. K.; Ruppelkerr, R., Urea oxidation-kinetics via cyclic voltammetry - Application to regenerative hemodialysis. *Bioelectrochem. Bioenerg.* **1989,** *22* (3), 341-353.
112. Bolzan, A. E.; Iwasita, T., Determination of the volatile products during urea oxidation on platinum by on line mass spectroscopy. *Electrochim. Acta* **1988,** *33*, 109-112.
113. Rumble, J. R., *CRC Handbook of Chemistry and Physics, 99th Edition (Internet Version 2018)*. CRC Press/Taylor & Francis: Boca Raton, FL., **2018**.
114. Nouri-Nigjeh, E.; Permentier, H. P.; Bischoff, R.; Bruins, A. P., Electrochemical oxidation by square-wave potential pulses in the imitation of oxidative drug metabolism. *Anal. Chem.* **2011,** *83* (14), 5519-25.
115. Nouri-Nigjeh, E.; Bischoff, R.; Bruins, A. P.; Permentier, H. P., Electrochemical oxidation by square-wave potential pulses in the imitation of phenacetin to acetaminophen biotransformation. *Analyst* **2011,** *136* (23), 5064-7.
116. T. Yuan. Nanostructured gold: applications in the study of drug metabolism. (**2017**). [ONLINE]. Retrieved from: https://www.rug.nl/research/portal/files/42215355/Complete_thesis.pdf. [Accessed 11 July 2019].
117. Cheng, Y. C.; Fu, C. C.; Hsiao, Y. S.; Chien, C. C.; Juang, R. S., Clearance of low molecular-weight uremic toxins p-cresol, creatinine, and urea from simulated serum by adsorption. *J Mol Liq* **2018,** *252*, 203-210.

118. Kameda, T.; Ito, S.; Yoshioka, T., Kinetic and equilibrium studies of urea adsorption onto activated carbon: Adsorption mechanism. *J Disper Sci Technol* **2017,** *38* (7), 1063-1066.
119. Yin, C. Y.; Aroua, M. K.; Daud, W. M. A. W., Review of modifications of activated carbon for enhancing contaminant uptakes from aqueous solutions. *Sep Purif Technol* **2007,** *52* (3), 403-415.
120. Eknoyan, G.; Beck, G. J.; Cheung, A. K.; Daugirdas, J. T.; Greene, T.; Kusek, J. W.; Allon, M.; Bailey, J.; Delmez, J. A.; Depner, T. A.; Dwyer, J. T.; Levey, A. S.; Levin, N. W.; Milford, E.; Ornt, D. B.; Rocco, M. V.; Schulman, G.; Schwab, S. J.; Teehan, B. P.; Toto, R.; Hemodialysis Study, G., Effect of dialysis dose and membrane flux in maintenance hemodialysis. *N. Engl. J. Med.* **2002,** *347* (25), 2010-9.
121. Gil, A.; Assis, F. C. C.; Albeniz, S.; Korili, S. A., Removal of dyes from wastewaters by adsorption on pillared clays. *Chem Eng J* **2011,** *168* (3), 1032-1040.
122. Kim, J. H.; Kim, J. C.; Moon, J. H.; Park, J. Y.; Lee, K. K.; Kang, E.; Kim, H. C.; Min, B. G.; Ronco, C., Development of a cold dialysate regeneration system for home hemodialysis. *Blood Purif.* **2009,** *28* (2), 84-92.
123. Giordano, C.; Esposito, R.; Bello, P.; Quarto, E.; Gonzalez, F. M., Cold carbon apparatus for hemodialysis. *J. Dial.* **1976,** *1* (2), 165-79.
124. Giordano, C.; Esposito, R.; Bello, P., A cold charcoal depurator for the adsorption of high quantities of urea. *Kidney Int. Suppl.* **1976,** (7), S284-8.
125. Deepak, D., Evaluation of adsorbents for the removal of metabolic wastes from blood. *Med. Biol. Eng. Comput.* **1981,** *19* (6), 701-6.
126. Wernert, V.; Schaf, O.; Ghobarkar, H.; Denoyel, R., Adsorption properties of zeolites for artificial kidney applications. *Micropor Mesopor Mat* **2005,** *83* (1-3), 101-113.
127. Ooi, C. H.; Cheah, W. K.; Sim, Y. L.; Pung, S. Y.; Yeoh, F. Y., Conversion and characterization of activated carbon fiber derived from palm empty fruit bunch waste and its kinetic study on urea adsorption. *J. Environ. Manage.* **2017,** *197*, 199-205.
128. Lehmann, H. D.; Marten, R.; Fahrner, I.; Gullberg, C. A., Urea elimination using a cold activated-carbon artificial tubulus for hemofiltration. *Artif. Organs* **1981,** *5* (4), 351-356.
129. Fujita, Y.; Okazaki, S., Adsorptive activity of activated carbon for urea in aqueous-solutions. *Nippon Kagaku Kaishi* **1990,** *1990* (4), 352-356.
130. Cheah, W. K.; Sim, Y. L.; Yeoh, F. Y., Amine-functionalized mesoporous silica for urea adsorption. *Mater Chem Phys* **2016,** *175*, 151-157.
131. Tijink, M. S.; Wester, M.; Glorieux, G.; Gerritsen, K. G.; Sun, J.; Swart, P. C.; Borneman, Z.; Wessling, M.; Vanholder, R.; Joles, J. A.; Stamatialis, D., Mixed matrix hollow fiber membranes for removal of protein-bound toxins from human plasma. *Biomaterials* **2013,** *34* (32), 7819-28.
132. Meng, F.; Seredych, M.; Chen, C.; Gura, V.; Mikhalovsky, S.; Sandeman, S.; Ingavle, G.; Ozulumba, T.; Miao, L.; Anasori, B.; Gogotsi, Y., MXene sorbents for removal of urea from dialysate: A step toward the wearable artificial kidney. *ACS Nano* **2018,** *12* (10), 10518-10528.
133. Coughlin, R. W., Effect of surface groups on adsorption of pollutants. *NSCEP* **1970,** *17020*.
134. Chaudhary, V.; Sharma, S., An overview of ordered mesoporous material SBA-15: Synthesis, functionalization and application in oxidation reactions. *J Porous Mat*

2017, *24* (3), 741-749.
135. Ukmar, T.; Planinsek, O., Ordered mesoporous silicates as matrices for controlled release of drugs. *Acta Pharm.* **2010,** *60* (4), 373-85.
136. Kruk, M.; Jaroniec, M.; Ko, C. H.; Ryoo, R., Characterization of the porous structure of SBA-15. *Chem Mater* **2000,** *12* (7), 1961-1968.
137. Huirache-Acuna, R.; Nava, R.; Peza-Ledesma, C. L.; Lara-Romero, J.; Alonso-Nuez, G.; Pawelec, B.; Rivera-Munoz, E. M., SBA-15 mesoporous silica as catalytic support for hydrodesulfurization catalysts-Review. *Materials (Basel)* **2013,** *6* (9), 4139-4167.
138. Cheung, O.; Hedin, N., Zeolites and related sorbents with narrow pores for CO2 separation from flue gas. *Rsc Adv* **2014,** *4* (28), 14480-14494.
139. Cheah, W. K.; Ishikawa, K.; Othman, R.; Yeoh, F. Y., Nanoporous biomaterials for uremic toxin adsorption in artificial kidney systems: A review. *J. Biomed. Mater. Res. B Appl. Biomater.* **2017,** *105* (5), 1232-1240.
140. Kumar, M. N. V. R.; Muzzarelli, R. A. A.; Muzzarelli, C.; Sashiwa, H.; Domb, A. J., Chitosan Chemistry and Pharmaceutical Perspectives. *Chemical Reviews* **2004,** *104* (12), 6017-6084.
141. Rinaudo, M., Chitin and chitosan: Properties and applications. *Progress in Polymer Science* **2006,** *31* (7), 603-632.
142. Pillai, C. K. S.; Paul, W.; Sharma, C. P., Chitin and chitosan polymers: Chemistry, solubility and fiber formation. *Progress in Polymer Science* **2009,** *34* (7), 641-678.
143. Benesch, J.; Tengvall, P., Blood protein adsorption onto chitosan. *Biomaterials* **2002,** *23* (12), 2561-8.
144. Pandit, K. R.; Nanayakkara, I. A.; Cao, W.; Raghavan, S. R.; White, I. M., Capture and direct amplification of DNA on chitosan microparticles in a single PCR-optimal solution. *Anal. Chem.* **2015,** *87* (21), 11022-9.
145. Parra-Barraza, H.; Burboa, M. G.; Sanchez-Vazquez, M.; Juarez, J.; Goycoolea, F. M.; Valdez, M. A., Chitosan-cholesterol and chitosan-stearic acid interactions at the air-water interface. *Biomacromolecules* **2005,** *6* (5), 2416-26.
146. R. Riva, H. Ragelle, A. des Rieux, N. Duhem, C. Jérôme, V. Préat, Chitosan and chitosan derivatives in drug delivery and tissue engineering, in: R. Jayakumar, M. Prabaharan, R.A.A. Muzzarelli (Eds.), *Chitosan for Biomaterials II*, Springer Berlin Heidelberg, Berlin, Heidelberg, **2011**, pp. 19-44.
147. Amidi, M.; Mastrobattista, E.; Jiskoot, W.; Hennink, W. E., Chitosan-based delivery systems for protein therapeutics and antigens. *Adv. Drug Deliv. Rev.* **2010,** *62* (1), 59-82.
148. Jing, S.; Yamaguchi, T., Selective Chemisorption of Urea by Chitosan Coated Dialdehyde Cellulose. *Nippon Kagaku Kaishi* **1990,** *1990* (1), 104-108.
149. X. Chen, W.J. Li, W. Zhong, T.Y. Yu, Investigation of adsorption properties of chitosan/Cu(II) compex in chitosan-silk fibroin blend membranes as adsorbents for urea, *Chin. J. Biomed. Eng.* 16(3), **1997,** 284-288.
150. Liu, J.; Chen, X.; Shao, Z.; Zhou, P., Preparation and characterization of chitosan/Cu(II) affinity membrane for urea adsorption. *J. Appl. Polym. Sci.* **2003,** *90* (4), 1108-1112.
151. Zhou, Y. G.; Yang, Y. D.; Guo, X. M.; Chen, G. R., Effect of molecular weight and degree of deacetylation of chitosan on urea adsorption properties of copper chitosan. *J. Appl. Polym. Sci.* **2003,** *89* (6), 1520-1523.
152. Pathak, A.; Bajpai, S. K., Preparation of Cu(II)-Immobilized chitosan (CIC) and

preliminary urea uptake study. *Polym-Plast Technol* **2008,** *47* (9), 925-930.
153. Pathak, A.; Bajpai, S. K., Chitosan-Magnetite Nanocomposites for Effective Removal of Urea in "Magnetic Hemodialysis Therapy": A Novel Concept. *J. App. Pol. Sci.* **2009,** *114* (5), 3106-3109.
154. Wilson, L. D.; Xue, C., Macromolecular sorbent materials for urea capture. *J. Appl. Polym. Sci.* **2013,** *128* (1), 667-675.
155. Xue, C.; Wilson, L. D., Kinetic study on urea uptake with chitosan based sorbent materials. *Carbohydr. Polym.* **2016,** *135*, 180-6.
156. Liu, X.; Sun, S. J.; Tang, Y. H.; Li, S. S.; Chang, J. H.; Guo, L. A.; Zhao, Y. D., Preparation and kinetic modeling of cross-linked chitosan microspheres immobilized Zn(II) for urea adsorption. *Anal. Lett.* **2012,** *45* (12), 1632-1644.
157. Zhou, Y. G., Sorption of Urea by the Complex of Chitosan-Cu(Ⅱ). *J Hebei University (Nat Sci Ed.)* **1999,** *19* (2), 140-143.
158. Pathak, A.; Bajpai, S. K., Cu(II)-cross-linked chitosan membrane (CCCM): Preparation, characterization and urea removal study using the diffusion-cell model (DCM). *Des. Monomers Polym.* **2009,** *12* (1), 43-55.
159. Penland, R. B.; Mizushima, S.; Curran, C.; Quagliano, J. V., Infrared absorption spectra of inorganic coördination complexes. X. Studies of some metal-urea Complexes. *J. Am. Chem. Soc.* **1957,** *79* (7), 1575-1578.
160. Theophanides, T.; Harvey, P. D., Structural and spectroscopic properties of metal-urea complexes. *Coord. Chem. Rev.* **1987,** *76*, 237-264.
161. Uragami, T.; Takigawa, K., Permeation and separation characteristics of ethanol-water mixtures through chitosan derivative membranes by pervaporation and evapomeation. *Polymer* **1990,** *31* (4), 668-672.
162. Chen, X.; Shao, Z. Z.; Huang, Y. F.; Huang, Y.; Zhou, P.; Yu, T. Y., Influence of crosslinking agent content on structure and properties of glutaraldehyde crosslinked chitosan membranes. *Acta Chim Sinica* **2000,** *58* (12), 1654-1659.
163. Zhou, Q. F.; Yang, F.; Guo, Q. X.; Xue, S., A new organocatalytic process of cyclotrimerization of acetylenic ketones mediated by 2,4-pentanedione. *Synlett* **2007,** *2007* (2), 215-218.
164. Verheyen, E.; Schillemans, J. P.; van Wijk, M.; Demeniex, M. A.; Hennink, W. E.; van Nostrum, C. F., Challenges for the effective molecular imprinting of proteins. *Biomaterials* **2011,** *32* (11), 3008-20.
165. Alexander, C.; Andersson, H. S.; Andersson, L. I.; Ansell, R. J.; Kirsch, N.; Nicholls, I. A.; O'Mahony, J.; Whitcombe, M. J., Molecular imprinting science and technology: A survey of the literature for the years up to and including 2003. *J. Mol. Recognit.* **2006,** *19* (2), 106-80.
166. Chen, L.; Wang, X.; Lu, W.; Wu, X.; Li, J., Molecular imprinting: Perspectives and applications. *Chem. Soc. Rev.* **2016,** *45* (8), 2137-211.
167. Haupt, K., Imprinted polymers—Tailor-made mimics of antibodies and receptors. *Chem. Comm.* **2003,** (2), 171-178.
168. Takeuchi, T.; Haginaka, J., Separation and sensing based on molecular recognition using molecularly imprinted polymers. *J. Chromatogr. B Biomed. Sci. Appl.* **1999,** *728* (1), 1-20.
169. Holthoff, E. L.; Bright, F. V., Molecularly imprinted xerogels as platforms for sensing. *Acc. Chem. Res.* **2007,** *40* (9), 756-767.
170. Alvarez-Lorenzo, C.; Concheiro, A., Molecularly imprinted polymers for drug

delivery. *J. Chromatogr. B* **2004,** *804* (1), 231-245.
171. Wulff, G.; Liu, J., Design of biomimetic catalysts by molecular imprinting in synthetic polymers: The role of transition state stabilization. *Acc. Chem. Res.* **2012,** *45* (2), 239-247.
172. Cheng, Y.; Xu, K. L.; Li, H.; Li, Y. F.; Liang, B., Preparation of urea-imprinted cross-linked chitosan and its adsorption behavior. *Anal. Lett.* **2014,** *47* (6), 1063-1078.
173. Alizadeh, T.; Akbari, A., A capacitive biosensor for ultra-trace level urea determination based on nano-sized urea-imprinted polymer receptors coated on graphite electrode surface. *Biosens. Bioelectron.* **2013,** *43* (1), 321-7.
174. Lian, H. T.; Liu, B.; Chen, Y. P.; Sun, X. Y., A urea electrochemical sensor based on molecularly imprinted chitosan film doping with CdS quantum dots. *Anal. Biochem.* **2012,** *426* (1), 40-6.
175. Chen, Y. P.; Liu, B.; Lian, H. T.; Sun, X. Y., Preparation and application of urea electrochemical sensor based on chitosan molecularly imprinted films. *Electroanalysis* **2011,** *23* (6), 1454-1461.
176. Lee, M. H.; Thomas, J. L.; Ho, M. H.; Yuan, C.; Lin, H. Y., Synthesis of magnetic molecularly imprinted poly(ethylene-co-vinyl alcohol) nanoparticles and their uses in the extraction and sensing of target molecules in urine. *ACS Appl. Mater. Interfaces* **2010,** *2* (6), 1729-36.
177. Khadro, B.; Sanglar, C.; Bonhomme, A.; Errachid, A.; Jaffrezic-Renault, N., Molecularly imprinted polymers (MIP) based electrochemical sensor for detection of urea and creatinine. *Procedia Eng.* **2010,** *5*, 371-374.
178. Alizadeh, T., Preparation of molecularly imprinted polymer containing selective cavities for urea molecule and its application for urea extraction. *Anal. Chim. Acta* **2010,** *669* (1-2), 94-101.
179. Alizadeh, T.; Akhoundian, M.; Movahed, Z., Indirectly determination of urea using chloride ion selective electrode after its extraction and preconcentration by molecularly imprinted polymer. *Anal. Bioanal. Electrochem.* **2009,** *1* (4), 246 - 256.
180. Huang, C. Y.; Tsai, T. C.; Thomas, J. L.; Lee, M. H.; Liu, B. D.; Lin, H. Y., Urinalysis with molecularly imprinted poly(ethylene-co-vinyl alcohol) potentiostat sensors. *Biosens. Bioelectron.* **2009,** *24* (8), 2611-7.
181. Grillon, E.; Gallo, R.; Pierrot, M.; Boileau, J.; Wimmer, E., Isolation and X-ray structure of the intermediate dihydroxyimidazolidine(Dhi) in the synthesis of glycoluril from glyoxal and urea. *Tetrahedron Lett.* **1988,** *29* (9), 1015-1016.
182. Shapiro, R.; Chatterjie, N., Cyclization reactions of ninhydrin with aromatic amines and ureas. *J. Org. Chem.* **1970,** *35* (2), 447-450.
183. Shimizu, T.; Fujishige, S., A newly prepared surface-treated oxystarch for removal of urea. *J. Biomed. Mater. Res.* **1983,** *17* (4), 597-612.
184. Abidin, M. N. Z.; Goh, P. S.; Ismail, A. F.; Said, N.; Othman, M. H. D.; Hasbullah, H.; Abdullah, M. S.; Ng, B. C.; Kadir, S.; Kamal, F., Highly adsorptive oxidized starch nanoparticles for efficient urea removal. *Carbohydr. Polym.* **2018,** *201*, 257-263.
185. Bing-Lin, H.; Zhao, X. B., Study of the oxidation of crosslinked β-cyclodextrin polymer and its use in the removal of urea. I. *React. Polym.* **1992,** *18* (3), 229-235.
186. M.S. Eisen, Urea sorbent, U.S. Patent 8,220,643 B2 (**2014**).
187. R.J. Wong, Materials for removal of toxins in sorbent dialysis and methods and systems using same, U.S. Patent 2014/0,336,568 A1 (**2014**).
188. Kuntz, E.; Quentin, J. P. Process for extracting urea from a solution with

alkenylaromatic polymers with a-ketoalhydic groups, **1977**.
189. J.P. Quentin, E. Kuntz, Alkenylaromatic polymers with α-ketoalhydic groups, U.S. Patent 3,933,753, **1976**.
190. Poss, M. J.; Blom, H.; Odufu, A.; Smakman, R., Macromolecular ketoaldehydes. U.S. Patent 6,861,473 B2: **2005**.
191. Smakman, R.; van Doorn, A. W., Urea removal by means of direct binding. *Clin. Nephrol.* **1986,** *26 Suppl 1*, S58-62.
192. R. Smakman, Macromolecular carbonyl groups containing material suitable for use as sorbent for nitrogen compounds., **1990**, U.S. Patent 4,897,200.
193. Stern, I. J.; Izzo, R. S.; Jo Wang, Z. W.; Beschorner, W. E., Mechanism of urea nitrogen binding by proposed oxidized starch gastrointestinal absorbents. *Experientia* **1975,** *31* (9), 1065-6.
194. Jong, J. A. W.; Smakman, R.; Moret, M. E.; Verhaar, M. C.; Hennink, W. E.; Gerritsen, K. G. F.; Van Nostrum, C. F., Reactivity of (vicinal) carbonyl compounds with urea. *ACS Omega* **2019,** *7* (4), 11928-11937.
195. van Doorn, A. W., Regeneration of dialysate. *Artif. Organs* **1979,** *3* (2), 190-2.
196. Jong, J. A. W.; Moret, M. E.; Verhaar, M. C.; Hennink, W. E.; Gerritsen, K. G. F.; van Nostrum, C. F., Effect of substituents on the reactivity of ninhydrin with urea. *ChemistrySelect* **2018,** *3* (4), 1224-1229.

3

Chapter 3

Effect of Substituents on the Reactivity of Ninhydrin with Urea

Jacobus A.W. Jong[a,c], Marc-Etienne Moret[b], Marianne C. Verhaar[c], Wim E. Hennink[a], Karin G.F. Gerritsen[c] and Cornelus F. Van Nostrum[a,*]

[a] Department of Pharmaceutics, Utrecht Institute for Pharmaceutical Sciences (UIPS), Utrecht University, Universiteitsweg 99, 3584 CG Utrecht, the Netherlands.
[b] Organic Chemistry and Catalysis, Debye Institute for Nanomaterials Science, Utrecht University, Universiteitsweg 99, 3584 CG Utrecht, the Netherlands.
[c] Department of Nephrology and Hypertension, University Medical Centre Utrecht, Heidelberglaan 100, 3584 CX Utrecht, The Netherlands.

Published in ChemistrySelect, 2018, 3, 1224–1229
DOI: 10.1002/slct.201800040

Abstract

Ninhydrin, i.e. the stable hydrate of the reactive species indanetrione, is a well-known compound used for the quantification of ammonia and amino acids. However, substituent effects on the reactivity of ninhydrin with nucleophiles are not described. In this work, the kinetics of the reaction of C4- and C5- substituted ninhydrins with urea was studied and monitored by ^{13}C-NMR. Surprisingly, the obtained results show that electron donating groups (EDGs) as well as electron withdrawing groups (EWGs) decrease the rate of the reaction. EDGs decrease the electrophilicity of indanetrione, resulting in slower overall kinetics than unsubstituted ninhydrin. The calculated Gibbs free energy differences for the dehydration of unsubstituted and substituted ninhydrins and the subsequent reaction with urea showed that the dehydration of the compounds is more sensitive to electronic effects than the subsequent reaction with urea. Therefore, although EWGs increase the electrophilicity of indanetrione, this is more than counterbalanced by an adverse shift of the hydration equilibrium towards the unreactive hydrate (i.e. ninhydrin), resulting in slower kinetics as well.

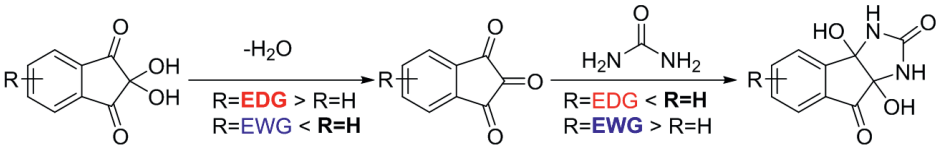

1. Introduction

More than a century ago, Ruhemann reported on the synthesis of ninhydrin (**1e**) and its remarkable reactivity towards amines and ammonia, yielding colored products.[1-2] He noted that ninhydrin reacts with amines on the central carbon rather than on the adjacent free carbonyls. In the years thereafter, applications such as quantification of ammonia and amino acids and fingerprint detection, using ninhydrin as reagent, were developed.[3-6] A number of publications reported on the kinetics and mechanism of the reaction of ninhydrin with amino acids, leading to the common understanding that the first step is the elimination of water, followed by nucleophilic attack of the non-protonated amine on the central ketone of indanetrione (**2e**). The latter is considered the rate-determining step (scheme 1).[7-10] The final compound that is formed, diketohydrindylidenediketo-hydrindamine or Ruhemann's Purple (scheme 1), adsorbs at 570 nm allowing quantification of e.g. amino acid concentrations in biological samples.

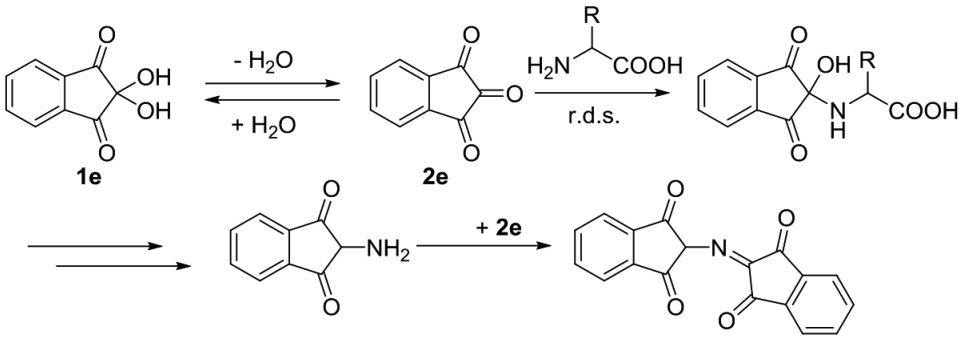

Scheme 1. The mechanism of reaction of ninhydrin with amino acids. R.d.s. = rate-determining step. **1e** = ninhydrin, table 1 entry e.

Ninhydrin is a powerful electrophile that reacts not only with amines, enamines, ammonia and amino acids, but also with weak nucleophiles such as anilines, alcohols, ureas and even amides.[11-16] Many studies have corroborated that upon dehydration of ninhydrin the central carbonyl of the resulting indanetrione is the most reactive towards amines. Devi *et al*. have recently reported on the reaction of ninhydrin with an aniline containing an amide functionality. They calculated, using Density Functional Theory at the B3LYP 6-31G(d,p) level,[17] that the central carbon is the least reactive when hydrated compared to the adjacent carbonyls, but becomes the most electron deficient and therefore the most reactive upon elimination of water, explaining that indanetrione reacts with the amide rather than ninhydrin itself.[14] In 1999 Bowden and Rumpal studied the effect of substituents on C4, C5, C6 and combinations thereof on the reactivity of indanetrione with water to form ninhydrin derivatives, and found a slope (ρ-value) of 1.05 in the Hammett Plot. The positive slope indicates that substituents that decrease the electron density in the three carbonyl groups increase the rate of hydration and *vice versa*.[18] However,

substituent effects on the reactivity of ninhydrin with other nucleophiles are still unknown.

In this paper we investigated the effect of both electron withdrawing groups (EWGs) and electron donating groups (EDGs) on the reactivity of ninhydrin with urea. We expected that EWGs increase and EDGs decrease the reactivity of ninhydrin with urea because ninhydrin is the electrophilic species in the reaction with amines. Urea was chosen as model nucleophile since its reaction with ninhydrin yields tetrahydroindeno-imidazole, a stable adduct (scheme 2), in contrast to that of ninhydrin with amino acids. [11-12, 19-22]

2. Results and Discussion

First, the order and rate constant of the reaction of ninhydrin with urea was determined in phosphate buffered aqueous saline (PBS) at 50 °C by the method of initial rates.[22-24] Various ninhydrin concentrations (5-20 mM) were reacted with a fixed amount of urea (10 mM) and *vice versa* (supporting information). The ninhydrin concentration was monitored over time by UV spectroscopy at 232 nm and the urea concentration was determined over time with urease, an enzyme that converts urea into CO_2 and ammonia that is subsequently quantified by its reaction with two equivalents of a phenol, yielding a dye that is quantified spectrophotometrically. The graphs of the initial reaction rate (mMh^{-1}) versus the initial concentration of the variable component showed linear correlations with similar rate constant (~0.2 h^{-1}, figures S3 and S5), and linear regression of the double logarithmic plots gave slopes of 0.95 ± 0.04 for urea and 1.13 ± 0.18 for ninhydrin (figures S4 and S6). Therefore it was concluded that the reaction of ninhydrin with urea (scheme 2) is first order in both urea and ninhydrin, and thus second order overall.

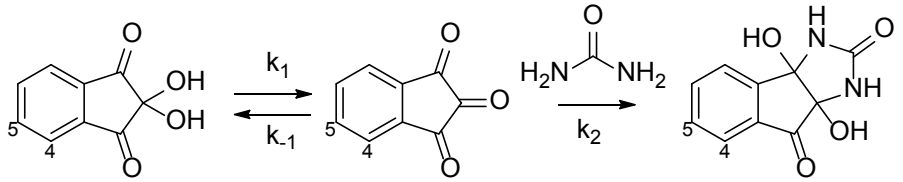

Scheme 2. Reaction of ninhydrin with urea.

The reaction mechanism (scheme 2) is composed of the equilibrium between elimination of water from **1e** and hydration of **2e** and the subsequent reaction of **2e** with urea to yield tetrahydroindeno-imidazole **3e**. Since the reaction is first order in both ninhydrin and urea, the rate of the formation of reaction product **3e** can be expressed by equation 1 and simplified by equation 2, in which k_{obs} is expressed by equation 3.

$$(1) \quad \frac{d[\mathbf{3e}]}{dt} = \frac{k_1 k_2 [ninhydrin][urea]}{k_{-1} + k_2[urea]}$$

$$(2) \quad \frac{d[\mathbf{3e}]}{dt} = k_{obs}[urea][ninhydrin]$$

$$(3) \quad k_{obs} = \frac{k_1}{k_{-1} + k_2[urea]} k_2$$

Because the rate-determining step is the nucleophilic attack of urea on the central carbonyl of indanetrione $k_{-1} >> k_2$[urea]. Therefore the numerator in equation 3 is dominated by k_{-1}, simplifying equation 3 to equation 4.

$$(4) \quad k_{obs} = \frac{k_1}{k_{-1}} k_2$$

By using both reactants in stoichiometric amounts, the urea concentration is equal to the ninhydrin concentration thereby simplifying the rate equation 2 to equation 5. The k_{obs}-value can thus be determined by only measuring the urea concentration in time. Solving differential equation 5 yields equation 6, k_{obs} is then obtained from the plot of the inverse of the urea concentration against time (an example is given in supporting information, figure S7).

$$(5) \quad \frac{d[\mathbf{3e}]}{dt} = k_{obs}[urea]^2$$

$$(6) \quad \frac{1}{[urea]_t} = k_{obs} t + \frac{1}{[urea]_{t=0}}$$

Several ninhydrins substituted at 4- and 5-position with EWGs (4- and 5-Br, 4- and 5-NO_2, 5-CF_3) and EDGs (4- and 5-Me, 5-OMe and 5-*t*Bu) were selected to investigate the electronic effects of the substituents on the reactivity of ninhydrin with urea. The ninhydrin derivatives were synthesized according to a recently published method in a versatile one-step procedure from the corresponding indane-1-ones in similar yields as reported.[23]

Since the pH of the medium influences the reaction rate of ninhydrin (scheme S1 and table S3), the pH was maintained at 7.4 using phosphate buffer saline (PBS). However, in contrast to unsubstituted ninhydrin (**1e**), the ninhydrin derivatives have low solubility in PBS (< 30 mM). Therefore, the different ninhydrin derivatives were dissolved in a 50/50 mixture of DMSO and PBS to study their reaction kinetics with urea. Since the urease assay is incompatible with DMSO presumably due to oxidation of DMSO rather than ammonia by hypochlorite, urea concentrations were determined by quantitative ^{13}C-NMR of ^{13}C-labeled urea (signal at 162.08 ppm) using Me_2SO_2 as internal standard (IS) at 42.15 ppm relative to the DMSO signal at 39.39 ppm. This new method was validated by comparing k_{obs}-values for the reaction of

ninhydrin with urea in PBS obtained by urea concentrations thus measured, with those measured by the urease assay. The new method yielded a k_{obs}-value for this reaction of 6.8 ± 0.3 $M^{-1}h^{-1}$ whereas the urea concentrations determined with the urease assay resulted in a k_{obs}-value of 6.7 ± 0.1 $M^{-1}h^{-1}$, thereby validating the ^{13}C-NMR urea concentration method (supporting information).

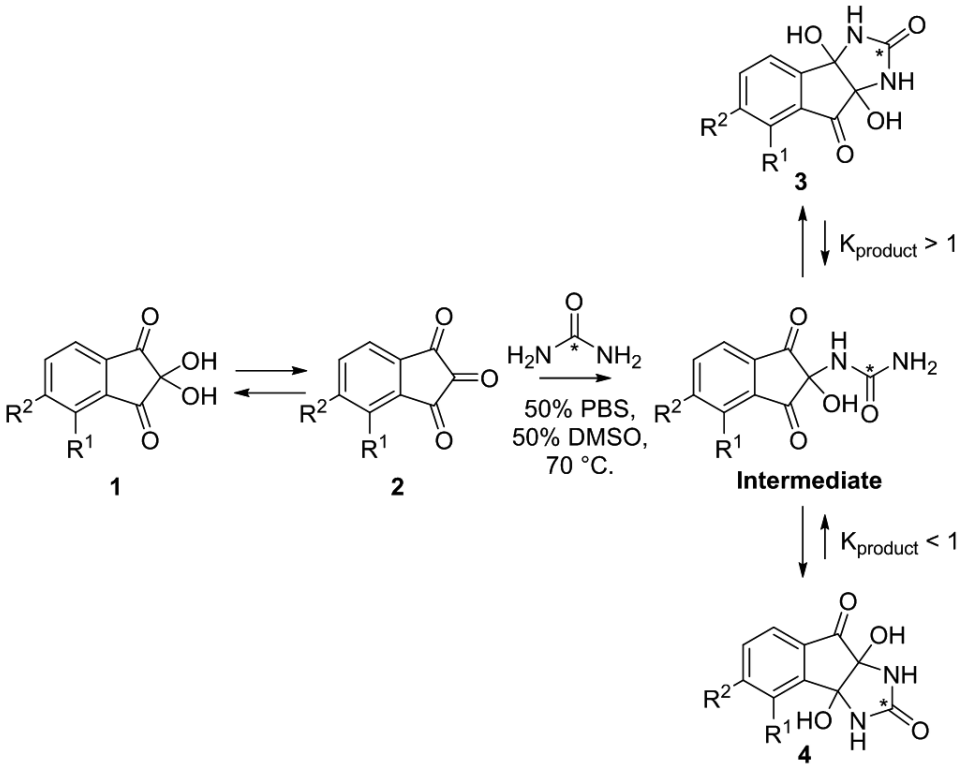

Scheme 3. Formation of regioisomers **3** and **4**.

The ninhydrin derivatives were reacted at 70 °C with urea in a 1:1 ratio. Notably, when a substituent is present on ninhydrin, two tetrahydroindeno-imidazole regioisomers **3** and **4** are formed that can be distinguished in the ^{13}C NMR spectra for urea quantification (scheme 3). The relative amounts of each regioisomer in the isolated products were determined by ^{1}H-NMR or 2D Heteronuclear Multiple Bond Correlation (HMBC) ^{13}C- ^{1}H- NMR (table 2).

Table 1 shows k_{obs}-values of the tested ninhydrin derivatives obtained from the kinetic plots. Under the experimental conditions (1:1 v/v PBS/DMSO at 70 °C) the reaction equilibrates, therefore the k_{obs} was derived from the initial slope of the plot of the inverse of the urea concentration in time. Unsubstituted ninhydrin gave a k_{obs}-value of 20.4 ± 2.2 $M^{-1}h^{-1}$ (entry e). As expected for an electrophile, EDGs such as methyl and *tert*-butyl (entry b-d) increase the electron density at the carbonyls and decrease the rate of the reaction with urea relative to unsubstituted ninhydrin (7.4

- 13.9 $M^{-1}h^{-1}$). Unexpectedly, EWGs such as bromo-, nitro- and trifluoromethyl (entry f-j) which decrease the electron density at the carbonyls also decreased the rate of the reaction (2.0 - 2.9 $M^{-1}h^{-1}$) and reacted even slower with urea than ninhydrins bearing an EDG.

Table 1. k_{obs}-Values for the reaction of ninhydrin derivatives with urea determined by quantitative ^{13}C NMR.

Entry 1[a]	R^1 (4-position)	R^2 (5-position)	Sigma-value[24] [a]	k_{obs}- value ($M^{-1}h^{-1}$) [b]
1a	H	OMe	-0.268	3.1
1b	H	tBu	-0.199[25]	13.9
1c	H	Me	-0.170	9.6
1d	Me	H	-0.069	7.4
1e	H	H	0	20.4±2.2[c]
1f	H	Br	0.232	2.0
1g	Br	H	0.391	2.9
1h	H	CF_3	0.54[26]	2.4
1i	NO_2	H	0.710	2.1
1j	H	NO_2	0.778	2.4

[a] Substituents in the 4-position are considered meta-substituted and substituents in the 5-position are considered para-substituted. [b] Reactions with urea were performed at 70 °C in 1:1 PBS/DMSO. [c] The error in the measurement was only determined for unsubstituted ninhydrin (n = 3).

To fit the kinetic data of the reaction of urea with substituted ninhydrins in a Hammett plot, the 5-position was taken as *para*-substituted and logically we chose the *meta*-parameter for 4-substituted ninhydrins.[27] Bowden and Rumpal fitted several Hammett parameters in their kinetic studies of the hydration of indanetrione and the ring fission of ninhydrin and found that the 5-position of indanetrione and ninhydrin correlates best with the *para*-parameter. The Hammett plot of the logarithm of the relative *k*-values (k_{obs} for substituted divided by k_{obs} for unsubstituted ninhydrin) as a function of the sigma constant for each substituent is shown in figure 1. In general the ninhydrin derivatives correlate poorly with the Hammett parameters, resulting in a scattered plot. However, when 5-OMe- and 5-Br-substituted ninhydrin and unsubstituted ninhydrin are left out, the other substituents follow a linear Hammett relationship. A possible explanation for the deviation of the 5-OMe group is that this group can be an EWG or EDG depending whether it is in the *meta*- or *para*-position, respectively. In the investigated reaction, the substituent is in fact in both positions whereas the sigma value that we used only corresponds to the *para*-position. The negative slope in the Hammett plot indicates that the reaction rate decreases with a decreasing electron density on the carbonyls, which is not expected for an electrophile such as ninhydrin.

To explain the unexpected negative influence of the EWGs on the reactivity of ninhydrin and the high reactivity of unsubstituted ninhydrin, we calculated the

energy changes (ΔG's) for the dehydration of ninhydrin **2** and for the subsequent formation of intermediate **I**, for each substituent. We used the same DFT method (B3LYP 6-31G(d,p)) as Devi *et al.* on ninhydrin and indanetrione (calculating the partial atomic (Mulliken) charges), but we performed all calculations using a polarizable continuum model for water instead of the gas phase.[14] Structure optimization was performed and the corresponding frequencies were calculated for the different ninhydrin derivatives, intermediates and products.

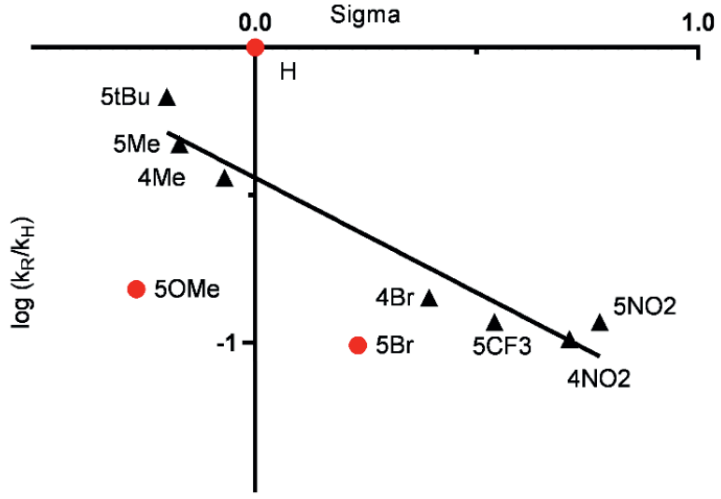

Figure 1. Hammett plot for the reaction of urea with ninhydrin derivatives; k_R and k_H are the k_{obs} for substituted and unsubstituted ninhydrin, respectively. Linear regression (excluding 5-OMe, H and 5-Br) gives y=-0.78x-0.44, R^2 = 0.93.

Because the reactions converge to an equilibrium instead of reaching full conversion, the reaction products are also expected to be at equilibrium with each other. Hence, the overall rate constant of the reaction (k_{obs}) does not affect the thermodynamic ratio of the two regioisomers. First we considered the isomerization of regioisomers **3** and **4**, by calculating the difference in Gibbs free energy of those products (equation 7) and calculated the corresponding equilibrium constants $K_{product}$ using equation 8 (figure S9 and table 2):

$$(7)\ \Delta G_{isomerization} = G_{Product3} - G_{Product4}$$

$$(8)\ \Delta G = -RTln(K)$$

A plot of the experimental versus the calculated $K_{product}$ is included in the supporting information section 8.5. The equilibrium constants calculated with the difference in energy of these regioisomers are overall in good agreement with the experimental $K_{product}$ (with exception of entry b), which shows that the chosen model correctly predicts which regioisomer is preferentially formed.

Table 2. Ratios of the isolated regioisomers, corresponding experimental equilibrium constants, and calculated equilibrium constants from ΔG's for the formation of each regioisomer.

Entry	Ninhydrin derivative	Isolated compound ratio 3:4[a]	Experimental $K_{product}$	Calculated $K_{product}$
a	5-OMe	1 : 5.0	0.20	0.037
b	5-tBu	1 : 1.4	0.71	1.375
c	5-Me	1 : 2.0	0.50	0.322
d	4-Me	1.5 : 1	1.5	2.155
f	5-Br	1 : 2.0	0.50	0.958
g	4-Br	1 : 1.5	0.67	0.128
h	5-CF_3	1.2 : 1	1.2	2.011
i	4-NO_2	<0.01 : 1	<0.01	0.003
j	5-NO_2	1.4 : 1	1.4	2.688

[a] Ratios were determined by NMR from the mixture of regioisomers after purification. Loss of product was not observed during the purification process (**3e** was isolated in a 69% yield after 70% conversion was observed in the corresponding kinetic experiment).

Using the calculated G-values, the differences in Gibbs free energy were determined according to equations 9-11:

Between the intermediate and indanetrione:

$$(9)\ \Delta G_{\mathrm{Intermediate}} = G_{\mathrm{intermediate}} - (G_{\mathrm{indanetrione}} + G_{\mathrm{urea}})$$

Between indanetrione and ninhydrin:

$$(10)\ \Delta G_{\mathrm{Dehydration}} = (G_{\mathrm{indanetrione}} + G_{\mathrm{water}}) - G_{\mathrm{ninhydrin}}$$

Between the intermediate and ninhydrin:

$$(11)\ \Delta G_{\mathrm{addition}} = (G_{\mathrm{intermediate}} + G_{\mathrm{water}}) - (G_{\mathrm{ninhydrin}} + G_{\mathrm{urea}})$$

In principle, for spontaneous processes like the hydration of indanetrione or its reaction with urea, ΔG values should be negative or close to zero. However, the opposite was found, which can be explained by several aspects of our computational model. First, differential solvation effects between reactant and products might not be accurately represented by a continuum solvent model which does not include specific interactions such as hydrogen bonding. Second, the contribution of translational entropy to the Gibbs free energy may be inaccurately treated in solution. For these reasons the obtained ΔG-values are not absolute values. Of note, these issues are not expected to significantly impact intrinsic substituent effects and trends within a series of analogous compounds can thus be accurately predicted.
The effect of a given substituent on the overall reaction can be determined by subtracting the ΔG of the addition of urea to ninhydrin ($\Delta G_{\text{H addition}}$) from the ΔG of the addition of urea to substituted ninhydrin ($\Delta G_{\text{R addition}}$), referred to as $\Delta\Delta G_{\text{R addition}}$ (equation 12).

$$(12)\ \Delta\Delta G_R = \Delta G_R - \Delta G_H$$

A positive $\Delta\Delta G_R$ implies that the substituted compound has a higher ΔG than the unsubstituted one, thus the substituent lowers the driving force for the reaction. To a first approximation, effects on the free energy of activation $\Delta G^{\ddagger}$ can be assumed to be proportional to effects on the driving force ΔG_R in a linear free energy relationship. According to the Eyring equation, the logarithm of the rate (log k) is proportional to the negative of the free enthalpy of activation ($-\Delta G^{\ddagger}$), implying that substituent effects on $-\Delta\Delta G_R$ should be proportional to those on log(k). In figure 2 A the $-\Delta\Delta G_{R\ addition.}$ is plotted against the Hammett sigma parameter and, in good agreement with the experimental Hammett plot, a negative slope is observed. To understand why EWGs – somewhat counterintuitively – decrease the reactivity of ninhydrin with urea, the $\Delta\Delta G_R$'s of both the dehydration of ninhydrin and the subsequent reaction of indanetrione with urea were calculated analogously ($-\Delta\Delta G_{R\ dehydration}$ and $-\Delta\Delta G_{R\ intermediate}$) and plotted against the Hammett sigma parameters (figure 2 B and C).
The effect of the substituent in terms of $-\Delta\Delta G_R$ on the dehydration of ninhydrin shows a negative slope in the Hammett plot, which means that EDGs increase the rate of the dehydration and EWGs decrease the rate of dehydration (figure 2B). This is in correspondence with the work of Bowden and Rumpal in which they investigated the influence of substituents on the reverse reaction (hydration of indanetrione) and found a positive slope (ρ=1.05) in the Hammett plot.[18] The ninhydrin-indanetrione equilibrium is defined by equation 13 and the equilibrium constant. K is calculated by equation 8, using the calculated ΔG for the formation of ninhydrin from indanetrione and water (table 3).

$$(13)\quad K = \frac{[ninhydrin]}{[indanetrione][H_2O]}$$

The higher calculated equilibrium constants for the EWGs relative to unsubstituted ninhydrin suggest that the indanetrione concentrations are indeed lower in the presence of an EWG, and higher in the presence of an EDG.
Using $-\Delta\Delta G_{R\ intermediate}$, figure 2C illustrates the substituent effect in a Hammett plot. In contrast to the dehydration of ninhydrin, a positive slope is observed, which indicates that EWGs increase the rate of the reaction of indanetrione with urea, and EDGs decrease this rate. Interestingly, the magnitude of the slope of the Hammett plot for the dehydration of ninhydrin (figure 2B) shows that this reaction is more affected by the substituent than the reaction of indanetrione with urea (figure 2C). In other words, the change in enthalpy for the dehydration of ninhydrin, and therefore the activation energy,[30] is more sensitive for electronic substituent effects than the reaction with urea.

Table 3. Calculated equilibrium constants K for the ninhydrin-indanetrione equilibria from calculated ΔG (J), T= 343 K.

Entry	Ninhydrin derivative	$K_{dehydration}$
a	5-OMe	0.08
b	5-tBu	0.17
c	5-Me	0.16
d	4-Me	0.24
f	5-Br	0.29
g	4-Br	0.37
h	5-CF_3	0.62
i	4-NO_2	0.46
j	5-NO_2	1.48

The computational results suggest that the introduction of an EWG on ninhydrin shifts the ninhydrin-indanetrione equilibrium towards ninhydrin, resulting in a decrease of the indanetrione concentration and slower steady state kinetics. Because the dehydration of ninhydrin is affected by the EWGs to a greater extent than the reaction of indanetrione with urea, the overall rate of the reaction is decreased, thereby explaining why the reactivity of electron-deficient ninhydrins towards urea is not increased compared to unsubstituted ninhydrin. The other way around, figure 2B shows that for EDGs the $\Delta\Delta G_{R\ dehydration}$ are negative and thus the indanetrione concentrations are higher. However, the experimental results (figure 1) show that also EDGs do not increase the reactivity of ninhydrin towards urea in water. The reason for this is that EDGs make the triketonesystem of indanetrione more electron-rich and thus less electrophilic than unsubstituted ninhydrin.
In addition, the experimental result that the electrophilicity of ninhydrin decreases with the introduction of an EWG is consistent with the mechanism in which the initial attack of the nucleophile on ninhydrin takes place at the C2 position, since an initial attack at the C1 position would be promoted by an EWG.

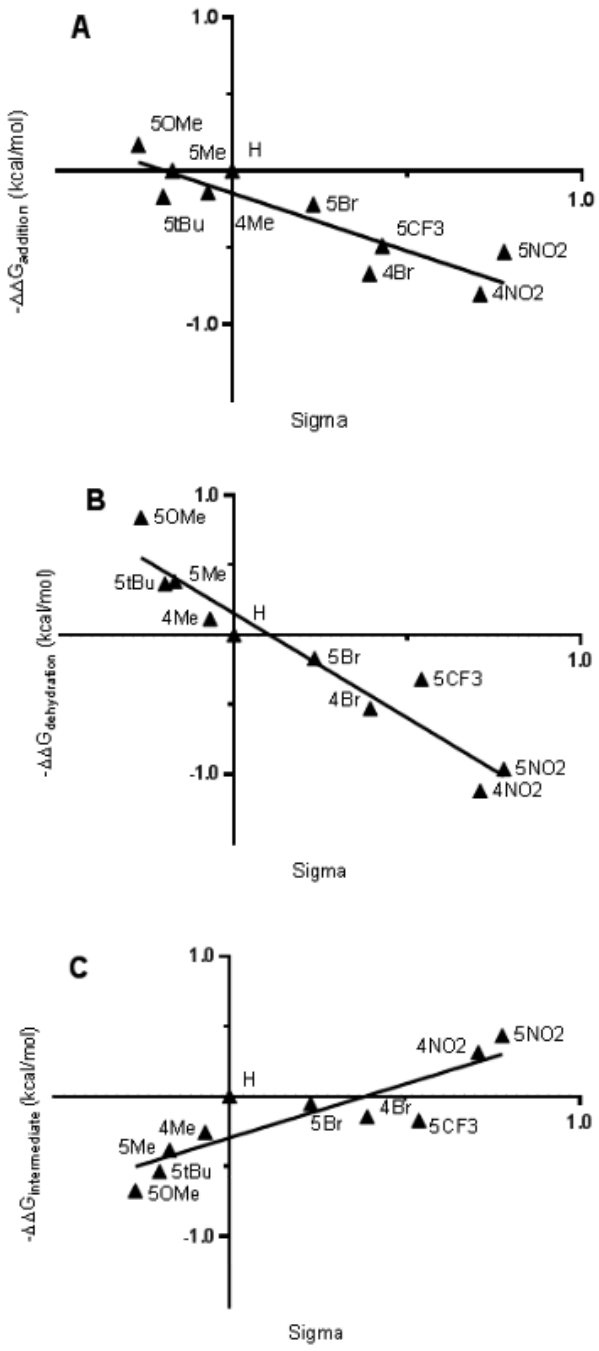

Figure 2. Calculated -ΔΔG's plotted against Hammett sigma constants for A) the reaction of ninhydrin with urea (y=-0.75x-0.15, R2 = 0.80) B) the dehydration of ninhydrin (y=-1.499x+0.15, R2 = 0.91) and C) the reaction of indanetrione with urea (y=0.77x – 0.30, R2 = 0.75).

3. Conclusions

A kinetic study is performed on the reaction of substituted ninhydrins with urea in water, which is first order in both ninhydrin and urea and second order overall. Two regioisomers are formed in the rate determining step, which is the reaction between the dehydrated form of ninhydrin (indanetrione) and urea. Because this reaction is a (pH dependent) equilibrium, the major regioisomer formed corresponds to the compound with the lowest calculated energy (G). The reactivity of the electrophilic indanetrione with urea in water showed surprising results. Both electron withdrawing and donating groups significantly decreased the rate of the reaction, EWGs even more than EDGs.

Computational studies on this system provided us with the suitable explanation that the dehydration of ninhydrin is more affected by the substituent than the reactivity towards urea. An EWG decreases rate of the dehydration of ninhydrin, thereby decreasing the indanetrione concentration, resulting in slower kinetics. Although EDGs do promote the dehydration of ninhydrin towards indanetrione, they decrease the electrophilicity of indanetrione towards urea, resulting in slower overall kinetics than unsubstituted ninhydrin but faster than EWG-substituted ninhydrins. This study shows that unsubstituted ninhydrin is the most reactive towards urea in water and that this result is an outlier in the Hammett plot.

4. Material and Methods

4. 1 General material and methods

All materials were obtained from Sigma-Aldrich (Zwijndrecht, The Netherlands) and used as received unless stated otherwise. 4-Nitroindane-1-one and 6-nitroindane-1-one were purchased from Key Organics (Camelford, UK). 5-bromoindane-1-one and 5-tertbutylindane-1-one were purchased from Combi Blocks (San Diego, USA). Phosphate buffered saline (PBS, pH = 7.4, ion composition: Na^+ 163.9 mM, Cl^- 140.3 mM, HPO_4^{2-} 8.7 mM, $H_2PO_4^-$ 1.8 mM) was obtained from B. Braun (Melsungen AG, Germany). All NMR experiments were performed on an Agilent 400-MR DD2 equipped with a OneNMR probe. All 1D NMR experiments were carried out according to the s2pul.c standard program with a spectral width of 24038.5 Hz and an acquisition time of 1.363 seconds. Residual solvent was used as internal standard (^{1}H: δ 2.50 ppm, ^{13}C {^{1}H}: δ 39.52 ppm for DMSO-d_6). Chemical shifts (δ) are given in ppm and coupling constants (*J*) are quoted in hertz (Hz). Resonances are described as s (singlet), d (doublet), t (triplet), q (quartet), bs (broad singlet) and m (multiplet) or combinations thereof. UV absorption was measured with a Shimadzu UV-2450 UV spectro-photometer using quartz cuvettes. Infrared (IR) spectra were recorded neat using a Thermo Scientific Nicolet iS5 FT-IR spectrometer and reported in cm^{-1}. Melting points were recorded on a manual Büchi Schmelzpunktbestimmungs-

apparat equipped with oil bath and are uncorrected. Electrospray Ionization (ESI) mass spectrometry was carried out using a Agilent 1100 Series LC/MSD Trap instrument in positive ion mode unless stated otherwise. Flash chromatography was performed over Silica Gel (particle size 40-63 µm, VWR Chemicals) using the indicated eluent. Thin Layer Chromatography (TLC) was performed using TLC plates from Merck (SiO2, Kieselgel 60 F254 neutral, on aluminium with fluorescence indicator) and compounds were visualized by UV detection (254 nm). The urease assay used to determine urea concentrations is the Urea CT* FS** colorimetric test purchased at DiaSys Diagnostic Systems GmbH (Holzheim, Germany). Urea concentrations were determined by a coupled enzyme reaction, which results in a colorimetric (570 nm) product proportional to the urea concentration. Samples were stored in a freezer (-20 °C) and thawed just before measurement.

4.2 Determination of the order in ninhydrin

A urea stock solution (20 mM) and several ninhydrin solutions (10, 20, 30 and 40 mM) were prepared in PBS. 5 mL of a ninhydrin solution was added to 5 mL urea solution (thereby decreasing the concentration of both urea and ninhydrin by half) and 75 µL was taken directly from the solution and diluted 300 times. The mixtures were heated to 50 °C and samples were taken after 5, 10, 15, 30 and 60 minutes. The ninhydrin concentration in the samples was determined with UV absorption at 232 nm. The ninhydrin concentrations at each time point and the corresponding initial rates are listed in table S1.

4.3 Determination of the order in urea

A ninhydrin stock solution (20 mM) and several urea solutions (10, 20, 30 and 40 mM) were prepared in PBS. 5 mL of the ninhydrin solution was added to 5 mL of each urea solution (thereby decreasing the concentration of both urea and ninhydrin by half) and 1 mL was directly taken from the solution and placed in an ice bath. The mixtures were heated to 50 °C and 1 mL was taken after 5, 30 and 60 minutes. The urea concentration in the samples was determined with an urease assay. The urea concentrations at each timepoint and the initial rate that is derived from these concentrations are listed in table S2.

4.4 Urea concentration determination procedure

For the calibration curve a stock solution of ^{13}C-labeled urea in PBS (50 mM) was prepared and diluted to the desired concentration. A solution of Me_2SO_2 in D_2O (1.50 mmol in 1000 µL, 1.34 M) was prepared and added to the analytes in a 10:1 ratio (1000 µL analyte and 100 µL internal standard). The mixture was shaken and 600 µL was transferred to an NMR tube. For reaction mixtures (in PBS or PBS:DMSO), 200 µL of internal standard solution was added to 1000 µL of reaction mixture and

transferred to an NMR tube. During the 1D ^{13}C- NMR experiments (101 MHz) proton signals were decoupled. To obtain a quantitative spectrum, the total relaxation delay was set to 40 seconds. To keep the total time of measurement short (> 6 minutes) the number of scans was set to 8 for all calibration curves and kinetic experiments (see supporting information section 4.3). Samples were measured twice and the average of the ratios obtained were used to determine the urea concentration. FIDs were Fourier transformed and automatic phase correction, third order polynomial baseline correction and automatic integration were applied with MestReNova Version 10.0.2-15465.

4.5 Synthesis of ninhydrin derivatives

General procedure I for the synthesis of ninhydrin derivatives.

Substituted indane-1-one (1.0 mmol) was dissolved in a 10:1 mixture of dioxane (3 mL) and H_2O (0.3 mL) in a microwave tube equipped with a magnetic stirrer. Selenium dioxide (3.1 mmol, 3.1 eq.) was added and the tube was sealed. The mixture was shaken vigorously and placed in the microwave where it was heated for 5 minutes at 180 °C. The crude reaction mixture was impregnated on silica and purified over column (Hex: EtOAc 2:1).

Synthesis of **2,2-dihydroxy-5-methoxy-1H-indene-1,3(2H)-dione (1a)**.
Following general procedure I the product was obtained as a red oil (0.98 mmol, 65%). ^{1}H- NMR (DMSO, 400 MHz) δ: 7.95 (d, *J* = 7.7 Hz, 1H), 7.56 (dd, *J* = 8.6 Hz, 2.4 Hz, 1H), 7.43 (s, 2H), 7.42 (d, *J* = 6.2 Hz, 1H), 3.98 (s, 3H) . ^{13}C- NMR (DMSO, 101 MHz) δ: 197.57 (C_q), 195.65 (C_q), 166.64 (C_q), 141.65 (C_q), 132.38 (C_q), 126.31 (CH), 125.84 (CH), 106.07 (CH), 88.42 (C_q), 56.93 (CH_3).

Synthesis of **5-(tert-butyl)-2,2-dihydroxy-1H-indene-1,3(2H)-dione (1b)**.
Following general procedure I, the product was obtained from 5-tertbutylindane-1-one as an orange solid (1.32 mmol, 88%). m.p.: 56.2-60.1 °C. ^{1}H-NMR (DMSO, 400 MHz) δ: 8.14 (dd, *J* = 8.2 Hz, 2.0 Hz, 1H), 7.96 – 7.93 (m, *2*H), 7.45 (bs, 2H), 1.37 (s, 9H). ^{13}C-NMR (DMSO, 101 MHz) δ: 197.22 (C_q), 196.51 (C_q), 161.01 (C_q), 138.74 (C_q), 136.38 (C_q), 134.89 (CH), 123.78 (CH), 119.75 (CH), 87.92 (C_q), 35.74 (C_q), 30.58 (CH_3). IR (neat): ν_{max} (cm^{-1}) = 3417 (br), 2962 (m), 1756 (w), 1720 (s), 1651 (w), 1600 (w), 1366 (w), 1201 (w), 1178 (s), 1080, 1029 (w), 979 (m), 921 (s), 837 (w), 779 (w), 691 (w). MS (ESI): m/z calculated for $C_{13}H_{14}O_4Na$ (M+Na) 257.08, found 257.1.

Synthesis of **2,2-dihydroxy-5-methyl-1H-indene-1,3(2H)-dione (1c)**.
Following general procedure I the product was obtained as an orange solid (1.11 mmol, 74%). ^{1}H- NMR (DMSO, 400 MHz) δ: 7.92-7.81 (m, 3H), 7.47 (s, 2H), 2.53 (s, 3H). ^{13}C- NMR (DMSO, 101 MHz) δ: 197.26 (C_q), 196.66 (C_q), 148.78 (C_q), 138.87 (C_q), 138.29 (CH), 136.43 (C_q), 123.88 (CH), 123.75 (CH), 87.93 (C_q), 21.74 (CH_3).

Synthesis of **2,2-dihydroxy-4-methyl-1H-indene-1,3(2H)-dione (1d)**.
Following general procedure I the product was obtained as a light brown solid (0.6 mmol, 60%). ^{1}H- NMR (DMSO, 400 MHz) δ: 7.90 (dd, *J* = 6.5 Hz, 2.1 Hz, 1H), 7.84-7.80 (m, 2H), 7.44 (s, 2H), 2.68 (s, 3H). ^{13}C- NMR (DMSO, 101 MHz) δ: 198.22 (C_q), 197.22 (C_q), 139.16 (C_q), 139.04(C_q), 138.89(CH), 136.50 (CH), 135.62 (C_q), 121.38 (CH), 87.30 (C_q), 18.26 (CH_3).

Synthesis of **5-bromo-2,2-dihydroxy-1H-indene-1,3(2H)-dione (1f)**.
Following general procedure I the product was obtained as an orange solid (0.73 mmol, 73%). ^{1}H- NMR (DMSO, 400 MHz) δ: 8.25-8.21 (m, 2H), 7.95 (dd, *J* = 8.0 Hz, 0.6 Hz, 1H), 7.60 (s, 2H). ^{13}C- NMR (DMSO, 101 MHz) δ: 196.16 (C_q), 195.86 (C_q), 140.15 (CH), 139.85 (C_q), 137.21 (C_q), 131.57 (C_q), 126.76 (CH), 125.94 (CH), 87.71 (C_q).

Synthesis of **4-bromo-2,2-dihydroxy-1H-indene-1,3(2H)-dione (1g)**.
Following general procedure I the product was obtained as an orange-red solid (0.92 mmol, 61%). ^{1}H- NMR (DMSO, 400 MHz) δ: 8.24 (dd, *J* = 7.8 Hz, 0.9 Hz, 1H), 8.01 (dd, *J* = 7.7 Hz, 1.0 Hz, 1H), 7.91, (t, *J* = 7.7 Hz), 7.59 (s, 2H). ^{13}C- NMR (DMSO, 101 MHz) δ: 195.70 (C_q), 194.90 (C_q), 141.63 (CH), 140.69 (C_q), 138.03 (CH), 135.39 (C_q), 123.22 (CH), 118.79 (C_q), 87.21 (C_q).

Synthesis of **2,2-dihydroxy-5-(trifluoromethyl)-1H-indene-1,3(2H)-dione (1h).**
Following general procedure I, the product was obtained from 6-trifluoromethylindane-1-one as an orange solid (0.11 mmol, 7%. m.p.: 45.9-52.4 °C. ^{1}H-NMR (DMSO, 400 MHz) δ: 8.40-8.34 (m, 2H), 8.22 (d, *J* = 8.0 Hz, 1H), 7.70 (s, 2H). ^{13}C-NMR (DMSO, 101 MHz) δ: 196.18 (C_q), 195.79 (C_q), 140.88 (C_q), 138.85 (C_q), 136.15 (d, *J* = 16.7 Hz, C_q), 133.66 (CH), 125.38 (CH), 121.14 (CH), 87.84 (C_q), 123.1 (d, *J* = 274.7 Hz, C_q). IR (neat): ν_{max} (cm^{-1}) = 3411 (w), 1732 (s), 1624 (m), 1326 (s), 1167 (m), 1128 (m), 1054 (m), 976 (m), 909 (m), 849 (m), 710 (m). MS (ESI): m/z calculated for $C_{10}H_4F_3O_4$ (M-H) 245.01, found 244.8.

Synthesis of **2,2-dihydroxy-4-nitro-1H-indene-1,3(2H)-dione (1i)**.
Following general procedure I the product was obtained as a light yellow solid (0.83 mmol, 55%). ^{1}H- NMR (DMSO, 400 MHz) δ: 8.46 (dd, *J* = 7.8 Hz, 1.0 Hz, 1H), 8.30 (dd, *J* = 7.6 Hz, 0.9 Hz, 1H), 8.23, (t, *J* = 7.7 Hz), 7.77 (s, 2H). ^{13}C- NMR (DMSO, 101 MHz) δ: 194.50 (C_q), 192.22 (C_q), 144.88 (C_q), 139.35 (C_q), 138.49 (CH), 130.70 (CH), 129.19 (C_q), 127.78 (CH), 87.68 (C_q).

Synthesis of **2,2-dihydroxy-5-nitro-1H-indene-1,3(2H)-dione (1j)**.
Following general procedure I the product was obtained as a red oil (0.76 mmol, 51%). ^{1}H- NMR (DMSO, 400 MHz) δ: 8.74 (dd, *J* = 7.6 Hz, 2.1 Hz, 1H), 8.61 (d, *J* = 2.0 Hz, 1H), 8.26 (d, *J* = 8.4 Hz, 1H), 7.77 (s, 2H). ^{13}C- NMR (DMSO, 101 MHz) δ: 195.79 (C_q), 195.37 (C_q), 152.80 (C_q), 141.59 (C_q), 139.23 (C_q), 131.42 (CH), 125.84 (CH),

118.89 (CH), 88.06 (C_q).

General procedure II for the kinetic experiments and isolation of the tetrahydroindeno-imidazoles.

(Substituted) ninhydrin (0.5 mmol, 1.0 eq.) was fully dissolved in DMSO (8.33 mL), and PBS (8.33 mL) was added slowly under continuous stirring to prevent the ninhydrin to precipitate. ^{13}C- labeled urea (31.5 mg, 0.5 mmol, 1.0 eq.) was dissolved in the ninhydrin solution, and the mixture was heated at 50 °C or 70 °C for 6 - 96 hours. Samples from the reaction were taken at suitable time points and the urea concentration in the sample was determined (see quantitative ^{13}C- NMR). The kinetic experiment was continued until over 50% conversion was reached and the k_{obs}-value for the ninhydrin was determined from the plot of $[urea]^{-1}$ over time. To isolate the indeno-imidazole product the crude reaction mixture was freeze-dried, impregnated on silica and purified over column (EtOAc : MeOH 20:1). The regioisomers were determined with ^1H or 2D (^1H-^{13}C) HMBC- NMR.

Second-order *k*-value determination of **3a,8a-dihydroxy-6-methoxy-1,3,3a,8a-tetrahydroindeno[1,2-d]imidazole-2,8-dione** and regioisomer **(3a and 4a)**.
Following general procedure II using 1a as a starting compound, the calculated *k*-value was 3.0 $M^{-1}h^{-1}$. The mixture of regioisomers in a 5:1 ratio was obtained as a light orange solid. m.p.: >200 °C [deg.]. ^1H-NMR (DMSO, 400 MHz) δ: 7.96 – 7.80 (m, $2H_a$ + $2H_b$), 7.69 - 7.65 (m, H_a + H_b), 7.43 (dd, *J* = 8.5 Hz, 2.4 Hz, H_b), 7.23 (d, *J* = 2.2 Hz ,H_a), 7.15 – 7.12 (m, H_a + H_b), 6.54 – 6.44 (m, $2H_a$ + $2H_b$), 6.59 (bs, H_b), 3.90 (s, $3H_a$), 3.84 (s, $3H_b$). ^{13}C-NMR (DMSO, 101 MHz) δ 195.97 (C_q), 165.89 (C_q), 156.66 (C^*_q), 154.93 (C_q), 125.52 (CH), 125.21 (C_q), 117.99 (CH), 107.97 (CH), 87.01 (C_q), 86.31 (C_q), 55.92 (CH_3). IR (neat): ν_{max} (cm^{-1}) = 3205 (br), 3054 (m), 3009 (m), 1697 (s), 1643 (s), 1596 (s), 1495 (w), 1433 (m), 1282 (m), 1212 (m), 1187 (m), 1103 (s), 1079 (w), 1057 (w), 1005 (s), 972 (w), 949 (m), 910 (w), 842 (w), 814 (w), 756 (w), 705 (w). MS (ESI): m/z calculated for $^{13}C^{12}C_{10}H_{10}N_2O_5Na$ (M+Na) 274.05, found 274.0.

Second-order *k*-value determination of **6-(tert-butyl)-3a,8a-dihydroxy-1,3,3a,8a-tetrahydroindeno[1,2-d]imidazole-2,8-dione** and regioisomer **(3b and 4b)**.
Following general procedure II using 1b as a starting compound, the calculated *k*-value was 13.9 $M^{-1}h^{-1}$. The mixture of regioisomers in a 1:1.4 ratio was obtained as an off-white solid. m.p.: 188 °C [deg.]. ^1H-NMR (DMSO, 400 MHz) δ: 7.79 (d, *J* = 2.0 Hz, H_a), 7.96 - 7.93 (m, H_a + H_b), 7.83 - 7.81 (m, H_a + H_b), 7.80 (m, H_a), 7.70 (d, *J* = 8.2 Hz, H_b), 7.67 - 7.65 (m, H_a +$2H_b$), 6.47 (bs, H_b), 6.47 (bs, H_a), 6.38 (bs, H_a), 6.35 (bs, H_b), 1.34 (s, $9H_a$), 1.32 (s, $9H_b$). ^{13}C-NMR (DMSO, 101 MHz) δ 197.35 (C_q), 197.33 (C_q), 160.11 (C_q), 156.69 (C^*_q), 156.66 (C^*_q), 153.02 (C_q), 152.15 (C_q), 134.45 (CH), 132.07 (C_q), 129.81 (C_q), 127.75 (CH), 124.80 (CH), 123.73 (C_q), 123.12 (CH), 121.37 (CH), 118.97 (CH), 86.93 (C_q), 86.88 (C_q), 86.65 (C_q), 86.60(C_q), 35.55 (C_q), 34.78 (C_q), 30.89 (CH_3), 30.80 (CH_3). IR (neat): ν_{max} (cm^{-1}) = 3343 (m), 2954 (m), 1721 (s), 1651

(s), 1632 (s), 1393 (m), 1363 (w), 1285 (w), 1249 (w), 1207 (w), 1114 (s), 1045 (w), 938 (w), 914 (m), 903 (m), 842 (w), 726 (w), 695 (w), 660 (w), 621 (w). MS (ESI): m/z calculated for $^{13}C^{12}C_{13}H_{16}N_2O_4Na$ (M+Na) 300.10, found 300.1.

Second-order *k*-value determination of **3a,8a-dihydroxy-6-methyl-1,3,3a,8a-tetrahydroindeno[1,2-d]imidazole-2,8-dione** and regioisomer **(3c and 4c)**.
Following general procedure II using 1c as a starting compound, the calculated *k*-value was 9.6 $M^{-1}h^{-1}$. The mixture of regioisomers in a 1:2 ratio was obtained as a white solid. m.p.: >200 °C [deg.].^{1}H-NMR (DMSO, 400 MHz) δ: 7.98-7.94 (m, H_a + H_b), 7.81 (bs, H_a + H_b), 7.69-7.62 (m, $2H_a$ + H_b), 7.55 – 7.53 (m, $2H_b$), 7.42 (d, *J* = 8.0 Hz, H_a), 6.51 (bs, H_a + H_b), 6.39 (m, H_a + H_b), 2.46 (s, $3H_a$), 2.40 (s, $3H_b$). ^{13}C-NMR (DMSO, 101 MHz) δ 197.30 (C_q), 197.28 (C_q), 159.11 (C_q), 156.63 (C_q*), 156.61 (C_q*), 152.38 (C_q), 147.43 (C_q), 139.87 (C_q), 137.58 (CH), 132.31 (C_q), 131.13 (CH), 129.89 (C_q), 125.03 (CH), 124.80 (CH), 123.37 (CH), 122.99 (CH), 86.88 (C_q), 86.84 (C_q), 86.56 (C_q), 86.51 (C_q), 21.89 (CH_3), 20.77 (CH_3). IR (neat): ν_{max} (cm^{-1}) = 3260 (br), 2940 (m), 2880 (m), 2840 (m), 1722 (s), 1641 (s), 1608 (m), 1407 (m), 1285 (s), 1131 (s), 1098 (s), 933 (m), 907 (m), 762 (m), 693 (m), 637 (m). MS (ESI): m/z calculated for $^{13}C^{12}C_{10}H_{10}N_2O_4Na$ (M+Na) 258.05, found 258.0.

Second-order *k*-value determination of **3a,8a-dihydroxy-7-methyl-1,3,3a,8a-tetrahydroindeno[1,2-d]imidazole-2,8-dione** and regioisomer **(3d and 4d)**.
Following general procedure II using 1d as a starting compound, the calculated *k*-value was 7.4 $M^{-1}h^{-1}$. The mixture of regioisomers in a 1.5:1 ratio was obtained as a white solid. m.p.: >200 °C [deg.]. ^{1}H-NMR (DMSO, 400 MHz) δ: 8.05 (bs, $1H_b$), 7.97 (bs, H_a), 7.87 (bs, H_b), 7.79 (bs, H_a), 7.70 (t, *J* = 7.6 Hz, H_a), 7.61 – 7.56 (m, $1H_a$ + $2H_b$), 7.47 (t, *J* = 7.4 Hz, H_b), 7.34 (d, *J* = 7.4 Hz, H_a), 6.55 (bs, 1 H_b), 6.48 (bs, H_a), 6.36 (bs, $1H_a$ + 1 H_b), 2.58 (s, 3 H_a), 2.55 (s, $3H_b$). ^{13}C-NMR (DMSO, 101 MHz) δ 199.41 (C_q), 198.44 (C_q), 157.44(C^*_q), 157.16 (C^*_q), 153.26 (C_q), 149.93 (C_q), 138.59 (CH), 138.47 (C_q), 136.77 (C_q), 136.19 (CH), 133.03 (C_q), 131.74 (CH), 130.29 (CH), 129.97 (C_q), 122.79 (CH), 121.33 (CH), 87.85 (C_q), 87.01 (C_q), 86.77 (C_q), 86.42 (C_q), 18.58 (CH_3), 18.30 (CH_3). IR (neat): ν_{max} (cm^{-1}) = 3230 (br), 1723 (s), 1647 (s), 1379 (br), 1107 (s), 1046 (m), 956 (m), 896 (m), 849 (m), 724(m). MS (ESI): m/z calculated for $^{13}C^{12}C_{10}H_{10}N_2O_4Na$ (M+Na) 258.05, found 258.0.

Second-order *k*-value determination of **3a,8a-dihydroxy-1,3,3a,8a-tetrahydroindeno[1,2-d]imidazole-2,8-dione (3e = 4e)**.
Following general procedure II using ninhydrin as a starting compound, the calculated *k*-value was 20.4 $M^{-1}h^{-1}$. The product was obtained as an off-white solid. ^{1}H-NMR (DMSO, 400 MHz) δ: 8.02 (bd, *J* = 2.1 Hz, 1H), 7.88-7.84 (m, 2H), 7.78-7.73 (m, 2H), 7.60 (dt, *J* = 7.8 Hz, 1.1 Hz, 1H), 6.50 (bd, *J* = 25.4 Hz, 2H). ^{13}C-NMR (DMSO, 101 MHz) δ 197.94 (d, *J* = 1.8 Hz, C_q), 156.71 (C^*_q), 152.01 (C_q), 136.65 (CH), 132.14 (C_q), 130.10 (CH), 125.12 (CH), 123.47 (CH), 86.71 (C_q), 86.66 (d, *J* = 1.0 Hz, C_q).

Second-order *k*-value determination of **6-bromo-3a,8a-dihydroxy-1,3,3a,8a-tetrahydroindeno[1,2-d]imidazole-2,8-dione** and regioisomer **(3f and 4f)**.

Following general procedure II using 1f as a starting compound, the calculated *k*-value was 2.0 $M^{-1}h^{-1}$. The mixture of regioisomers in a 1:2 ratio was obtained as an orange solid. m.p.: >200 °C [deg.]. ^{1}H-NMR (DMSO, 400 MHz) δ: 8.08-8.04 (m, H_a + H_b), 7.99 - 7.90 (m, $2H_a$ + $3H_b$), 7.81 (dd, *J* = 8.2 Hz, 2.2 Hz, H_a), 7.73 – 7.68 (m, H_a + H_b), 6.69 (bs, H_a + H_b), 6.65 (bs, H_a), 6.59 (bs, H_b). ^{13}C-NMR (DMSO, 101 MHz) δ 196.95 (C_q), 156.47 (C^*_q), 153.48 (C_q), 133.36 (CH), 131.05 (C_q), 130.33 (C_q), 128.18 (CH), 125.56 (CH), 86.75 (C_q), 86.16 (C_q). IR (neat): ν_{max} (cm^{-1}) =3271 (br), 1725 (s), 1638 (s), 1593 (m), 1398 (m), 1240 (w) , 1213 (w), 1176 (w), 1094 (m), 1046 (w), 1007 (w), 950 (w), 897 (m), 838 (w), 739 (w). MS (ESI): m/z calculated for $^{13}C^{12}C_9H_7N_2O_4Na$ (M+Na) 321.95, found 322.0.

Second-order *k*-value determination of **7-bromo-3a,8a-dihydroxy-1,3,3a,8a-tetrahydroindeno[1,2-d]imidazole-2,8-dione** and regioisomer **(3g and 4g)**.

Following general procedure II using 1g as a starting compound, the calculated *k*-value was 2.9 $M^{-1}h^{-1}$. The mixture of regioisomers in a 1:1.5 ratio was obtained as a light brown solid. m.p.: >200 °C [deg.]. ^{1}H-NMR (DMSO, 400 MHz) δ: 8.07 (bs, $1H_a$), 8.04 (d, *J* = 7.8 Hz, H_b), 7.96 (bs, H_a), 7.90 (bs, H_b), 7.79-7.76 (m, $2H_a$ + $3H_b$), 7.54 (t, *J* = 7.6 Hz, H_a), 6.75 (bs, 1 H_a), 6.67 (bs, H_b), 6.56 (bs, $1H_a$ + 1 H_b). ^{13}C-NMR (DMSO, 101 MHz) δ 196.86 (C_q), 195.75 (C_q), 156.77 (C^*_q), 156.56 (C^*_q), 154.84 (C_q), 149.12 (C_q), 140.60 (CH), 137.54 (CH), 134.74 (C_q), 134.60 (CH), 131.93 (CH), 129.43 (C_q), 124.43 (CH), 122.93 (CH), 119.37 (C_q), 118.42 (C_q), 87.81 (C_q), 87.76 (C_q), 86.69 (C_q), 86.63 (C_q). IR (neat): ν_{max} (cm^{-1}) = 3393 (m), 3265 (br), 2960 (m), 2923 (m), 2852 (m), 1707 (s), 1624 (s), 1587 (m), 1389 (m), 1259 (m), 1214 (m), 1180 (m), 1102 (s), 1020 (m), 943 (m), 798 (m), 736 (m). MS (ESI): m/z calculated for $^{13}C^{12}C_9H_7N_2O_4Na$ (M+Na) 321.95, found 322.0.

Second-order *k*-value determination of **3a,8a-dihydroxy-6-(trifluoromethyl)-1,3,3a,8a-tetrahydroindeno[1,2-d]imidazole-2,8-dione** and regioisomer **(3h and 4h)**.

Following general procedure II using 1h as a starting compound, the calculated *k*-value was 2.3 $M^{-1}h^{-1}$. The mixture of regioisomers in a 1.2:1 ratio was obtained as an off-white solid. m.p.: >200 °C [deg.]. ^{1}H-NMR (DMSO, 400 MHz) δ: 8.25 (dd, *J* = 8.2 Hz, 1.2 Hz, H_a), 8.16 (d, J = 2.6 Hz, H_a), 8.07 – 8.04 (m, H_a + H_b), 8.01 – 7.95 (m, $2H_a$ + $4H_b$), 6.78 (bs, H_b), 6.76 (bs, H_a), 6.74 (bs, H_b), 6.71 (bs, H_a). ^{13}C-NMR (DMSO, 101 MHz) δ 196.99 (C_q), 196.97 (C_q), 156.51 (C^*_q), 156.45 (C^*_q), 155.10 (C_q), 152.18 (C_q), 135.71 (C_q), 135.39 (C_q), 134.97 (C_q), 133.14 (CH), 132.55 (C_q), 130.86 (C_q), 130.54 (C_q), 126.96 (CH), 126.69 (CH), 124.92 (CH), 122.47 (CH), 120.60 (CH), 86.88 (C_q), 86.84 (C_q), 86.42 (C_q), 86.36 (C_q). IR (neat): ν_{max} (cm^{-1}) = 3345 (br), 3258 (br), 1741 (w), 1722 (s), 1692 (s), 1651 (s), 1625 (m), 1398 (w), 1330 (m), 1269 (m), 1170 (m), 1118 (s), 1058 (m), 926 (w), 848 (w), 714 (w). MS (ESI): m/z calculated for $^{13}C^{12}C_{10}H_7F_3N_2O_4Na$ (M+Na) 312.03, found 312.0.

Second-order *k*-value determination of **3a,8a-dihydroxy-4-nitro-1,3,3a,8a-tetrahydroindeno[1,2-d]imidazole-2,8-dione (4i)**.
Following general procedure II using 1i as a starting compound, the calculated *k*-value was 2.1 $M^{-1}h^{-1}$. One regioisomer was obtained as an off-white solid. m.p.: >200 °C [deg.]. ^{1}H-NMR (DMSO, 400 MHz) δ: 8.55 (dd, *J* = 8.0 Hz, 0.7 Hz, 1H), 8.22 - 8.19 (m, 2H), 7.90 (t, *J* = 7.8 Hz, 1H), 7.32 (m, 1H), 6.87 (bs, 2H). ^{13}C-NMR (DMSO, 101 MHz) δ 196.23 (C_q), 156.59 (C_q*), 152.92 (C_q), 145.65 (C_q), 134.66 (C_q), 132.41 (CH), 131.94 (CH), 130.05 (CH), 86.90 (d, *J* = 9.1 Hz, C_q), 86.83 (d, *J* = 4.0 Hz, C_q). IR (neat): ν_{max} (cm^{-1}) = 3386 (m), 3049 (w), 2651 (w), 1735 (s), 1655 (s), 1610 (m), 1543 (m), 1406 (w), 1381 (w), 1346 (m), 1328 (w), 1203 (w), 1165 (w), 1130 (s), 1013 (w), 962 (w), 868 (w), 841 (w), 760 (w), 718 (s), 688 (w). MS (ESI): m/z calculated for $^{13}C^{12}C_9H_7N_3O_6Na$ (M+Na) 289.02, found 289.0.

Second-order *k*-value determination of **3a,8a-dihydroxy-6-nitro-1,3,3a,8a-tetrahydroindeno[1,2-d]imidazole-2,8-dione** and regioisomer **(3j and 4j)**.
Following general procedure II using 1j as a starting compound, the calculated *k*-value was 2.3 $M^{-1}h^{-1}$. The mixure of regioisomers in a 1.4:1 ratio was obtained as a brown solid. m.p.: >200 °C [deg.]. ^{1}H-NMR (DMSO, 400 MHz) δ: (3j) 8.68 (dd, *J* = 8.5 Hz, 2.1 Hz, 1H), 8.42 (d, *J* = 2.0 Hz, 1H), 8.21 (bs, 1H), 8.05 – 8.00 (m, 2H), 6.87 (bs, 2H). ^{13}C-NMR (DMSO, 101 MHz) δ (3j) 196.67 (C_q), 156.45(C^*_q), 156.39 (C_q), 148.89 (C_q), 132.89 (C_q), 131.11 (CH), 126.96 (CH), 118.66 (CH), 87.13 (C_q), 86.25 (C_q). ^{1}H-NMR (DMSO, 400 MHz) δ: (4j) 8.60 (s, 1H), 8.38 (d, *J* = 8.6 Hz, 1H), 8.15 (bs, 1H), 8.04 – 8.00 (m, 2H), 6.86 (bs, 2H). ^{13}C-NMR (DMSO, 101 MHz) δ (4j) 196.95 (C_q), 156.39 (C^*_q), 152.65 (C_q), 152.48 (C_q), 136.09 (C_q), 125.39 (CH), 125.19 (CH), 120.58 (CH), 87.01 (C_q), 86.28 (C_q). IR (neat): ν_{max} (cm^{-1}) = 3260 (br), 2922 (m), 2852 (m), 1721 (m), 1689 (s), 1651 (s), 1536 (s), 1403 (w), 1347 (s), 1200 (w), 1174 (m), 1116 (s), 938 (w), 910 (w), 845 (m), 731 (m), 686 (w), 643 (w). MS (ESI): m/z calculated for $^{13}C^{12}C_9H_6N_3O_6$ (M-H) 265.03, found 265.8.

5. Acknowledgement

This research was supported by the Dutch organization for Scientific Research (NWO-TTW, project 14433) and the Dutch Kidney Foundation. MEM acknowledges the Sectorplan Natuur- en Scheikunde (Tenure-track grant at Utrecht University) for financial support.

6. References

1. Ruhemann, S., Cyclic di- and tri-ketones. *J Chem Soc* **1910,** *97*, 1438-1449.
2. Ruhemann, S., CCXII.—Triketohydrindene hydrate. *J. Chem. Soc. Trans.* **1910,** *97* (0), 2025-2031.
3. MacFadyen, D. A., Determination of ammonia evolved from alpha-amino acids by ninhydrin. *J. Biol. Chem.* **1944,** *153* (2), 507-513.
4. Troll, W.; Cannan, R. K., A modified photometric ninhydrin method for the analysis of amino and imino acids. *J. Biol. Chem.* **1953,** *200* (2), 803-11.
5. Vonhofsten, B., Detection of fingerprints by the ninhydrin reaction. *Nature* **1954,** *173* (4401), 449-450.
6. Yemm, E. W.; Cocking, E. C., The determination of amino-acids with ninhydrin. *Analyst* **1955,** *80* (948), 209-213.
7. MacFadyen, D. A., On the mechanism of the reaction of ninhydrin with alpha-amino acids. I. Absorption spectra of ninhydrin and certain derivatives. *J. Biol. Chem.* **1950,** *186* (1), 1-12.
8. Friedman, M.; Sigel, C. W., A kinetic study of the ninhydrin reaction. *Biochemistry* **1966,** *5* (2), 478-85.
9. Hansen, D. B.; Joullie, M. M., The development of novel ninhydrin analogues. *Chem. Soc. Rev.* **2005,** *34* (5), 408-17.
10. Mccaldin, D. J., The chemistry of ninhydrin. *Chem Rev* **1960,** *60* (1), 39-51.
11. Roberts, C. W., The synthesis and properties of ninhydrin ureide. *J. Biol. Chem.* **1943,** *150*, 471-476.
12. Shapiro, R.; Chatterjie, N., Cyclization reactions of ninhydrin with aromatic amines and ureas. *J Org Chem* **1970,** *35* (2), 447-450.
13. Simakov, V. I.; Kurbatov, S. V.; Borbulevych, O. Y.; Antipin, M. Y.; Olekhnovich, L. P., Structures of condensation products of ortho-aminophenols with ninhydrin. *Russ Chem B+* **2001,** *50* (6), 1064-1067.
14. Devi, R. V.; Garande, A. M.; Maity, D. K.; Bhate, P. M., A serendipitous synthesis of 11a-hydroxy-11,11a-dihydrobenzo[e]indeno[2,1-b][1,4]diazepine-10,12-dione derivatives by condensation of 2-aminobenzamides with ninhydrin in water. *J. Org. Chem.* **2016,** *81* (4), 1689-95.
15. Chen, N. Y.; Zou, M. M.; Tian, X.; Zhu, F. J.; Jiang, D. P.; Cheng, J. G.; Shao, X. S.; Li, Z., Isomerization of ninhydrin-heterocyclic ketene aminal adducts: Kinetic versus thermodynamic control, solvent dependency and mechanism. *Eur J Org Chem* **2014,** (28), 6210-6218.
16. Leinweber, D.; Wartchow, R.; Butenschon, H., Synthesis, characterization, and some reactions of the tricarbonylchromium complexes of 1,3-indandione and Ninhydrin. *Eur J Org Chem* **1999,** (1), 167-179.
17. Becke, A. D., Density-functional thermochemistry .3. The role of exact exchange. *J. Chem. Phys.* **1993,** *98* (7), 5648-5652.
18. Bowden, K.; Rumpal, S., The hydration of indane-1,2,3-triones and related triones. *J Chem Res* **1997,** (2), 35.
19. Caputo, R.; Ferreri, C.; Palumbo, G.; Adovasio, V.; Nardelli, M., Ninhydrylurea: X-ray crystal s tructure and ^{13}C NMR spectrum. *Gazz. Chim. It.* **1987,** *117* (12), 731 - 738.
20. Kaupp, G.; Naimi-Jamal, M. R.; Schmeyers, J., Quantitative reaction cascades of ninhydrin in the s olid state. *Chem.: Eur. J.* **2002,** *8* (3), 594-600.

21. Azizian, J.; Karimi, A. R.; Soleimani, E.; Mohammadi, A. A.; Mohammadizadeh, M. R., Highly functionalized dihydrofuran derivatives: Synthesis by diastereoselective intramolecular Wittig reaction. *Heteroatom Chem* **2006,** *17* (4), 277-279.
22. Rifat, S.; Jahan, K.; Romman, U. K. R.; Akhter, K.; Halim, M. E., A green approach to synthesize and in vitro antimicrobial activity of indeno-imidazole derivatives and ninhydrin-nucleophile adducts. *Asian J. Chem.* **2016,** *28* (7), 1611-1616.
23. Marminon, C.; Nacereddine, A.; Bouaziz, Z.; Nebois, P.; Jose, J.; Le Borgne, M., Microwave-assisted oxidation of indan-1-ones into ninhydrins. *Tetrahedron Lett* **2015,** *56* (14), 1840-1842.
24. Hammett, L. P., The effect of structure upon the reactions of organic compounds benzene derivatives. *J. Am. Chem. Soc.* **1937,** *59*, 96-103.
25. Herbst, R. L.; Jacox, M. E., The effects of alkyl groups linked to conjugated systems. I. The alkaline hydrolysis of some ethyl *p*-alkylbenzoates. *J. Am. Chem. Soc.* **1952,** *74* (12), 3004-3006.
26. Hansch, C.; Leo, A.; Taft, R. W., A survey of Hammett substituent constants and resonance and f ield parameters. *Chem Rev* **1991,** *91* (2), 165-195.
27. Bowden, K.; Rumpal, S., Reactions of carbonyl compounds in basic solutions .23. The mechanism of the base-catalysed ring fission of 2,2-dihydroxyindane-1,3-diones. *J Chem Soc Perk T 2* **1997,** (5), 983-988.

7. Supporting information

Online available are plots of the inverse urea concentration in time for all kinetic experiments, calculated G vales for all ninhydrins, products and intermediates, ΔG values for all ninhydrins and intermediates, coordinates for optimized structures of all products and intermediates and ^{1}H- and ^{13}C NMR spectra of all new compounds.

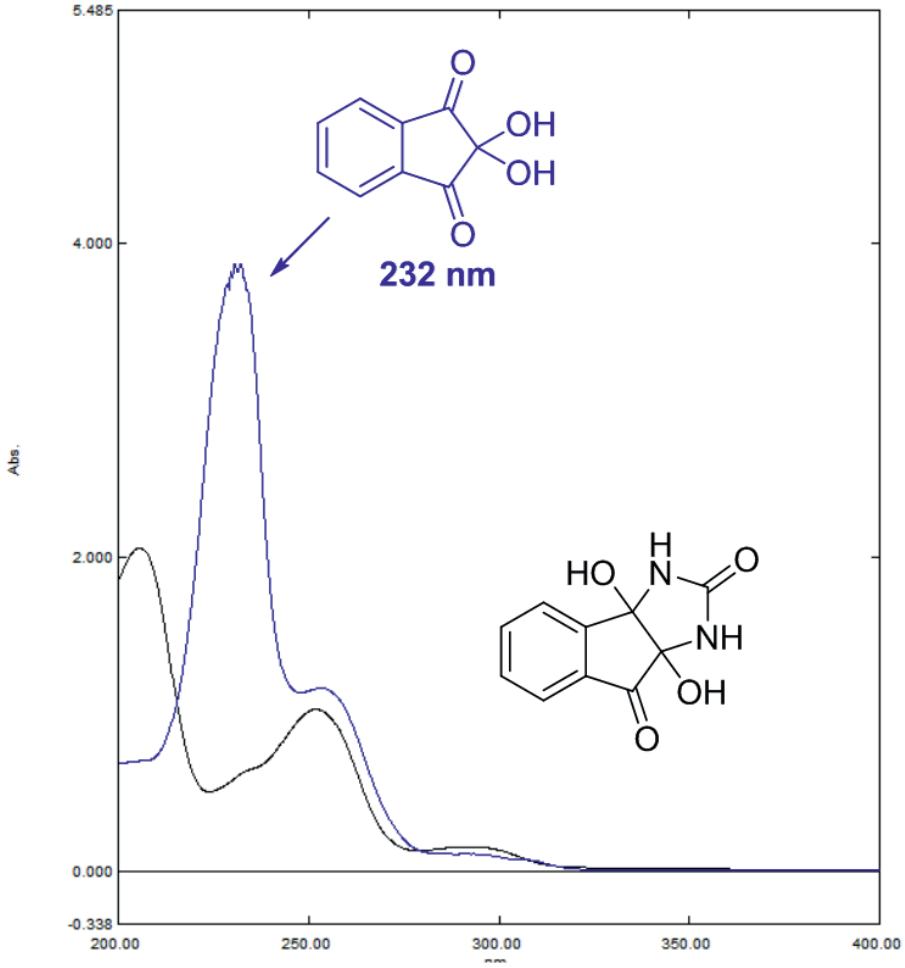

Figure S1: UV absorption spectrum of ninhydrin and 3a,8a-dihydroxy-1,3,3a,8a-tetrahydroindeno[1,2-d]imidazole-2,8-dione.

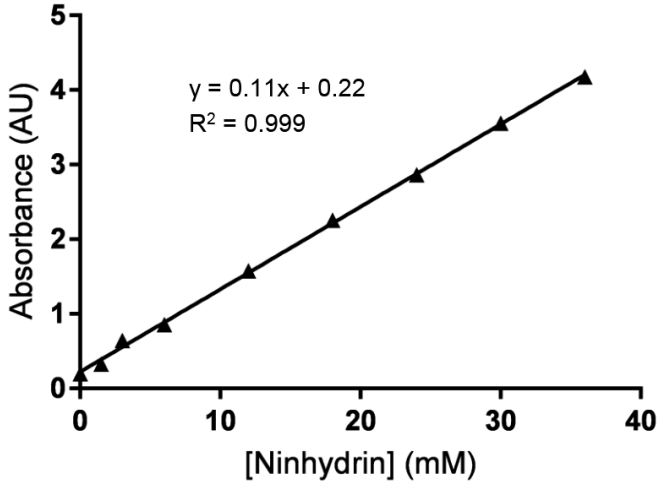

Figure S2: Calibration curve of absorption at 232 nm with the ninhydrin concentration.

Table S1: Measured ninhydrin concentrations in time. Conditions: 10 mM urea and given amount of ninhydrin in PBS at 50 °C. [a] Considered an outlier.

Initial [nin] (mM)	[nin] (mM) t=0 h	[nin] (mM) t = 0.083 h	[nin] (mM) t = 0.17 h	[nin] (mM) t = 0.25 h	[nin] (mM) t = 0.5 h	[nin] (mM) t = 1.0 h	Initial Rate (mMh^{-1})
5	4.66	5.00[a]	4.70	4.44	4.36	4.17	0.78
10	9.73	9.75	9.44	9.36	9.25	8.80	1.31
15	15.67	14.68	14.64	14.65	14.28	13.73	3.25
20	20.26	19.75	20.93[a]	19.54	19.19	19.52[a]	3.79

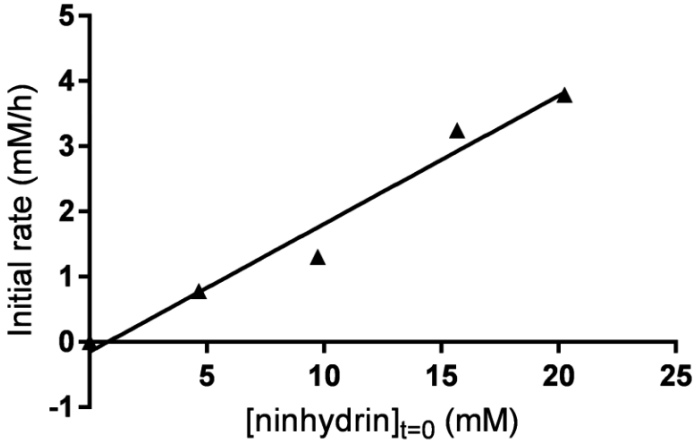

Figure S3: Plot of the initial rate versus the initial ninhydrin concentration. Linear regression gives y=0.20x-0.02, R^2 = 0.97.

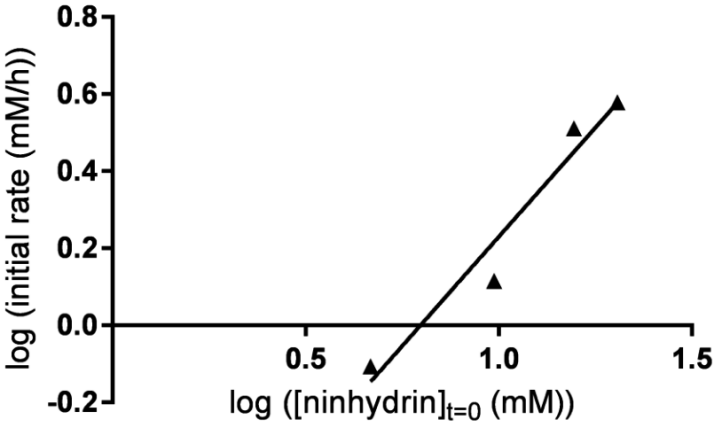

Figure S4: Plot of the logarithm of the initial rate versus the logarithm of the initial ninhydrin concentration. The slope of the linear regression corresponds to the order of ninhydrin in the reaction with urea. Linear regression gives y=1.13x-0.90, R^2 = 0.95.

Table S2: Measured urea concentrations in time. Conditions: 10 mM ninhydrin in PBS at 50 °C. [a] The urea concentration measured with the urease assay after addition of ninhydrin is lower than the actual concentration, probably due to the reaction of remaining ninhydrin with ammonia during the urea determination.

Initial [Urea] (mM)	[Urea] (mM)[a] t=0 h	[Urea] (mM) t= 0.083 h	[Urea] (mM) t=0.5 h	[Urea] (mM) t= 1.0 h	Initial rate (mMh^{-1})
5	4.0	4.0	3.6	3.2	0.82
10	8.7	8.7	7.8	7.3	1.52
15	13.9	13.6	12.4	11.3	2.61
20	18.9	18.7	16.4	13.4	4.03

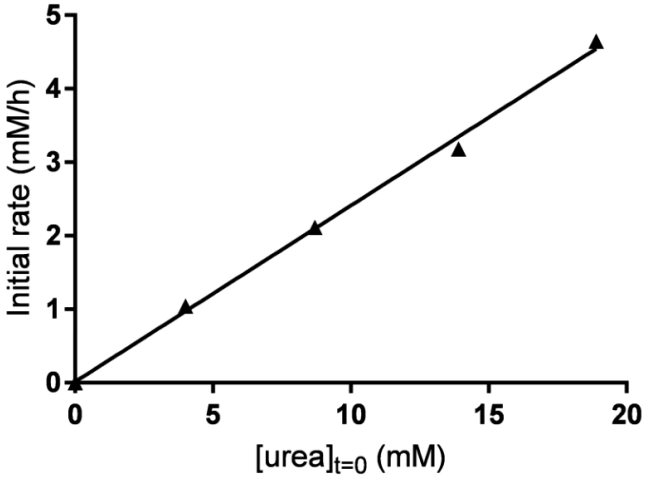

Figure S5: Plot of the initial rate versus the initial urea concentration. Linear regression gives y=0.24x+0.02, R^2=0.99.

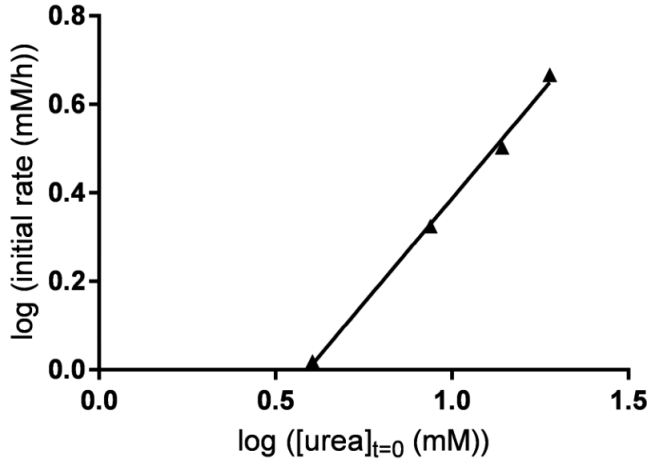

Figure S6: Plot of the logarithm of the initial rate versus the logarithm of the initial urea concentration. The slope of the linear regression corresponds to the order of urea in the reaction with ninhydrin. Linear regression gives y=0.95x-0.55, R^2 = 0.99.

pH Dependence of the rate of the reaction of ninhydrin with urea

The effect of pH on the reaction rate of ninhydrin with urea was tested in aqueous PBS at 50 °C (table S2). The results show that a more acidic medium decreased the rate. Presumably the acid labile hemiaminal bonds of product **3e** hydrolyze faster in acidic medium resulting in a reverse reaction and slower overall kinetics (scheme S1). To preserve a constant pH, phosphate buffered saline (PBS, pH = 7.4, Braun) was used during all experiments.

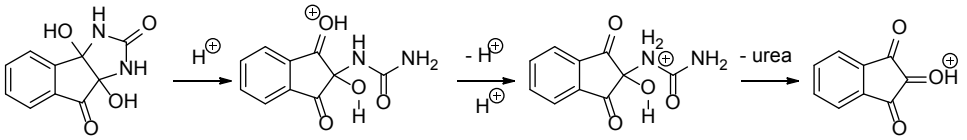

Scheme S1: Acid-promoted cleavage of urea from tetrahydroindeno-imidazole (proposed mechanism).

Table S3: The influence of the pH on the k_{obs} for the reaction of urea with ninhydrin at 50 °C.

Entry	Solvent	k_{obs} ($M^{-1}h^{-1}$)
1	PBS, pH = 6	3.6
2	PBS, pH = 7.4	6.8
3	PBS, pH = 9	7.5

Urea concentration determination by ^{13}C- NMR
Validation

To a solution of ninhydrin (89.1 mg, 0.5 mmol, 30 mM) in PBS (16.7 mL) ^{13}C-urea was added (30.5 mg, 0.5 mmol, 30 mM) and the mixture was stirred at 50 °C. Samples were taken and cooled to 0 °C directly every 2 hours. The urea concentration in these samples were determined by ^{13}C- NMR and by an urease assay (separate samples) according to the procedures described in Experimental Section. This experiment was performed in triplo.

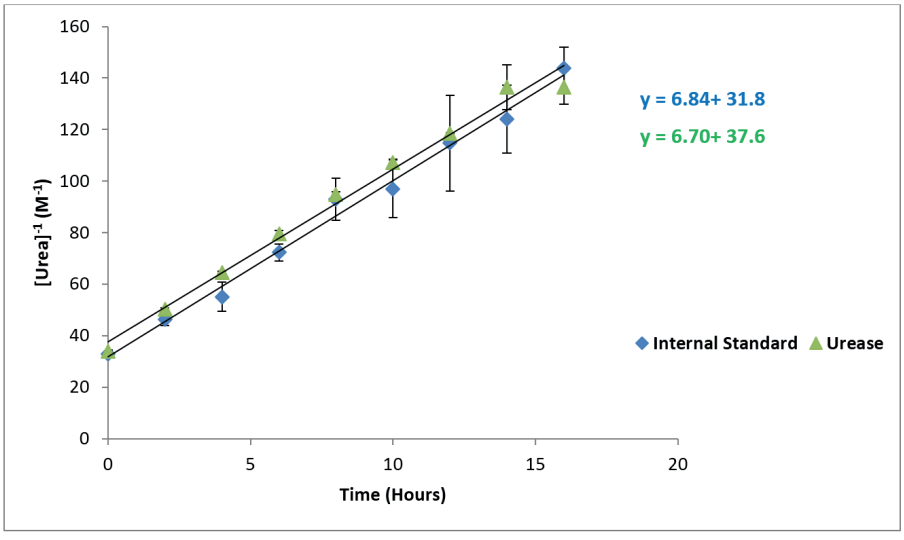

Figure S7. Determination of urea during the reaction with ninhydrin in PBS at 50 °C by quantitatine ^{13}C- NMR and by urease assay.

Table S4: $[Urea]^{-1}$ over time measured by the 13C - NMR and an urease assay, in triplo.

Time (hours)	$[Urea]^{-1}$ by ^{13}C-NMR #1 (M^{-1})				$[Urea]^{-1}$ by Urease (M^{-1})			
	#1	#2	#3	Standard deviation ^{13}C- NMR	#1	#2	#3	Standard deviation Urease
0	32.67	32.42	33.12	0.36	33.53	33.67	34.47	0.51
2	44.37	45.44	49.22	2.55	49.46	50.94	49.93	0.76
4	58.54	58.11	48.46	5.70	65.02	64.10	64.60	0.46
6	74.02	68.35	74.37	3.38	78.19	80.19	80.19	1.16
8	83.42	97.53	97.73	8.20	94.25	95.97	94.16	1.02
10	103.96	102.83	84.16	11.12	106.95	108.58	105.71	1.44
12	111.56	134.76	97.93	18.62	118.76	118.48	118.20	0.28
14	116.22	116.50	139.12	13.14	137.55	144.51	127.23	8.70
16	140.77	137.50	153.07	8.21	130.72	134.95	143.47	6.50

With the data from table S4 the k_{obs}-value for the reaction of ninhydrin with urea at 50 °C in PBS was determined three times with the ^{13}C-NMR method and three times with the urease assay. The k_{obs}-values, mean and standard deviation obtained in these experiments are listed in table S5.

Table S5: k_{obs}-Values of the reaction of ninhydrin with urea in PBS at 50 °C by ^{13}C-NMR and an urease assay.

Overview	k_{obs}-value ^{13}C-NMR ($M^{-1}h^{-1}$)	k_{obs}-value Urease ($M^{-1}h^{-1}$)
#1	6.53	6.58
#2	6.84	6.86
#3	7.15	6.67
stdev	0.31	0.14
mean	6.84	6.70

During the kinetic experiment the urea peak (162 ppm) decreases and a product peak (158 ppm) arises.

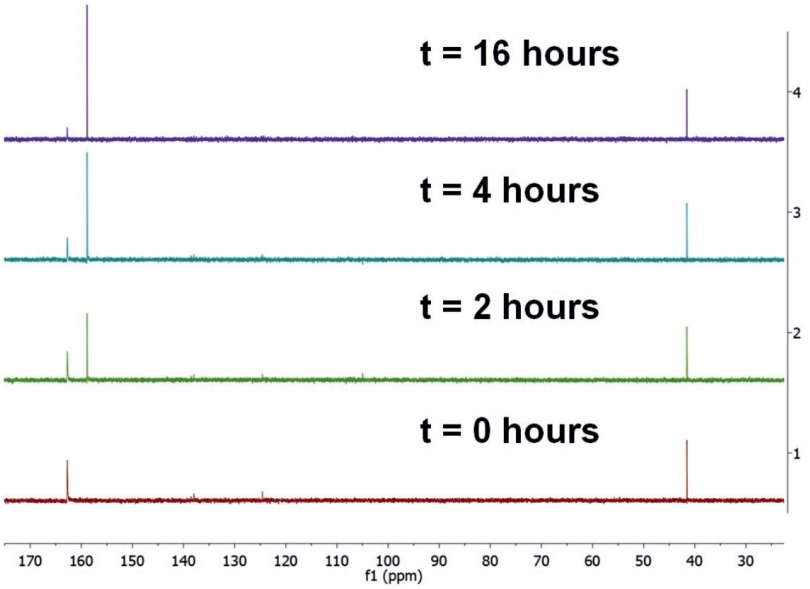

Figure S8: Quantitative ^{13}C- NMR spectrum over time. ^{13}C - labeled urea gives a signal at162.08 ppm and Me_2SO_2 (internal standard) gives a signal at 39.39 ppm).

Error analysis of quantitative ^{13}C- NMR

To increase the signal of the quaternary carbon in urea, the relaxation time was increased to 40 seconds. In that case, a linear correlation between the urea concentration and the urea : internal standard area ratio was found. To determine the urea concentration of an aqueous solution a calibration curve was made with the internal standard.

Duplicate measurements of the exact same sample resulted in deviating ratios. Four calibration curves, originating from four independent stock solutions, were made in the 5 - 30 mM range. The sets of dilutions were measured once, twice, thrice or four times (table S6). With increasing number of duplicate measurement of the same sample, the standard error of the mean and the error in the slope decreased whereas the slope and the intercept stayed similar. The standard deviation of 12 measurements was calculated for different number of scans per measurement (table S7). The standard deviation, and therefore the error in the measurement, strongly decreased as the number of scans is increased to 32 or higher. In order to save measuring time, 8 scans and the mean ratio of two measurements was used in all experiments. If necessary, depending on the purpose of the urea concentration determination, the number of scans or the number of measurements can be increased to decrease the error in the urea determination at the expense of the speed of the determination.

Table S6: Error analysis of quantitative ^{13}C-NMR method per number of duplicate measurements.

Number of duplicate measurements	Slope (*a*)	Error in *a*	Intercept (*b*)	Standard error
1	0.2318	0.014	0.2291	0.455
2	0.2418	0.007	0.1921	0.213
3	0.2293	0.006	0.2047	0.206
4	0.2315	0.009	0.1898	0.283

Table S7: Error analysis of quantitative ^{13}C-NMR method per increasing number of scans.

Number of Scans	Average Ratio	Std. Dev.	Relative Std. Dev
8	6.37	0.63	0.10
16	6.76	0.59	0.09
32	6.60	0.22	0.03
64	6.44	0.20	0.03
128	6.51	0.13	0.02

Computational data

DFT calculations were performed using the Gaussian 09 software package,[1] using B3LYP (Becke, three-parameter, Lee-Yang-Parr) functional with 6-31g(d,p) as basis set on all atoms. Structure optimizations were carried out with water as solvent without any symmetry restrains in water. Frequency analyses were performed on all calculations. Input: #B3LYP/6-31G(d,p) opt=tight freq scf=tight int=ultrafine pop=regular SCRF=(Solvent=Water).

Experimental vs Caluclated $K_{product}$ plot

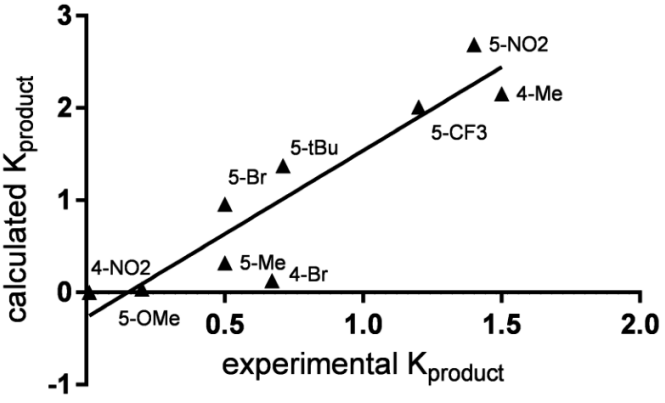

Figure S9: The plot of the experimental $K_{product}$ versus the calculated $K_{product}$. Linear regression gives y=1.8x-0.27, R^2=0.84.

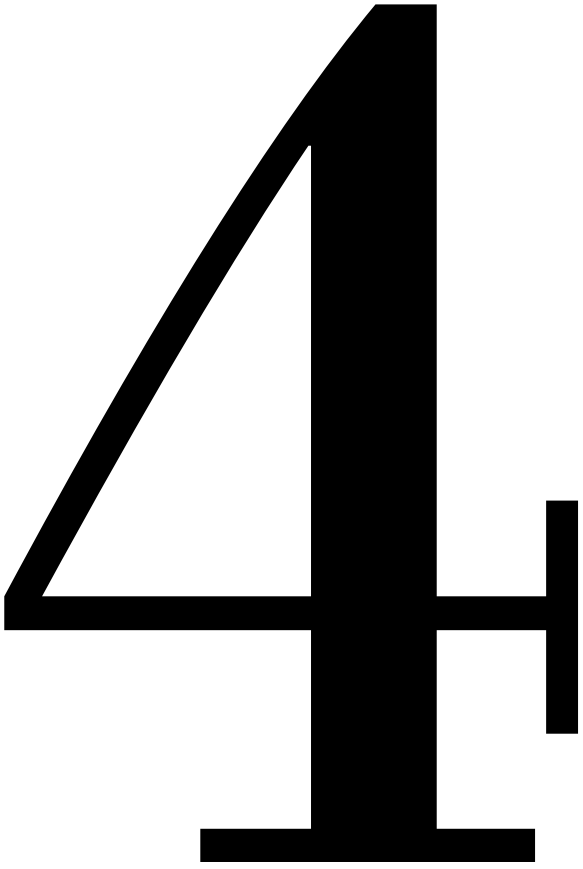

Chapter 4

Reactivity of (Vicinal) Carbonyl Compounds with Urea

Jacobus A.W. Jong[a,d], Robert Smakman[b], Marc-Etienne Moret[c], Marianne C. Verhaar[d], Wim E. Hennink[a], Karin G.F. Gerritsen[d] and Cornelus F. Van Nostrum[a,*]

[a] Department of Pharmaceutics, Utrecht Institute for Pharmaceutical Sciences (UIPS), Utrecht University, Universiteitsweg 99, 3584 CG Utrecht, the Netherlands.
[b] Innovista, Raadhuisstraat 1, 1393 NW Nigtevecht, the Netherlands.
[c] Organic Chemistry and Catalysis, Debye Institute for Nanomaterials Science, Utrecht University, Universiteitsweg 99, 3584 CG Utrecht, the Netherlands.
[d] Department of Nephrology and Hypertension, University Medical Centre Utrecht, Heidelberglaan 100, 3584 CX Utrecht, The Netherlands.

Published in: ACS Omega, 2019, 4, 7, 11928-11937
DOI: 10.1021/acsomega.9b01177

Abstract

Urea removal from dialysate is the major obstacle in realization of a miniature dialysis device, based on continuous dialysate regeneration in a closed loop, used for the treatment of patients suffering from end stage kidney disease. For the development of a polymeric urea sorbent, capable of removing urea from dialysate with high binding capacities and fast reaction kinetics, a systematic kinetic study was performed on the reactivity of urea with a library of low molecular weight carbonyl compounds in phosphate buffered saline (pH 7.4) at 323 K. It was found that di-aldehydes do not react with urea under these conditions, but need to be activated under acidic conditions and require the aldehyde groups in close proximity to each other to allow a reaction with urea. Among the 31 (hydrated) carbonyl compounds tested, triformylmethane, ninhydrin and phenylglyoxaldehyde were the most reactive ones with urea. This is attributed to the low dehydration energies of these compounds, as calculated by Gibbs free energy differences between the hydrated and the dehydrated carbonyl compound, which is favourable for the reaction with urea. Therefore, future urea sorbents should contain such functional groups at the highest possible density.

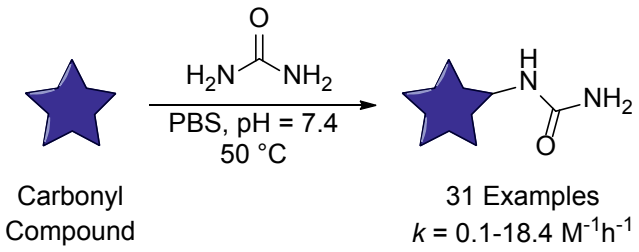

1. Introduction

In the human body urea is a metabolite of nitrogen-containing nutrients such as amino acids. These nutrients are metabolized in the liver into the toxic base ammonia, which is rapidly converted into urea by enzymatic processes. Urea is then transported through the bloodstream to the kidneys, where it is excreted into the urine.[1] The production of urea in the human body is 230-400 mmol per day.[1-2] The majority of patients suffering from end stage kidney disease undergoes single pass hemodialysis in a center 3-4 times per week in order to remove urea and other soluble waste products such as potassium, phosphate and organic compounds from their body. However, the frequent and long visits to a dialysis center compromise their participation in economic and social life. Home hemodialysis therefore offers more flexibility and autonomy for dialysis patients. However, a large complex dialysis machine is required at home in combination with a large supply of dialysis fluids (~120 L per treatment) or a bulky immobile water purification system which discourages many patients from selecting home hemodialysis. A miniature dialysis device based on continuous regeneration and reuse of dialysate in a closed-loop system, free from a fixed water supply, that can easily be used at home and during travel, would greatly enhance patient's freedom and autonomy.[3,4] It would also facilitate more frequent and longer hemodialysis enhancing blood purification, which is expected to improve clinical outcomes and quality of life.[5]

In current miniaturize dialysis devices that are under development, ion-exchangers are used to remove excess of ions such as phosphate and potassium while most organic waste solutes such as creatinine and uric acid can effectively be removed by activated carbon.[6] However, efficient urea removal is still a major obstacle in the development of a light-weight dialysis device.[7] In principle, three strategies to remove urea from blood dialysate are available: enzymatic conversion, electrochemical degradation and adsorption by a sorbent.[8] Enzymatic conversion by immobilized urease, which has been used in the first commercial portable dialysis device that was marketed from 1973 to 1993 (REDY), results in formation of ammonium (NH_4^+) and carbon dioxide (CO_2).[9] The ammonium is removed by a large quantity of zirconium phosphate ion exchanger which also captures calcium and magnesium ions that need to be replenished from a reservoir, which limits miniaturization of the device.[3, 10] Electrochemical degradation of urea into nitrogen (N_2), hydrogen (H_2) and carbon dioxide (CO_2) does allow miniaturization of hemodialysis. However, this urea removal method also produces harmful side-products such as active chlorine species and reaction products thereof such as chloroamines.[8] Therefore, ideally, a sorbent is applied that efficiently removes urea from dialysate by physi- or chemisorption. These sorbent materials are required to be stable, should not leach harmful compounds into the dialysate and should adsorb high quantities of urea from aqueous solution at a sufficient rate. Physisorption in general is a very fast, reversible and concentration dependent process. However all urea sorbents based

on physisorption known so far, such as activated carbon and zeolites, have relatively low affinity for urea and desorption will occur as the urea concentration in the dialysate decreases in time.[11-12] On the other hand, several polymeric chemisorbents that can bind urea covalently through carbonyl groups have been reported.[13-18] Despite the weak nucleophilicity of urea nitrogen it still can react with electrophilic carbonyl groups present in these sorbents such as glyoxaldehydes,[13, 15] ninhydrin-groups,[14] α-keto-esters[16] and oxidized alcohols.[17-18] Covalent urea sorbents with binding capacities up to 2.0 mmol/g have been reported. However, these materials suffer from slow urea binding kinetics at 37 °C, because only a part (1.2 mmol/g at most) of the urea-reactive groups has reacted after 8 hours, still requiring more than 330 grams of this material to remove the daily urea production (400 mmol).[19]

In the search for a more efficient polymeric urea sorbent suitable for incorporation in a miniature dialysis device, with high binding capacity and fast reaction kinetics, we performed a kinetic study on the covalent binding of urea with a library of low molecular weight carbonyl compounds. In literature, uncatalyzed covalent binding of urea (derivatives) in water has been reported with compounds such as ninhydrin,[20-22] aromatic glyoxaldehydes[23] and other aldehydes.[24] Based on these reports we systematically analyzed the kinetics of the reaction of several aromatic carbonyl compounds and non-aromatic analogues thereof with urea, in aqueous solution representative for dialysate, and determined the second order rate constant. It is expected that the kinetics of the reaction of carbonyl compounds with urea decreases upon incorporation of the carbonyl groups in a polymeric sorbent, due to substituent effects[22] and decreased accessibility of polymeric groups as compared with molecules in solution. Still, this fundamental knowledge can be used for the future design of urea sorbents with fast kinetics and high binding capacities.

2. Results and Discussion

A carbonyl compound can react with urea in a 1:1 molar ratio. Therefore, first order dependence in both urea and the carbonyl compound is expected according to equation 1. Indeed, in our previous work we analyzed the kinetics of urea with ninhydrin substituted with Electron Donating Groups (EDGs) and Electron Withdrawing Groups (EWGs) and concluded that the reaction of these ninhydrin derivatives with urea is first order in both urea and ninhydrin and thus second order overall.[22] Also the reaction of phenylglyoxaldehyde (PGA) with nucleophilic groups in enzymes such as NH_2 groups of arginine residues has been shown to be first order in PGA.[25-26]

$$(Eq.1)\ \frac{d[urea]}{dt} = -k_2[urea][carbonyl\ compound]$$

Quantitative ^{13}C-NMR was previously used as a robust method to determine the k_2-value of the reaction of urea with ninhydrin (scheme 1).[22] Using this method,

^{13}C-enriched urea and ninhydrin are reacted in stoichiometric amounts and therefore their relative concentrations remain equal throughout the reaction (equation 2). Simplification of equation 1 using equation 2 results in equation 3, in which the second order k_2-value is determined by only measuring urea concentrations in time.

$$(Eq.2)\ [urea] = [carbonyl\ compound]$$

$$(Eq.3)\ \frac{d[urea]}{dt} = -k_2[urea]^2$$

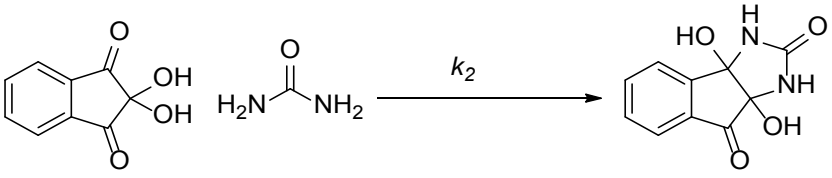

Scheme 1: The reaction of ninhydrin, a vicinal tricarbonyl hydrate, with urea.[21]

The influence of temperature on the rate of reaction of ninhydrin with urea was determined in phosphate buffered aqueous saline (PBS) at temperatures between 20 °C (293 K) and 70 °C (343 K). The second order k_2-values were determined from the plot of the inverse urea concentration in time (figure S2) and the ln(k_2) values were plotted against the inverse of the absolute temperature in the Arrhenius plot (figure 1). Linear regression and use of Arrhenius equation resulted in a pre-exponential constant (A) of (23.3 ± 0.6) × 10^9 $M^{-1}h^{-1}$ and an activation energy (E_a) of 14.0 ± 0.4 kcal/mol. To have reasonably fast kinetics, the reaction of the carbonyl compounds with urea was carried out at 323 K unless stated otherwise.

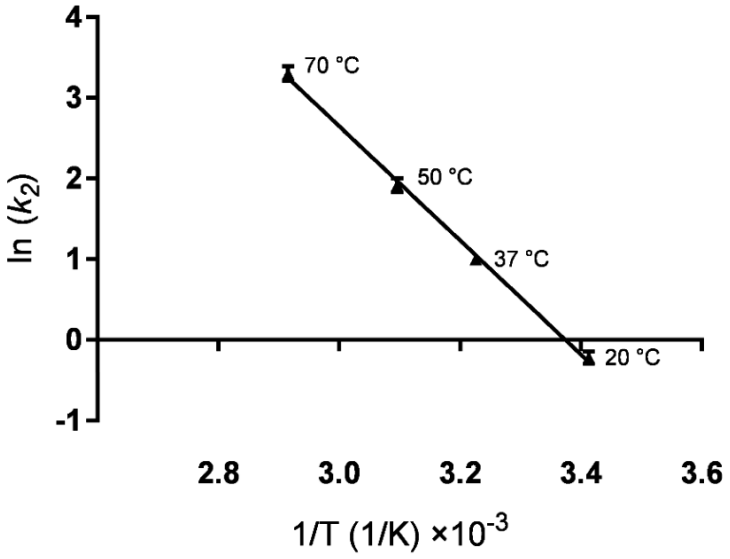

Figure 1: Arrhenius plot of the reaction of ninhydrin with urea in PBS. Linear regression gives ln (k_2) = -7073 (1/K) + 23.87. Arrhenius equation: ln (k_2) = (-E_a/RT) + ln (A), thus -E_a/R = -7073 K and ln (A) = 23.87.

First, hydrates of a variety of similar vicinal tri- and tetra-ketones were reacted with urea in PBS at 323 K. The structures of the tested carbonyl compounds and the corresponding k_2-values are listed in table 1. 2,2-Dihydroxy-4,4,5,5-tetramethylcyclopentane-1,3-dione (entry 2) is an aliphatic analog of ninhydrin and was tested to investigate the influence of the aromatic ring on the reactivity of the vicinal triketone with urea. 2,2,3,3-Tetrahydroxy-2,3-dihydronaphthalene-1,4-dione (entry 3) is an analogue of ninhydrin that consists of four vicinal ketones of which two form hydrates. To increase the number of urea-reactive groups per gram of material also 2,2,6,6-tetrahydroxy-s-indacene-1,3,5,7(2H,6H)-tetraone (entry 4), which contains two triketone groups, was tested, together with its non-aromatic analog 2,2,5,5-tetrahydroxy-3a,6a-dimethyl-6-methylenetetrahydropentalene-1,3,4(2H)-trione (entry 5).

Table 1: Structural formulas of tested vicinal ketone hydrates and the determined k_2-values of their reaction with urea in PBS at 323K. [a] Compound is probably converted into ninhydrin during the reaction with urea.[27] [b] Tested in 1:1 (v/v) DMSO:PBS at 343K due to its low aqueous solubility.

Entry	Structure	k_2 ($M^{-1}h^{-1}$)
1	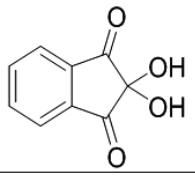	6.8 ± 0.6
2	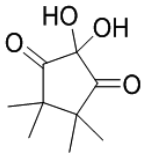	<0.1
3	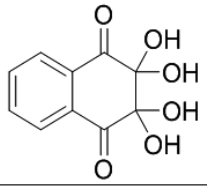	0.55 ± 0.07[a]
4	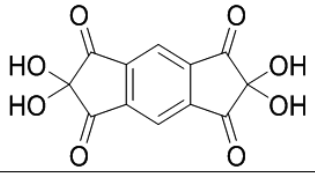	0.32 ± 0.09[b]
5	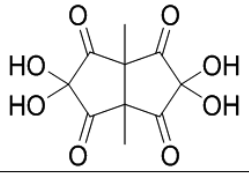	<0.1

Only the aromatic derivatives of the tested vicinal ketone hydrates in table 1 (entry 1,3, and 4) reacted with urea. The urea concentration in the reaction mixture containing oxolin (entry 3) did decrease in time, however the shift of the urea carbon peak in the ^{13}C-NMR of the product corresponds to the shift of the same carbon in the ninhydrin-urea adduct (figure S1). This suggests that the decrease in the urea concentration is not because of the reaction of oxolin with urea, but rather due to the conversion of oxolin into ninhydrin,[27] that subsequently reacts with urea forming the ninhydrin-urea product. In this case the equations 1-3 are invalid and the rate observed cannot be used to calculate *k*-value of oxolin with urea. Interestingly, the k_2 value of the reaction of entry 4 with urea substantially decreased by a factor ~20 when compared to ninhydrin (entry 1), presumably due to the presence of two EWGs on the opposite site of the aromatic ring, that

decreases the rate of dehydration of the hydrate which is a required step to allow subsequent reaction with urea.[22]

Because phenylglyoxaldehyde (PGA) has been reported to react with urea derivatives,[23] this compound (table 2, entry 6) as well as an aliphatic analogue (entry 7) were tested for reaction with urea. To increase the amount of urea-reactive groups per gram of material, also 2,2'-(1,3-phenylene)bis(2-oxoacetaldehyde), a compound with an aromatic ring with two glyoxaldehyde functionalities, was tested (entry 8). For the reaction of phenylglyoxaldehyde with urea, the inverse of the urea concentration in time showed a non-linear correlation (figure S5). Identification of the isolated reaction product after 24 hours at 323 K in PBS by ^{1}H- and ^{13}C-NMR spectroscopy showed that the initially formed urea-PGA product reacted with another equivalent of PGA. This means that the urea concentration did not remain equal to the PGA concentration during the reaction and equation 2 and 3 are therefore invalid, explaining the non-linear correlation observed in the plot of the inverse urea concentration in time. Scheme 2 shows the reaction of PGA with urea (A) and the proposed mechanism for the formation of the isolated product (B). Since the final product was isolated in a 57% yield with respect to PGA, and is therefore the major formed product, the reaction of the 1:1 adduct with a second molecule of PGA must be faster than the initial reaction of urea with PGA.

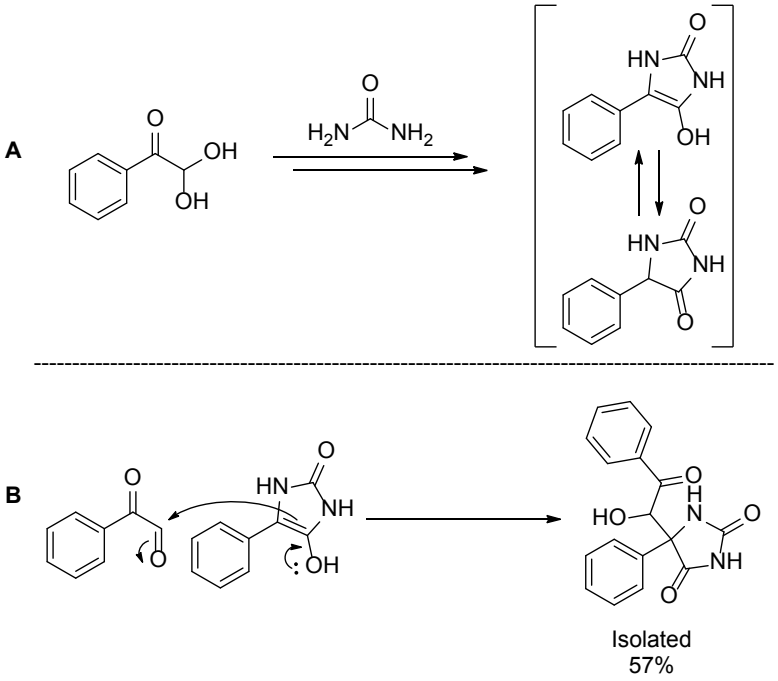

Scheme 2: A) The reaction of hydrated PGA with urea. B) Proposed mechanism of the reaction of the 1:1 PGA urea adduct with a second PGA molecule. Conditions: 0.5 mmol urea and 0.5 mmol PGA in 16.7 mL PBS (30 mM of urea and PGA) at 50 °C.

The k_2-values of the reaction of the glyoxaldehydes (table 2 entry 6, 7 and 8) with urea were determined from the initial slope of the plot of the inverse urea concentration in time using second order polynomial regression (figure S5). The k_2-values for the different glyoxaldehydes tested are listed in table 2. To validate whether the slopes of the lines of figure S5 can indeed be used for the calculation of the second order reaction rate constants, PGA was reacted with an excess (3-50 equivalents) of urea to decrease the probability of the reaction of the 1:1 adduct with another PGA molecule. Thus, pseudo-first order (PFO) conditions were obtained and the rate constants (k_{PFO}) were measured. In a control experiment, ninhydrin (30 mM) was reacted with 5 equivalents of urea (150 mM) in PBS and the k_{PFO}-value was determined to be 1.0 ± 0.1 h^{-1} (figure S6), which corresponds to a k_2 of 6.7 $M^{-1}h^{-1}$ (1.0 h^{-1}/0.15 M = 6.7 $M^{-1}h^{-1}$) which is similar to the k_2 for ninhydrin (table 1, entry 1). This validates that the k_{PFO} can indeed be used to determine the k_2 for the reaction of the carbonyl compound with urea.

The k_{PFO}-values for the reaction of PGA with excess urea were plotted against the [urea] (figure S8) and this figure shows that k_2 (as defined of the derivative of dk_{PFO}/d[urea]) is not proportional with [urea], but decreases with increasing urea concentration. This is likely because the dielectric constant of the medium changes, which influences the reactivity of PGA greatly.[25-26, 28] Determination of k_2 for PGA by extrapolating k_{PFO} to 30 mM using polynomial regression resulted in a k_2 of 3.7 $M^{-1}h^{-1}$ (figure S8 and table S3), which is similar to k_2 determined by the initial slope of the plot of the inverse urea concentration in time (table 2, entry 6), thereby validating that this method is an accurate method to determine the k_2 of glyoxaldehydes.
As for the vicinal ketone hydrates, the aromatic glyoxaldehyde (entry 6) showed a faster reaction with urea than the aliphatic (entry 7) and doubly substituted analogues (entry 8), the latter presumably also due to the decreased rate of dehydration of the hydrate in the presence of the meta positioned EWG.

Table 2: Structural formulas of tested glyoxaldehydes and the corresponding k_2 of their reaction with urea in PBS at 323 K.

Entry	Structure	k_2 ($M^{-1}h^{-1}$)
6	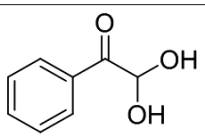	3.7 ± 0.1
7	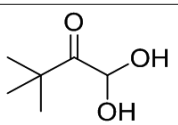	1.2 ± 0.0
8	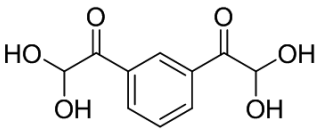	0.78 ± 0.07

The enol form of triformylmethane (TFM), entry 9 of table 3, is a very electrophilic aldehyde which has been reported to react with urea to yield an enamine (scheme 3).[24] To further investigate the reaction of urea with other aldehydes than TFM, one monoaldehyde and several dialdehydes were selected and their reaction kinetics with urea were tested (entry 10-13). In addition, electron-poor perfluorated ketones and aldehydes were also tested (entry 14 and 15), as well as a strained 4-membered ring diketone (entry 16) and a dialdehyde that potentially forms an aromatic system upon reaction with urea (entry 17 and scheme S1). The structures of the selected aldehydes and ketones and the corresponding k_2-values are listed in table 3.

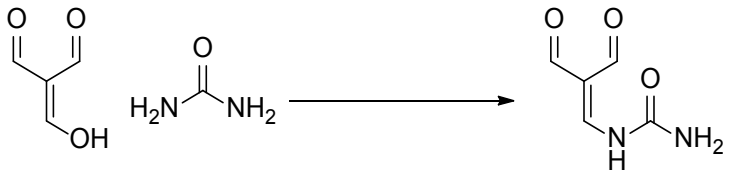

Scheme 3: The reaction of triformylmethane with urea.[24]

Table 3: Structural formulas of tested aldehydes and ketones and the determined k_2-values of their reaction with urea in PBS at 323 K. [a] Measured at 293 K instead of 323 K to decrease the reaction rate. [b] 1,1,3,3-Tetramethoxypropane was stirred in PBS at pH 2 for 30 minutes at RT, after which the pH was adjusted (to pH 2 or 7.4) and urea was added to the reaction mixture. [c] 2,5-Dimethoxytetrahydrofuran was stirred in PBS at pH 2 for 30 minutes at RT, after which the pH was adjusted (to pH 2 or 7.4) and urea was added to the reaction mixture. [d] Measured both in PBS and 1:1 PBS:DMSO as solvent at 323 K.

Entry	Structure	k_2 ($M^{-1}h^{-1}$) in PBS pH 7.4	k_2 ($M^{-1}h^{-1}$) in PBS pH 2.0
9	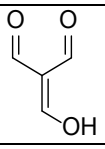	18.4 ± 5.2[a]	
10	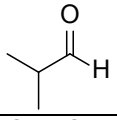	<0.1	<0.1
11[b]		<0.1	18.1 ± 2.3
12[c]	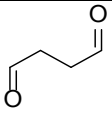	<0.1	10.8 ± 0.8
13	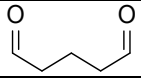	<0.1	1.0 ± 0.1
14	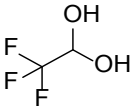	<0.1 [d]	
15	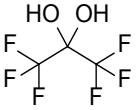	<0.1 [d]	
16	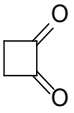	<0.1[d]	
17	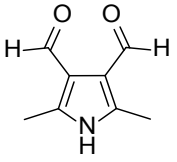	<0.1 [d]	

In the reaction mixture of urea with TFM (entry 9) the urea concentration dropped very rapidly and remained constant after the first measurement at 30 minutes and 323 K. Therefore, besides reacting with urea, we assume that TFM was completely consumed by reacting with itself within this timeframe (as reported by others, see scheme S2).[29] In order to determine the k_2-value with sufficient accuracy, the reaction temperature was lowered to room temperature (293 K) and the initial slope of the plot of inverse TFM concentration versus time (figure S9) showed a k_2-value of 18.4 $M^{-1}h^{-1}$, which is 23 times faster than the reaction of urea with ninhydrin at the same temperature (figure 1, table S2) making TFM a very interesting compound to build in a urea sorbent.

In contrast to entry 9, the mono-aldehyde (entry 10) and the 1,1- 1,2- and 1,3-dialdehydes (table 3, entries 11-13) did not react with urea within 24 hours at 323 K and pH 7.4. To allow the initially formed hemi-aminal to dehydrate and form a more stable imine, the pH was decreased to pH 2 (at this pH urea is not protonated, pK_a 0.1).[30] Under these conditions the mono-aldehyde still did not react with urea, whereas the di-aldehydes did react with urea (table 3, entry 11, 12 and 13). The formed hemi-aminal will be in equilibrium with the (hydrated) aldehyde. However, the presence of a second aldehyde group makes a second intramolecular nucleophilic attack of urea possible, thereby driving the equilibria towards the urea-bound aromatic product (scheme 4). The results presented in table 3 show that the kinetics of the reaction with urea decreased with increasing number of carbon atoms between the two aldehyde groups, presumably due to the decreasing mutual inductive electron withdrawing effect of the aldehydes. Also, intramolecular ring closure likely becomes less favorable when the distance between the urea nitrogen and the aldehyde increases.

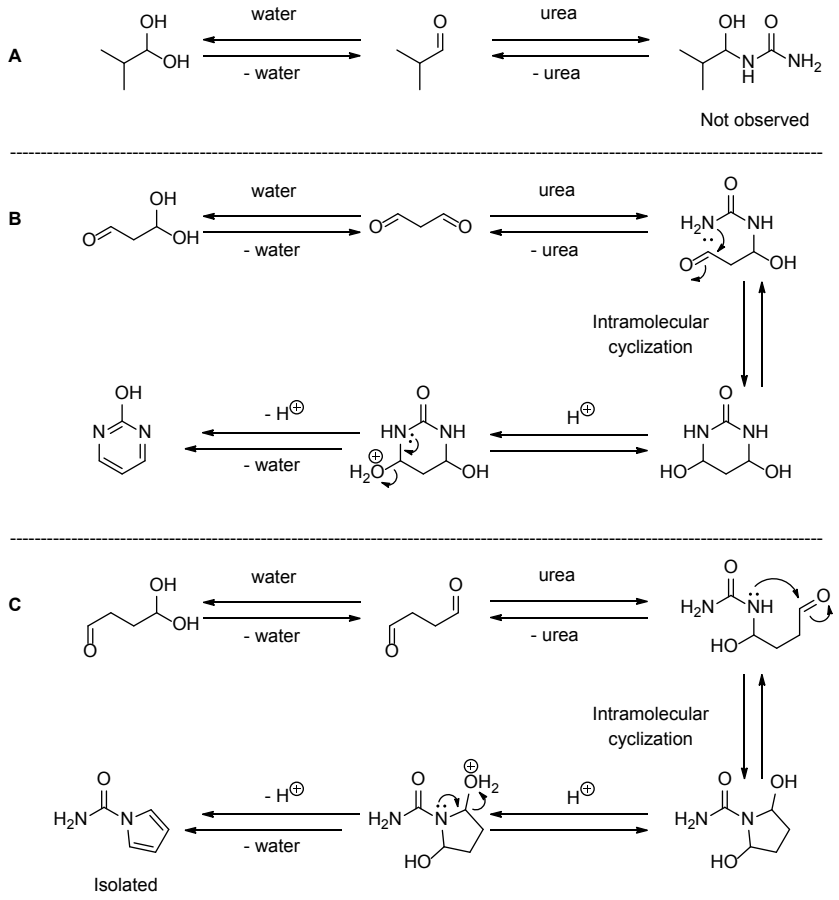

Scheme 4: A) Proposed mechanism of the equilibrium between a mono-aldehyde and urea in H_2O; B) Proposed mechanism of the acid-catalyzed terminating reaction between a 1,3-di-aldehyde and urea in H_2O,[31] and C) between a 1,4-di-aldehyde and urea in H_2O.

Based on these results we conclude that in order to drive the equilibrium with water towards the urea-adduct, at least two carbonyl groups in close proximity are required allowing urea to react with both its nitrogens, forming a 5- or 6-membered ring. TFM did not undergo an intramolecular ring closure towards a cyclic product at pH 7.4, because it can easily form a stable enamine at this pH (scheme 3). Maltsec *et al*. have shown that under acidic conditions TFM, like the di-aldehydes tested (entries 11, 12 and 13), undergoes an intramolecular ring closure into a 6-membered ring.[32]

The electron deficient fluorinated aldehyde and ketone hydrates (entries 14 and 15) did not react with urea under the applied experimental conditions. Also, cyclobutanedione (entry 16) did not react with urea, despite that the reaction with urea could cause release of ring strain because the hybridization of the carbonyl

carbon would change from sp^2 to sp^3 upon reaction with urea (table 3, entry 16). The one with the possibility to form an aromatic system upon reaction with urea (table 3, entry 17) as the possible driving forces did not react with urea, like many other carbonyl compounds that were expected to react with urea but did in fact not (listed in table S1).

To understand why certain carbonyl compounds and hydrates such as ninhydrin and PGA react with urea whereas carbonyl compounds and hydrates such as hexafluoroacetone (entry 15) and 2,2-dihydroxy-4,4,5,5-tetramethylcyclopentane-1,3-dione (entry 2) do not, we calculated the changes in Gibbs free energy (ΔG) for these reactions using a computational model that we used in our previous study on the reaction of ninhydrin derivatives with urea.[22] Most of the carbonyl compounds that we tested are predominately present in their hydrated forms. Consequently, the first step in the reaction mechanism is the dehydration of the hydrate and thus the formation of the carbonyl (shown in scheme 5 for ninhydrin).[22, 33] The ΔG of the dehydration of the carbonyl compound was calculated ($\Delta G_{dehydration}$) as well as the subsequent reaction of the dehydrated carbonyl compound with urea to form the intermediate adduct ($\Delta G_{intermediate}$).

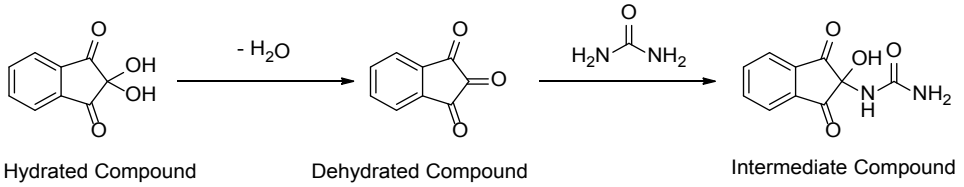

Scheme 5: The dehydration of ninhydrin and subsequent reaction with urea.

Table 4: Structural formulas, rate constants (323 K in PBS, pH 7.4) and $\Delta G_{dehydration}$ and $\Delta G_{intermediate}$ of selected aldehydes and ketones. [a] Measured at 293 K in PBS pH 7.4. [b] Data also reported in our earlier work.[22] [c] Measured at 343 K PBS:DMSO 1:1 (v/v). [d] Oxolin is converted into ninhydrin.

Entry	Hydrated Compound	k_2-value ($M^{-1}h^{-1}$)	$\Delta G_{dehydration}$ (kcal/mol)	$\Delta G_{intermediate}$ (kcal/mol)
A	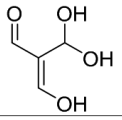	18.4±5.2[a]	-10.7	14.1
B[b]	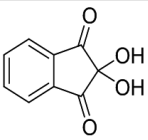	6.8±0.6	-0.8	5.4
C	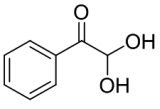	3.7±0.1	-6.1	7.6

Entry	Hydrated Compound	k_2-value ($M^{-1}h^{-1}$)	$\Delta G_{dehydration}$ (kcal/mol)	$\Delta G_{intermediate}$ (kcal/mol)
D	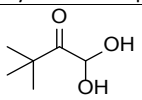	1.2 ± 0.0	-5.7	8.8
E	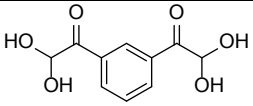	0.78 ± 0.07	-3.5	9.2
F	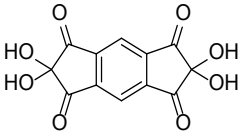	0.32 ± 0.09[c]	0.4	4.3
G	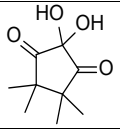	<0.1	1.4	3.9
H	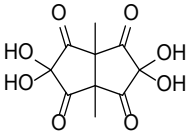	<0.1	0.0	4.3
I	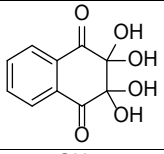	<0.1 [d]	2.3	8.3
J	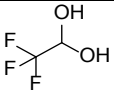	<0.1	1.3	2.9
K	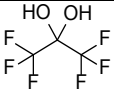	<0.1	5.1	2.5

By using a continuum solvent model as an approximation in the calculations, the solvation effects might not be accurately represented because the model does not include interactions such as hydrogen bonding. Additionally, the contribution of translational entropy to the Gibbs free energy in the gas phase may be inaccurately treated in solution. For these reasons, the obtained ΔG-values should not be considered absolute values, but they can be compared relatively to each other as all reactions are dehydration or condensation reactions. In fact, actual $\Delta G_{dehydration}$ should be positive in most cases because the compounds listed in table 5 are present as the hydrate in water (with exception of TFM, entry A), and the free energy of the hydrate should be lower than the free energy of the corresponding carbonyl compound. NMR analysis showed that TFM is indeed mainly present in its non-hydrated form, which corresponds to the lowest calculated $\Delta G_{dehydration}$ for this compound. Interestingly, the compounds that react with urea at 323 K (entries A-E) show a low ΔG value for dehydration (-10.7 to -3.5 kcal/mol), whereas the hydrates that show a relatively high value for dehydration (0.0 to 5.1 kcal/mol) react

slowly (entry F) or not (entries G-K) with urea at 343 K. This shows that the Gibbs free energy for dehydration of carbonyl compounds gives a good indication for the reaction rate of the carbonyl compound with urea, and can be used to screen promising carbonyl compounds.

TFM shows a rapid reaction with urea (table 4, entry A) despite the high $\Delta G_{intermediate}$ because it is primarily dehydrated in solution. Ninhydrin (entry B) has a less favorable dehydration, but a relatively low $\Delta G_{intermediate}$ and shows relatively fast kinetics for the reaction with urea as compared to the other hydrated carbonyl compounds. A clear trend that lower values of $\Delta G_{dehydration}$ and $\Delta G_{intermediate}$ coincide with a fast reaction rate with urea is observed for entries C-E. Carbonyl compounds F-K all have a relatively high $\Delta G_{dehydration}$, therefore the concentration of the urea-reactive species will be low, resulting in a rate-constant < 0.1 $M^{-1}h^{-1}$.

3. Conclusions

In our aim to design an efficient polymeric urea sorbent, the kinetics of the reaction of urea with carbonyl compounds was systematically analyzed. TFM, ninhydrin and PGA showed the fastest kinetics of their respective class of compounds among the ones tested. Importantly, in order to react with urea, at least two carbonyl groups are needed in close proximity to allow both nitrogens of urea to react, resulting in the formation of a stable 5- or 6-membered ring and effectively driving the equilibrium with water towards the urea adduct. This trend is shown for vicinal triketones, glyoxaldehydes and di-aldehydes. TFM, a tri-aldehdye that is predominately present in its dehydrated form, showed the highest reaction rate with urea and did not form a cyclic product but a stable enamine instead. Computational studies suggest that for carbonyl compounds with a relatively high $\Delta G_{dehydration}$ the dehydration of the hydrate is unfavorable and therefore the concentration of the urea-reactive species is low resulting in a very slow, often not measurable, reaction with urea.

In order to design urea sorbents with fast reaction kinetics at physiological conditions, suitable for incorporation in a miniature dialysis device, the focus should be on introducing a high density of functional groups such as TFM, ninhydrin or PGA, in for example a polymer matrix.

4. Material and Methods

4.1 General

All chemicals were obtained from Sigma-Aldrich (Zwijndrecht, the Netherlands) and used as received unless stated otherwise. Phosphate buffered saline (PBS, pH = 7.4, ion composition: Na^+ 163.9 mM, Cl^- 140.3 mM, HPO_4^{2-} 8.7 mM, $H_2PO_4^-$ 1.8 mM) was obtained from B. Braun (Melsungen AG, Germany). 1,1,3,3-Tetramethoxypropane

and 2,6-dimethylhepta-2,5-dien-4-one (phorone) were obtained from Combi Blocks (CA, USA). 4-Bromo-2-hydroxybenzaldehyde and 1,1'-(1,3-Phenylene)bis(ethan-1-one) were obtained from AK Scientific (CA, USA). 2-Phenylmalonaldehyde was obtained from Apollo Scientific (Manchester, UK). 2,2,3,3-Tetrahydroxy-2,3-dihydronaphthalene-1,4-dione and [1,1'-biphenyl]-2,2'-dicarbaldehyde were obtained from Santa Cruz Biotechnology (CA, USA). 1,1-Dihydroxy-3,3-dimethylbutan-2-one was obtained from Enamine (NJ, USA). 3-Isothiocyanatoprop-1-ene was obtained from FluoroChem (Hadfield, UK). NMR spectra of the different compounds were recorded on an Agilent 400-MR DD2 equipped with a OneNMR probe or a Bruker 600 MHz with a BBI probe at RT. The quantitative 1D ^{13}C- NMR experiments were carried out on the Agilent 400-MR DD2 using the standard s2pul.c pulse system with a spectral width of 24038.5 Hz and an acquisition time of 1.363 seconds. Residual solvent signals were used as internal standard (^{1}H: δ 2.50 ppm, ^{13}C (^{1}H): δ 39.52 ppm for DMSO-d_6, ^{1}H: δ 7.26 ppm, ^{13}C (^{1}H): δ 77.16 ppm for $CDCl_3$, ^{1}H: δ 5.32 ppm, ^{13}C (^{1}H): δ 53.84 ppm for CD_2Cl_2). Chemical shifts (δ) are given in ppm and coupling constants (J) are given in hertz (Hz). Resonances are described as s (singlet), d (doublet), t (triplet), q (quartet), bs (broad singlet) and m (multiplet) or combinations thereof. UV absorption spectra and intensities were recorded with a BMG LABTECH SpectroStar Nano platereader using UV-Star Microplate 96 well obtained from Greiner Bio-One (Alphen aan de Rijn, the Netherlands). Flash chromatography was performed over silica gel (particle size 40-63 µm, VWR Chemicals, Leuven, Belgium) using the indicated eluent. Thin Layer Chromatography (TLC) was performed using TLC plates from Merck Darmstadt, Germany, (SiO_2, Kieselgel 60 F254 neutral, on aluminum with fluorescence indicator) and the compounds were visualized by UV detection (254 nm).

4.2 General procedure for the kinetic analysis of the carbonyl compounds with urea.

The carbonyl compound of interest (0.5 mmol, 1.0 eq.) was dissolved in 16.7 mL PBS or a 1:1 (v/v) mixture of DMSO and PBS. ^{13}C-labeled urea (31.5 mg, 0.5 mmol, 1.0 eq.) was added to the solution, and the mixture was stirred magnetically at the indicated temperature for 2 - 96 hours. Samples from the reaction were taken at different time points and the urea concentrations in the different samples were determined by quantitative ^{13}C- NMR (see below). The kinetic experiment was continued until more than 50% conversion was reached or when the urea concentration remained constant. The k_2-values for the carbonyl compounds were determined from the plots of 1/[urea] versus time.

4.3 Determination of urea concentration by ^{13}C-NMR.[22]

For the calibration curve a stock solution of ^{13}C-labeled urea in PBS (50 mM) was prepared and diluted to 5, 10, 15, 20, 25, 30 and 35 mM. A solution of Me_2SO_2

in D_2O (1.50 mmol in 1000 µL, 1.34 M) was prepared and added to the analytes in a 10:1 ratio (1000 µL analyte and 100 µL internal standard). The mixture was shaken and 600 µL was transferred into an NMR tube. For reaction mixtures in 1:1 PBS:DMSO, 200 µL of internal standard solution was added to 1000 µL of reaction mixture and transferred into an NMR tube. During the 1D ^{13}C- NMR experiments (101 MHz) proton signals were decoupled. FIDs were Fourier transformed and automatic phase correction, third order polynomial baseline correction and automatic integration were applied with MestReNova Version 10.0.2-15465. Intra- and interassay coefficients of variation were within 10%. Ratio of integrals for urea at 162.08 ppm and internal standard at 42.15 ppm were compared with those of the calibration curve for calculating urea concentration in the samples.

4.4 Identification of urea-dialdehyde adduct under acidic conditions.

2,5-Dimethoxytetrahydrofuran (mixture of cis and trans) (0.5 mmol, 1.0 eq.) was dissolved in PBS and the pH was adjusted with 1M HCl to pH 2 and stirred for 30 minutes at RT. Urea (300.3 mg, 5 mmol, 10 eq.) was added and the reaction mixture was heated to 50 °C and stirred for 5 hours. The mixture was allowed to cool to RT and freeze dried. The crude mixture was purified over silica (EtOAc:MeOH 19:1) and the ^1H-NMR spectra of the isolated compound corresponded with 1H-pyrrole-1-carboxamide.[34]

4.5 Determination of carbonyl compound concentration by UV.

A carbonyl compound stock solution (30 mM) in PBS was diluted 30 times (4350 µL PBS + 150 µL 30 mM stock solution) to a 1 mM stock solution. A calibration curve was prepared by diluting the 1 mM stock solution to 0.005, 0.010, 0.020, 0.040, 0.060, 0.080, 0.100 and 0.120 mM with PBS. Samples of the solutions (200 µL) were transferred into a UV-Star 96-well plate in triplo. The concentration of the carbonyl compound in the reaction mixture was determined by taking a sample and directly diluting it 300 times at RT (30 times dilution (150 µL reaction mixture + 4350 µL PBS) followed by 10 times dilution (150 µL sample + 1350 µL PBS), after which 200 µL was transferred into the UV-Star 96-well plate in triplo. The TFM, ninhydrin or PGA concentration in the samples was determined with the average UV absorption of 3 wells at 248, 232 and 250 nm respectively.

4.6 Computational Studies

DFT calculations were performed using the Gaussian 09 software package, using B3LYP (Becke, three-parameter, Lee-Yang-Parr) functional with 6-31g(d,p) as basis set on all atoms.[35] Structure optimizations were carried out with water as solvent without any symmetry restrains in water. Frequency analyses were performed on all calculations. Input: #B3LYP/6-31G(d,p) opt=tight freq scf=tight int=ultrafine pop=regular SCRF=(Solvent=Water).

4.7 Syntheses and spectroscopic data

Synthesis of **4,4,3,3-tetramethylcyclopentane-1,2,3-trione hydrate**.[36-37]

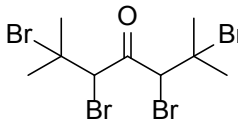

Bromine (10.3 mL, 145 mmol, 2.0 eq.) was dissolved in CH_2Cl_2 (50 mL). The solution was cooled to 0 °C and 2,6-dimethylhepta-2,5-dien-4-one (10 g, 72.5 mmol, 1.0 eq.) was dissolved CH_2Cl_2 (50 mL) and added dropwise. Next, the reaction mixture was stirred for 1 hour at 0 °C. The solvent was evaporated and the crude mixture was recrystallized from EtOH, yielding 2,3,5,6-tetrabromo-2,6-dimethylheptan-4-one as a white solid (27.8 g, 60.9 mmol, 84%). ^{1}H- NMR ($CDCl_3$, 400 MHz) δ main isomer: 5.15 (s, 2H), 2.02 (s, 12H). ^{13}C- NMR ($CDCl_3$) δ main isomer: 193.88 (C_q), 62.83 (C_q), 59.62 (CH), 33.90 (CH_3), 29.29 (CH_3).

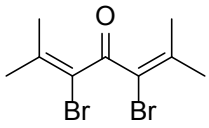

2,3,5,6-Tetrabromo-2,6-dimethylheptan-4-one (50 mmol, 1.0 eq.) was dissolved in cold pyridine (30 mL) and kept for 24 hours at 0 °C without stirring. The reaction mixture was transferred into a separation funnel with CH_2Cl_2 and washed with 30% H_2SO_4 (twice), H_2O, brine and dried over Na_2SO_4. After evaporation of the solvent, 3,5-dibromo-2,6-dimethylhepta-2,5-dien-4-one was isolated as a brown oil which started crystalizing when dried undervacuum and at RT (5.35 g, 49 mmol, 98%). ^{1}H- NMR ($CDCl_3$, 400 MHz) δ: 2.04 (s, 6H), 1.99 (s, 6H). ^{13}C- NMR ($CDCl_3$, 101 MHz) δ: 190.25 (C_q), 144.98 (C_q), 115.64 (C_q), 25.99 (CH_3), 22.55 (CH_3).

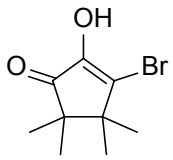

3,5-Dibromo-2,6-dimethylhepta-2,5-dien-4-one (4.158 g, 16 mmol, 1.0 eq.) was dissolved in cold H_2SO_4 (2.56 mL, 48 mmol, 3.0 eq.) and stirred at 0 °C for 24 hours. The mixture was poured over crushed ice during which 3-bromo-2-hydroxy-4,4,5,5-tetramethylcyclopent-2-en-1-one precipitated. The resulting suspension was filtered, the obtained solid material was washed with water and dried under vacuum at RT, yielding 3-bromo-2-hydroxy-4,4,5,5-tetramethylcyclopent-2-en-1-one in 76 % yield (2.8 g, 12 mmol). ^{1}H- NMR ($CDCl_3$, 400 MHz) δ: 5.82 (bs, OH), 1.13 (s, 6H), 1.11 (s, 6H). ^{13}C- NMR ($CDCl_3$, 101 MHz) δ: 204.73 (C_q), 147.49 (C_q), 138.72 (C_q), 51.18 (C_q), 46.60 (C_q), 24.99 (CH_3), 22.64 (CH_3).

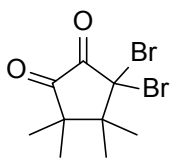

3-Bromo-2-hydroxy-4,4,5,5-tetramethylcyclopent-2-en-1-one (3.5 mmol, 1.0 eq) was dissolved in cold acetic acid (4 mL), to which bromine (178 µL, 3.5 mmol, 1.0 eq.) in acetic acid (4 mL) was slowly added at 0 °C. The reaction mixture was allowed to heat to RT and stirred for 2 hours. The mixture was poured over ice and rested for 10 minutes. The suspension was filtrated, the obtained solid material was washed with water and dried under vacuum, yielding 3,3-dibromo-4,4,5,5-tetramethylcyclopentane-1,2-dione as brown solid in a 38% yield (419 mg, 1.34 mmol). ^{1}H-NMR ($CDCl_3$, 400 MHz) δ: 1.39 (s, 6H), 1.34 (s, 6H). ^{13}C- NMR ($CDCl_3$, 101

MHz) δ: 214.13 (C_q), 204.74 (C_q), 73.32 (C_q), 50.68 (C_q), 46.92 (C_q), 25.45 (CH_3), 24.10 (CH_3).

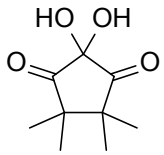

The procedure as described by Gill and Shoppee[36-37] did not yield 2,2-dihydroxy-4,4,5,5-tetramethylcyclopentane-1,3-dione in our hands. Therefore we modified the procedure inspired by the work of Liang *et al*.[38] 3,3-Dibromo-4,4,5,5-tetramethylcyclopentane-1,2-dione (157 mg, 0.5 mmol, 1.0 eq.) was dissolved in DMSO (1 mL) and iodine (0.1 mmol, 0.2 eq.) and water (0.5 mmol, 1.0 eq.) were added. The reaction mixture was stirred at 50 °C for 24 hours after which the resulting mixture was freeze dried to remove DMSO. Purification of the crude mixture over silica (hexane:EtOAc 1:1) yielded 2,2-dihydroxy-4,4,5,5-tetramethylcyclopentane-1,3-dione as a yellow solid in a 90% yield. ^{1}H- NMR ($CDCl_3$, 400 MHz) δ: 6.02 (bs, 2H), 1.14 (s, 6H), 1.12 (s, 6H). These peak shifts differ from those reported by Gill and Shoppee (δ: 1.20 (s, 6H) and 1.08 (s, 6H)). ^{13}C- NMR ($CDCl_3$, 101 MHz) δ: 214.21 (C_q), 137.78 (C_q), 51.10 (C_q), 24.97 (CH_3), 22.61 (CH_3).

Synthesis of **s-indacene-1,2,3,5,6,7-hexaone hydrate**.

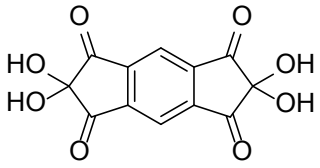

s-Indacene-1,3,5,7(2H,6H)-tetraone was synthesized according to the procedure of Krief *et al*.[39] (^{1}H- NMR (CD_2Cl_2, 400 MHz) δ 8.48 (s, 2H), 3.42 (s, 4H)) and oxidized into s-indacene-1,2,3,5,6,7-hexaone hydrate according to the procedure reported by Marminon *et al*.[40] s-Indacene-1,3,5,7(2H,6H)-tetraone (171 mg, 0.8 mmol, 1.0 eq.) was dissolved in a 10:1 mixture of dioxane (3 mL) and H_2O (0.3 mL) in a microwave tube equipped with a magnetic stirrer. Selenium dioxide (275 mg, 2.5 mmol, 3.1 eq.) was added and the tube was sealed. The mixture was shaken vigorously until selenium dioxide was dissolved and the tube placed in the microwave where it was heated for 5 minutes at 180 °C. The crude reaction mixture was impregnated on silica and purified over silica (8:1 CH_2Cl_2 : MeOH), obtaining the product in a 30% yield (66 mg, 0.24 mmol). ^{1}H- NMR (DMSO, 600 MHz) δ 8.45 (s, 2H), 7.82 (bs, 4H). ^{13}C- NMR (DMSO, 125 MHz) δ: 195.66 (C_q), 143.66 (C_q), 119.68 (CH), 88.31 (C_q).

Synthesis of **3a,6a-dimethyldihydropentalene-1,2,3,4,5,6-hexaone**.

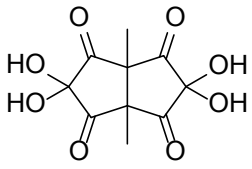

3a,6a-Dimethyltetrahydropentalene-2,5(1H,3H)-dione (499 mg, 3.0 mmol, 1.0 eq.) was dissolved in DMSO and 48% HBr (4.1 mL, 36 mmol, 12 eq.), 57% HI (171 µL, 1.5 mmol, 0.5 eq.) and I_2 (380 mg, 1.5 mmol, 0.5 eq.) were added. The mixture was stirred magnetically at 80 °C for 4 hours. Afterwards the mixture was allowed to cool to RT and was extracted with CH_2Cl_2 5 times. The organic layers were combined, dried over Na_2SO_4 and concentrated, during

which red crystals precipitated from the solution. After filtration, the crystals were collected in a 36% yield (279 mg, 1.1 mmol). ^{1}H- NMR (DMSO, 400 MHz) δ: 10.68 (bs, 4H), 1.41 (s, 3H), 1.32 (s, 3H). ^{13}C- NMR (DMSO, 101 MHz) δ: 191.81 (C_q), 148.24 (C_q), 133.28 (C_q), 65.11 (C_q), 52.39 (C_q), 19.47 (CH_3), 17.08 (CH_3).

Synthesis of **5-(1-hydroxy-2-oxo-2-phenylethyl)-5-phenylimidazolidine-2,4-dione.**

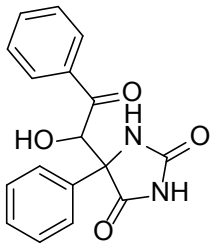

Phenylglyoxaldehyde (456 mg, 3.0 mmol, 1.0 eq.) was dissolved under continuous stirring in PBS (100 mL) and urea (180 mg, 3.0 mmol, 1.0 eq.) was added. The reaction mixture was heated to 50 °C and stirred for 24 hours. Afterwards the mixture was allowed to cool to RT and the solvent was removed by freeze-drying. The crude reaction mixture was impregnated on silica and purified over silica (hexanes:EtOAc = 5:1), obtaining 5-(1-hydroxy-2-oxo-2-phenylethyl)-5-phenylimidazolidine-2,4-dione as a mixture of diastereomers (266 mg, 0.86 mmol) as a white solid in a 57% yield with respect to phenylglyoxaldehyde. Major diastereomer: ^{1}H- NMR (DMSO, 400 MHz) δ: 10.77 (bs, 1H), 8.23 (bs, 1H), 7.82 (d, *J* = 8.3 Hz, 2H), 7.59 (d, *J* = 8.2 Hz, 2H), 7.53 (m, 1H), 7.40 (t, J = 7.6 Hz, 2H), 7.25 (t, *J* = 7.6 Hz, 2H), 7.18 (m, 1H), 6.65 (d, *J* = 8.7 Hz, 1H), 5.71 (d, J = 8.5 Hz, 1H). ^{13}C- NMR (DMSO, 101 MHz) δ: 196.77 (C_q), 174.88 (C_q), 157.11 (C_q), 136.02 (C_q), 135.48 (C_q), 133.33 (CH), 128.69 (CH), 128.43 (CH), 128.09 (CH), 127.68 (CH), 125.78 (CH), 73.64 (CH), 70.60 (C_q).

Synthesis of **1,1'-(1,3-phenylene)bis(2,2-dihydroxyethan-1-one)**.

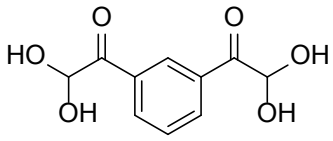

1,1'-(1,3-Phenylene)bis(ethan-1-one) (162 mg, 1.0 mmol, 1.0 eq.) was dissolved in a 10:1 mixture of dioxane (3 mL) and H_2O (0.3 mL) in a microwave tube equipped with a magnetic stirrer. Selenium dioxide (344 mg, 3.1 mmol, 3.1 eq.) was added and the tube was sealed. The mixture was shaken vigorously until selenium dioxide was completely dissolved and the tube placed in the microwave in which it was heated for 5 minutes at 180 °C. The crude reaction mixture was impregnated on silica and purified over silica (EtOAc), obtaining an orange oil in a 41% yield (93 mg, 0.41 mmol). ^{1}H- NMR (DMSO, 600 MHz) δ: 8.71 (t, *J* = 2.0 Hz, 1H), 8.32 (m, 2H), 7.66 (t, *J* = 7.6 Hz, 1H), 6.90 (bs, 4OH), 5.68 (s, 2H). ^{13}C- NMR (DMSO, 125 MHz) δ: 188.67 (C_q), 133.92 (CH), 133.84 (C_q), 130.07 (CH), 128.64 (CH), 89.64 (CH).

Synthesis of **triformylmethane**.

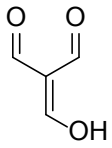

Triformylmethane was synthesized according to the procedure of Budeninsky *et al*.[41] ^{1}H- NMR ($CDCl_3$, 400 MHz) δ: 9.50 (s, 1H), 9.02 (s, 2H). ^{13}C- NMR ($CDCl_3$, 101 MHz) δ: 186.60 (CH), 118.42 (C_q). One ^{13}C- signal is not observed, possibly due to tautomerization.

5. Acknowledgement

This research was supported by the Dutch organization for Scientific Research (NWO-TTW, project 14433) and the Dutch Kidney Foundation. MEM acknowledges the Sectorplan Natuur- en Scheikunde (Tenure-track grant at Utrecht University) for financial support.

6. References

1. Weiner, I. D.; Mitch, W. E.; Sands, J. M., Urea and ammonia metabolism and the control of renal nitrogen excretion. *Clin. J. Am. Soc. Nephrol.* **2015,** *10* (8), 1444-58.
2. Shinaberger, C. S.; Kilpatrick, R. D.; Regidor, D. L.; McAllister, C. J.; Greenland, S.; Kopple, J. D.; Kalantar-Zadeh, K., Longitudinal associations between dietary protein intake and survival in hemodialysis patients. *Am. J. Kidney. Dis.* **2006,** *48* (1), 37-49.
3. Davenport, A.; Gura, V.; Ronco, C.; Beizai, M.; Ezon, C.; Rambod, E., A wearable haemodialysis device for patients with end-stage renal failure: a pilot study. *Lancet* **2007,** *370* (9604), 2005-10.
4. Davenport, A., Dialysis: A wearable dialysis device: the first step to continuous therapy. *Nat. Rev. Nephrol.* **2016,** *12* (9), 512-4.
5. Rocco, M. V.; Lockridge, R. S., Jr.; Beck, G. J.; Eggers, P. W.; Gassman, J. J.; Greene, T.; Larive, B.; Chan, C. T.; Chertow, G. M.; Copland, M.; Hoy, C. D.; Lindsay, R. M.; Levin, N. W.; Ornt, D. B.; Pierratos, A.; Pipkin, M. F.; Rajagopalan, S.; Stokes, J. B.; Unruh, M. L.; Star, R. A.; Kliger, A. S.; Frequent Hemodialysis Network Trial, G.; Kliger, A.; Eggers, P.; Briggs, J.; Hostetter, T.; Narva, A.; Star, R.; Augustine, B.; Mohr, P.; Beck, G.; Fu, Z.; Gassman, J.; Greene, T.; Daugirdas, J.; Hunsicker, L.; Larive, B.; Li, M.; Mackrell, J.; Wiggins, K.; Sherer, S.; Weiss, B.; Rajagopalan, S.; Sanz, J.; Dellagrottaglie, S.; Kariisa, M.; Tran, T.; West, J.; Unruh, M.; Keene, R.; Schlarb, J.; Chan, C.; McGrath-Chong, M.; Frome, R.; Higgins, H.; Ke, S.; Mandaci, O.; Owens, C.; Snell, C.; Eknoyan, G.; Appel, L.; Cheung, A.; Derse, A.; Kramer, C.; Geller, N.; Grimm, R.; Henderson, L.; Prichard, S.; Roecker, E.; Rocco, M.; Miller, B.; Riley, J.; Schuessler, R.; Lockridge, R.; Pipkin, M.; Peterson, C.; Hoy, C.; Fensterer, A.; Steigerwald, D.; Stokes, J.; Somers, D.; Hilkin, A.; Lilli, K.; Wallace, W.; Franzwa, B.; Waterman, E.; Chan, C.; McGrath-Chong, M.; Copland, M.; Levin, A.; Sioson, L.; Cabezon, E.; Kwan, S.; Roger, D.; Lindsay, R.; Suri, R.; Champagne, J.; Bullas, R.; Garg, A.; Mazzorato, A.; Spanner, E.; Rocco, M.; Burkart, J.; Moossavi, S.; Mauck, V.; Kaufman, T.; Pierratos, A.; Chan, W.; Regozo, K.; Kwok, S., The effects of frequent nocturnal home hemodialysis: the frequent hemodialysis network nocturnal trial. *Kidney Int.* **2011,** *80* (10), 1080-91.
6. Agar, J. W., Review: understanding sorbent dialysis systems. *Nephrology (Carlton)* **2010,** *15* (4), 406-11.
7. Lehmann, H. D.; Marten, R.; Gullberg, C. A., How to catch urea? Considerations on urea removal from hemofiltrate. *Artif. Organs* **1981,** *5* (3), 278-85.
8. Urbanczyk, E.; Sowa, M.; Simka, W., Urea removal from aqueous solutions-a review. *J. Appl. Electrochem.* **2016,** *46* (10), 1011-1029.
9. Roberts, M., The regenerative dialysis (REDY) sorbent system. *Nephrology* **1998,** *4* (4), 275-278.
10. Gura, V.; Rivara, M. B.; Bieber, S.; Munshi, R.; Smith, N. C.; Linke, L.; Kundzins, J.; Beizai, M.; Ezon, C.; Kessler, L.; Himmelfarb, J., A wearable artificial kidney for patients with end-stage renal disease. *JCI Insight* **2016,** *1* (8), 15.
11. Cheng, Y. C.; Fu, C. C.; Hsiao, Y. S.; Chien, C. C.; Juang, R. S., Clearance of low molecular-weight uremic toxins p-cresol, creatinine, and urea from simulated serum by adsorption. *J. Mol. Liq.* **2018,** *252*, 203-210.
12. Wernert, V.; Schaf, O.; Ghobarkar, H.; Denoyel, R., Adsorption properties of zeolites for artificial kidney applications. *Micropor. Mesopor. Mat.* **2005,** *83* (1-3), 101-113.
13. Poss, M. J.; Blom, H.; Odufu, A.; Smakman, R., Macromolecular ketoaldehydes. U.S.

Patent 6,861,473 B2: **2005**.
14. Smakman, R. Macromolecular carbonyl groups containing material suitable for use as sorbent for nitrogen compounds. U.S. Patent 4,897,200, **1990**.
15. Wong, R. J. Materials for removal of toxins in sorbent dialysis and methods and systems using same. U.S. Patent 2014/0,336,568 A1, **2014**.
16. Eisen, M. S. Urea sorbent. U.S. Patent 8,220,643 B2, **2014**.
17. Shimizu, T.; Fujishige, S., A newly prepared surface-treated oxystarch for removal of urea. *J. Biomed. Mater. Res.* **1983,** *17* (4), 597-612.
18. Deepak, D., Evaluation of adsorbents for the removal of metabolic wastes from blood. *Med. Biol. Eng. Comput.* **1981,** *19* (6), 701-6.
19. Smakman, R.; van Doorn, A. W., Urea removal by means of direct binding. *Clin. Nephrol.* **1986,** *26 Suppl 1*, S58-62.
20. Roberts, C. W., The synthesis and properties of ninhydrin ureide. *J. Biol. Chem.* **1943,** *150*, 471-476.
21. Shapiro, R.; Chatterjie, N., Cyclization reactions of ninhydrin with aromatic amines and ureas. *J. Org. Chem.* **1970,** *35* (2), 447-450.
22. Jong, J. A. W.; Moret, M. E.; Verhaar, M. C.; Hennink, W. E.; Gerritsen, K. G. F.; van Nostrum, C. F., Effect of substituents on the reactivity of ninhydrin with urea. *ChemistrySelect* **2018,** *3* (4), 1224-1229.
23. Kostyanovsky, R. G.; Shtamburg, V. G.; Shishkin, O. V.; Zubatyuk, R. I.; Shtamburg, V. V.; Anishchenko, A. A.; Mazepa, A. V., Pyramidal nitrogen in the crystal of N-[(benzoyl)(hydroxy)methyl]-N-benzyloxy-N '-(2-bromophenyl)urea. *Mendeleev Commun* **2010,** *20* (3), 167-169.
24. Arnold, Z.; Budesinsky, M.; Pankova, M., Reactivity of triformylmethane .1. Reactions of triformylmethane with selected types of amino-compounds. *Collect. Czech. Chem. Commun.* **1991,** *56* (5), 1019-1031.
25. Gadda, G.; Negri, A.; Pilone, M. S., Reaction of phenylglyoxal with arginine groups in D-amino-acid oxidase from Rhodotorula Gracilis. *J. Biol. Chem.* **1994,** *269* (27), 17809-14.
26. Bohren, K. M.; von Wartburg, J. P.; Wermuth, B., Inactivation of carbonyl reductase from human brain by phenylglyoxal and 2,3-butanedione: A comparison with aldehyde reductase and aldose reductase. *Biochim. Biophys. Acta* **1987,** *916* (2), 185-92.
27. Zenkova, E. A.; Degterev, E. V., Optimization of ninhydrin reagent synthesis from 1,2,3,4-tetrahydro-1,4-dioxo-2,2,3,3-tetrahydroxynaphthalene (oxolin) and possible applications. *Pharm. Chem. J.* **2000,** *34* (3), 135-137.
28. Ramakrishna, S.; Benjamin, W. B., Evidence for an essential arginine residue at the active-site of ATP citrate lyase from rat-liver. *Biochem. J.* **1981,** *195* (3), 735-743.
29. Koissi, N.; Neuvonen, K.; Munter, T.; Kronberg, L.; Lonnberg, H., Condensation of triformylmethane with guanosine. *Nucleos. Nucleot. Nucl.* **2001,** *20* (10-11), 1761-74.
30. Clayden, J.; Warren, S.; Greeves, N.; Wothers, P. *Organic Chemistry*; Oxford University Press: **2000**, pp 349.
31. Tserng, K. Y.; Kalhan, S. C., Gas chromatography/mass spectrometric determination of [15N]urea in plasma and application to urea metabolism study. *Anal. Chem.* **1982,** *54* (3), 489-91.
32. Maltsev, O. V.; Pothig, A.; Hintermann, L., Synthesis of Soai aldehydes for asymmetric

autocatalysis by desulfurative cross-coupling. *Org. Lett.* **2014,** *16* (5), 1282-5.
33. Rubln, M. B., The chemistry of vicinal polyketones. *Chem. Rev.* **1975,** *2* (2), 177-202.
34. Alvarez, M.; Fernandez, D.; Joule, J. A., Synthesis of 1,2-dihydropyrrolo[1,2-c] pyrimidin-1-ones. *J. Chem. Soc.-Perkin Trans. 1* **1999,** (3), 249-255.
35. M. J. Frisch, G. W. T., H. B. Schlegel, G. E. Scuseria, M. A. Robb, J. R. Cheeseman, G. Scalmani, V. Barone, B. Mennucci, G. A. Petersson, H. Nakatsuji, M. Caricato, X. Li, H. P. Hratchian, A. F. Izmaylov, J. Bloino, G. Zheng, J. L. Sonnenberg, M. Hada, M. Ehara, K. Toyota, R. Fukuda, J. Hasegawa, M. Ishida, T. Nakajima, Y. Honda, O. Kitao, H. Nakai, T. Vreven, J. A. Montgomery, Jr., J. E. Peralta, F. Ogliaro, M. Bearpark, J. J. Heyd, E. Brothers, K. N. K ; udin, V. N. S., R. Kobayashi, J. Normand, K. Raghavachari, A. Rendell, J. C. Burant, S. S. Iyengar, J. Tomasi, M. Cossi, N. Rega, J. M. Millam, M. Klene, J. E. Knox, J. B. Cross, V. Bakken, C. Adamo, J. Jaramillo, R. Gomperts, R. E. Stratmann, O. Yazyev, A. J. Austin, R. Cammi, C. Pomelli, J. W. ; Ochterski, R. L. M., K. Morokuma, V. G. Zakrzewski, G. A. Voth, P. Salvador, J. J. Dannenberg, S. Dapprich, A. D. Daniels, O. Farkas, J. B. Foresman, J. V. Ortiz, J. Cioslowski and D. J., Gaussian 09, Revision A.02. *Gaussian, Inc., Wallingford CT,* **2009**.
36. Gill, G. B.; Idris, M. S. H.; Kirollos, K., Ene reactions of indane-1, 2, 3-trione (a super-enophile) and related vicinal tricarbonyl systems. *J. Chem. Soc. Perkin Trans. 1* **1992,** (18), 2355-2365.
37. Shoppee, C. W., 1,2,3-Triketotetramethylcyclopentane: A blue triketone. *J. Chem. Soc. Perkin Trans. 1* **1936**, 269-274.
38. Liang, Y. F.; Li, X.; Wang, X.; Zou, M.; Tang, C.; Liang, Y.; Song, S.; Jiao, N., Conversion of simple cyclohexanones into catechols. *J. Am. Chem. Soc.* **2016,** *138* (37), 12271-7.
39. Khodorkovsky, V.; Becker, J. Y.; Krief, P.; Ellern, A.; Neilands, O.; Shapiro, L., s-Indacene-1,3,5,7(2H,6H)-tetraone ('Janusdione') and 1,3-dioxo-5,6-indanedicarboxylic acid: Old and new 1,3-indandione derivatives. *Synthesis* **2004,** *2004* (15), 2509-2512.
40. Marminon, C.; Nacereddine, A.; Bouaziz, Z.; Nebois, P.; Jose, J.; Le Borgne, M., Microwave-assisted oxidation of indan-1-ones into ninhydrins. *Tetrahedron Lett.* **2015,** *56* (14), 1840-1842.
41. Budeninsky, M.; Fiedler, P.; Arnold, Z., Triformylmethane: An efficient preparation, some derivatives, and spectra. *Synthesis* **1989,** (1), 1-5.

7. Supporting Information

Online available structural formulas, calculated G-values and optimized coordinates of all hydrated, dehydrated and intermediate compounds and ^{1}H and ^{13}C NMR spectra of synthesized compounds.

7.1 List of carbonyl compounds investigated for reactivity with urea that were not included in the main manuscript

Table S1: Carbonyl compounds tested for urea binding. Conditions: 30 mM urea and 30 mM carbonyl compound at 323 K.

Entry	Compound	k_2 ($M^{-1}h^{-1}$) in PBS	k_2 ($M^{-1}h^{-1}$) in PBS:DMSO 1:1 (v/v)
18	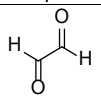	0.33 ± 0.03	Not Determined
19	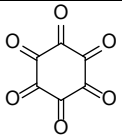	<0.1	<0.1
20	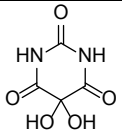	0.14 ± 0.02	Not Determined
21	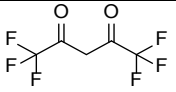	<0.1	<0.1
22	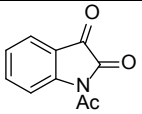	<0.1	<0.1
23	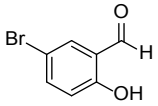	<0.1	<0.1
24	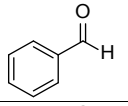	<0.1	<0.1
25	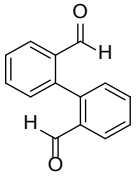	Not Determined	<0.1

Entry	Compound	k_2 ($M^{-1}h^{-1}$) in PBS	k_2 ($M^{-1}h^{-1}$) in PBS:DMSO 1:1 (v/v)
26	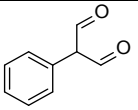	Not Determined	<0.1
27	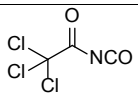	<0.1	<0.1
28		<0.1	<0.1
29		Not Determined	<0.1
30	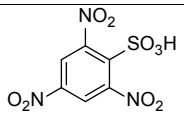	<0.1	Not Determined
31	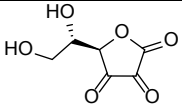	<0.1	Not Determined

7.2 Product analysis of the reaction of oxolin with urea

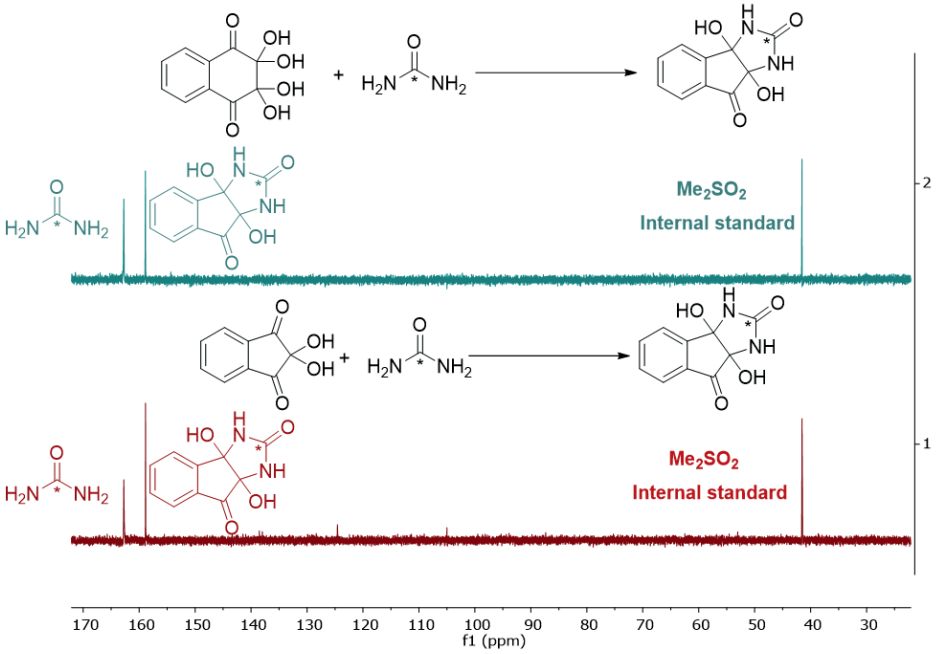

Figure S1: Quantitative ^{13}C- NMR spectra of the reaction mixture of urea with oxolin urea (upper) and the reaction mixture of urea with ninhydrin (lower), showing the formation of the same compound 3a,8a-dihydroxy-1,3,3a,8a-tetrahydroindeno[1,2-d]imidazole-2,8-dione.

7.3 The influence of temperature on the reaction of ninhydrin with urea

Integration of equation 3 yields equation S1. The slope in the plot of the inverse urea concentration in time gives the k_2-value of the reaction.

$$(Eq.S1)\frac{1}{[urea]} = k_2 t + \frac{1}{[urea]_{t=0}}$$

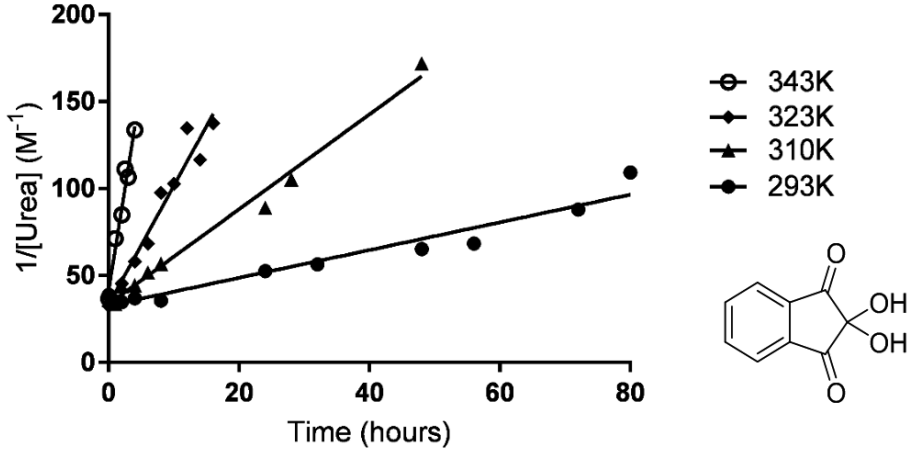

Figure S2: Plot of the inverse urea concentration in time of the reaction of ninhydrin (30 mM) with urea (30 mM) in PBS at different temperatures.

Table S2: k_2 Rate constants of the reaction of ninhydrin with urea at various temperatures. Conditions: 30 mM urea and 30 mM ninhydrin in PBS pH 7.4.

T (°C)	T (K)	1/T	k_2($M^{-1}h^{-1}$)	ln(k)
20	293	3.41×10^{-3}	0.80±0.06	-0.22
37	310	3.23×10^{-3}	2.7±0.1	1.00
50	323	3.10×10^{-3}	6.8±0.6	1.92
70	343	2.92×10^{-3}	23.5±2.4	3.30

7.4 Second order kinetics of the reaction of urea with carbonyl compounds

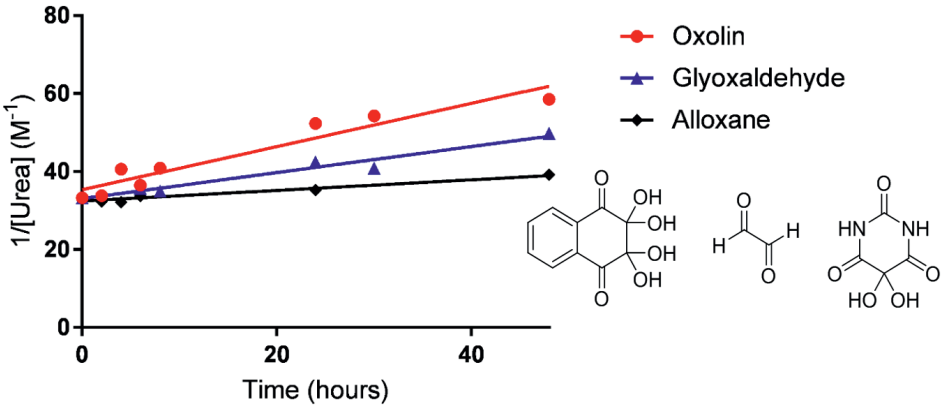

Figure S3: Plot of the inverse urea concentration in time of the reaction of urea (30 mM) with oxolin, glyoxaldehdye and alloxane (30 mM) in PBS at 323 K.

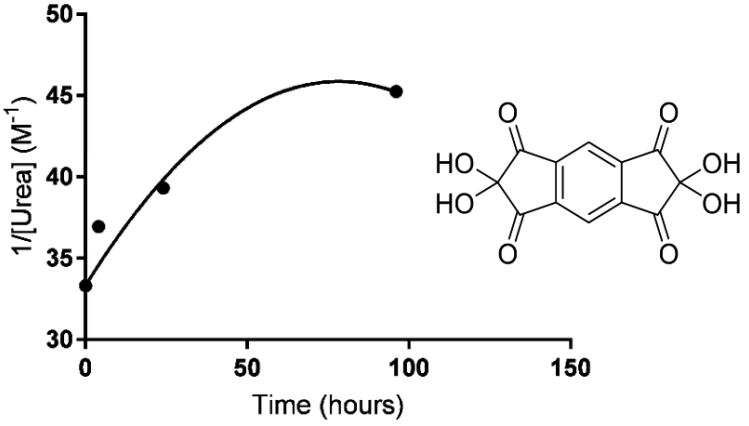

Figure S4: Plot of the inverse urea concentration in time of the reaction of 2,2,6,6-tetrahydroxy-s-indacene-1,3,5,7(2H,6H)-tetraone (15 mM, corresponding to 30 mM (1.0 eq.) of triketone hydrate groups) with urea (30 mM, 1.0 eq.) in DMSO : PBS 1:1 v/v at 343 K.

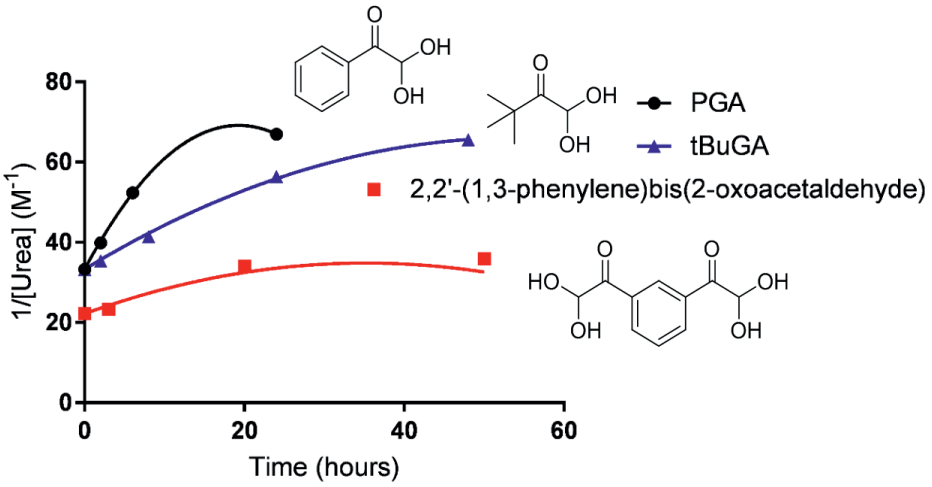

Figure S5: Plot of the inverse urea concentration in time of the reaction of urea (30 or 45 mM. 1.0 eq.) with phenylglyoxaldehyde (PGA, 30 mM, 1.0 eq.), tertbutyl glyoxaldehyde (tBuGA, 30 mM, 1.0 eq.) and 2,2'-(1,3-phenylene)bis(2-oxoacetaldehyde) (22.5 mM, corresponding to 45 mM (1.0 eq.) of glyoxaldehyde groups) in PBS at 323 K.

7.5 Comparison of the PFO kinetics for the reaction of phenylglyoxaldehyde and ninhydrin with urea

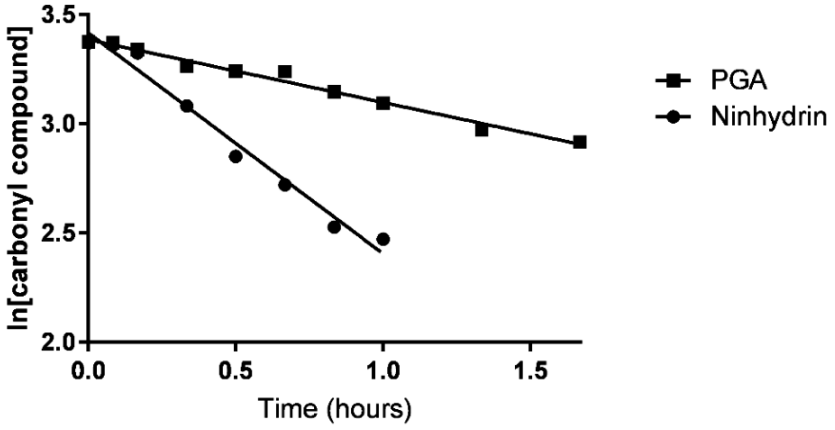

Figure S6: Kinetics of the reaction of ninhydrin or PGA (30 mM, 1.0 eq.) with urea (150 mM, 5 eq.) in PBS at 323 K. Linear regression gives y = -1.01x + 3.42 (R^2 = 0.98) for ninhydrin and y = -0.29 x + 3.38 (R^2 = 0.98) for PGA.

7.6 PFO kinetics for the reaction of phenylglyoxaldehyde with urea

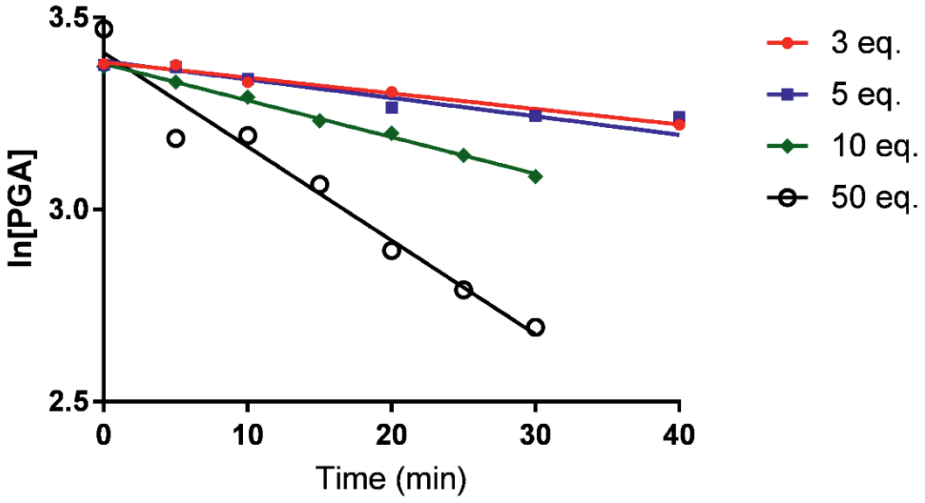

Figure S7: Kinetics of the reaction of PGA (30 mM, 1.0 eq.) with urea (90-1500 mM, 3 - 50 eq.) in PBS at 323 K.

The second order k_2-value can be derived from the pseudo first order k_{PFO}-value by using the following formulas.
(1) Rate = k_2 [urea]^1[carbonyl compound]^1
If [urea]>>[carbonyl compound] than:
(2) Rate = k_{PFO} [carbonyl compound]^1 and (3) $k_{PFO} = k_2$ [urea].
Rewrite as: (4) $k_2 = k_{PFO}$ / [urea].

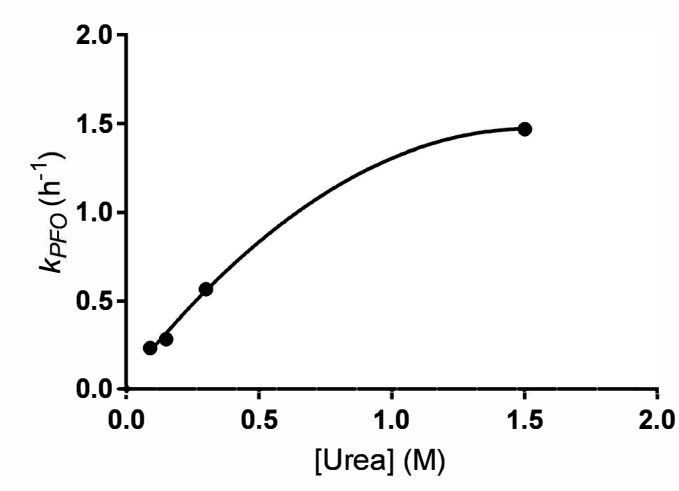

Figure S8: Plot of k_{PFO} versus [urea] in the reaction of PGA with urea. Polynomial regression gives $y = -0.62x^2 + 1.87x + 0.06$.

Table S3: The influence of the urea concentration on the k_{PFO}- and k_2-values of the reaction of PGA with excess urea. [a] Extrapolated from figure S8 using polynomial regression.

[PGA] (mM)	[urea] (mM), eq.	k_{PFO} (h^{-1})	k_2 ($M^{-1}h^{-1}$)
30	30, 1 eq.	0.11[a]	3.7[a]
30	90, 3 eq.	0.24	2.7
30	150, 5 eq.	0.29	1.9
30	300, 10 eq.	0.57	1.9
30	1500, 50 eq.	1.47	0.98

7.7 Second order kinetics of the reaction of urea with aldehydes

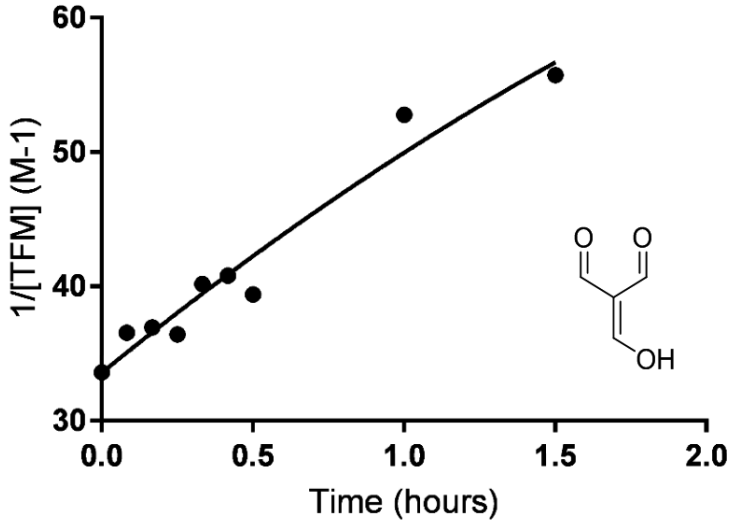

Figure S9: Plot of the inverse urea concentration in time of the reaction of triformylmethane (30 mM) with urea (30 mM) in PBS at 323K.

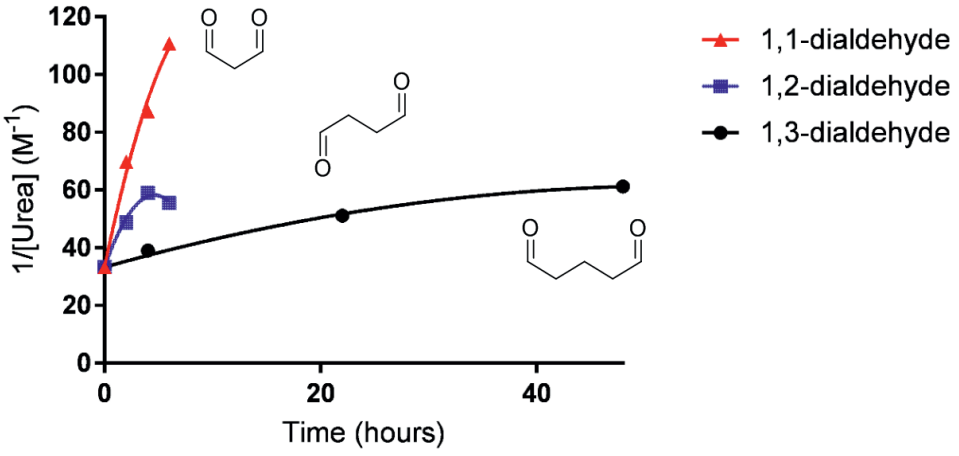

Figure S10: Plot of 1/[urea] in time of the reaction of urea (30 mM) with a 1,1-, 1,2-, and a 1,3-dialdehyde (30 mM) in PBS (pH 2) at 323 K.

7.8 Possible formation of aromatic system from 3,4-diformylpyrrole

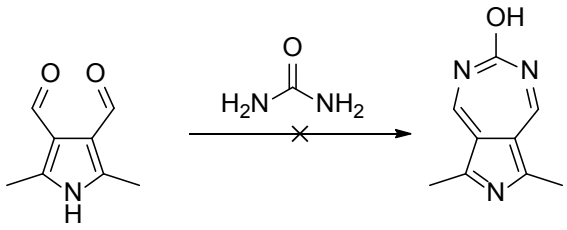

Scheme S1: Possible reaction of 3,4-diformylpyrrole with urea.

7.9 Side reactions of triformylmethane in solution

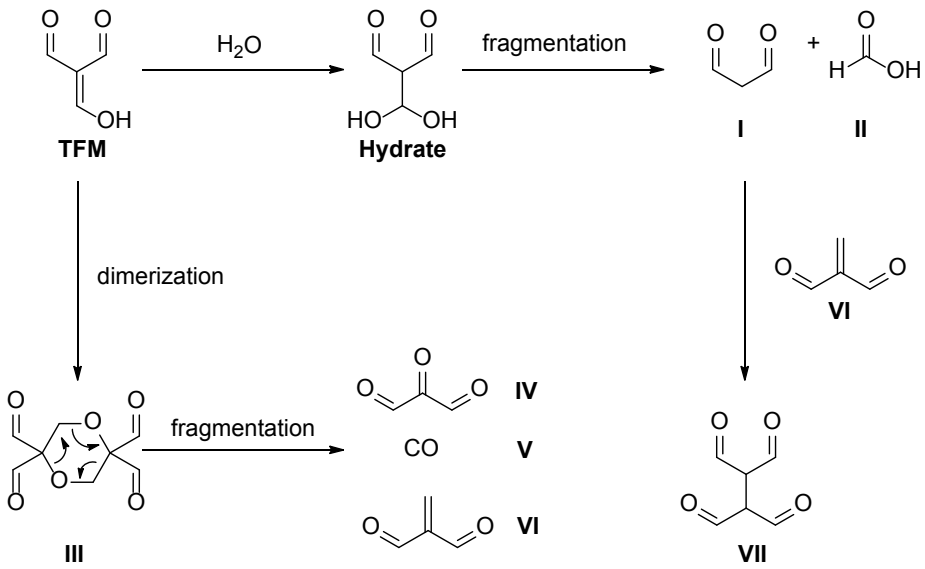

Scheme S2: Overview of the reported reactions of TFM in aqueous solution.[29]

5

Chapter 5

Phenylglyoxaldehyde-functionalized Polymeric Sorbents for Urea Removal from Aqueous Solutions

Jacobus A.W. Jong[a,b], Yong Guo[a], Cas Veenhoven[a], Marc-Etienne Moret[c], Johan van der Zwan[d], Alessandra Lucini Paioni[d], Marc Baldus[d], Karina C. Scheiner[a], Remco Dalebout[e], Mies J. van Steenbergen[a], Marianne C. Verhaar[b], Robert Smakman[f], Wim E. Hennink[a], Karin G.F. Gerritsen[b] and Cornelus F. van Nostrum[a]*

[a]Department of Pharmaceutics, Utrecht Institute for Pharmaceutical Sciences (UIPS), Utrecht University, Universiteitsweg 99, 3584 CG Utrecht, the Netherlands.
[d]Department of Nephrology and Hypertension, University Medical Centre Utrecht, 3584 CX
[c]Organic Chemistry and Catalysis, Debye Institute for Nanomaterials Science, Utrecht University, Universiteitsweg 99, 3584 CG Utrecht, the Netherlands.
[d]NMR Spectroscopy, Bijvoet Center for Biomolecular Research Department of Chemistry, Faculty of Science, Utrecht University, Padualaan 8, 3584 CH Utrecht, the Netherlands.
[e]Inorganic Chemistry and Catalysis, Debye Institute for Nanomaterials Science, Utrecht University, Universiteitsweg 99, 3584 CG Utrecht, the Netherlands.
[f]Innovista, Raadhuisstraat 1, 1393 NW Nigtevecht, the Netherlands.

Submitted

Abstract

For realization of a wearable artificial kidney based on regeneration of a small volume of dialysate, urea removal from such dialysate is a major challenge. Here a potentially suitable polymeric sorbent based on phenylglyoxaldehyde (PGA), able to covalently bind urea under physiological conditions is described. Sorbent beads containing PGA groups were obtained by suspension polymerization of either styrene or vinylphenylethan-1-one (VPE), followed by modification of the aromatic groups of poly(styrene) and poly(VPE) into PGA. It was found that PGA functionalized sorbent beads removed ~0.6 mmol urea/g under static conditions at 37 °C from urea-enriched phosphate-buffered saline. This means that the daily urea production of a dialysis patient can be removed with a few hundred grams of this sorbent which is an important step forward in the development of wearable artificial kidney.

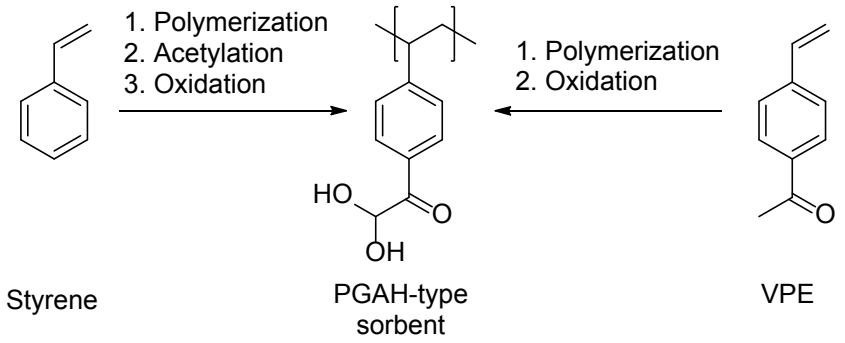

1. Introduction

Uremic toxins such as creatinine and urea accumulate in the body of patients suffering from end-stage kidney disease (ESKD).[1] In order to remove these waste compounds, ESKD patients undergo hemodialysis (HD) 3-6 times a week for 2-8 hours, usually performed in a dialysis center or hospital. To improve the flexibility and quality of life of dialysis patients, a wearable HD device is urgently needed which uses a small volume of dialysate (preferably < 0.5 L, compared to 120 L presently used for a conventional HD session) that is continuously regenerated by a purification unit so that it can be reused in a closed-loop system.[2-4] Urea removal from dialysate is crucial in realizing such a wearable HD device. Urea is the uremic toxin with the highest daily production (~400 mmol per day[5]) and currently there is no adequate urea removal technology available that enables reduction of the dialysate volume to < 0.5 L.[6]

Ideally, a suitable urea sorbent has a high density of functional groups that are able to form covalent or non-covalent bonds with urea at 37 °C resulting in its removal from dialysate,[7] without forming toxic side-products that can be released into the patient. As non-covalent bonds between urea and physisorbents are reversible and generally weaker than covalent bonds, these sorbents have low binding capacities. Chemisorption by the formation of covalent bonds between urea and the sorbent is therefore preferred to remove high amounts of urea from dialysate at 37 °C. A few urea chemisorbents have been reported, in which urea removal was based on the reaction with an electrophilic carbonyl group, such as an aldehyde,[8-9] an indanetrione [10-11] or a phenylglyoxaldehyde (PGA).[12-14] PGA is a very electrophilic functional group (**2a,** PGA), and forms a (reversible) hydrate in contact with water, *i.e.* phenylglyoxaldehyde hydrate (**1a**, PGAH). In our previous work, we systematically studied the reactivity of urea with a variety of carbonyl compounds in phosphate-buffered saline (PBS) spiked with urea (30 mM) and found that PGAH was one of the compounds with the highest reactivity. Importantly, PGAH is synthetically easily accessible and a urea sorbent based on PGAH would therefore be a logical choice for application in dialysate regeneration. In addition, we found that PGAH and urea can irreversibly react in a 1:1 ratio (**3a**) and a 2:1 ratio (**3'a**) (scheme 1).[15]

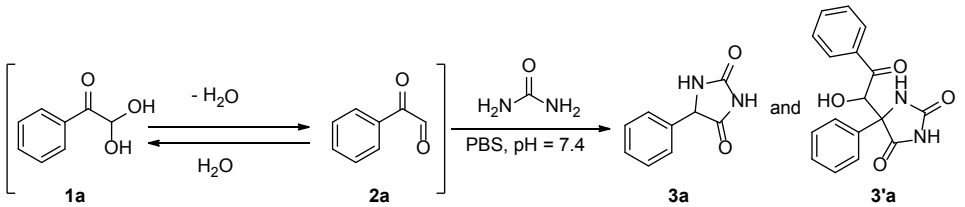

Scheme 1: The reaction of PGAH with urea.[15]

PGAH-type urea sorbent beads based on polystyrene were claimed in a few patents. These beads were obtained via acetylation of polystyrene, followed by halogenation of the acetyl group and Kornblum oxidation of the primary halide.[12-14] Poss *et al.* synthesized macroporous particles based on this procedure, to allow easier diffusion of urea into the polymeric matrix and thereby faster and higher urea removal was achieved than with non-porous beads (binding capacity of 1.5 *vs* 0.29 mmol/g, respectively).[12-13] However, the experimental procedures to obtain these materials and their characteristics were not described in detail. In theory, a polymeric sorbent based on vinyl-substituted PGAH has a maximum urea binding capacity of 2.8 or 5.6 mmol/g, depending whether PGAH and urea react in a 2:1 ratio or a 1:1 ratio, which is much higher than those reported by Poss *et al*. which suggests a low extent of conversion of the phenyl groups into PGAH groups. In the present work we aim to develop PGAH-type sorbents for urea removal from dialysate by studying and optimizing the modification of the aromatic groups of polystyrene into PGAH groups. In addition, we explored a new route to obtain PGAH-functionalized sorbents which circumvents the acetylation step by polymerization of vinylphenylethanone (VPE), an acetylated styrene-like monomer, and potentially results in higher amount of PGAH groups per gram of sorbent. The kinetics of the urea uptake by PGAH-type sorbents under physiological conditions were studied. Finally, we determined whether the PGAH-groups in the sorbents react with urea in a 1:1 or a 2:1 molar ratio.

2. Results and Discussion

First, we investigated whether the reactivity of a phenylglyoxaldehyde hydrate (PGAH)-based urea sorbent could be increased by appropriate substituents, since in our previous publication about the reactivity of ninhydrin with urea we found that substituents on the aromatic ring have a substantial impact on the reaction rate due to their effect on the indanetrione-ninhydrin equilibrium in water.[16] Thus, the kinetics of the reaction of urea with *para*-methyl-PGAH (**1b**), a PGAH-derivative with an electron donating group (EDG), and with *para*-nitro-PGAH (**1c**), a PGAH-derivative with an electron withdrawing group (EWG) (figure 1), were analyzed and compared to the kinetics of unsubstituted PGAH (**1a**) with urea. Substituents on the *meta*-position were not investigated because in our previous study on substituent effects on the reaction of ninhydrin-analogues with urea we found that the position of the EDG has a marginal effect on the overall reactivity of ninhydrin-derivatives with urea.[16] Moreover, the Friedel Crafts acetylation of the aromatic group in polystyrene (as the first step towards the PGAH sorbent) lead to *ortho*/*para* substitution, because the aliphatic polymeric backbone is considered as an activating group[17] and therefore acetylation will not take place at the *meta*-position.

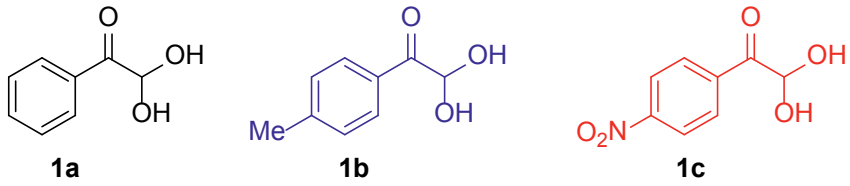

Figure 1: Structures of phenylglyoxaldehyde hydrate (PGAH) (**1a**), *para*-methyl PGAH (**1b**) and *para*-nitro PGAH (**1c**).

As urea and PGAH can react with each other in aqueous solution both in a 1:1 and 1:2 ratio (scheme 1),[15] a large excess (50 equivalents) of urea was used to limit the formation of the 1:2 urea-PGA adduct (scheme 2). The rate of the reaction of PGAH with urea is expressed by equation 1.[15] Because the urea concentration is much higher than the PGAH concentration, its concentration stays almost constant, and thus pseudo-first order conditions are valid (equation 2), thereby making the reaction rate (-d[PGAH]/dt) dependent on the PGAH concentration only (equation 3). The pseudo-first order kinetics of the reaction of PGAH (and its derivatives) with urea were analyzed by determining the concentrations of **1a-c** in time using UV spectroscopy (see supporting information section 7.1 for the raw data and calculations). The solvent for this reaction was a 1:1 (v/v) PBS/DMSO mixture due to the very low solubility of **1b** and **1c** in PBS only. The pseudo-first order rate constants (k_{PFO}) correspond with the negative slopes in the plot of the logarithm of the PGAH-(derivatives) concentration divided by log (e) *versus* time (figure 2) and are reported in table 1.

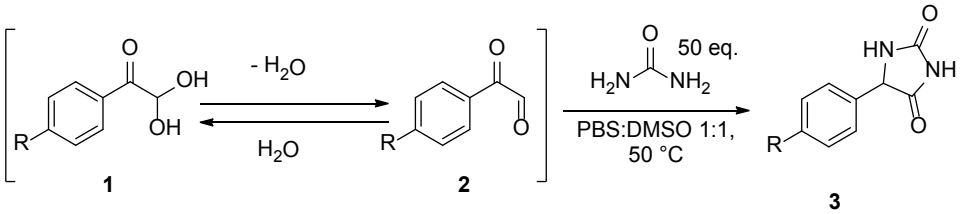

Scheme 2: Reaction of the PGAH-(derivatives)with urea. Reaction conditions: PGAH-(derivatives) (compound **1**, 0.3 mmol, 1.0 eq., 30 mM) and urea (15 mmol, 50 eq. 1.5 M) in 1:1 (v/v) mixture of PBS and DMSO (10 mL) at 50 °C.

$$(1) \quad -\frac{[PGAH]}{dt} = k_2\,[urea][PGAH]$$

$$(2) \quad k_{PFO} = k_2[urea]$$

$$(3) \quad -\frac{[PGAH]}{dt} = k_{pfo}\,[PGAH]$$

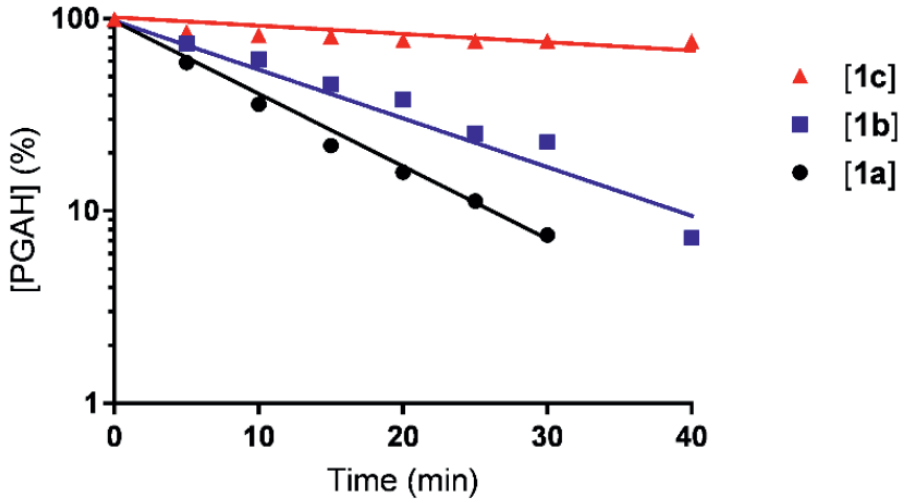

Figure 2: Logarithm of the concentration of PGAH-(derivatives) *versus* time upon reaction with an excess of urea (50 eq.) in a 1:1 (v/v) PBS:DMSO mixture at 50 °C.

Table 1: Pseudo-first order rate constants of the reaction of PGAH(-analogues) with 50 eq. of urea in 1:1 (v/v) PBS:DMSO at 50 °C. The k_{PFO} was calculated from the negative slope divided by log(e) in the plot of log[**1a**, **1b**, **1c**] in time (figure 2).

Entry	Substituent	k_{PFO} (min^{-1})
1a	H	0.085 ± 0.003
1b	*p*-Me	0.061 ± 0.005
1c	*p*-NO_2	0.006 ± 0.002

The results presented in figure 2 and table 1 show that methyl-substituted PGAH (**1b**) reacted slightly slower with urea than unsubstituted PGAH (**1a**) (k_{PFO} = 0.061 versus 0.085 min^{-1}), however nitro-substituted PGAH (**1c**) reacted more than a factor 10 slower than unsubstituted PGAH (**1a**) (k_{PFO} = 0.006 min^{-1}). In our previous work we found that electron donating groups and electron withdrawing groups decrease the reaction rate of urea with ninhydrin-derivatives due to the changes in the rate of dehydration of these derivatives, as suggested by calculations of the Gibbs free energies (G) of the starting material and intermediates.[16] Similarly, we calculated G-values of PGAH (**1**), PGA (**4**) and the first urea-PGA intermediate (**5**) at the the B3LYP/6-31G(d,p) DFT level and calculated the change in energy for dehydration of PGAH ($\Delta G_{dehydration}$) and the reaction of PGA with urea ($\Delta G_{intermediate}$) (scheme 3). The influence of the substituent (Me and NO_2) on both reaction steps was quantified by subtraction of the ΔG-values of unsubstituted species from the ΔG of substituted species, thereby yielding a ΔΔG-value for each substituent (equations 4 and 5).

$$\Delta\Delta G_{Me} = \Delta G_{Me} - \Delta G_{H} \quad (4)$$

$$\Delta\Delta G_{NO_2} = \Delta G_{NO_2} - \Delta G_{H} \quad (5)$$

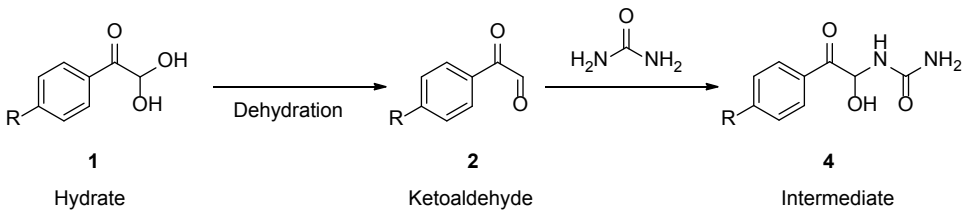

Scheme 3: Dehydration of PGAH into PGA and subsequent reaction of PGA with urea.

Based on the ΔΔG-values of the substituents, we found that an EDG (*i.e.* compound **1b**) results in a more favorable, and hence presumably faster dehydration into **2b** as compared to the dehydration of PGAH (**1a**) into PGA (**2a**) ($\Delta\Delta G_{Me,\ dehydration}$ = -0.27 kcal/mol). On the other hand, the subsequent reaction of **2b** with urea is less favorable as compared to reaction of **2a** with urea ($\Delta\Delta G_{Me,\ intermediate}$ = 0.35 kcal/mol). In other words, the reaction of **2b** with urea is enhanced to a greater extent than the dehydration of **1b**, thus explaining the slightly lower k_{PFO} value of **1b** as compared to that of **1a.** In opposite, the influence of the EWG (*i.e.* compound **1c**) results in an increase of Gibbs free energy for the dehydration of **1c** into **2c** ($\Delta\Delta G_{NO2,\ dehydration}$ = 0.94 kcal/mol) and in a more favorable reaction of **2c** with urea ($\Delta\Delta G_{NO2,\ intermediate}$ = -0.41 kcal/mol), as compared to unsubstituted PGAH. For PGAH bearing an EWG (**1c**), the less favorable dehydration is affecting the overall rate to a greater extent than the reaction with urea, resulting in substantially slower reaction kinetics as well. Based on this analysis, it is concluded that a PGAH-containing sorbent in which the aromatic ring is directly connected to an electron donating polycarbon backbone (such as in polystyrene) has probably a somewhat reduced reactivity as compared to unsubstituted PGAH, but that this cannot readily be compensated by other or additional (EDG or EWG) substituents.

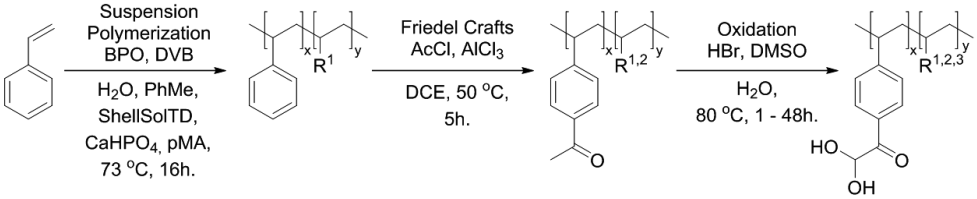

Scheme 4: Synthesis of PGA-type sorbents from styrene. R^1 = crosslinker, R^2 = unmodified styrene, R^3 = side product, see scheme 5 and 8.

An overview of the synthesis route towards PGAH-type sorbents based on polystyrene is shown in scheme 4. For the preparation of polystyrene we essentially used a method as described by Jong *et al*.[18] Macroporous polystyrene beads (PS) were synthesized by suspension co-polymerization of styrene and a low content of

divinylbenzene (DVB, 2.5%) in a cylindrical reactor with mechanical stirrer (supporting information section 7.2). A mixture of toluene and ShellSolTD® (9:91 v/v) was used as a non-solvating porogen[19] and spherical beads (figure 3A) were obtained in a 97% yield. The average diameter of the beads as determined by light microscopy was 0.49 ± 0.18 mm. Scanning electron microscopy (SEM) analysis (figure 3B) showed that pores are clearly visible on the surface of the beads. The surface area (S_{BET}) and pore volume of the beads as determined by nitrogen physisorption were 36.3 m^2/g and 0.32 mL/g, respectively. The plot of the pore volume *versus* the pore diameter (figure 3C) shows that the pores present in the material were mainly in the range of 50-100 nm, demonstrating that the obtained beads are indeed macroporous.[20]

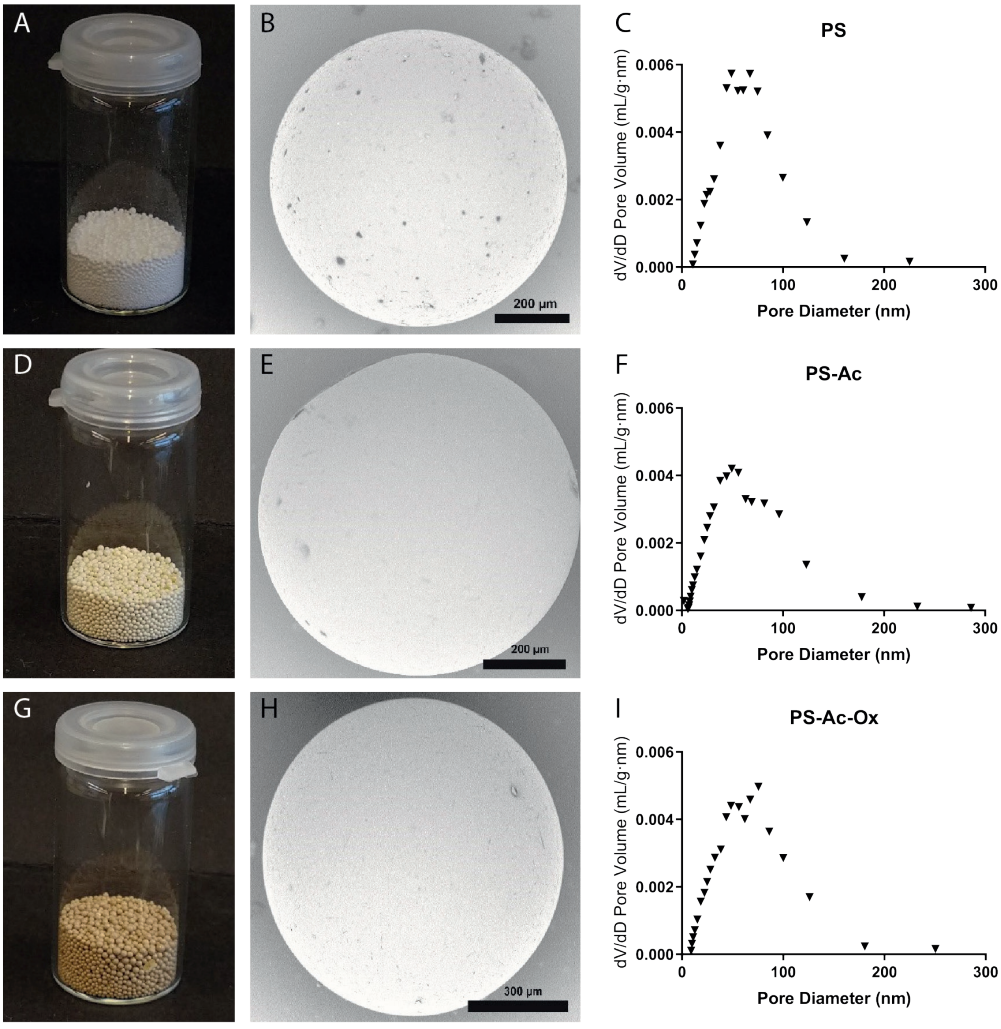

Figure 3: Characteristics of the styrene-based PGAH-sorbent (PS-Ac-Ox: G-I) and its precursors (PS beads: A-C; PS-Ac beads: D-F): photographs (left images), typical SEM images (middle) and pore size/volume distribution (right figures).

The aromatic groups of the PS beads suspended in 1,2-dichloroethane (DCE) were subsequently acetylated in a Friedel-Crafts reaction using acetylchloride as reactant and $AlCl_3$ as catalyst. The obtained acetylated PS beads (71.6 g, PS-Ac, figure 3D) were characterized using SEM (figure 3E), light microscopy and nitrogen physisorption (3F). The PS-Ac beads showed similar characteristics as PS; the S_{BET} surface area was similar (43.4 m^2/g), as did the size (0.61 ± 0.17 mm) and the pore size/volume distribution (figure 3F), demonstrating that the Friedel-Crafts reaction did not adversely affect the macroporosity or degrade the beads, possibly because the reaction temperature (50 °C) was far below the glass transition temperatures of both the PS and PS-Ac beads (T_g were 119 °C and 184 °C respectively, supporting information section 7.3). Infrared spectroscopic (IR) analysis of PS-Ac showed the presence of a new peak at 1675 cm^{-1}, assigned to the C=O stretching vibration of the acetyl group,[21] demonstrating that acetylation indeed had taken place (supporting information section 7.4). To quantify the degree of acetylation of the aromatic groups, the PS-Ac beads were analyzed by quantitative ^{13}C-solid state NMR spectroscopy (supporting information section 7.9). Comparison of the integral from the carbonyl carbons (180-200 ppm) with that from the aromatic peaks (110-160 ppm) and the aliphatic peaks (10-50 ppm) shows that approximately 60% of the styrene units have been acetylated.

The acetyl aromatic groups in PS-Ac beads were halogenated and subsequently converted into PGAH-groups by a Kornblum oxidation in a one-pot procedure using a mixture of concentrated aqueous HBr and DMSO, thereby yielding PS-Ac-Ox beads.[22-23] To establish the optimal reaction time for these oxidizing conditions to obtain the highest PGAH-density, beads were taken from the reaction mixture at different time points, and their urea binding capacity was determined (supporting information section 7.5 and 7.7 and figure 4).

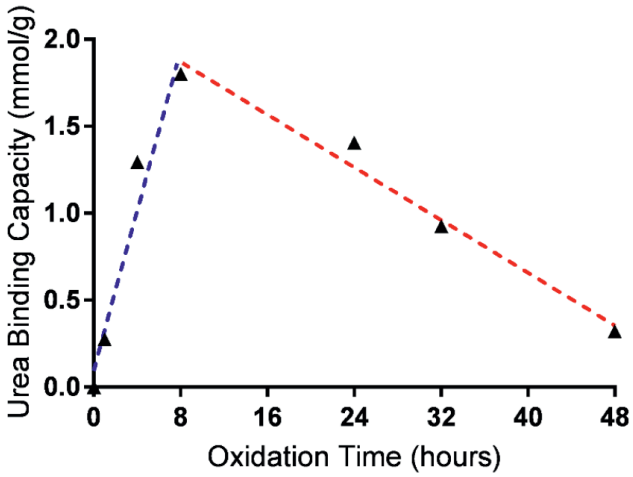

Figure 4: Urea binding capacity of Ps-Ac-Ox beads as a function of oxidation time of Ps-Ac. Conditions for oxidation: Ps-Ac (3.5 g) in DMSO (35 mL) and 48% aqueous HBr (10 mL) stirred mechanically at 80 °C.

Figure 4 shows that the urea binding capacity of the beads increased with oxidation time during the first 8 hours to 1.8 mmol/g, demonstrating successful oxidation of the acetyl group into PGAH/PGA (figure 4, blue line). However, at longer reaction times, the binding capacity decreased (figure 4, red line). IR analysis of the sorbent obtained after 8 of oxidation (Ps-Ac-Ox-8h; which had the highest binding capacity) showed a single carbonyl peak at 1675 cm^{-1} with a minor shoulder peak at 1740 cm^{-1}, whereas the sorbent obtained after 48 hours of oxidation (Ps-Ac-Ox-48h) showed two carbonyl peaks at 1675 cm^{-1} and 1740 cm^{-1} (figure 5). Floyd *et al*. reported that oxidation of 2-bromoacetophenone with DMSO resulted in a mixture of PGAH and phenylglyoxilic acid (PGOA, structure shown in scheme 5). It is therefore concluded that over-oxidation occurred when the beads were exposed to the oxidizing mixture for more than ~8 hours resulting in the formation of carboxylic acids groups (scheme 5). The shoulder peak at 1740 cm^{-1} in the PS-Ac-Ox-8h sample indicates that the over-oxidation of PGA/PGAH into PGOA already occurred during the first 8 hours of reaction, but it is slower than the oxidation of the acetyl group into the PGA/PGAH group.

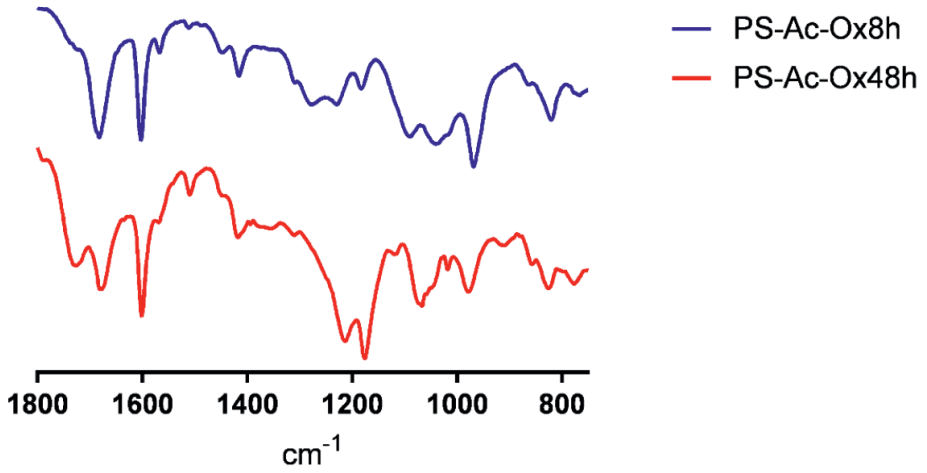

Figure 5: IR spectra of PS-Ac-Ox-8h (lower spectrum) and PS-Ac-Ox-48h (upper spectrum).

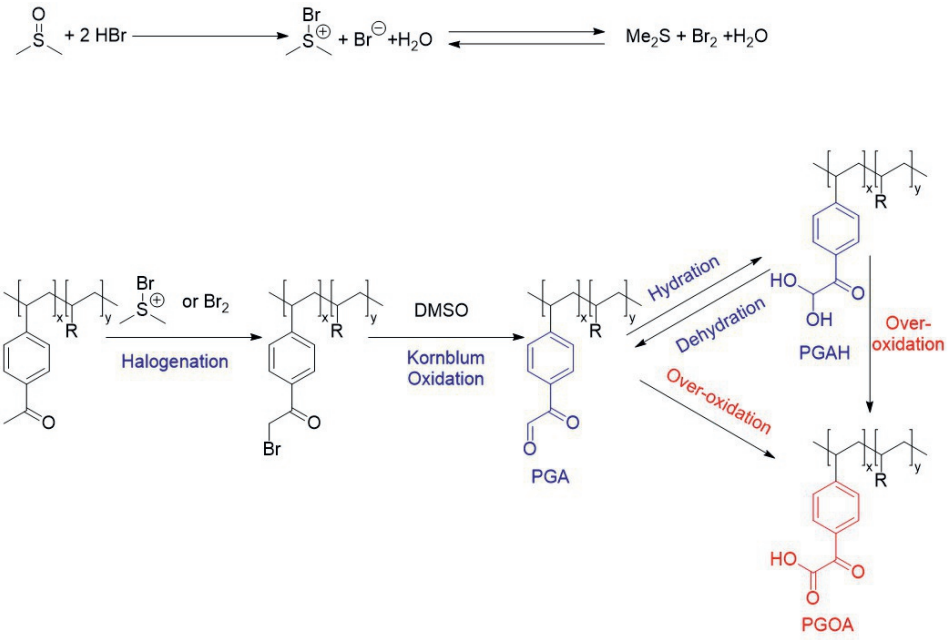

Scheme 5: Oxidation of PS-Ac using HBr and DMSO. PGA = Phenylglyoxaldehyde, PGAH = phenylglyoxaldehyde hydrate, PGOA = phenylglyoxilic acid.

The sorbent was analyzed by quantitative ^{13}C-solid state NMR to quantify the amount of PGAH groups in Ps-Ac-Ox. The CH_3 peak of the acetyl group detected in ^{13}C-NMR spectrum of PS-Ac had disappeared, indicating that all acetyl groups had been converted (supporting information section 7.9). Comparison of the area under the hydrate carbon peak (80-100 ppm) with that of the aromatic peaks (110-160 ppm) and the aliphatic peaks (10-50 ppm) shows that ~40% of the aromatic groups (thus ~67% of the acetyl groups) had been converted into PGAH groups. In addition, a minor peak around 165 ppm was detected, which is assigned to the carboxylic acid carbonyl peak from PGOA.

PS-Ac beads were also oxidized for 8 hours on a larger scale (*i.e.* 60 instead of 3.5 gram), and the obtained beads (PS-Ac-Ox) were characterized by SEM, light microscopy and nitrogen physisorption (figure 3G-I). PS-Ac-Ox beads had similar size (0.54 ± 0.11 mm), surface area (37.0 m^2/g) and pore volume and pore size/volume distribution (figure 3I) as PS and PS-Ac. This confirms that also the oxidation reaction had neither affected the macroporosity nor degraded the beads, likely because the reaction temperature (80 °C) was below the glass transition temperatures (T_g) of both the PS-Ac and PS-Ac-Ox beads (T_g of dry beads were 184 °C and >230 °C, respectively (supporting information section 7.3)). The PGAH content of the sorbent according to ^{13}C-NMR (supporting information section 7.9) was similar to the sorbent prepared at small scale, while the urea binding capacity of PS-Ac-Ox was lower than the batch prepared at small scale (*i.e.* 1.4 mmol/g, *versus* 1.8 mmol/g at 3.5 g scale) (table 2 and supporting information section 7.7). This difference can be

explained by the relatively large error (~10%) in quantification of the PGAH groups by ^{13}C NMR.

Table 2: Characteristics of PS, PS-Ac and PS-Ac-Ox beads (after 8 h oxidation of PS-Ac). [a]Determined by light microscopy. [b]Determined by N_2 physisorption. [c]Determined by ^{13}C solid state NMR.

Beads	Diameter (mm)[a]	Surface Area (m^2/g)[b]	Pore Volume (mL/g)[b]	Functionalization[c]	Urea Binding Capacity (mmol/g)
PS	0.49 ± 0.18	36.3	0.32	-	-
PS-Ac	0.61 ± 0.17	43.4	0.31	~60% acetylation	-
PS-Ac-Ox (small scale)	n.d.	n.d.	n.d.	~40 % PGAH-groups	1.8
Ps-Ac-Ox (large scale)	0.54 ± 0.11	37.0	0.31	~40 % PGAH-groups	1.4

One option to obtain a sorbent with higher binding capacity is to increase the density of reactive PGAH units. We hypothesized that this can be accomplished by bypassing the incomplete Friedel-Crafts acetylation of polystyrene (~60 %). Therefore, a novel route was explored in which vinylphenylethanone (VPE) was used as monomer, which can be polymerized yielding a polymer with 100% of acetylated aromatic groups, which requires only one post polymerization step, *i.e.* the oxidation of the acetyl group (scheme 5). To allow proper comparison with the route based on styrene (scheme 4) we selected VPE with the vinylgroup at the *para*-position with respect to the acetyl group. The VPE monomer (**7**) was synthesized on a 10 gram scale from ethynylphenylethanone (**6**) in which the triple bond was reduced to a double bond using Lindlar's catalyst and hydrogen (scheme 6). The reaction time was carefully monitored to prevent over-reduction of the double bond into the single bond (**9**).

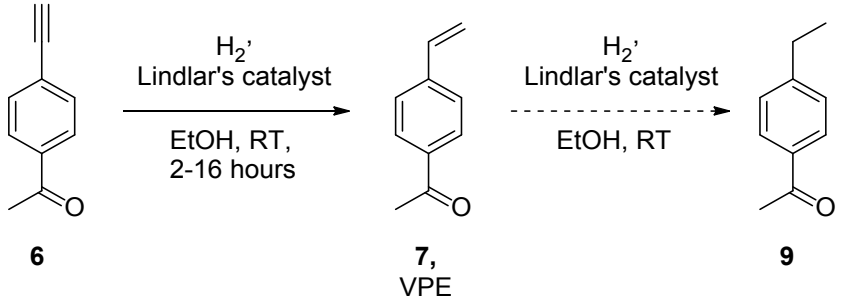

Scheme 6: The synthesis of vinylphenylethanone (**7**, VPE).

Next, the conditions needed to obtain macroporous sorbent beads based on the monomer VPE (scheme 7). Crucial to obtain macroporous sorbent beads is the identification of the optimal porogen.[20,24-25] The suspension polymerization conditions of styrene were selected as a starting point, *i.e.* using toluene with ShellSolTD as

non-solvating porogen. Importantly, the non-solvating porogen should dissolve VPE and precipitate pVPE. When the crosslinked polymer does not swell in the porogen, this will result in phase separation and yield porosity.[19] However, ShellSolTD and VPE are not miscible and therefore ShellSolTD/toluene mixtures with high volumes of ShellSolTD are non-solvents for VPE, and no polymeric beads were obtained by suspension polymerizations at various volumetric ratios of ShellSolTD as porogen.
The Hildebrand solubility parameter (δ) of a molecule or polymer, which is defined as the square root of the cohesive energy density, is commonly used to predict the miscibility of solvents, monomers and polymers, because compounds with a similar δ-value are likely miscible. This solubility parameter can be determined experimentally or calculated based on the molecular structure, *i.e.* by the method reported by Fedors.[26] ShellSolTD is a mixture of alkanes and therefore ShellSolTD was replaced by heptane, for which δ = 15.2 $J^{1/2}m^{-3/2}$,[27] and the heptane/toluene ratio was adjusted to vary the δ-value between 15.2 and 18.2 $J^{1/2}m^{-3/2}$ (*i.e.* the δ -value of toluene).[27-28] The calculated δ-values of VPE (δ = 19.0 $J^{1/2}m^{-3/2}$)[26] and of pVPE (δ = 21.1 $J^{1/2}m^{-3/2}$)[26] are higher than those of styrene (17.8 $J^{1/2}m^{-3/2}$)[29] and polystyrene (δ = 17.4-19.0 $J^{1/2}m^{-3/2}$)[27, 30], thus the δ of a suitable porogen mixture (δ_{mix}) is also expected to be higher than the δ_{mix} of the porogen used for the suspension polymerization of polystyrene. Volumetric mixtures of 75:25 and 50:50 heptane and toluene with δ_{mix}-values of 15.6 and 16.9 $J^{1/2}m^{-3/2}$, respectively, did dissolve VPE and resulted in the formation polymeric beads (table 3, entry 1-2). However, the S_{BET} surface areas of the beads as determined with nitrogen physisorption were low (S_{BET} < 0.05 m^2/g), indicating that δ_{mix}-value of these porogen mixtures is too low, resulting in early precipitation of pVPE without the formation of macropores.

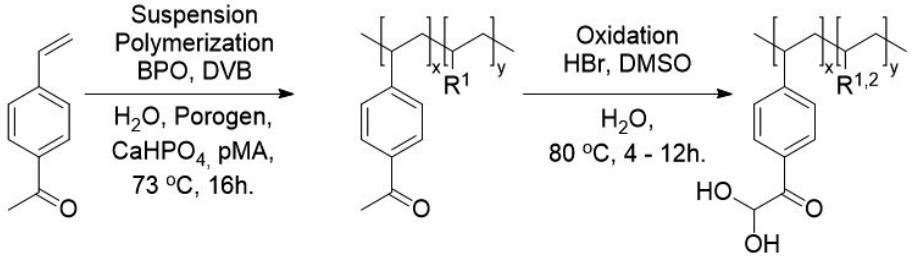

Scheme 7: Synthesis of PGAH-type sorbents from VPE. R^1 = crosslinker, R^2 = side product, see scheme 5 and 8.

Table 3: Effect of the porogen in the suspension copolymerization of VPE with DVB on the surface area of polyvinylphenylethanone. [a]Aggregated particles were obtained. [b]Surface area after oxidation of pVPE. *δ-Values of the porogen mixtures (δ_{mix}) were determined according to equation 6, in which x_i and V*i* are the molar fraction and the volume fraction of the solvents and monomer, respectively.[28-29]

Entry	Porogen	Porogen ratio	δ_{mix} porogen ($J^{1/2}m^{-3/2}$)*	% DVB	Bead diameter (mm)	Yield (%)	S_{BET} surface area (m^2/g)
1[a]	heptane/ toluene	75:25	15.6	3	0.62 ± 0.22	93%	< 0.05
2	heptane/ toluene	50:50	16.9	3	0.40 ± 0.28	99%	< 0.05
3	heptane/ toluene	40:60	17.5	3	0.48 ± 0.14	65%	0.1
4	heptane/ toluene	30:70	17.8	3	0.61 ± 0.23	75%	2.0 (1.9[b])
5	heptane/ toluene	20:80	18.1	3	0.66 ± 0.21	66%	0.2
6	heptane/ toluene	10:90	18.2	3	0.47 ± 0.10	70%	< 0.05
7	toluene	-	18.2	6	0.71 ± 0.23	69%	0.2
8[a]	toluene/ nitrobenzene	90:10	18.2	3	0.57 ± 0.34	52%	< 0.05
9	toluene/ nitrobenzene	80:20	18.4	6	0.55 ± 0.19	82%	< 0.05

$$(6) \qquad \delta_{mix} = \frac{\Sigma\, x_i V_i \delta_i}{\Sigma x_i V_i}$$

To further tune the porogen mixture to induce precipitation in a later stage of the polymerization, the δ-value of the porogen mixture (δ_{mix}) was stepwise increased, and therefore closer to the δ-value of pVPE, from 16.9 to 18.2 $J^{1/2}m^{-3/2}$ using mixtures of heptane and toluene (table 3, entries 2 - 7). To further increase the δ_{mix}, mixtures of nitrobenzene (δ = 21.7 $J^{1/2}m^{-3/2}$)[31] and toluene (δ = 18.2 $J^{1/2}m^{-3/2}$)[27] were used in a 10:90 and 20:80 ratio (table 3, entries 8 and 9). The 30:70 mixture of heptane and toluene (entry 4), for which the calculated δ_{mix}-value of the porogen mixture is 17.8 $J^{1/2}m^{-3/2}$, yielded the sorbent with the largest S_{BET} surface area of 2.0 m^2/g. Interestingly, the difference in calculated δ-value of pVPE and the 30:70 heptane/ toluene mixture (21.1-17.8 = 3.3 $J^{1/2}m^{-3/2}$) is similar to difference between the δ-value of polystyrene and the 91:9 ShellSolTD/heptane mixture (18.2 ± 0.8 - 15.2 = 3.0 ± 0.8 $J^{1/2}m^{-3/2}$). However, the surface area of the obtained pVPE beads was substantially smaller than that of the PS beads (2.0 and 36.3 m^2/g, respectively). It is important to note that at the start of the polymerization the δ_{mix} of the porogen is higher than at the end of the polymerization, due to VPE dissolved in the porogen (δ_{mix} = 18.3 $J^{1/2}m^{-3/2}$, the δ_{mix} gradually decreases during the polymerization reaction as a result

of VPE depletion). Therefore, the initial difference between the calculated δ-value of pVPE and the porogen-VPE mixture (21.1-18.3 = 2.8 $J^{1/2}m^{-3/2}$) is actually bigger than the initial difference between the δ-value of polystyrene and the porogen-styrene mixture (18.2±0.8 - 16.5 = 1.7±0.8 $J^{1/2}m^{-3/2}$), and therefore precipitation of pVPE probably occurred at an earlier stage of the polymerization reaction than PS did.

To assess the influence of porosity on the urea binding capacity, the pVPE beads of entry 2 (S_{BET} < 0.05 m^2/g) and 4 (S_{BET} = 2.0 m^2/g) were selected for oxidation. The beads of low surface area (entry 2) were oxidized for 4-12 hours under the same conditions as applied for PS-Ac. The urea binding capacities of the resulting oxidized pVPE beads (pVPE-Ox-(2) were 1.8-2.2 mmol/g, of which the highest binding capacity (2.2 mmol/g) was obtained after 12 hours of oxidation (supporting information section 7.6 and 7.7). The pVPE beads with the highest surface area (entry 4) were therefore oxidized for 12 hours and the urea binding capacity of these beads (pVPE-Ox-(4)) was 1.8 mmol/g (supporting information section 7.7). The surface area of the pVPE-Ox-(4) determined by nitrogen physisorption was similar to that of the corresponding pVPE beads (1.9 vs 2.0 m^2/g), most likely because the reaction temperature of the oxidation reaction (80 °C) is much lower than the T_g of pVPE beads (147 °C, supporting information section 7.3) and the beads therefore remain dimensionally stable under these oxidizing reaction conditions.

As hypothesized, the VPE-based materials showed a higher urea binding capacity than the styrene-based materials because of the increase in the density of acetyl groups and therefore a higher PGAH content after oxidation (1.4-1.8 *vs.* 1.8-2.2 mmol/g). Surprisingly, the surface area of pVPE beads had no influence on the urea binding capacity (1.8-2.2 and 1.8 mmol/g for pVPE-Ox-(2) and pVPE-Ox-(4) respectively). This shows that PGAH groups are accessible for urea also in materials without macroporosity, possibly because the sorbents swell to a minor but sufficient extent in water due to the polar and hydrophilic carbonyl groups and the carboxylic acid groups of PGOA due to overoxidation of PGA/PGAH (scheme 5). In addition, upon urea binding the beads become more hydrophilic further enhancing accessibility for water and urea thereby further improving urea binding kinetics.

The average size of pVPE-Ox-(4) beads determined by light microscopy was slightly larger than that of the pVPE beads (0.77 ± 0.20 and 0.61 ± 0.23 mm, respectively). Due to the swelling/deswelling of the beads during nitrogen physisorption experiments, the pore/volume distribution for these materials could not be determined.

The pVPE-Ox-(4) and corresponding pVPE beads were analyzed by SEM (figure 6B, C, E and F). Unlike the beads obtained in the suspension polymerization of styrene, the obtained pVPE beads were hollow as they were deflated after drying under vacuum, which suggests core-shell phase separation during the polymerization

reaction. In general, core-shell structures are thermodynamically favorable in water-oil-polymer mixtures when the surface tension between the water and the oil phase (γ_{WO}) is greater than the surface tension between the water and the polymer phase (γ_{WP}) and the polymer and oil phase (γ_{PO}) combined ($\gamma_{WO} > \gamma_{WP} + \gamma_{PO}$).[32-33] Apparently, due to the polar carbonyl groups present in pVPE, γ_{WP} decreased as compared to the γ_{WP} between water and polystyrene.

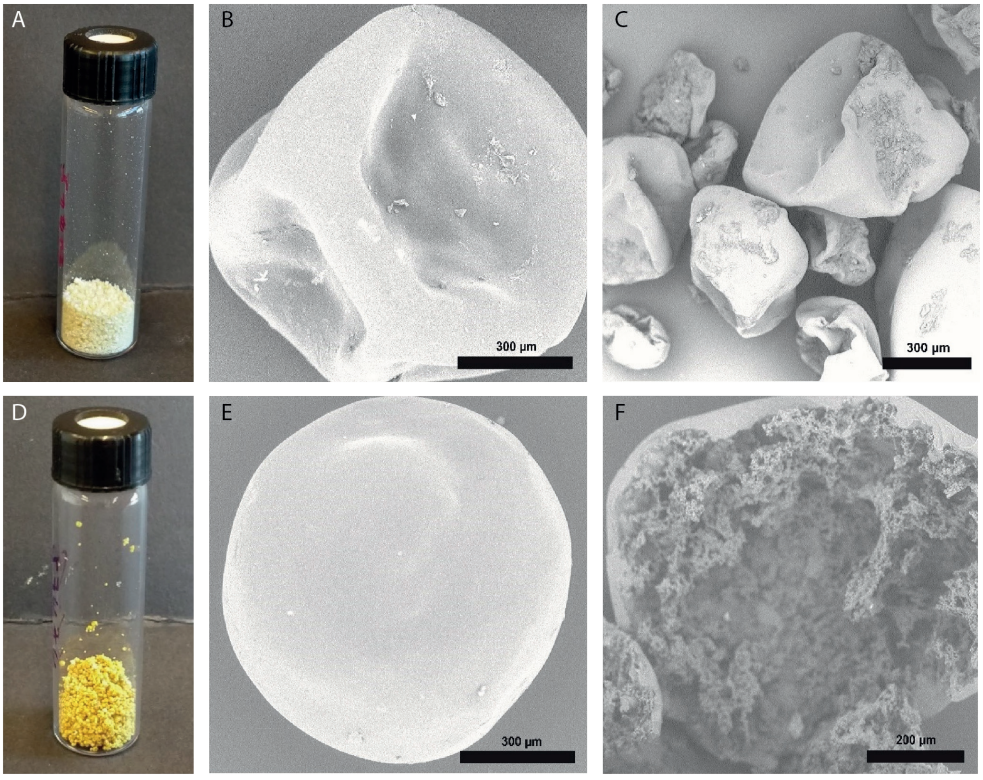

Figure 6: Photographs of the VPE-based PGAH-sorbent beads (pVPE-Ox-(4): D-F) and their precursor (pVPE beads: A-C): photographs (left images) and typical SEM images (middle and right).

To determine the density of PGAH-groups in pVPE-Ox-(2) and pVPE-Ox-(4), these materials were analyzed by ^{13}C solid state NMR spectroscopy (supporting information section 7.9). Comparison of the hydrate peak integral (80-100 ppm) with the backbone peak integral (10-50 ppm) demonstrates a PGAH-content of ~50% for both pVPE-Ox-(2) and pVPE-Ox-(4), which confirms that higher PGAH contents are obtained using the VPE instead of the styrene route (~50 and ~40% respectively).

Like PS-Ac-Ox beads, pVPE-Ox beads also clearly show the peak around 165 ppm (assigned to carboxylic acid group of PGOA) due to over-oxidation of PGAH, resulting in the formation of phenylglyoxilic acid (scheme 5). Moreover, an additional peak around 70 ppm was detected in the ^{13}C- NMR spectrum of pVPE-Ox. Presumably,

due to the higher density of acetyl groups in pVPE as compared to PS-Ac, an aldol condensation between neighboring PGA and remaining acetyl groups had occurred during the oxidation reaction, as was described for the oxidation of acetophenone into PGA/PGAH (scheme 8).[34-35] Because PS was only acetylated for 60%, this side reaction likely also occurred to a smaller extent in this material, as indicated by a very minor peak at 70 ppm in the spectrum of PS-Ac-Ox (supporting information section 7.9).

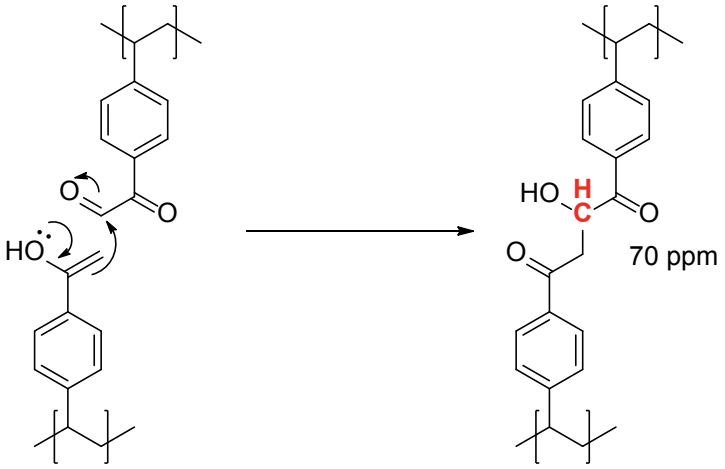

Scheme 8: Aldol reaction between a dehydrated PGA group and the enol-tautomer of the acetyl group, giving rise to the signal at 70 ppm in the quantitative ^{13}C solid state NMR spectrum.

It was found that the pVPE-Ox sorbent beads, which were for ~50% functionalized with PGAH groups, had a urea binding capacity of ~2 mmol/g. However, a 100% functionalized sorbent contains 5.5 mmol/g PGAH groups (including 3 mol% crosslinker) based on molecular weight of the monomer (178 g/mol), which implies that a sorbent with ~50% PGAH groups would have a urea binding capacity of 2.8 mmol/g at most. There are two reasons why the actual urea binding capacity for a sorbent functionalized with PGAH groups is lower than theoretical urea binding capacity based on a 1:1 reaction of urea with PGAH. First, some of the PGAH groups might be inaccessible for urea. Second, PGAH can react with urea in both a 1:1 and a 2:1 ratio (scheme 1) and therefore one potential binding site is lost when PGAH reacts with urea in a 2:1 ratio.

Quantification of the inaccessible and therefore unreacted PGAH groups in beads with ~2 mmol urea per gram sorbent with ^{13}C- NMR spectroscopy is not possible because unreacted PGAH and reacted PGAH give rise to signals in the same region of the spectrum. Therefore the sorbent beads which had reacted with urea (PS-Ac-Ox@urea and pVPE-Ox-(4)@urea) were analyzed with IR spectroscopy, along with PGAH, and the 2:1 adduct of PGAH and urea (**3'a**) (figure 7). PGAH shows a clear ketone-carbonyl stretching vibration at 1700 cm^{-1} and a C-O stretching vibration at

1210 cm^{-1}. However, these peaks have a lower intensity in the IR spectra of PS-Ac-Ox@urea and pVPE-Ox-(4)@urea, and the main carbonyl peak is clearly shifted (from 1700 to 1740 cm^{-1}). Based on these observations it is concluded that the majority of the PGAH groups were indeed accessible for reaction with urea and had reacted. This agrees with the observation that the surface area does not influence the urea binding capacity. Moreover, the IR spectra of PS-AC-Ox@urea and pVPE-Ox-(4)@urea are more similar to the IR spectrum of the isolated 2:1 addition product **3'a** (figure 7). The several peaks arising from the carbonyl stretching vibration in the region of 1650-1800 cm^{-1} of **3'a** are also present in the spectra of PS-AC-Ox@urea and pVPE-Ox-(4)@urea. Therefore it is concluded that reaction of the 1:1 PGAH : urea adduct with a second PGA group takes place in the sorbent beads at least to some extent, thereby explaining the difference between the urea binding capacity of the sorbents (~2.0 mmol/g) and the theoretical capacity based on the actual PGAH content (2.8 mmol/g). From this difference we then calculate that (2.8-2.0=) 0.8 mmol/g PGAH was lost because it reacted with the 1:1 PGAH:urea adduct. Therefore (2*0.8=) 1.6 mmol/g (57%) of PGAH reacted in a 2:1 ratio with urea, and thus (2.8-1.6=) 1.2 mmol/g (43%) of the PGAH groups present in the sorbent reacted in a 1:1 ratio with urea.

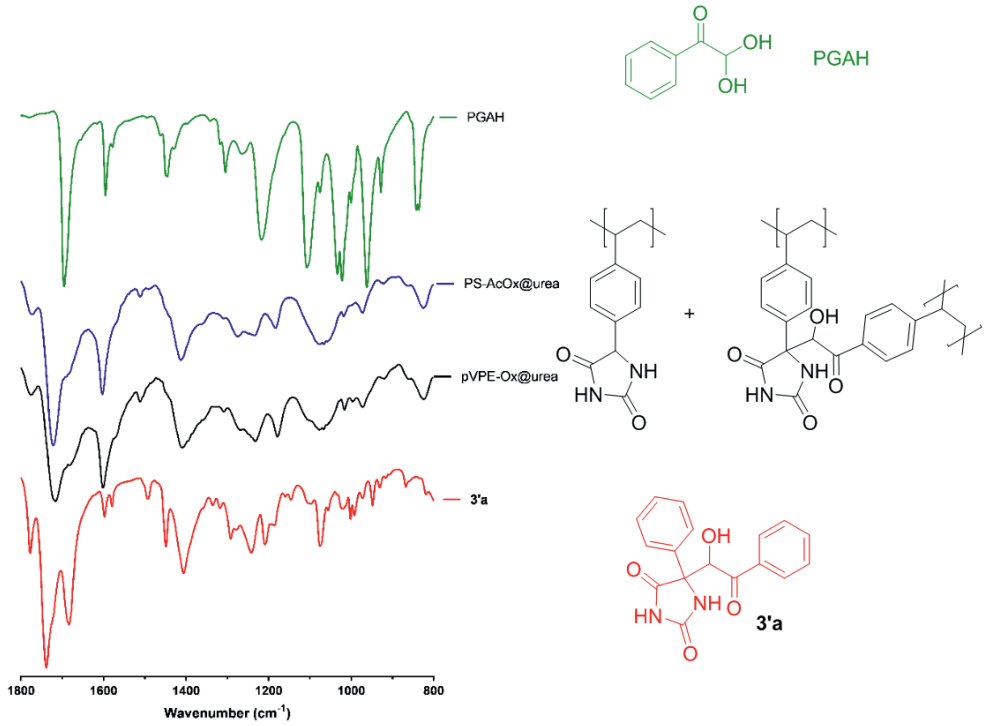

Figure 7: IR spectra of PGAH, PS-AC-Ox@urea, pVPE-Ox-(4)@urea and the 2:1 addition product of PGAH and urea (**3'a**).

The kinetics of the urea binding of the two different types of PGAH-type sorbents was investigated by incubating them in a 30 mM urea solution in phosphate-buffered saline (PBS) at 37 °C, conditions representative for the regeneration of dialysate.[7] The urea binding was determined by measuring the urea concentration in the solution at different time points (supporting information section 7.8 and figure 8A). The PS-Ac-Ox sorbent showed a binding of 0.5-0.6 mmol/g after 24 hours. The sorbent pVPE-Ox-(4) bound 0.5-0.6 mmol per gram already in 8 hours which increased to 0.8-0.9 mmol/g after 24 hours, reaching around 50% of its maximum binding capacity. Figure 8B shows that both materials reached ~45% of the maximum binding capacity after 24 hours.

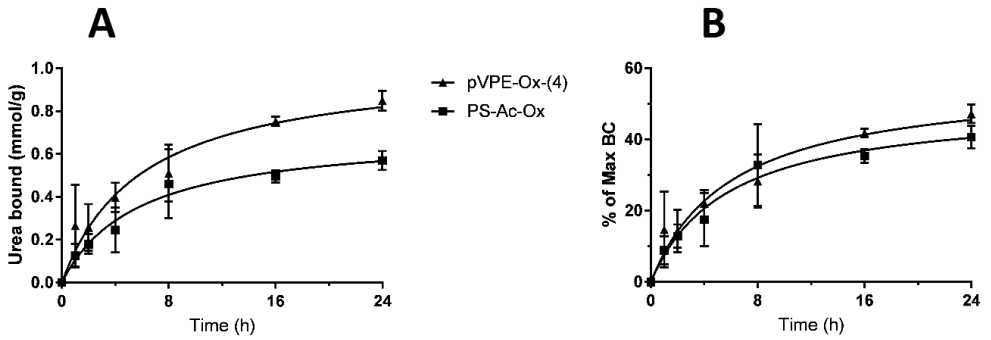

Figure 8: Urea binding of PS-Ac-Ox and pVPE-Ox-(4) in time. A) Binding expressed in mmol urea/g sorbent. B) Relative urea binding (percentage of the maximum binding capacity). Conditions: sorbent (10 mg/mL) in 30 mM urea solution in PBS at 37 °C (N=4).

3. Conclusion

Urea sorbent beads containing phenylglyoxaldehyde hydrate (PGAH) groups were successfully prepared via suspension polymerization of either styrene or vinylphenylethanone (VPE) followed by acetylation and oxidation, or oxidation only, respectively. The VPE route turned out to be the best choice, at it saves one post polymerization modification step, and, importantly, resulted in a sorbent with higher PGAH content (~50%, *vs* ~40% for PS-based sorbents) and concomitantly higher binding capacity (1.8 mmol/g, *vs* 1.4 mmol/g for PS-based sorbents). These beads are potentially suitable for application as urea sorbents in a wearable artificial kidney.

The accessibility of the PGAH groups in the VPE-based sorbents is not dependent on the surface area of the material, possibly because the beads swell to a minor extent. The kinetics of urea sorption from simulated dialysate showed that ~30% of the binding capacity is reached after 8 hours at 37 °C. The best sorbent developed (pVPE-Ox-(4)) bound ~0.5-0.6 mmol/g in 8 hours, which demonstrates that ~700 grams of this PGAH-type sorbent is needed to remove the daily urea production of 400 mmol of end-stage kidney disease patients during a dialysis session of 8 hours.

4. Materials and Methods

4.1 General

4-Nitrophenylglyoxaldehyde and 4-methylphenylglyoxaldehyde were purchased from CombiBlocks (CA, USA). 4-Ethynylacetophenone was purchased from Acros Organics (NJ, USA). Phosphate-buffered saline (PBS, pH = 7.4, ion composition: Na^+ 163.9 mM, Cl^- 140.3 mM, HPO_4^{2-} 8.7 mM, $H_2PO_4^-$ 1.8 mM) was obtained from B. Braun (Melsungen AG, Germany). Anhydrous dicalcium phosphate ($CaHPO_4$) was obtained from Chemtrade International (Bussum, the Netherlands). Polymethacrylic acid (Degalan® RG S mv) was obtained from Evonik Industries (Darmstadt, Germany). ShellSolTD®, a mixture of alkenes, was a kind gift from Shell (Amsterdam, the Netherlands). All other chemicals were obtained from Sigma-Aldrich (Zwijndrecht, the Netherlands) and used as received unless stated otherwise. Nickel filters with a cut-off of 200 μm were obtained from Veco B.V. (Eerbeek, the Netherlands).

4.2 NMR, UV and IR spectroscopy

NMR spectra were recorded on a Bruker 600 MHz with a BBI probe at room temperature (RT). Residual solvent signals were used as internal standard (^{1}H: δ 7.26 ppm, ^{13}C (^{1}H): δ 77.16 ppm for $CDCl_3$). Chemical shifts (δ) are given in ppm and coupling constants (J) are given in hertz (Hz). Resonances are reported as s (singlet), d (doublet), t (triplet), q (quartet), bs (broad singlet) and m (multiplet) or combinations thereof. UV absorption spectra were recorded in triplicate with a BMG LABTECH SpectroStar Nano plate reader using a UV-Star Microplate 96 well obtained from Greiner Bio-One (Alphen aan de Rijn, the Netherlands). Infrared (IR) spectra were recorded neat using a Perkin Elmer ATRU Spectrum 2.

4.3 Determination of the Pseudo-First Order Rate Constants

PGAH (**1a**) and two PGAH derivatives (**1b** and **1c**) (0.3 mmol, 1.0 eq.) were individually dissolved in 1:1 v/v mixture of PBS:dimethylsulfoxide (DMSO) (10 mL). Urea (901 mg, 15 mmol, 50 eq.) was dissolved in the PGAH solution which was subsequently magnetically stirred at 50 °C. Samples (50 μL) from the reaction mixture were taken at different time points, diluted 10 (**1a**) or 15 (**1b** and **1c**) times with 1:1 v/v DMSO:PBS (500 or 700 μL) and subsequently diluted another 10× using the same solvent mixture (thus resulting in a final 100 or 150 times dilution, respectively). The concentrations of the PGAH (derivatives) **1a-c** in the 100 or 150 times diluted samples were determined by UV spectroscopy (260, 263 and 270 nm, for **1a**, **1b** and **1c**, respectively). A calibration curve was prepared using a dilution series in 1:1 v/v mixture of PBS:DMSO (final concentrations varied from 0.030-0.360 mM) from a stock solution of the PGAH (derivatives) (30 mM) in 1:1 (v/v) DMSO:PBS. The k_{PFO}-values for the PGAH analogues were determined from the slopes of the plots of ln [PGAH] *versus* time.

4.4 Calculation of Gibbs Free Energy (G)

Density functional theory (DFT) calculations were performed using the Gaussian 09 software package, using B3LYP (Becke, three-parameter, Lee-Yang-Parr) functional with 6-31g(d,p) as basis set on all atoms.[36] Structure optimizations were carried out with water as solvent without any symmetry restraints. Frequency analyses were performed on all optimized geometries to check that they are in fact minima. Standard temperature (298.15 K) and pressure (1 atm) were used for thermochemical calculations. Input: #B3LYP/6-31G(d,p) opt=tight freq scf=tight int=ultrafine pop=regular SCRF=(Solvent=Water).

4.5 Preparation of 10% Polymethacrylic Acid Sodium Salt Solution in Water

In a glass reactor equipped with mechanical stirrer, polymethacrylic acid (10 grams) was dissolved in water (84 mL) by heating to 80 °C and stirring for 30 minutes. Next an aqueous 50% NaOH (2.67 mL; 68 mmol NaOH) solution was added and stirring was continued for 60 minutes at the same temperature. The obtained viscous solution was transferred into a Falcon tube and stored at 4 °C for later use as thickening agent of the aqueous phase in suspension polymerization.

4.6 Suspension Polymerization of Styrene

For the suspension polymerization of styrene we essentially used a method as described by Jong et al.[18] However, ShellSolTD and a poly(methacrylic acid) sodium salt solution were used instead of hexane and polyacrylic acid sodium salt. The detailed procedure was as follows.

The aqueous phase was prepared by addition of NaCl (340 mg), poly(methacrylic acid) sodium salt solution (8.32 g of a 10% solution in water) and $CaHPO_4$ (3.06 g) to water (540 mL) in a glass reactor equipped with a teflon blade stirrer (see figure S7 for a picture). The aqueous phase was stirred for 30 minutes at RT and the pH was 6.9. The organic phase was prepared by mixing styrene (229 mL, 2.0 mol), ShellSolTD (276 mL) and toluene (27 mL) in a beaker. Next, 55% technical grade divinylbenzene (DVB) (13 mL, 50 mmol, 2.5 mol%) and a 50% benzoylperoxide blend with dicyclohexyl phthalate (6.0 g, 12.4 mmol, 0.6 mol%) was added to the organic phase and stirred until the initiator was dissolved and a homogeneous solution was formed at room temperature (RT). The organic phase was subsequently added to the aqueous phase in the glass reactor under continuous mechanical stirring at 180 rpm, by which an o/w emulsion was formed, and oxygen was removed by flushing with nitrogen gas for 20 minutes. Next, the emulsion was heated at 73 °C in an oil bath for 16 hours under mechanical stirring. The resulting suspension was allowed to cool to RT and was poured over a sieve (cut-off 200 µm, Veco B.V.) and washed with acetone and water. The white beads were collected and dried over P_2O_5 under

vacuum, resulting in 216 g polystyrene (PS) beads. TGA analysis showed ~14% volatiles present, indicating a yield of solid material of ~186 gram (86%).

4.7 Friedel-Crafts Acetylation of Polystyrene[12]

In a glass reactor equipped with a teflon blade stirrer, PS beads (80.9 g, 0.77 mol aromatic groups, 1.0 eq.) were swollen in 1,2-dichloroethane (DCE, 750 mL) for 30 minutes under mechanical stirring. Anhydrous $AlCl_3$ (156 g, 1.17 mol, 1.5 eq.) was added portion wise (3-5 gram) to the suspension over the course of 15 minutes. After all $AlCl_3$ was added, acetyl chloride (66 mL, 0.94 mol, 1.2 eq.) was added slowly and the suspension was heated to 50 °C in an oil bath for 5 hours, after which the formation of HCl-gas (caused by the reaction of aromatic group and acetyl chloride) stopped. The suspension was allowed to cool to RT, after which the suspension was filtered (cut-off 200 µm). The residue was suspended in a 500 mL of 6 M HCl solution at 0 °C in an ice bath and stirred for 30 minutes to remove aluminum salts; this step was repeated twice. The suspension was filtered (cut-off 200 µm, Veco B.V.) and washed with acetone and water until the pH of the filtrate was > 5. The residue was dried over P_2O_5 under vacuum, resulting in acetylated polystyrene (PS-Ac, 71.6 g).

4.8 Halogenation and Kurnblum Oxidation of Acetylated Polystyrene[12]

In a glass reactor equipped with a teflon blade stirrer, PS-Ac beads (60.0 g) were swollen in DMSO (600 mL, 8.45 mol) for 30 minutes under continuous stirring, after which an aqueous solution of 48% HBr (175 mL, 1.55 mol) was slowly added. One of the outlets of the reactor was capped with a septum containing a needle allowing escape of the formed Me_2S. The suspension was stirred at 80 °C for 8 hours, after which the reaction mixture was filtered (cut-off 200 µm, Veco B.V.). The residue was washed with water until the pH of the filtrate was > 5. The residue was dried over P_2O_5 under vacuum, resulting in PS-Ac-Ox (55.2 grams).

4.9 Synthesis of *p*-(Vinylphenyl)ethenone (VPE)

In a 3-neck round bottom flask *p*-(ethynylphenyl)ethenone (**6**, 10.0 g, 69.4 mmol) was suspended in EtOH (350 mL) and Lindlar's catalyst (300 mg, 3 w%) was added. Air was replaced by H_2 (balloon) and the suspension was stirred at RT for 2-16 hours. To monitor the conversion (and thus preventing over-reduction of VPE (**7**) into the alkane (**8**)), samples were frequently taken from the reaction mixture and, after evaporation of EtOH under reduced pressure, the conversion was determined by ^{1}H-NMR ($CDCl_3$). After the conversion was >90%, the H_2-filled balloon was removed and the reaction mixture was concentrated under reduced pressure. The crude product was re-dissolved in CH_2Cl_2 and purified by filtration over Hyflo. The filtrate was concentrated under reduced pressure, giving crude VPE (**7**) as a yellow liquid in a 99% yield (10.1 g, 69.0 mmol). Melting point 29 °C, melt enthalpy 90.6 J/g

(supporting information section 7.3). ^{1}H-NMR ($CDCl_3$, 600 MHz) δ 7.92 (d, *J* = 8.3 Hz, 2H), 7.48 (d, *J* = 8.2 Hz, 2H), 6.75 (dd, *J* = 17.6 Hz, 10.9 Hz, 1H), 5.87 (d, *J* = 17.6 Hz, 1H), 5.39 (d, *J* = 10.9 Hz, 1H), 2.59 (s, 3H). The melting point and the NMR spectrum correspond with the ones reported in literature.[37-39]

4.10 Suspension Polymerization of *p*-(Vinylphenyl)ethenone

The same procedure as for the preparation of polystyrene beads was employed, with some minor modifications. In brief, the aqueous phase was prepared by addition of NaCl (11 mg), polymethacrylic acid sodium salt solution (452 mg of a 10% gel in water) and $CaHPO_4$ (84 mg) to water (15 mL). The organic phase was composed of VPE (2.1 g, 14.4 mmol, 2 mL), porogen (2.9 mL, com position see table 3), 80% technical grade DVB (3-6 mol%) and a 50% benzoylperoxide blend with dicyclohexyl phthalate (174 mg, 0.36 mmol, 2.5 mol%). After mixing and polymerization (same procedure followed as for 'Suspension Polymerization of Styrene'), the resulting suspension was allowed to cool to RT and poured over a filter (cut-off 200 µm, Veco B.V.). The residue was washed with acetone and water, and finally dried over P_2O_5 under vacuum, resulting in pVPE (1.1-1.9 grams, yield 52-90%).

4.11 Halogenation and Kurnblum Oxidation of pVPE

The same procedure as for the halogenation and Kurnblum oxidation of acetylated polystyrene beads was employed for 12 hours, downscaled to 600 mg pVPE. After washing, 606 mg of yellow beads (pVPE-Ox) was obtained.

4.12 Scanning Electron Microscopy Analysis of Sorbent Particles

The morphology of the beads was analyzed by scanning electron microscopy (SEM, Phenom, FEI Company, the Netherlands). Dried beads were transferred onto 12-mm diameter aluminum specimen stubs (Agar Scientific Ltd., England) using double-sided adhesive tape. Prior to analysis, the beads were coated with platinum using an ion coater under vacuum. The samples were imaged using a 5 kV electron beam.

4.13 Determination of the Size of the Beads by Light Microscopy

The diameters of the beads were measured using optical microscopy, utilizing a size calibrated Nikon eclipse TE2000-U microscope equipped with a digital camera (Nikon DS-2Mv camera and Nikon DS-U1 digital adapter, with a 4× magnification) and the NIS-elements basic research software package. Images of the beads were taken in the dry state and for 30 arbitrary beads 3 points on the perimeter of the beads were identified to allow calculation of circular diameter by the program.[40] The average diameters and standard deviations are reported.

4.14 Quantitative ^{13}C Solid State NMR Analysis of the Different Beads

For solid-state ^{13}C NMR measurements, beads were crushed and transferred into a 3.2 mm rotor for the magic-angle spinning (MAS) solid-state NMR analysis. The analysis of the samples was performed either on a Bruker 700 MHz wide-bore magnet with an AVANCE-III console or on a Bruker 400 MHz spectrometer. The spectra were recorded at room temperature (298 K) and using Magic Angle Spinning (MAS) frequency between 10 and 14 kHz, chosen to minimize the overlap of the signal with spinning sidebands. For the ^{13}C direct excitation spectra, 30˚ pulses were applied with field strength of 55 kHz and 80 kHz SPINAL64.[41] ^{1}H decoupling was applied during acquisition. The ^{13}C T1 relaxation time for each sample was determined using inverse recovery and used to establish the repetition time for the different samples, set to 2*T1. Except for the pVPE-Ox-(4) sample, which showed a very short relaxation time of 1 s, for the other samples the T1 varied from 40 to 80 s. Details for the specific analyses are given in the supporting information section 7.9. The NMR spectra were processed with 200 Hz line-broadening and analyzed with Bruker Topspin3.5.

4.15 Determination of Surface Area of the Beads using Nitrogen Physisorption

N_2 physisorption isotherms were measured at -196 °C using a Micromeritics TriStar 3000 and TriStar II Plus apparatus. Prior to analysis, the samples were dried under vacuum for 16 hours at RT. Surface areas of the beads were determined using the Brunauer-Emmett-Teller (BET) method and the total pore volumes were derived from the amount of N_2 adsorbed at p/p_0 = 0.995.[42] A Barrett-Joyner-Halenda (BJH) analysis was employed to determine pore size/volume distributions of the samples with the use of a Harkins-Jura thickness curve.[43-44] Due to the shrinking of the porous polymeric beads and collapsing of the pores with increasing pressure, and subsequent expansion and with decreasing pressure, the correction of the dead volume is incorrect, as by default it assumes that the solid fraction of the sample does not change in volume with pressure. As the dead volume was determined at $p/p_0 \approx 0$ and assumed constant during the measurement, the default dead volume-corrected isotherms decreased slightly with increasing pressures, which is physically meaningless. The relative deviation is largest for materials with low surface areas (< 5 m^2/g) and high materials volume fractions in the measurement tubes, such as for pVPE-Ox. A correction for this deformation *i.e.* change in dead volume with pressure was applied to these isotherms by a linear swelling function ($V_{adjusted} = a \cdot (p/p_0) + V_{original}$), in which a represents the swelling factor relative to the material's volume at $p/p_0 \approx 0$, until $dV/d(p/p_0) > 0$ was achieved for all pressures. Values for a were between 1.2 and 7.2, indicating a significant deformation of these materials. The S_{BET} surface areas of the pVPE-Ox beads were calculated from the isotherms that were corrected for these volume changes as a function of pressure.

4.16 Determination of Urea Binding

The sorbent beads (15 mg) were dispersed with urea solution (1.5 mL, 30 mM) in PBS in Eppendorf tubes. The samples were placed in an oven at 37 °C on a rotating device. After 1, 2, 4, 8, 16 and 24 hours, two Eppendorf tubes per time point were taken and the beads were allowed to settle and the supernatant was removed. To determine the maximum binding capacity (control experiment shown in the supporting information section 7.5), the sorbent beads (50 mg per vial) were incubated for 24 hours at 70 °C with a urea solution (5 mL, 30 or 50 mM) in PBS in two glass vials, after which the beads were allowed to settle and the urea concentrations in the supernatants were determined with an AU 5800 routine chemistry analyzer (Beckman Coulter, Brea, CA) using a coupled enzyme reaction, which results in a colorimetric (570 nm) product proportional to the urea concentration.[45]

4.17 Thermal Analysis of Monomer and Beads

Thermographic analysis (TGA) was done as follows. In a platinum pan the beads were heated at a rate of 10 °C/minute. The weight loss during the ramp heating (and thereby the decomposition temperature) was determined on a TA Instruments TGA Q50.

Differential scanning calorimetry (DSC) analysis of the different samples was done as follows. In an open aluminum pan the monomer or beads were heated from -50 till 250 °C at a rate of 10 °C/minute and the heat flow was monitored. Next, the sample was quickly cooled from 250 to -50 °C and subsequently heated again to 250 °C at a rate of 10 °C/min. The T_g or melting point was determined with a TA instruments Discovery DSC. For the beads, residual solvent evaporated during the first run and therefore the results of the second run are reported. For the monomer (VPE) events of the first run are reported.

4.18 Synthesis of 5-(1-Hydroxy-2-oxo-2-phenylethyl)-5-phenylimidazolidine-2,4-dione

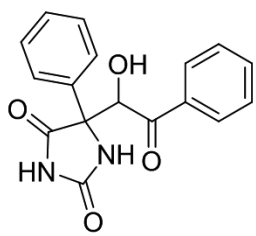

5-(1-Hydroxy-2-oxo-2-phenylethyl)-5-phenylimidazolidine-2,4-dione was synthesized as described earlier,[15] and used as reference compound for the IR analysis of the sorbent beads before and after urea saturation.

5. Acknowledgement

The authors like to thank Carl C.L Schuurmans for his help with determining the size of the sorbent particles, Lies A.L. Fliervoet for making figures 3 and 6 and

Shell Amsterdam for the gift of ShellSolTD. This research was supported by the Dutch organization for Scientific Research (NWO-TTW, project 14433) and the Dutch Kidney Foundation. The NMR experiments were supported by a TOP-PUNT grant to MB (NWO Grant number 718.015.001). RD acknowledges the European Research Council (ERC) for funding (ERC-2014-CoG 648991). MEM acknowledges the Sectorplan Natuur- en Scheikunde (Tenure-track grant at Utrecht University) for financial support.

6. References

1. Vanholder, R.; Gryp, T.; Glorieux, G., Urea and chronic kidney disease: the comeback of the century? (in uraemia research). *Nephrol. Dial. Transplant.* **2018,** *33* (1), 4-12.
2. Gura, V.; Rivara, M. B.; Bieber, S.; Munshi, R.; Smith, N. C.; Linke, L.; Kundzins, J.; Beizai, M.; Ezon, C.; Kessler, L.; Himmelfarb, J., A wearable artificial kidney for patients with end-stage renal disease. *JCI Insight* **2016,** *1* (8), 15.
3. Agar, J. W., Review: understanding sorbent dialysis systems. *Nephrology (Carlton)* **2010,** *15* (4), 406-11.
4. Davenport, A.; Gura, V.; Ronco, C.; Beizai, M.; Ezon, C.; Rambod, E., A wearable haemodialysis device for patients with end-stage renal failure: a pilot study. *Lancet* **2007,** *370* (9604), 2005-10.
5. Wester, M.; van Gelder, M. K.; Joles, J. A.; Simonis, F.; Hazenbrink, D. H. M.; van Berkel, T. W. M.; Vaessen, K. R. D.; Boer, W. H.; Verhaar, M. C.; Gerritsen, K. G. F., Removal of urea by electro-oxidation in a miniature dialysis device: a study in awake goats. *Am. J. Physiol. Renal. Physiol.* **2018,** *315* (5), F1385-F1397.
6. Lehmann, H. D.; Marten, R.; Fahrner, I.; Gullberg, C. A., Urea elimination using a cold activated-carbon artificial tubulus for hemofiltration. *Artif. Organs* **1981,** *5* (4), 351-356.
7. van Gelder, M. K.; Mihaila, S. M.; Jansen, J.; Wester, M.; Verhaar, M. C.; Joles, J. A.; Stamatialis, D.; Masereeuw, R.; Gerritsen, K. G. F., From portable dialysis to a bioengineered kidney. *Expert Rev. Med. Devices* **2018,** *15* (5), 323-336.
8. Shimizu, T.; Fujishige, S., A newly prepared surface-treated oxystarch for removal of urea. *J. Biomed. Mater. Res.* **1983,** *17* (4), 597-612.
9. Deepak, D., Evaluation of adsorbents for the removal of metabolic wastes from blood. *Med. Biol. Eng. Comput.* **1981,** *19* (6), 701-6.
10. Smakman, R. Macromolecular carbonyl groups containing material suitable for use as sorbent for nitrogen compounds. U.S. Patent 4,897,200, **1990**.
11. Smakman, R.; van Doorn, A. W., Urea removal by means of direct binding. *Clin. Nephrol.* **1986,** *26 Suppl 1*, S58-62.
12. Poss, M. J.; Blom, H.; Odufu, A.; Smakman, R., Macromolecular ketoaldehydes. U.S. Patent 6,861,473 B2: **2005**.
13. Kuntz, E.; Quentin, J. P., Alkenylaromatic polymers with α-ketoalhydic groups, U.S. Patent 3.933.753, **1976**.
14. Kuntz, E.; Quentin, J. P., Process for extracting urea from a solution with alkenylaromatic polymers with a-ketoalhydic groups. U.S. Patent 3.933.753 **1977**.
15. Jong, J. A. W.; Smakman, R.; Moret, M.-E.; Verhaar, M. C.; Hennink, W. E.; Gerritsen, K. G. F.; Van Nostrum, C. F., Reactivity of (vicinal) carbonyl compounds with urea. *ACS Omega* **2019,** *4* (7), 11928-11937.
16. Jong, J. A. W.; Moret, M. E.; Verhaar, M. C.; Hennink, W. E.; Gerritsen, K. G. F.; van Nostrum, C. F., Effect of substituents on the reactivity of ninhydrin with urea. *ChemistrySelect* **2018,** *3* (4), 1224-1229.
17. Clayden, J.; Warren, S.; Greeves, N.; Wothers, P.; *Organic Chemistry*. Oxford University Press: **2000**, p. 561.
18. Jong, G. J. D. Ion exchangers from poly(aminostyrene) and ethylene imine. U.S. Patent US3582505A , **1971**.
19. Gokmen, M. T.; Du Prez, F. E., Porous polymer particles—A comprehensive guide

to synthesis, characterization, functionalization and applications. *Prog. Polym. Sci.* **2012,** *37* (3), 365-405.
20. Durie, S.; Jerabek, K.; Mason, C.; Sherrington, D. C., One-Pot Synthesis of branched poly(styrene−divinylbenzene) suspension polymerized resins. *Macromolecules* **2002,** *35* (26), 9665-9672.
21. Cacchi, S.; Fabrizi, G.; Gavazza, F.; Goggiamani, A., Palladium-catalyzed reaction of aryl iodides with acetic anhydride. A carbon monoxide-free synthesis of acetophenones. *Org. Lett.* **2003,** *5* (3), 289-291.
22. Floyd, M. B.; Du, M. T.; Fabio, P. F.; Jacob, L. A.; Johnson, B. D., The oxidation of acetophenones to arylglyoxals with aqueous hydrobromic acid in dimethyl sulfoxide. *J. Org. Chem.* **1985,** *50* (25), 5022-5027.
23. Kornblum, N.; Jones, W. J.; Anderson, G. J., A new and selective method of oxidation - the conversion of alkyl halides and alkyl tosylates to aldehydes. *J. Am. Chem. Soc.* **1959,** *81* (15), 4113-4114.
24. Liu, Q. Q.; Wang, L.; Xiao, A. G., Research progress in macroporous styrene-divinylbenzene co-polymer microspheres. *Des. Monomers Polym.* **2007,** *10* (5), 405-423.
25. Wood, C. D.; Cooper, A. I., Synthesis of macroporous polymer beads by suspension polymerization using supercritical carbon dioxide as a pressure-adjustable porogen. *Macromolecules* **2001,** *34* (1), 5-8.
26. Fedors, R. F., A method for estimating both the solubility parameters and molar volumes of liquids. *Polym. Eng. Sci.* **1974,** *14* (2), 147-154.
27. Van Krevelen, D. M., *Properties of Polymers*. Amsterdam, **1990**, 198-203.
28. Cameron, N. R.; Barbetta, A., The influence of porogen type on the porosity, surface area and morphology of poly(divinylbenzene) PolyHIPE foams. *J. Mat. Chem.* **2000,** *10* (11), 2466-2471.
29. Cai, Y.; Yan, W.; Peng, X.; Liang, M.; Yu, L.; Zou, H., Influence of solubility parameter difference between monomer and porogen on structures of poly (acrylonitrile–styrene-divinylbenzene) resins. *J. Appl. Polym. Sci.* **2019,** *136* (3), 46979.
30. Matsukawa, H.; Yoda, S.; Okawa, Y.; Otake, K., Phase behavior of a carbon dioxide/methyl trimethoxy silane/polystyrene ternary system. *Polymers* **2019,** *11* (2), 11.
31. Hanssen, C. M., *The three dimensional solubility parameter and solvent diffusion coefficient, their importance in surface coating formulation*. Danish Technical Press: Copenhagen, **1967**.
32. Jonsson, M.; Nordin, O.; Malmström, E.; Hammer, C., Suspension polymerization of thermally expandable core/shell particles. *Polymer* **2006,** *47* (10), 3315-3324.
33. Sundberg, D. C.; Casassa, A. P.; Pantazopoulos, J.; Muscato, M. R.; Kronberg, B.; Berg, J., Morphology development of polymeric microparticles in aqueous dispersions. I. Thermodynamic considerations. *J. Appl. Polym. Sci.* **1990,** *41* (7-8), 1425-1442.
34. Liu, Y.; Zhao, H.; Tian, G.; Du, F.; Qi, Y.; Wen, Y., A novel coupling reaction of α-halo ketones promoted by SmI3/CuI. *RSC Advances* **2016,** *6* (31), 26317-26322.
35. Dudley, H. W.; Ochoa, S., 157. Benzoylphenacylcarbinol. *J. Chem. Soc.* **1933,** (0), 625.
36. M. J. Frisch, G. W. T., H. B. Schlegel, G. E. Scuseria, M. A. Robb, J. R. Cheeseman, G. Scalmani, V. Barone, B. Mennucci, G. A. Petersson, H. Nakatsuji, M. Caricato, X. Li, H. P. Hratchian, A. F. Izmaylov, J. Bloino, G. Zheng, J. L. Sonnenberg, M. Hada, M. Ehara, K. Toyota, R. Fukuda, J. Hasegawa, M. Ishida, T. Nakajima, Y. Honda, O. Kitao, H. Nakai, T. Vreven, J. A. Montgomery, Jr., J. E. Peralta, F. Ogliaro, M. Bearpark, J. J.

Heyd, E. Brothers, K. N. K ; udin, V. N. S., R. Kobayashi, J. Normand, K. Raghavachari, A. Rendell, J. C. Burant, S. S. Iyengar, J. Tomasi, M. Cossi, N. Rega, J. M. Millam, M. Klene, J. E. Knox, J. B. Cross, V. Bakken, C. Adamo, J. Jaramillo, R. Gomperts, R. E. Stratmann, O. Yazyev, A. J. Austin, R. Cammi, C. Pomelli, J. W. ; Ochterski, R. L. M., K. Morokuma, V. G. Zakrzewski, G. A. Voth, P. Salvador, J. J. Dannenberg, S. Dapprich, A. D. Daniels, O. Farkas, J. B. Foresman, J. V. Ortiz, J. Cioslowski and D. J., Gaussian 09, Revision A.02. *Gaussian, Inc., Wallingford CT,* **2009**.

37. Bassetti, M.; Ciceri, S.; Lancia, F.; Pasquini, C., Hydration of aromatic terminal alkynes catalyzed by iron(III) sulfate hydrate under chlorine-free conditions. *Tetrahedron Lett.* **2014,** *55* (9), 1608-1612.
38. Molander, G. A.; Brown, A. R., Suzuki-Miyaura cross-coupling reactions of potassium vinyltrifluoroborate with aryl and heteroaryl electrophiles. *J. Org. Chem.* **2006,** *71* (26), 9681-6.
39. Denmark, S. E.; Butler, C. R., Vinylation of aryl bromides using an inexpensive vinylpolysiloxane. *Org. Lett.* **2006,** *8* (1), 63-66.
40. Schuurmans, C. C. L.; Abbadessa, A.; Bengtson, M. A.; Pletikapic, G.; Eral, H. B.; Koenderink, G.; Masereeuw, R.; Hennink, W. E.; Vermonden, T., Complex coacervation-based loading and tunable release of a cationic protein from monodisperse glycosaminoglycan microgels. *Soft Matter* **2018,** *14* (30), 6327-6341.
41. Fung, B. M.; Khitrin, A. K.; Ermolaev, K., An improved broadband decoupling sequence for liquid crystals and solids. *J. Magn. Reson.* **2000,** *142* (1), 97-101.
42. Thommes, M.; Kaneko, K.; Neimark Alexander, V.; Olivier James, P.; Rodriguez-Reinoso, F.; Rouquerol, J.; Sing Kenneth, S. W., Physisorption of gases, with special reference to the evaluation of surface area and pore size distribution (IUPAC Technical Report). In *Pure and Applied Chemistry*, **2015**; Vol. 87, p 1051.
43. Barrett, E. P.; Joyner, L. G.; Halenda, P. P., The determination of pore volume and area distributions in porous substances. I. Computations from nitrogen isotherms. *J. Am. Chem. Soc.* **1951,** *73* (1), 373-380.
44. Jura, G.; Harkins, W. D., Surfaces of Solids. XI. Determination of the decrease (π) of free surface energy of a solid by an adsorbed film. *J. Am. Chem. Soc.* **1944,** *66* (8), 1356-1362.
45. Talke, H.; Schubert, G. E., Enzymatic urea determination in the blood and serum in the warburg optical test. *Klin. Wochenschr.* **1965,** *43*, 174-5.

7. Supporting Information

On request are available; Calculated G values for all PGAH analogues, PGA-analogues and intermediates, and ΔG and ΔΔG values for dehydration and the reaction of PGA analogues with urea; Coordinates for optimized structures calculated compounds and intermediates.

7.1 Pseudo-first order rate constants of the reactions of PGAH-analogues with urea

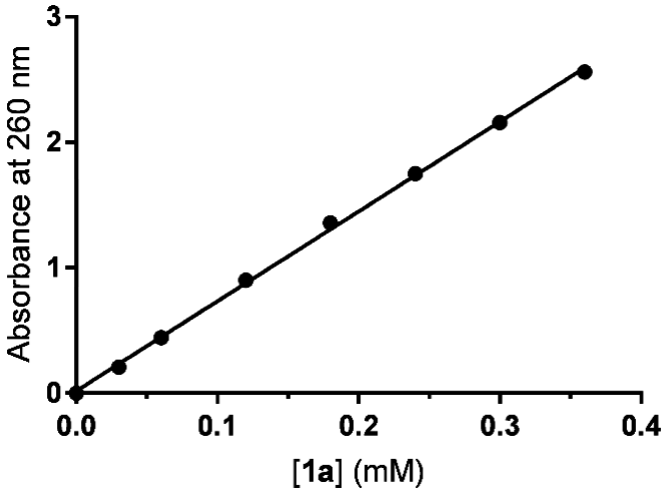

Figure S1: The absorbance at 260 nm versus the PGAH (**1a**) concentration in a 1:1 (v/v) mixture of PBS and DMSO used for calculation of the non-reacted PGA upon incubation with urea.

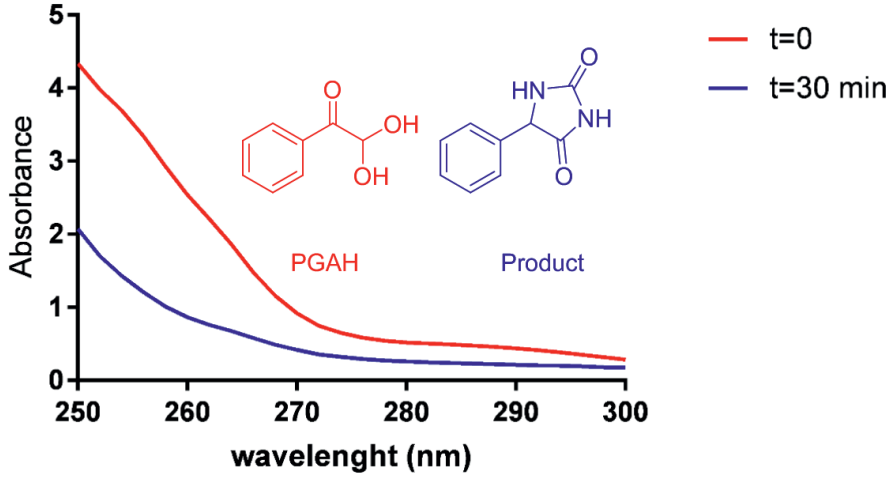

Figure S2: Absorbance spectrum of the reaction mixture of PGAH (**1a,** concentration = 0.30 mM) with 50 equivalents of urea in a 1:1 (v/v) mixture of PBS and DMSO.

Figure S2 shows that reaction of PGA with urea resulted in the formation of a product with a lower absorbance at 260 nm. Since the $Abs_{observed}$ did not further decrease after t=60, it is assumed that PGAH was fully converted into the product at 60 minutes.

Thus, $Abs_{t=0}$ is only due to the PGAH present in solution. This absorption corresponds to a [PGAH] of 27.7 mM according to figure S1.
$Abs_{t=60}$ is only due to the product present in solution, which concentration should thus be 27.7 mM as well.

The concentration of unreacted PGAH at different time points was calculated using the following equations:

Equation S1: $\mathbf{Abs_t = Abs_{PGAH} + Abs_{product}}$
Equation S2: $\mathbf{Abs_{PGAH} = a[PGAH]}$ (based on figure S1, in which a is the slope)
Equation S3: $\mathbf{Abs_{product} = c[product]}$ (in which $c=(Abs_{t=60}-Abs_{solvent})/([product]_{t=60})$
Equation S4: $\mathbf{[product]_t = [PGAH]_{t=0} - [PGAH]_t}$

Substitution of S4 in S3 results in S5:

Equation S5: $\mathbf{Abs_{product} = c[PGAH]_{t=0} - c[PGAH]_t}$

Substitution of S5 and S2 in S1 results in S6.

Equation S6: $\mathbf{[PGAH]_t = (Abs_t - c[PGAH]_{t=0})/(a-c)}$

Table S1: The PGAH concentration in time during the reaction with 50 equivalents of urea in a 1:1 (v/v) mixture of PBS:DMSO at 50 °C.

Time (min)	Absorption	[**1a**] (mM)	ln[**1a**]
0	2.00	27.7	3.32
5	1.35	16.4	2.80
10	0.97	9.9	2.30
15	0.75	6.1	1.80
20	0.65	4.4	1.48
25	0.58	3.1	1.14
30	0.52	2.1	0.73

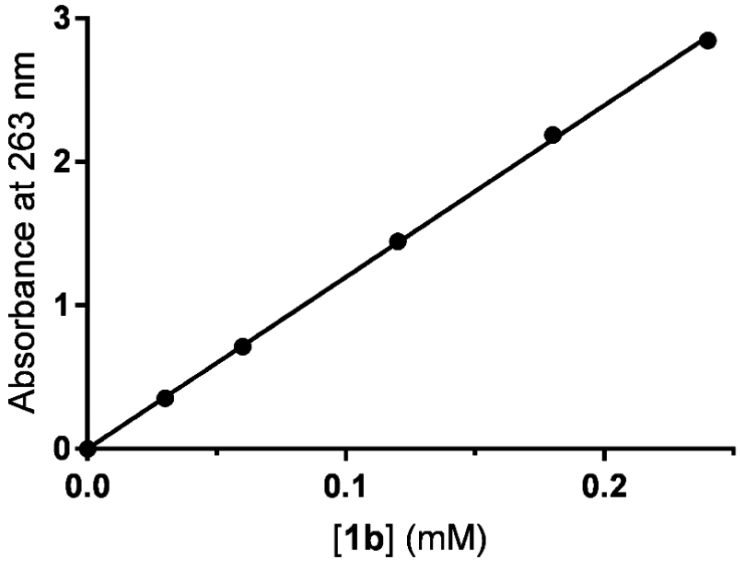

Figure S3: Absorbance at 263 nm versus the Me-PGAH (**1b**) concentration in a 1:1 (v/v) mixture of PBS and DMSO.

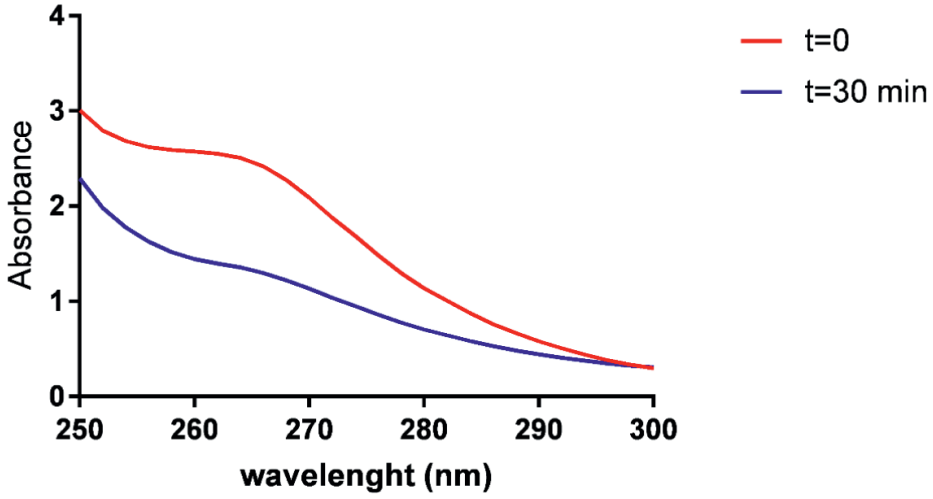

Figure S4: Absorbance spectrum of the reaction mixture of Me-PGAH (**1b,** concentration = 0.20 mM) with 50 equivalents of urea in a 1:1 (v/v) mixture of PBS and DMSO.

Table S2: The concentration of **1b** in time during the reaction with 50 equivalents of urea in a 1:1 (v/v) mixture of PBS:DMSO at 50 °C. A similar correction was made to the [**1b**] using equation S6 as described above for **1a**.

Time (min)	Absorption	[**1b**] (mM)	ln[**1b**]
0	2.17	27.2	3.30
5	1.95	20.2	3.00
10	1.84	16.7	2.82
15	1.71	12.4	2.52
20	1.64	10.3	2.33
25	1.54	6.9	1.93
30	1.52	6.2	1.83
40	1.38	2.0	0.68

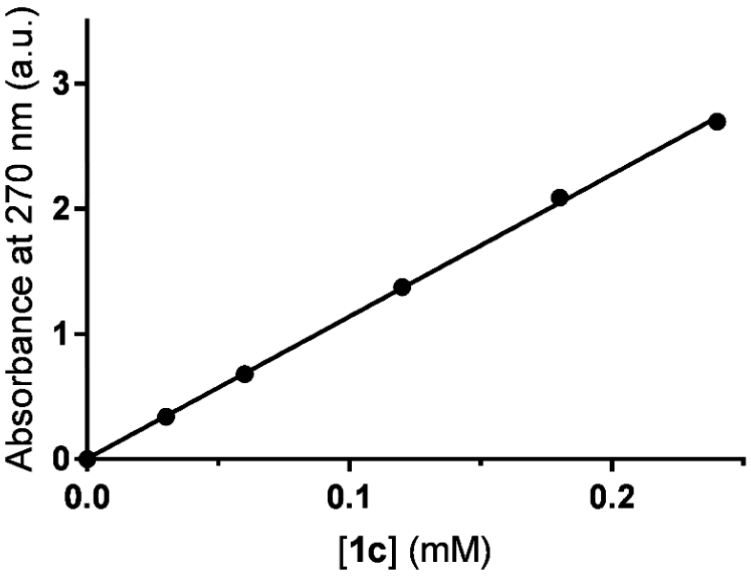

Figure S5: Absorbance at 270 nm versus the NO_2-PGAH (**1c**) concentration in a 1:1 (v/v) mixture of PBS and DMSO.

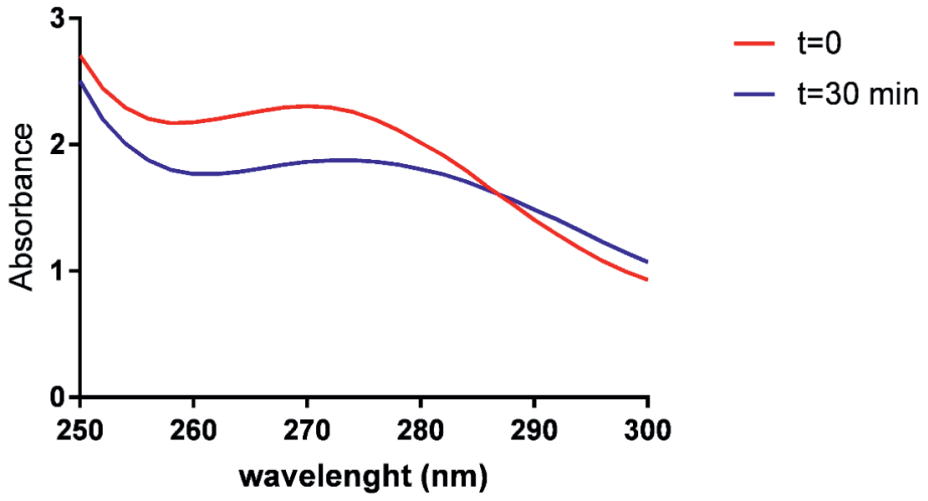

Figure S6: Absorbance spectrum of the reaction mixture of NO_2-PGAH (**1c,** concentration = 0.20 mM) with 50 equivalents of urea in a 1:1 (v/v) mixture of PBS and DMSO.

Table S3: The concentration of **1c** in time during the reaction with 50 equivalents of urea in a 1:1 (v/v) mixture of PBS:DMSO at 50 °C.

Time (min)	Absorption	[**1c**] (mM)	ln[**1c**]
0	2.09	27.6	3.32
5	1.78	23.5	3.16
10	1.73	22.7	3.12
15	1.70	22.4	3.11
20	1.62	21.3	3.06
25	1.61	21.2	3.05
30	1.61	21.2	3.05
40	1.60	21.1	3.05

7.2 Suspension polymerization reactor

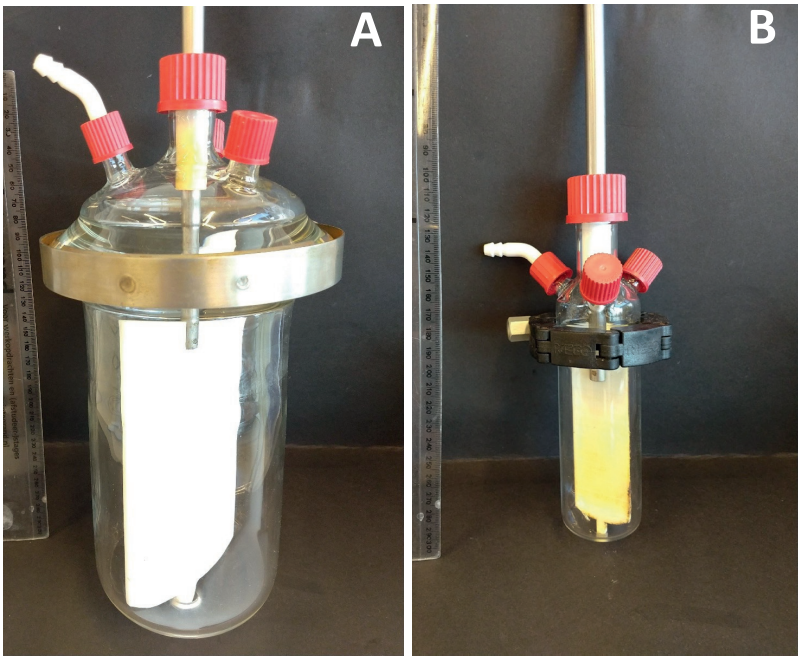

Figure S7: Photographs of the used reactor for suspension polymerization with a volume of A) ± 1.0 Liter and B) ± 200 mL.

7.3 DSC and TGA analysis of monomer and polymeric beads

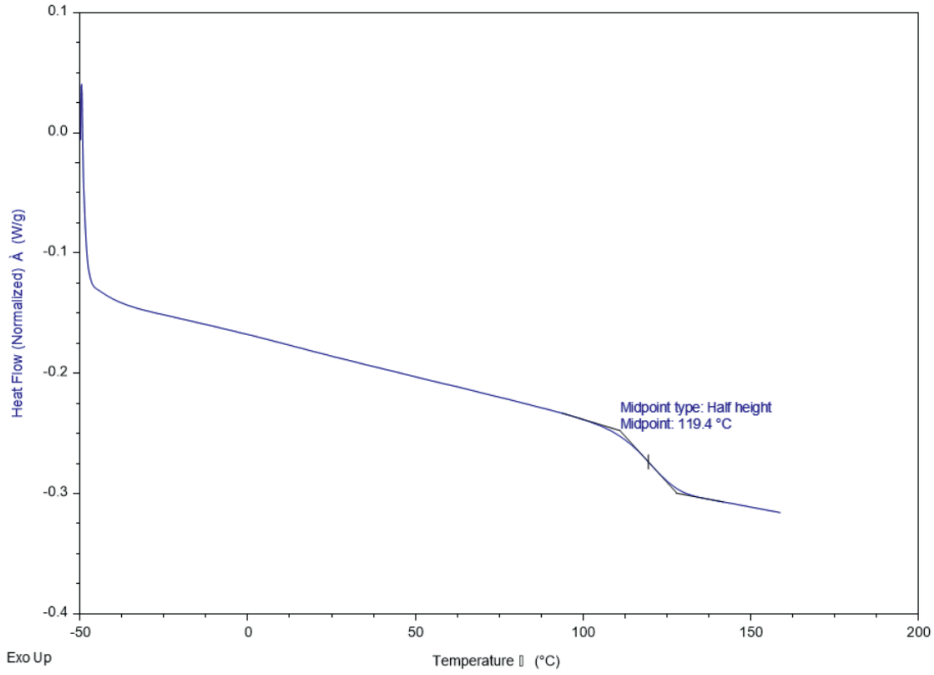

Figure S8: DSC thermogram of polystyrene beads (PS). Glass transition temperature (T_g) is 119 °C.

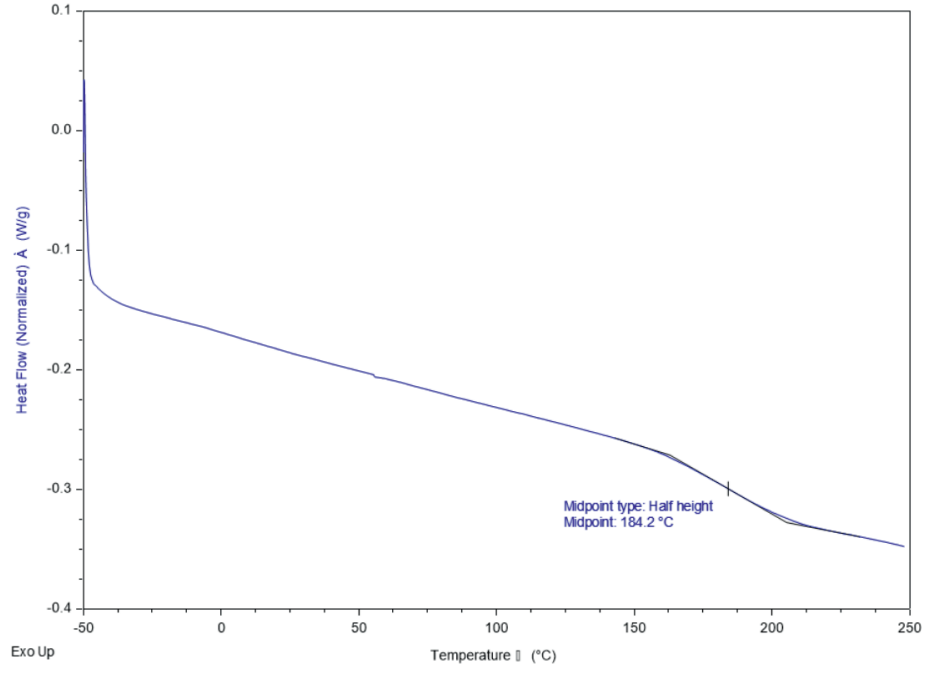

Figure S9: DSC thermogram of acetylated polystyrene beads (PS-Ac). Glass transition temperature (T_g) is 184 °C.

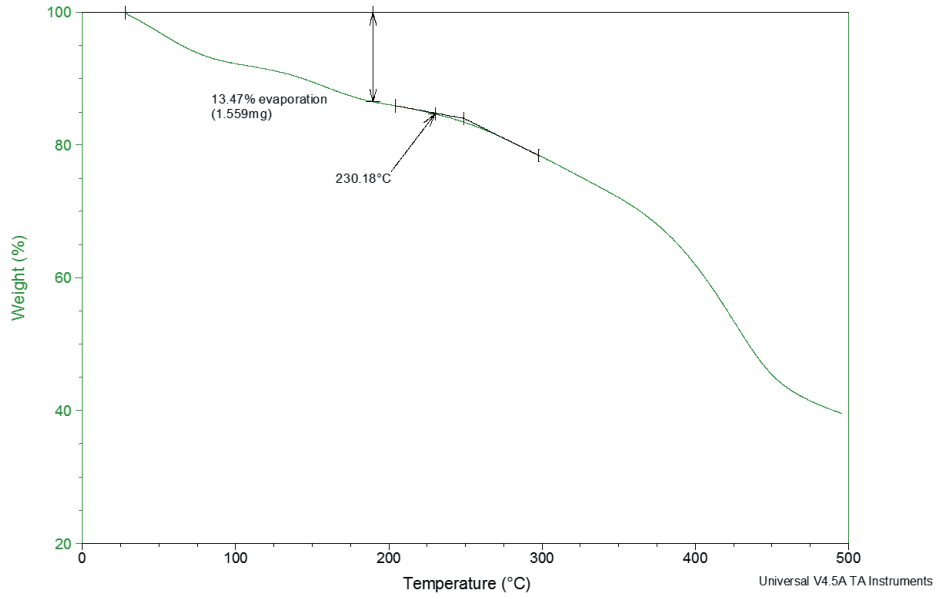

Figure S10: TGA plot of oxidized acetylated polystyrene beads (PS-Ac-Ox). Decomposition starts at ~230 °C; no glass transition temperature (T_g) was observed below 230 °C by DSC analysis.

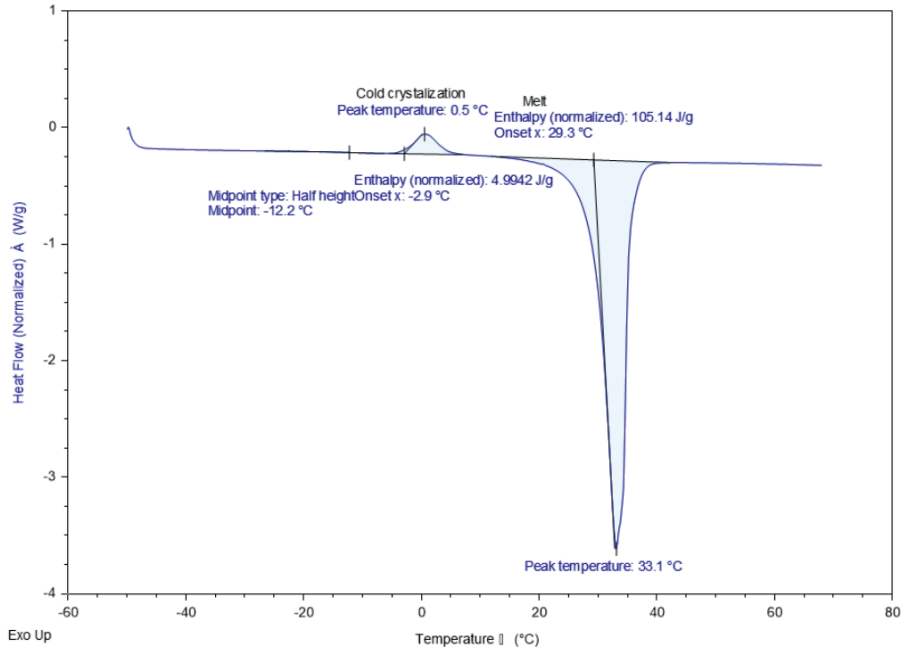

Figure S11: DSC thermogram of the VPE monomer. The melting temperature is 29 °C; Melting enthalpy 105 J/g.

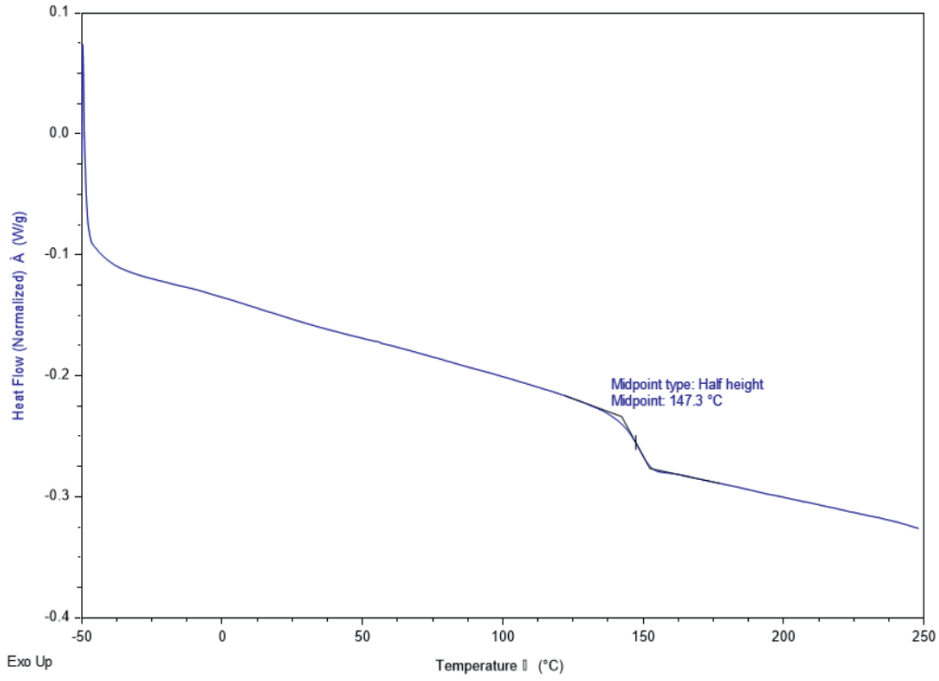

Figure S12: DSC thermogram of polyvinylphenylethanone (pVPE). Glass transition temperature (T_g) is 147 °C.

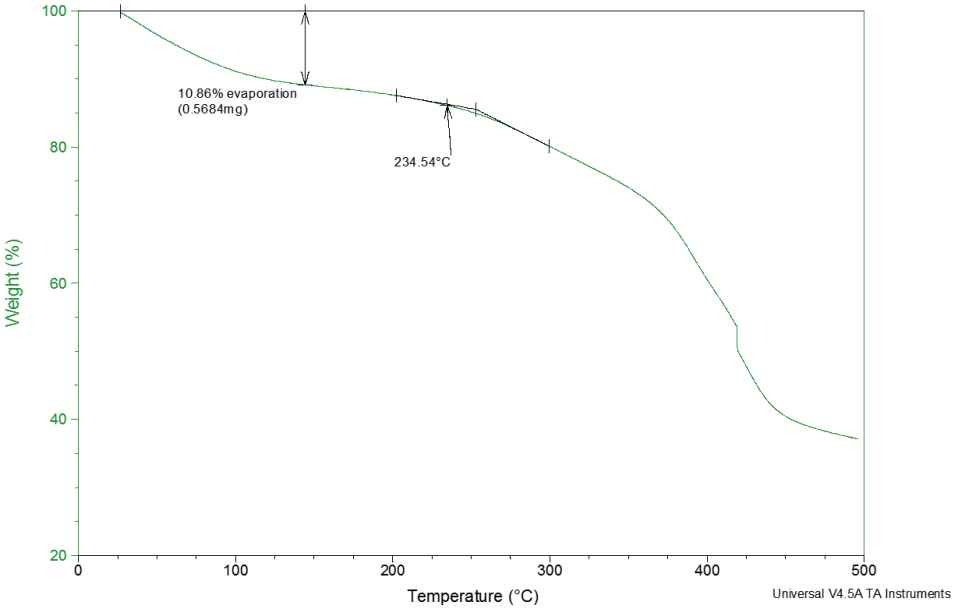

Figure S13: TGA plot of oxidized polyvinylphenylethanone (pVPE-Ox-(4)). Decomposition of starts at ~230 °C; no glass transition temperature (T_g) was observed below 235 °C by DSC.

7.4. IR Characterization of Sorbents

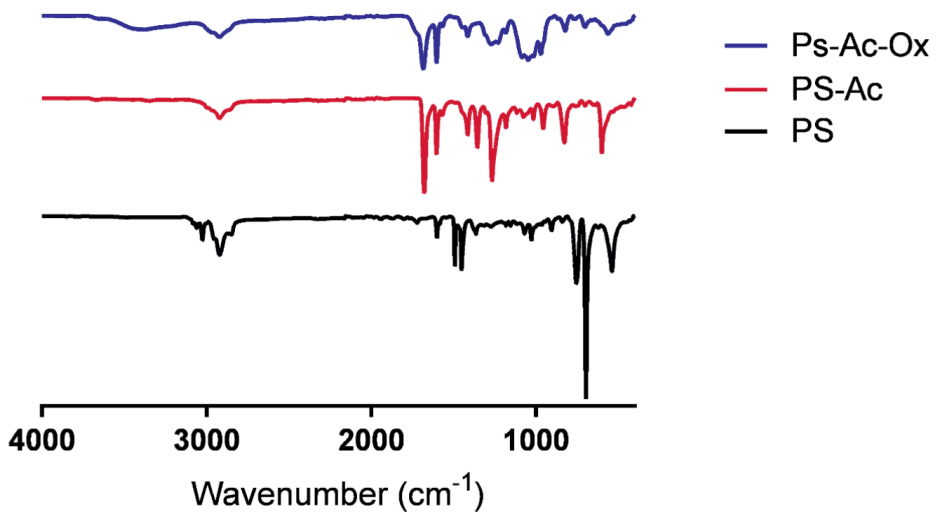

Figure S14: Full IR spectra of PS, PS-Ac and PS-Ac-Ox.

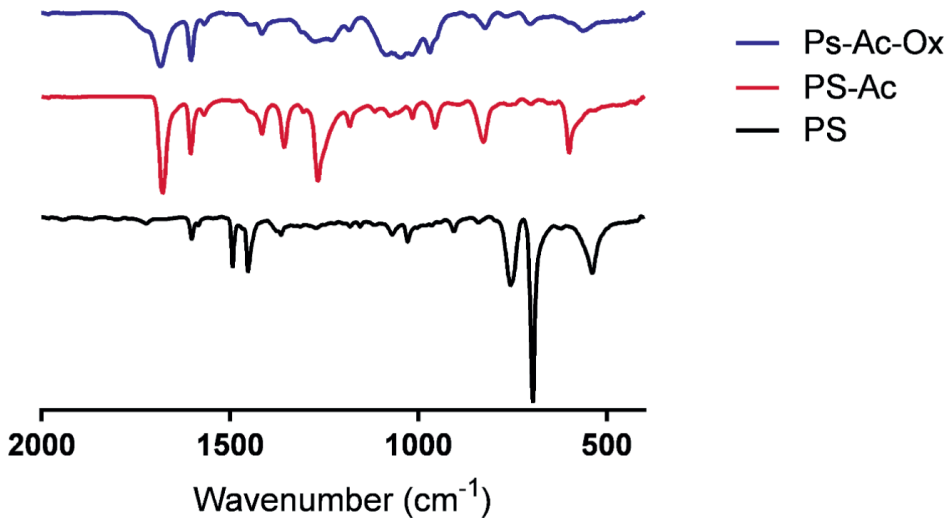

Figure S15: IR spectra of PS, PS-Ac and PS-Ac-Ox in the region of 2000-400 cm^{-1}.

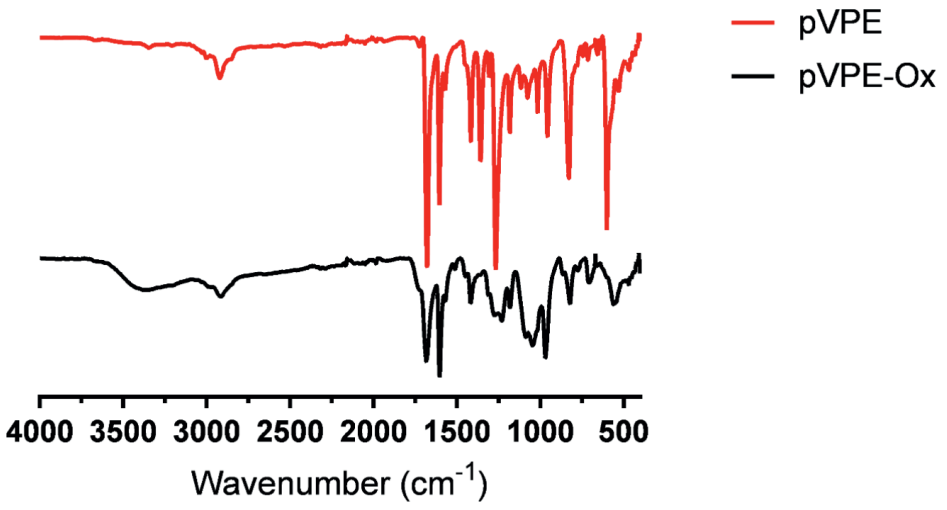

Figure S16: Full IR spectra of pVPE and pVPE-Ox.

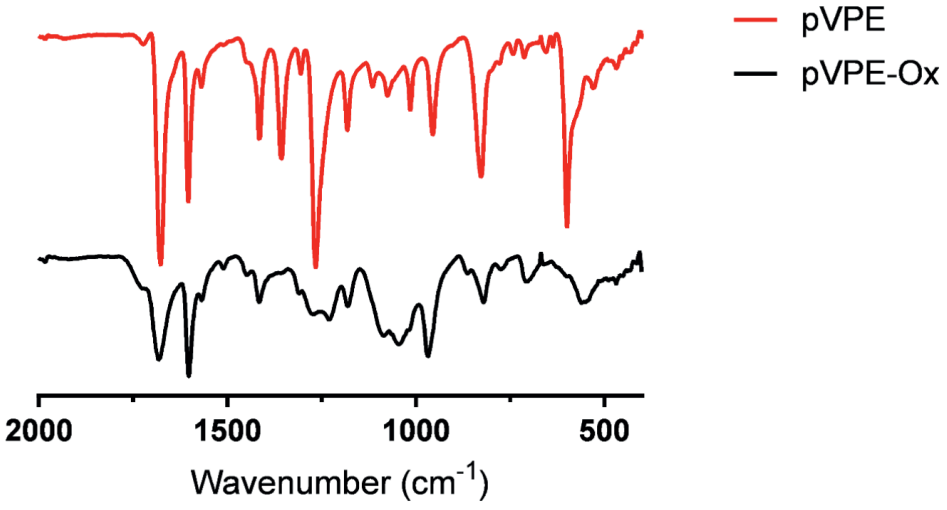

Figure S17: IR spectra of pVPE and pVPE-Ox in the region of 2000-400 cm^{-1}.

7.5 Conditions to determine the maximum urea binding capacity

Sorbent beads (PS-Ac-Ox, 15 mg) in an Eppendorf tube were dispersed in a urea solution (30 mM, 1.5 mL) and placed in an rotating oven at 70 °C. Per time point 2 eppendorf tubes were removed and after sedimentation of the beads, the urea concentration was determined in the supernatant. It was found the urea concentration did not change after ~24 hours (table S4), indicating that under these conditions (24 hours reaction at 70 °C) all available PGAH groups have reacted with urea. Therefore for determination of the maximum binding capacity, the beads were incubated for 24 hours at 70 °C, after which the urea concentration was determined (Table S4).

Table S4: Kinetics of urea sorption by PS-Ac-Ox in urea solution (30 mM) in PBS (10 mg/mL) at 70 °C under static conditions.

Time (h)	$[Urea]_{t=24h}$ (mM)		Urea bound (mmol/g)
	Duplicate#1	Duplicate#2	
0	31.4	31.1	0
16	18.6	19.0	1.25 ± 0.03
24	17.9	18.2	1.32 ± 0.02
32	17.2	18.1	1.36 ± 0.06

7.6 Oxidation of pVPE-beads

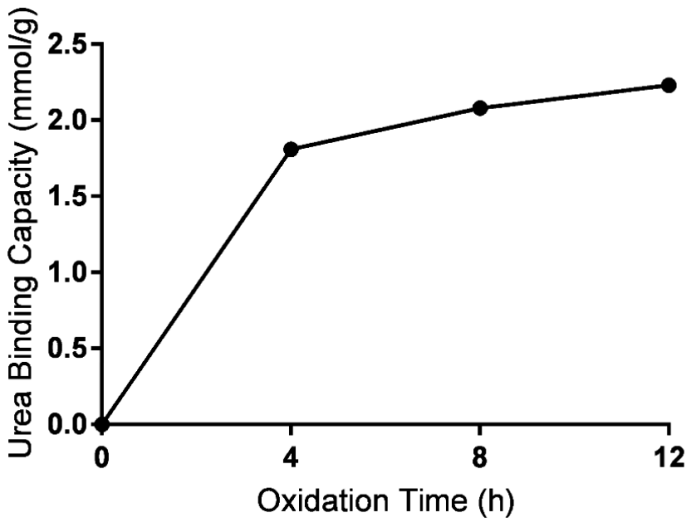

Figure S18: The urea binding capacity of pVPE beads (table 3 entry 2) as a function of oxidation time of pVPE. Conditions for oxidation: pVPE (500 mg) in DMSO (5.0 mL) and 48% aqueous HBr (1.45 mL) stirred with a Teflon blade stirrer at 80 °C for 4-12 hours. Per timepoint ± 150 mg beads was removed from the suspension and tested for urea binding according to the procedure described in supporting information section 7.5. Raw data are presented in table S5.

7.7. Maximum Binding Capacity Urea Sorbents

Table S5: Urea sorption by the sorbent beads in urea solution in PBS (10 mg/mL) at 70 °C for 24 hours under static conditions.

Sorbent	$[Urea]_{t=0}$ (mM)		$[Urea]_{t=24h}$ (mM)		Max Binding Capacity (mmol/g)
	Duplicate#1	Duplicate#2	Duplicate#1	Duplicate#2	
PS-Ac-Ox-1h	30.5	30.4	28.1	27.3	0.28 ± 0.06
PS-Ac-Ox-4h	30.5	30.4	17.4	17.6	1.30 ± 0.01
PS-Ac-Ox-8h	30.5	30.4	12.1	12.8	1.80 ± 0.05
PS-Ac-Ox-24h	30.5	30.4	16.2	16.6	1.41 ± 0.03
PS-Ac-Ox-32h	30.5	30.4	21.6	20.8	0.93 ± 0.06
PS-Ac-Ox-48h	30.5	30.4	27.0	27.5	0.32 ± 0.04
PS-Ac-Ox (60 g, 8h)	29.8	29.8	16.7	16.1	1.34 ± 0.04
PS-Ac-Ox (60 g, 8h)	46.1	43.4	30.6	30.8	1.41 ± 0.01
pVPE-Ox-(2)-4h	49.8	50.0	32.1	31.6	1.81 ± 0.04
pVPE-Ox-(2)-8h	49.8	50.0	29.0	29.2	2.08 ± 0.01
pVPE-Ox-(2)-12h	49.8	50.0	27.3	27.9	2.23 ± 0.04
pVPE-Ox-(4)	46.1	43.4	28.0	26.4	1.76 ± 0.11

7.8 Static urea sorption of PS-Ac-Ox and pVPE-Ox beads

Table S6: Urea sorption of PS-Ac-Ox sorbent beads (15 mg) in 1.5 mL urea solution (~30 mM) in PBS under static conditions.

Time (h)	[Urea] (mM)				Urea removed (mmol/g)
	Duplicate#1	Duplicate#2	Duplicate#3	Duplicate#4	
0	27.7	27.7	29.3	29.3	0
1	26.1	25.8	28.2	28.8	0.13 ± 0.16
2	25.3	25.7	28.1	27.6	0.18 ± 0.05
4	24.2	24.2	27.9	27.8	0.25 ± 0.11
8	21.2	21.9	26.7	25.7	0.46 ± 0.16
16	22.9	23.1	23.9	24.2	0.50 ± 0.03
24	21.6	21.8	24.3	24.3	0.57 ± 0.04

Table S7: Urea sorption of pVPE-Ox-(4) sorbent beads (15 mg) in 1.5 mL urea solution (~30 mM) in PBS under static conditions.

Time (h)	[Urea] (mM)				Urea removed (mmol/g)
	Duplicate#1	Duplicate#2	Duplicate#3	Duplicate#4	
0	27.7	27.7	30.8	30.8	0
1	23.4	22.9	29.8	30.2	0.27 ± 0.19
2	24.4	25.0	29.1	29.1	0.26 ± 0.11
4	23.6	22.7	27.6	27.1	0.40 ± 0.07
8	22.5	20.7	27.5	25.8	0.51 ± 0.13
16	20.3	19.8	23.3	23.4	0.75 ± 0.02
24	18.5	19.1	22.8	22.5	0.85 ± 0.05

7.9. Quantitative ^{13}C- Solid State NMR Spectroscopy

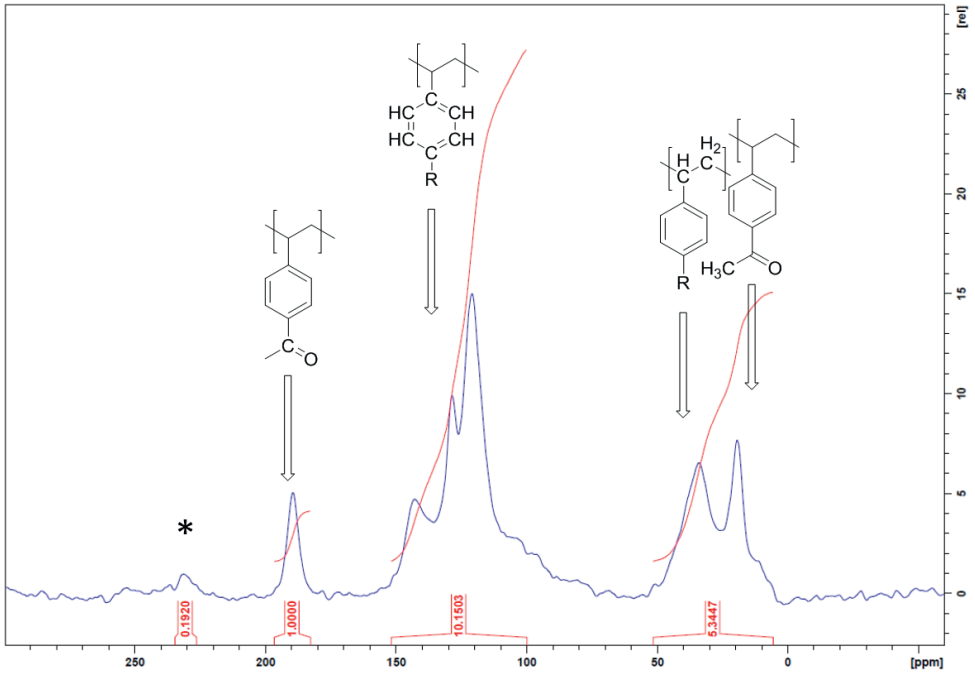

Figure S19: Quantitative ^{13}C solid state NMR spectrum of PS-Ac. The spectrum was recorded on a Bruker 400 MHz spectrometer using a 100 s recycle delay, 20 ms acquisition time, 11 kHz MAS frequency and an accumulation of 4947 scans. Spinning sideband originating from aromatic peak indicated with a star (*) was included in the integration of the aromatic and aliphatic peaks.

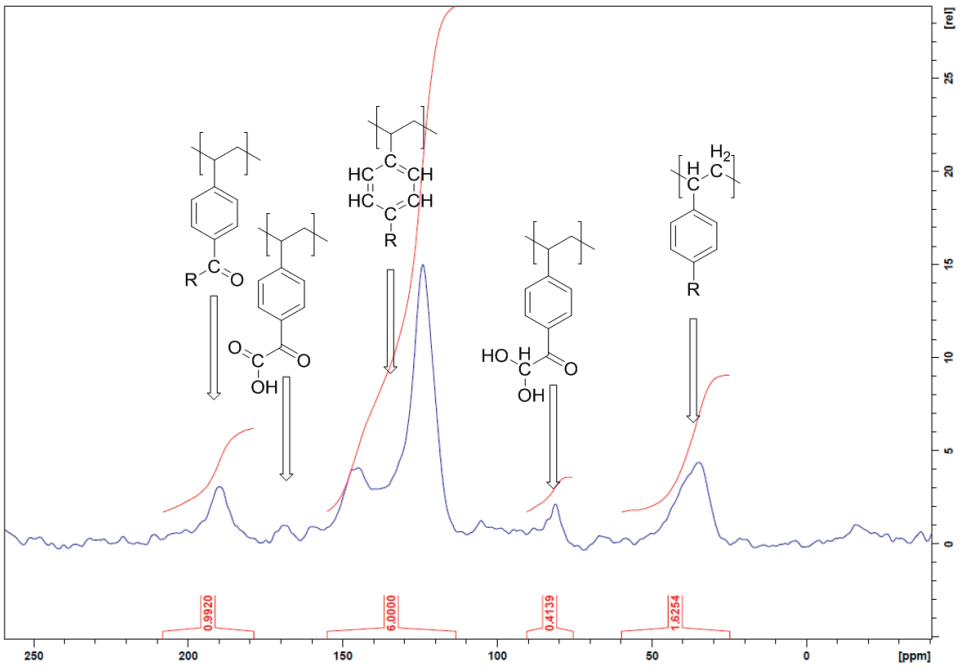

Figure S20: Quantitative ^{13}C solid state NMR spectrum of PS-Ac-Ox (prepared at small scale (ca. 500 mg). The spectrum was recorded on a Bruker 400 MHz spectrometer using a 150 s recycle delay, 20 ms acquisition time, 14 kHz MAS frequency and an accumulation of 3400 scans.

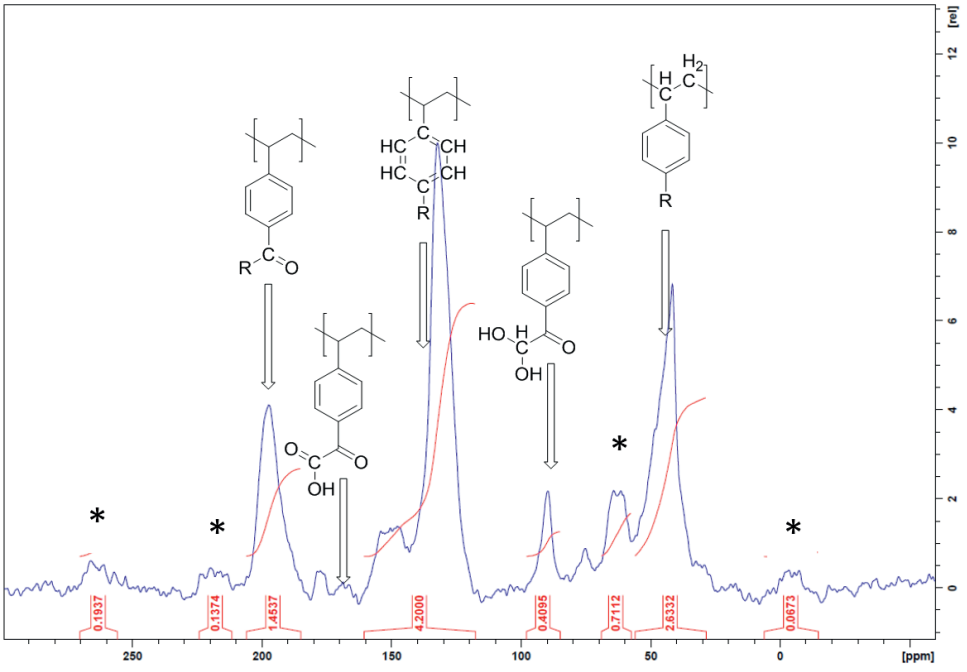

Figure S21: Quantitative ^{13}C solid state NMR spectrum of PS-Ac-Ox (synthesized at large scale (60 grams)). The spectrum was recorded on a Bruker 700 MHz spectrometer using a 75 s recycle delay, 11 ms acquisition time, 12 kHz MAS frequency and an accumulation of 4482 scans. Spinning sidebands originating from the aromatic peak indicated with a star (*) were included in the integration of the aromatic peak.

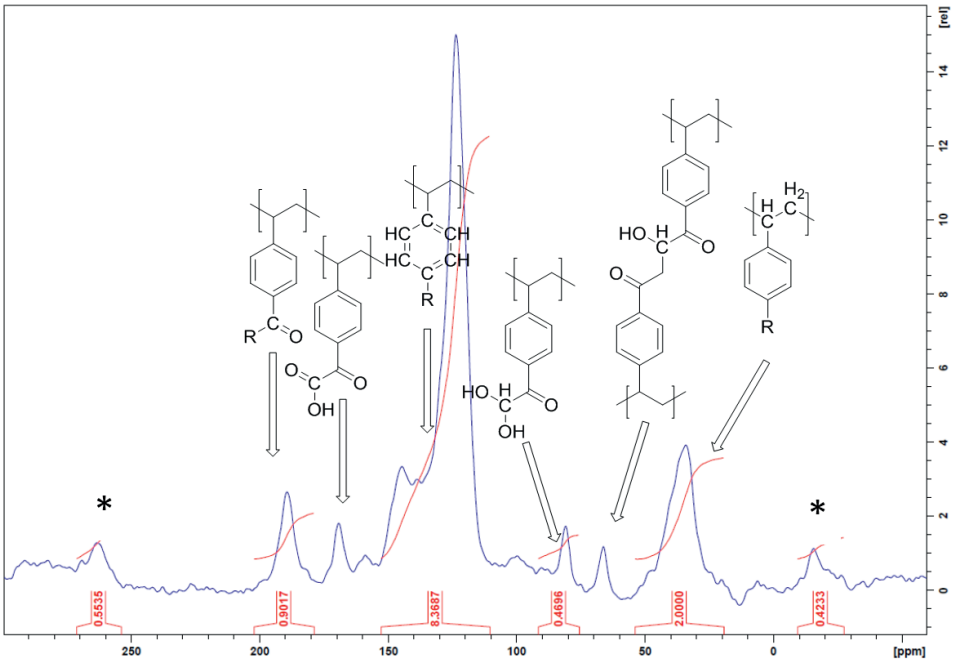

Figure S22: Quantitative ^{13}C solid state NMR spectrum of pVPE-Ox-(2). The spectrum was recorded on a Bruker 700 MHz spectrometer using a 50 s recycle delay, 11 ms acquisition time, 13.5 kHz MAS frequency and an accumulation of 4771 scans. Spinning sidebands originating from aromatic peak indicated with a star (*) were included in the integration of the aromatic peak.

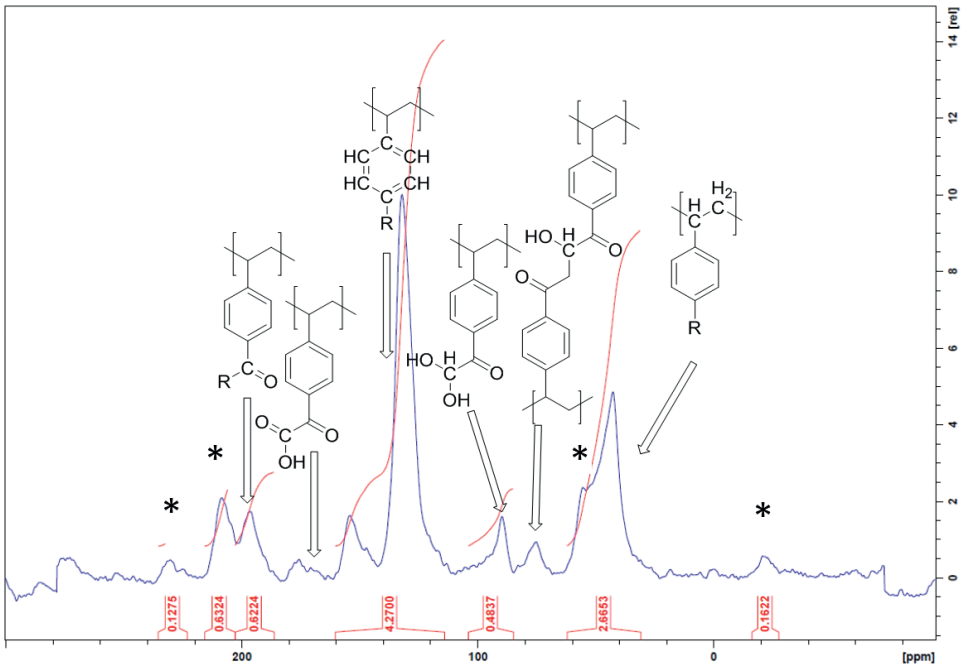

Figure S23: Quantitative ^{13}C solid state NMR spectrum of pVPE-Ox-(4). The spectrum was recorded on a Bruker 400MHz spectrometer. The spectrum was recorded using a 150 s recycle delay, 20 ms acquisition time, 14 kHz MAS frequency and an accumulation of 5623 scans. Spinning sidebands originating from aromatic peak indicated with a star (*) were included in the integration of the aromatic and carbonyl peaks.

6

Chapter 6

A Ninhydrin-type Urea Sorbent for the Development of a Wearable Artificial Kidney

Jacobus A.W. Jong[a,b*], Yong Guo[a*], Diënty Hazenbrink[b], Stefania Douka[a], Dennis Verdijk[c], Johan van der Zwan[d], Klaartje Houben[d], Marc Baldus[d], Karina C. Scheiner[a], Remco Dalebout[e], Marianne C. Verhaar[b], Robert Smakman[f], Wim E. Hennink[a], Karin G.F. Gerritsen[b] and Cornelus F. van Nostrum[a**]

[a]Department of Pharmaceutics, Utrecht Institute for Pharmaceutical Sciences (UIPS), Utrecht University, Universiteitsweg 99, 3584 CG Utrecht, the Netherlands.
[d]Department of Nephrology and Hypertension, University Medical Centre Utrecht, 3584 CX Utrecht, the Netherlands.
[c]MercaChem B.V., Kerkenbos 1013, 6546 BB Nijmegen, the Netherlands.
[d]NMR Spectroscopy, Bijvoet Center for Biomolecular Research Department of Chemistry, Faculty of Science, Utrecht University, Padualaan 8, 3584 CH Utrecht, the Netherlands.
[e]Inorganic Chemistry and Catalysis, Debye Institute for Nanomaterials Science, Utrecht University, Universiteitsweg 99, 3584 CG Utrecht, the Netherlands.
[f]Innovista, Raadhuisstraat 1, 1393 NW Nigtevecht, the Netherlands.
*Authors contributed equally.

Submitted

Abstract

The aim of this study was to develop polymeric chemisorbents with a high density of ninhydrin groups, able to covalently bind urea under physiological conditions and thus potentially suitable for use in a wearable artificial kidney. Macroporous beads were prepared by suspension polymerization of 5-vinyl-1-indanone (vinylindanone) using a 90:10 (v/v) mixture of toluene and nitrobenzene as a porogen. The indanone groups were subsequently oxidized in a one-step procedure into ninhydrin groups. Their urea absorption kinetics were evaluated under both static and dynamic conditions at 37 °C in simulated dialysate (urea in phosphate buffered saline). Under static conditions and at a 1:1 molar ratio of ninhydrin : urea the pVI-Ox beads removed ~0.6-0.7 mmol/g and under dynamic conditions and at a 2:1 molar excess of ninhydrin ~0.6 mmol urea/g sorbent in 8 hours at 37 °C, which is a step towards a wearable artificial kidney.

1. Introduction

Patients suffering from end-stage kidney disease are treated with hemodialysis or peritoneal dialysis to remove waste compounds such as urea, creatinine, potassium and phosphate, as well as excess water from their body. To improve the quality of life of dialysis patients, wearable artificial kidney devices are being developed which use a small volume of dialysate (preferably <0.5 L) that is continuously regenerated by a purification unit and re-used in a closed loop system.[1-3] Removal of urea from dialysate is a major challenge in the realization of such a wearable dialysis device,[4] since urea has low reactivity and high aqueous solubility while it is the metabolite with the highest daily molar production (240-470 mmol/day)[5-6]. Several strategies for urea removal from dialysate have been explored, including enzymatic hydrolysis,[7-8] electro-oxidation[9] and adsorption of urea[10-14]. However, each of these strategies has drawbacks that do not allow reduction of the dialysate volume to <0.5 L as required for a wearable device.[15]

Chemisorption of urea by a sorbent, that is able to form irreversible covalent bonds with urea at 37 °C, seems an attractive strategy as 1) high urea binding capacities (BC) have been reported[11, 16-17] and 2) no potentially harmful side products are formed. Several urea chemisorbents have been reported in literature, however the main drawbacks are that the kinetics of urea adsorption are generally very slow and that these sorbents need multi step synthesis, which routes are difficult and expensive to scale up.[11-12, 17-18]

Our aim is to develop urea sorbents with fast urea removal kinetics which are relatively easy to synthesize. Recently, we reported the second order reaction rate constants (k_2-values) of more than 30 carbonyl compounds with urea in buffered aqueous solution, of which ninhydrin was one of the compounds with the fastest binding kinetics.[19] The reaction of 5-substituted-ninhydrin with urea is shown in scheme 1. In addition, we investigated the effect of electron donating and electron withdrawing substituents on the reactivity of ninhydrin towards urea, and found that an electron donating group such as a methyl- or a *tert*-butyl- group on the 5-position shows the highest reactivity of the ninhydrin derivates with urea.[20] Therefore, we concluded that a sorbent with an electron donating carbon-carbon backbone, functionalized with ninhydrin groups on the 5-position would structure-wise be optimal.

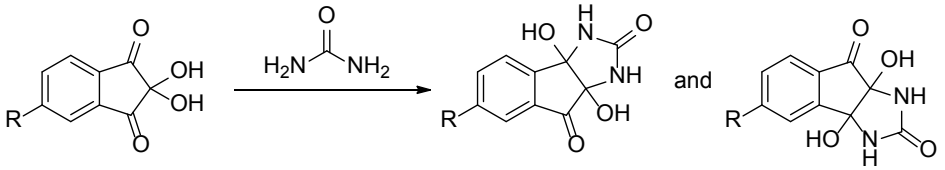

Scheme 1: The reaction of 5-substituted ninhydrin with urea.[20]

Smakman and Van Doorn previously developed urea sorbents containing ninhydrin-groups.[17, 21] These sorbents were obtained by suspension copolymerization of styrene with divinylbenzene (DVB), followed by a 6-step modification which resulted in sorbent particles of which 55% of the styrene groups were modified into ninhydrin groups (supporting information section 7.1).[17, 21] The intermediate obtained after 5 modification steps is one in which the aromatic groups of polystyrene were modified into 1-indanone groups, which were subsequently oxidized to ninhydrin groups in a one-pot halogenation and Kornblum oxidation reaction (scheme 2).[17] The resulting sorbents are among the best performing in terms of binding capacity (BC) so far (2.2 mmol/g).[16, 21]

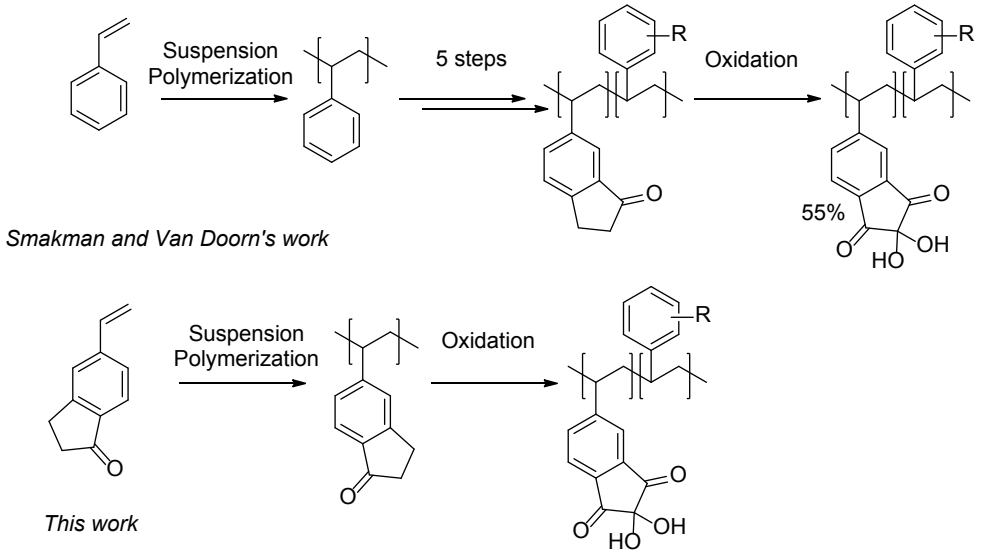

Scheme 2: Comparison of synthetic route of Smakman's ninhydrin sorbents[17, 21] with the route described in this work. R= side products.

We hypothesized that the density of ninhydrin groups in such a sorbent could be increased by directly polymerizing a 1-indanone-based monomer followed by a single final oxidation step, thereby avoiding the first 5 post-polymerization modification steps which yielded incomplete conversion of the aromatic groups into ninhydrin groups. Therefore, we selected 5-vinyl-1-indanone[22] (vinylindanone) as the monomer instead of styrene, because this results in a 5-alkyl-substituted ninhydrin group after oxidation, which, as discussed above, has structure-wise optimal reactivity towards urea (scheme 2).

Further, microparticles with a size of 100-1000 µm are preferred for application in a sorbent cartridge to prevent pressure building up in the dialysate circuit.[23] In addition, we assumed that a macroporous system would be required to increase the accessibility of the ninhydrin groups in the beads for urea and to obtain fast binding kinetics.[11]

The aim of this study is therefore to design, prepare and characterize macroporous sorbent beads with a high density of ninhydrin groups obtained by suspension polymerization of vinylindanone, followed by a one-step oxidation of the indanone groups into ninhydrin groups. The urea binding of the obtained beads was studied under both static and dynamic (flow) conditions from simulated dialysate (urea in PBS), aiming for the application of regeneration of dialysate in a wearable dialysis device.

2. Results and Discussion

2.1 5-Vinyl-1-indanone Synthesis and Upscaling

The functional monomer 5-vinyl-1-indanone (vinylindanone) was synthesized on a relatively small scale of 4 gram in 3 steps from 5-bromoindan-1-one (scheme 3). The first and the second step, a Sonogashira cross-coupling of 5-bromo-1-indanone with ethynyltrimethylsilane followed by deprotection of the TMS-group, was reported by Ortega *et al*. yielding 5-ethynylindan-1-one.[24] In the third step, the alkyne was reduced to a vinyl-group using H_2 and Lindlar's catalyst. The overall yield over these three steps (of which two steps included purification by column chromatography) was 73%.

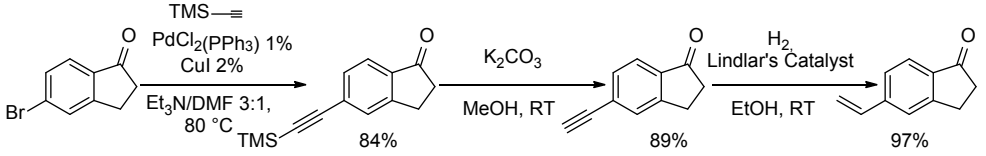

Scheme 3: Three step synthesis of 5-vinyl-1-indanone.

Although this route is suitable to obtain vinylindanone on a small scale (up to 40 grams), the purification by column chromatography (needed for two steps) proved to be cumbersome on a larger scale. Therefore, in order to obtain vinylindanone on 500 g scale, a one-step synthesis by a Suzuki-Molander coupling of 5-bromo-1-indanone with potassium vinyltrifluoroborate was exploited (scheme 4).[25] The reaction conditions were optimized until almost quantitative conversion (supporting information section 7.2) and vinylindanone was isolated after filtration over a silica plug in a 85% yield. Vinylindanone obtained via the Suzuki-Molander route yielded a monomer with higher purity than vinylindanone synthesized on a small scale, as both the melting point and the melting enthalpy were substantially higher (26 and 42 °C; 22.9 and 92.8 J/mol, respectively).

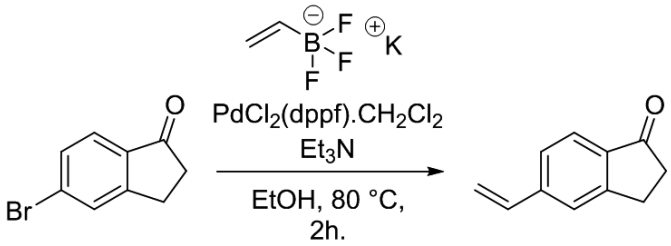

Scheme 4: One step synthesis of 5-vinylindan-1-one.

2.2 Polyvinylindanone Synthesis and Optimization

Macroporous polyvinylindanone (pVI) particles can be obtained by suspension polymerization of vinylindanone and divinylbenzene (DVB) using a non-solvating porogen, which is able to dissolve the used monomers (vinylindanone and DVB), and on the other hand precipitates the resulting polymer. This in turn causes phase separation between the monomer solution and the precipitated polymer yielding porous structures.[26] A commonly used method to predict the miscibility of solvents, monomers and polymers, is comparing the Hildebrand solubility parameters (δ) as similar δ values indicate miscibility. This solubility parameter, which is defined as the square root of the cohesive energy density, can either be determined experimentally or calculated based on the molecular structure via various methods.[27-28] For the preparation of porous particles using a non-solvent, a porogen is needed with a δ-value close to that of the monomer to ensure its dissolution, and different (preferable lower) than that of the resulting polymer, resulting in its precipitation. The δ-values of vinylindanone and poly-vinylindanone (pVI), as calculated based on the method reported by Fedors,[28] are much larger that the δ-values of styrene and polystyrene (20.5 and 22.9 vs. 17.8 and 17.4-19.0 $J^{1/2}m^{-3/2}$, respectively see supporting information section 7.3[27, 29]). The porogen mixture used for the preparation of porous polystyrene particles has a delta-value (δ_{mix}) of 15.2 $J^{1/2}m^{-3/2}$, which is lower than the δ-values of both styrene and polystyrene (lower by 2.6 and 2.2-3.8 $J^{1/2}m^{-3/2}$, respectively). Therefore, a porogen is needed with a larger δ-value than the one used for the suspension polymerization of polystyrene. Vinylindanone is soluble in both toluene (δ = 18.2 $J^{1/2}m^{-3/2}$)[27, 30] and nitrobenzene (δ = 21.7 $J^{1/2}m^{-3/2}$)[31] whereas pVI is insoluble in toluene but soluble in nitrobenzene. The δ-value of a mixture (δ_{mix}) is calculated with equation 1, in which x_i, V_i and δ_i are the molar fraction, the volume fraction and the (calculated) δ-values of the solvents and monomer, respectively.

$$(1) \qquad \delta_{mix} = \frac{\Sigma\, x_i V_i \delta_i}{\Sigma x_i V_i}$$

Using mixtures of nitrobenzene and toluene as non-solvating porogen, the conditions (i.e. toluene : nitrobenzene ratio) to obtain macroporous pVI beads

prepared by suspension copolymerization of vinylindanone and DVB were systematically optimized. First, the volume fraction of nitrobenzene used in the porogen mixture was increased with steps of 5%, and the S_{BET} surface areas of the obtained beads were measured with N_2 physisorption. The highest S_{BET} surface area of 1.7 m^2/g was obtained using a mixture of 90% toluene and 10% nitrobenzene as porogen (δ_{mix} = 18.9 $J^{1/2}m^{-3/2}$ with ~43 % v/v vinylindanone and 18.2 $J^{1/2}m^{-3/2}$ without vinylindanone), which indeed has a lower δ_{mix}-value than the calculated δ-value of the monomer (20.4 $J^{1/2}m^{-3/2}$) (figure 1). Therefore this mixture was identified as the optimal porogen for the preparation of macroporous pVI beads via suspension polymerization.

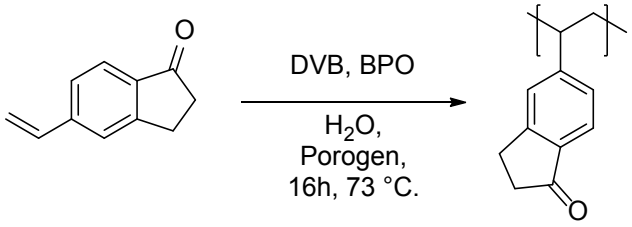

VI **pVI**

Scheme 5: Suspension polymerization of 5-vinylindan-1-one (vinylindanone).

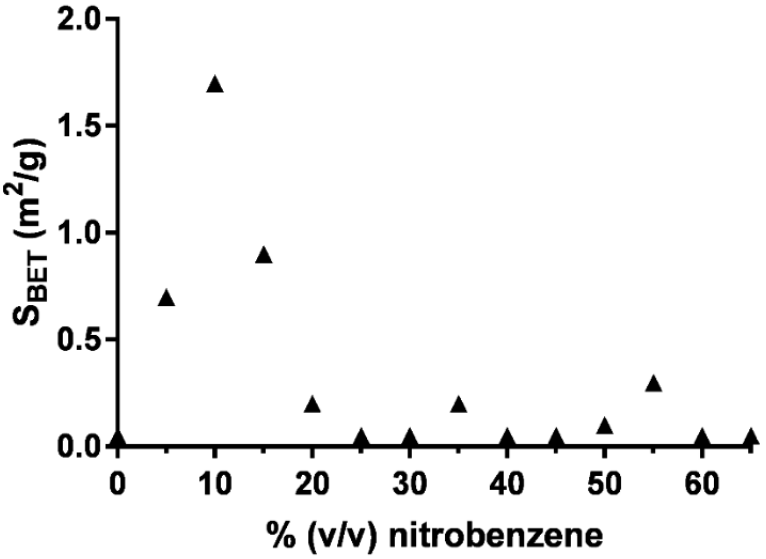

Figure 1: S_{BET} surface area of the obtained poly(VI) (with 2.5% DVB) beads versus the volume fraction (% v/v) nitrobenzene in toluene used as porogen in the suspension polymerization.

With the optimized porogen composition established for the suspension polymerization of vinylindanone at hand, the synthesis of the beads was scaled up to 24 and 50 grams yielding beads with a S_{BET} of 1.5 and 3.3 m^2/g in 80 and 92% yield, respectively.

2.3 Oxidation of Polyvinylindanone

The oxidation of indanone groups present in the macroporous sorbent particles into ninhydrin groups was studied by a one-step halogenation and Kornblum oxidation reaction using HBr, HI and I_2 in DMSO at 90 °C (scheme 6). Beads were removed from the suspension at different time points and their urea binding capacity (BC) was determined (figure 2).

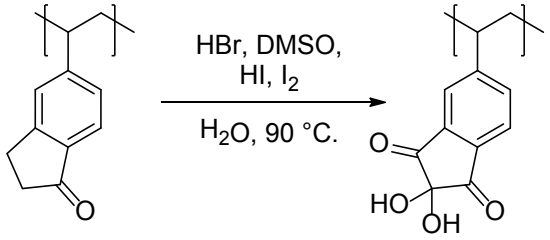

Scheme 6: Oxidation of indanone groups in pVI into ninhydrin groups (pVI-Ox).

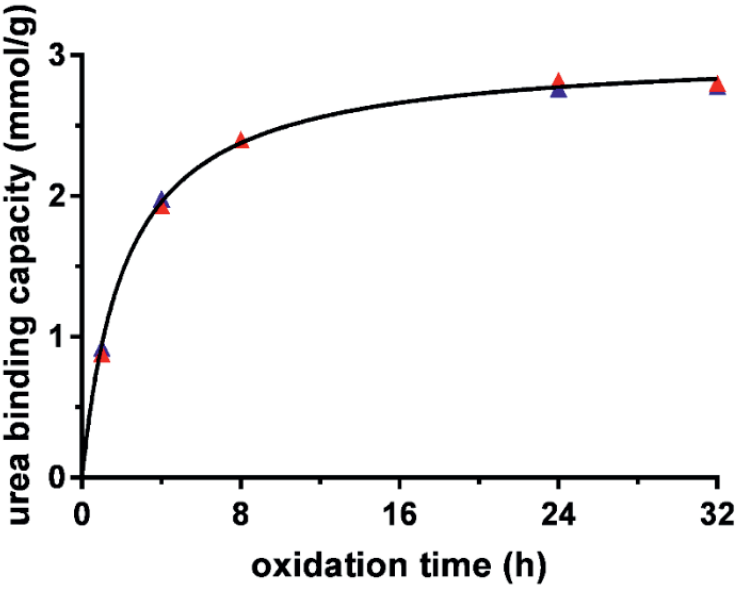

Figure 2: Urea binding capacity (average of 2 independent experiments, red and blue) of sorbent beads as function of oxidation time of pVI.

Figure 2 shows that indanone groups in pVI were gradually oxidized into ninhydrin groups to reach a BC for urea of 2.8 mmol/g in 24 hours. The observation that the BC reaches a plateau value demonstrates that the formed ninhydrin groups are stable under these harsh oxidizing conditions. Next, pVI beads were oxidized on a 40 gram scale under these conditions for 24 hours, yielding 49.1 gram sorbent beads containing ninhydrin groups (pVI-Ox). The BC of the obtained pVI-Ox beads was 3.2 mmol/g, which is one of the highest reported urea binding capacities of sorbents reported so far.[16, 32-33]

2.4 Characterization of pVI and pVI-Ox

Photographs of pVI and pVI-Ox beads are shown in figure 3A and D, respectively, and their morphologies were analyzed with scanning electron microscopy (SEM, figure 3B, C, E and F). The images of figure 3 show typical examples of both pVI and pVI-Ox beads, which are present as single beads (B and E) and as aggregates of several beads (C and F). The diameters of the pVI and pVI-Ox (aggregated) beads as determined by light microscopy were 0.74 ± 0.31 and 0.73 ± 0.28 mm, respectively. The surface area of pVI-Ox beads as determined by N_2 physisorption was 1.7 m^2/g, demonstrating that the porosity was not affected during the oxidation of the indanone groups (S_{BET} = 1.5 m^2/g). Thermal analysis by differential scanning calorimetry (DSC) showed that the glass transition temperature of both polymers was >160 °C (supporting information section 7.5) explaining their dimensional stability under the oxidizing conditions.

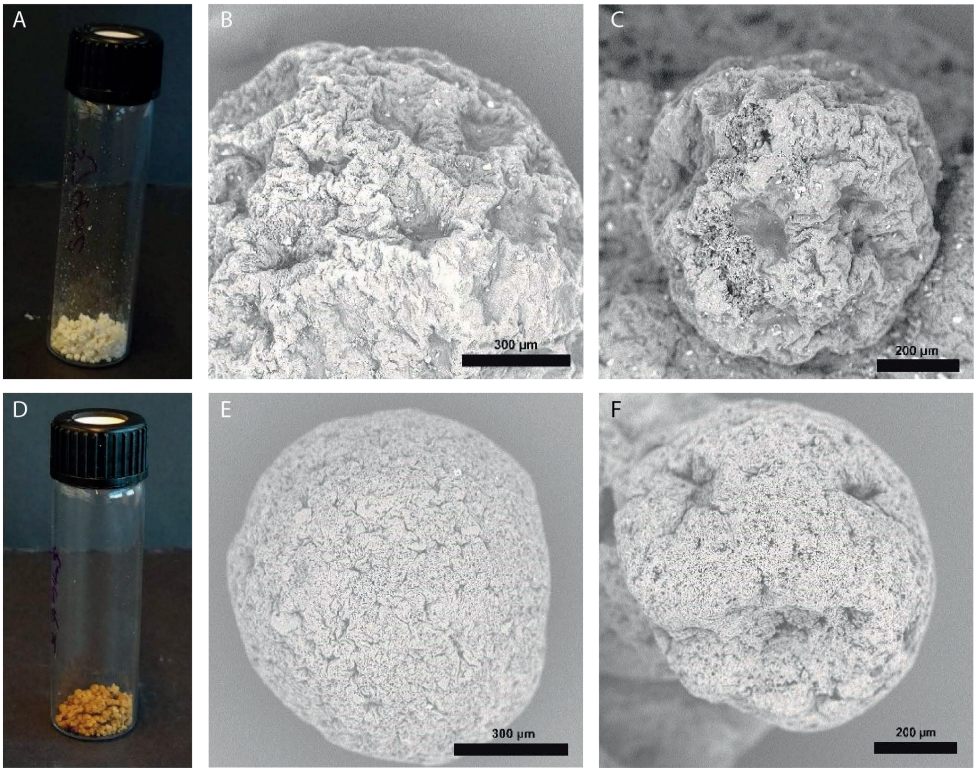

Figure 3: Photographs (A and D) and SEM pictures (B, C, E and F) of pVI and pVI-Ox beads.

The pVI and pVI-Ox beads were analyzed by infrared (IR) spectroscopy, and their spectra were compared with those of commercial 1-indanone and ninhydrin (figure 4A and B). The stretching vibration of the C=O bond (1700 cm^{-1}) and of the aromatic C=C bonds (1600 cm^{-1}) in the spectrum of pVI correspond to their respective peaks in the spectrum of 1-indanone. Similarly, the stretching vibrations of the C=O bonds (1700 and 1750 cm^{-1}), the aromatic C=C bonds (1600 cm^{-1}) and the C-O bonds (1090 cm^{-1}) in the IR spectrum of pVI-Ox are very similar to those of ninhydrin. In addition, the C-O stretching vibration peak (1090 cm^{-1}) as well as the splitting of the C=O peak observed (1780-1700 cm^{-1}) in the IR spectrum of pVI-Ox are not present in that of pVI, thereby confirming that the indanone groups have indeed been converted into ninhydrin groups during the oxidation step.

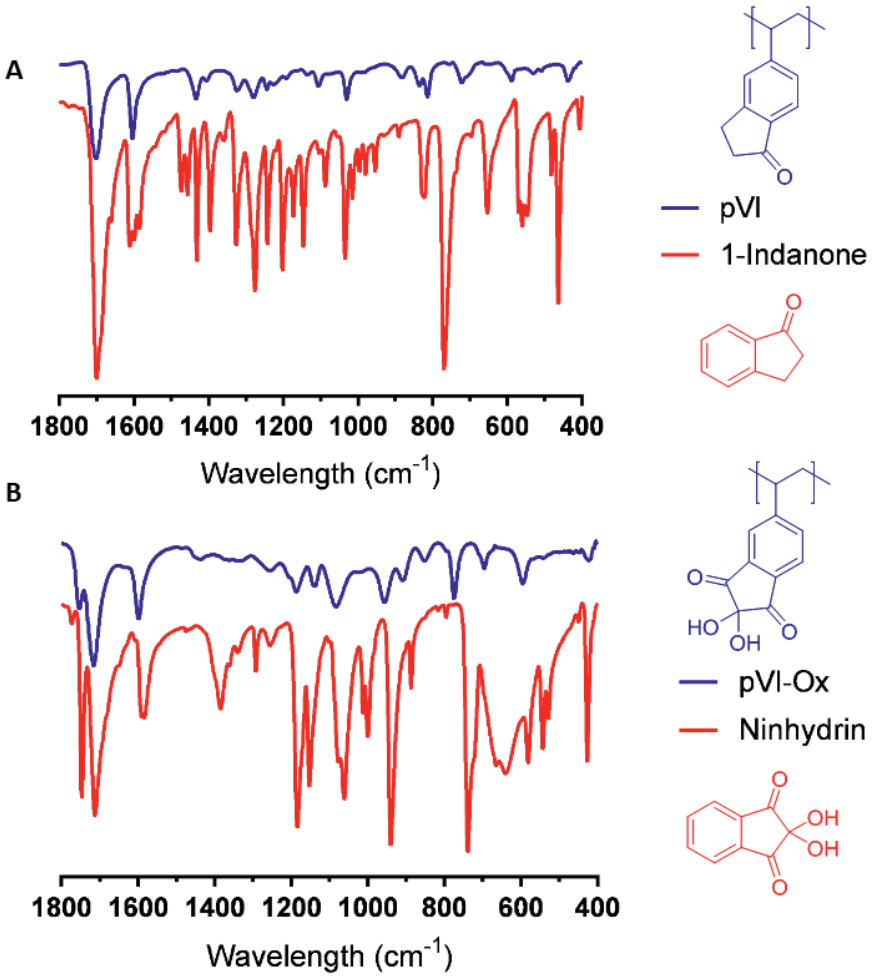

Figure 4: A) Infrared spectra of pVI (blue) and indanone (red) in the region of 400-1800 cm^{-1}. B) Infrared spectra of pVI-Ox (blue) and ninhydrin (red) in the region of 400-1800 cm^{-1}. Full IR spectra are shown in supporting information section 7.4.

Because IR analysis does not provide information on the extent of oxidation of the indanone groups, both pVI and pVI-Ox were analyzed with ^{13}C-solid state NMR spectroscopy. The different carbon signals present in the spectrum of the beads were intensified using cross-polarization (CP)[34], which however does not allow quantitative integration of the peaks (figure 5A). In the CP-spectrum of pVI (upper spectrum) a sharp peak at 30 ppm is observed, corresponding to the CH_2 groups of the indanone moiety. In the CP spectrum of pVI-Ox (lower spectrum) this sharp peak has disappeared, which demonstrates that the indanone groups were fully converted. In addition, a new peak around 90 ppm was detected, which is assigned to the hydrate carbon of ninhydrin. In order to quantify the density of ninhydrin groups present in pVI-Ox, the recycle delay (time in between the pulses) has to

be increased to allow all carbons to reach the equilibrium position. Therefore, the relaxation time (T_1) of pVI-Ox was determined to be 40 s and a quantitative solid state ^{13}C- NMR spectrum was obtained using a recycle delay of 80 s (2*T_1), applying a 30° pulse. The quantitative ^{13}C- solid state NMR spectrum is shown in figure 5B. Integration of the C-C backbone peak (30-50 ppm) and the hydrate carbon peak (90 ppm) demonstrates that 74% of the indanone groups were converted into ninhydrin groups. The structure of the remaining ~24% of the converted indanone groups could not be established as these side products did not give rise to new peaks in the ^{13}C-NMR spectrum (figure 5A and B). Based on the molecular weight of vinyl-substituted ninhydrin (204 g/mmol), the maximum binding capacity that could be obtained using sorbent beads consisting of 97.5% vinylninhydrin and 2.5% DVB is 4.8 mmol/g. A binding capacity of pVI-Ox of 3.2 mmol/g implies that 67% (3.2/4.8 mmol/g *100%) of the indanone groups are converted into accessible ninhydrin groups. Considering the error in both the urea binding capacity and the quantitative solid state ^{13}C-NMR analysis (~5%) as well as the likely presence of residual water in the beads, it is concluded that all ninhydrin groups present in pVI-Ox are accessible for urea.

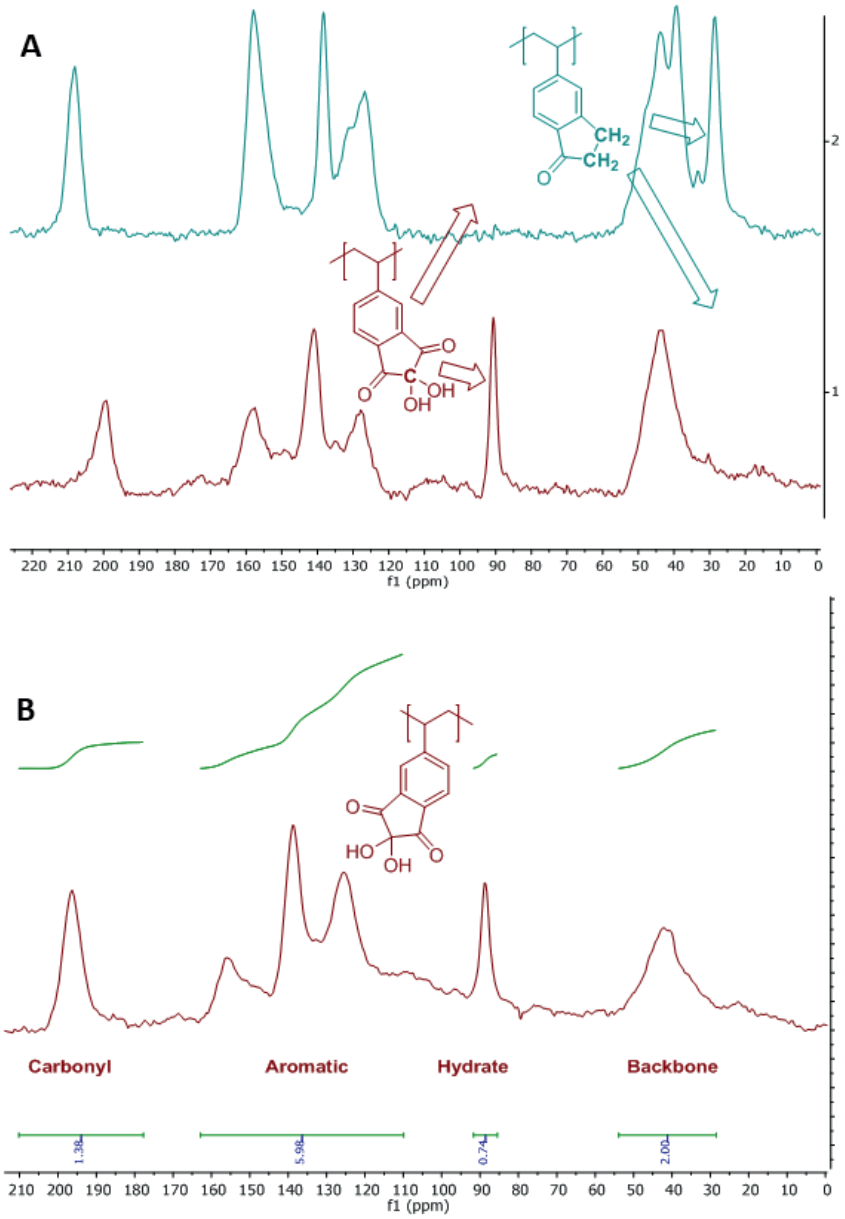

Figure 5: A) Solid state ^{13}C NMR (CP) spectra of pVI (upper) and pVI-Ox (lower). B) Quantitative solid state ^{13}C-NMR (30° pulse and recycle delay = $2*T_1$) of pVI-Ox. Integration of the hydrate carbon (90 ppm) and the backbone (30-50 ppm) shows that 74 % of the indanone groups were converted into ninhydrin groups.

2.5 Kinetics of Static Urea Absorption by pVI-Ox beads

To establish the potential of pVI-Ox beads as a suitable urea sorbent for dialysate regeneration, their urea removal kinetics were evaluated. First, to assess the urea absorption kinetics of pVI-Ox beads and the influence of temperature under static conditions, the beads were incubated with a 30 mM urea solution in PBS at 37, 50 and 70 °C and the urea concentration in the supernatant was monitored for 24 hours (figure 6).

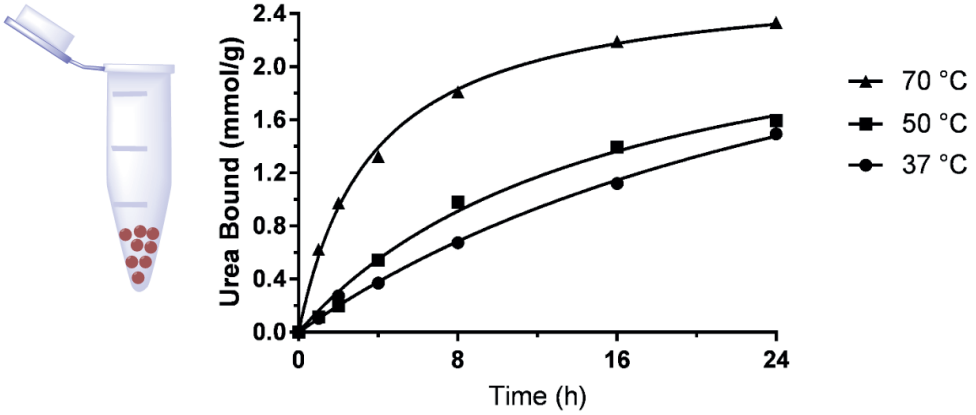

Figure 6: Binding of urea by pVI-Ox beads in time under static conditions at 37, 50 and 70 °C. Glass vials were charged with pVI-Ox beads (50 mg, 0.16 mmol ninhydrin groups), suspended in a 30 mM urea solution in PBS (5 mL, 0.15 mmol urea) and incubated in an oven under constant rotation and at the indicated temperatures. At regular time points the urea concentrations in the supernatants were measured. Each data point is the average of 2 independent measurements.

At 37 °C and 50 °C the rate of the urea binding is relatively slow and therefore the amount of urea bound is almost linear with time during the first 8 hours, as the amount of available ninhydrin groups is still large (≥78% (2.5 mmol/g) at 37 °C and ≥69 % (2.2 mmol/g) at 50 °C). At 70 °C however, the urea binding kinetics is much faster, and the binding kinetics decrease quickly after 6-8 hours because both the amount of available ninhydrin groups and the urea concentration have decreased by >50%.

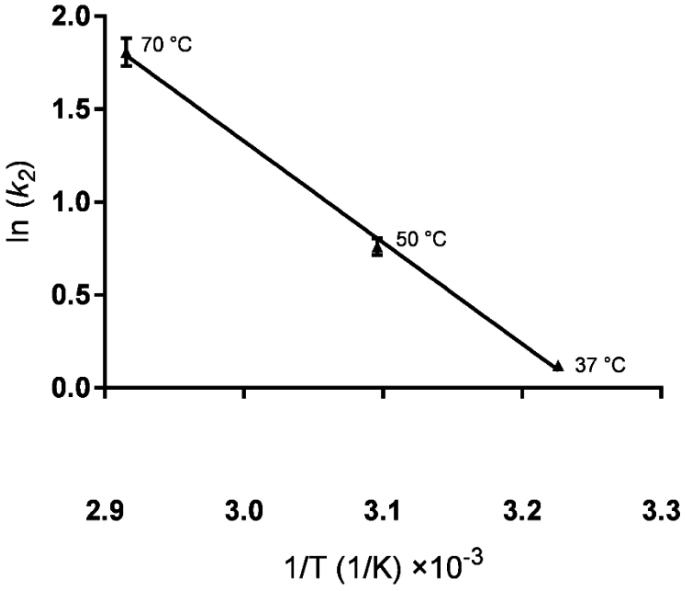

Figure 7: Arrhenius plot of the reaction of urea with ninhydrin-groups in pVI-Ox in PBS.

The second-order rate constant (k_2) of the reaction of urea with the ninhydrin-groups at 37 °C, as determined from the slope of the plot of the inverse urea concentration in time (supporting information section 7.8),[20] was determined to be 1.1 ± 0.1 $M^{-1}h^{-1}$. This is close to our earlier reported k_2-value of the reaction of urea with ninhydrin at 37 °C (2.7±0.1 $M^{-1}h^{-1}$)[19] and our earlier observation that alkyl substituents decrease the reactivity of ninhydrin-derivatives towards urea with factor ~2.[20] The natural logarithm of the k_2-values was plotted versus the inverse absolute temperature (figure 7). From this Arrhenius plot the activation energy (E_a) and pre-exponential factor (A) for the reaction of urea with the ninhydrin-groups in pVI-Ox were determined to be 10.8 ± 0.5 kcal/mol and (48.4 ± 2.1) × 10^6 $M^{-1}h^{-1}$. Interestingly, the activation energy of this reaction is lower than that of the reaction of ninhydrin with urea in solution (14.0 ± 0.4 kcal/mol), and the pre-exponential factor, which is correlated to the number of collisions between the reactants, is greatly reduced with a factor ~10^3 ((23.2 ± 0.6) × 10^9 $M^{-1}h^{-1}$),[19] likely due to the strongly reduced mobility of the ninhydrin groups in the beads as compared to ninhydrin in solution. Apparently, it is an coincidence that the k_2-value of the reaction of the ninhydrin groups in the sorbent with urea at 37 °C is similar to that of ninhydrin with urea in solution as the decrease in the pre-exponential factor (A) is compensated by a decrease in activation energy (E_A).

2.6 Effect of Ninhydrin: Urea Molar Ratio on the Urea Removal

To study the effect of the molar ratio between urea in solution and the ninhydrin

groups in pVI-Ox on urea removal, the amount of sorbent was doubled as compared to the conditions in figure 6. Figure 8A shows that, as expected, the urea concentration dropped more rapidly at a higher molar ratio of ninhydrin : urea. The determined k_2 value for the reaction of ninhydrin and urea at a 1:1 molar ratio and at 37 °C was (1.1 ± 0.1 $M^{-1}h^{-1}$, figure S8 and table S9). To determine the k_2-value for the reaction of ninhydrin groups with urea in a 2:1 molar ratio, pseudo-first order conditions are assumed for the first 4 hours. The pseudo-first order rate constant (k_{PFO}) was determined to be 0.060 h^{-1}, which corresponds a k_2-value of 1.0 ± 0.1 $M^{-1}h^{-1}$ (supporting information figure S9) and is in good agreement with the value determined at a 1:1 molar ratio. The data of figure 8A were used to calculate the amount of urea bound per gram of sorbent. Figure 8B shows that the pVI-Ox beads bound ~0.5 and ~0.6 mmol urea/g in 8 hours when the molar ratio ninhydrin : urea were 2:1 and 1:1, respectively.

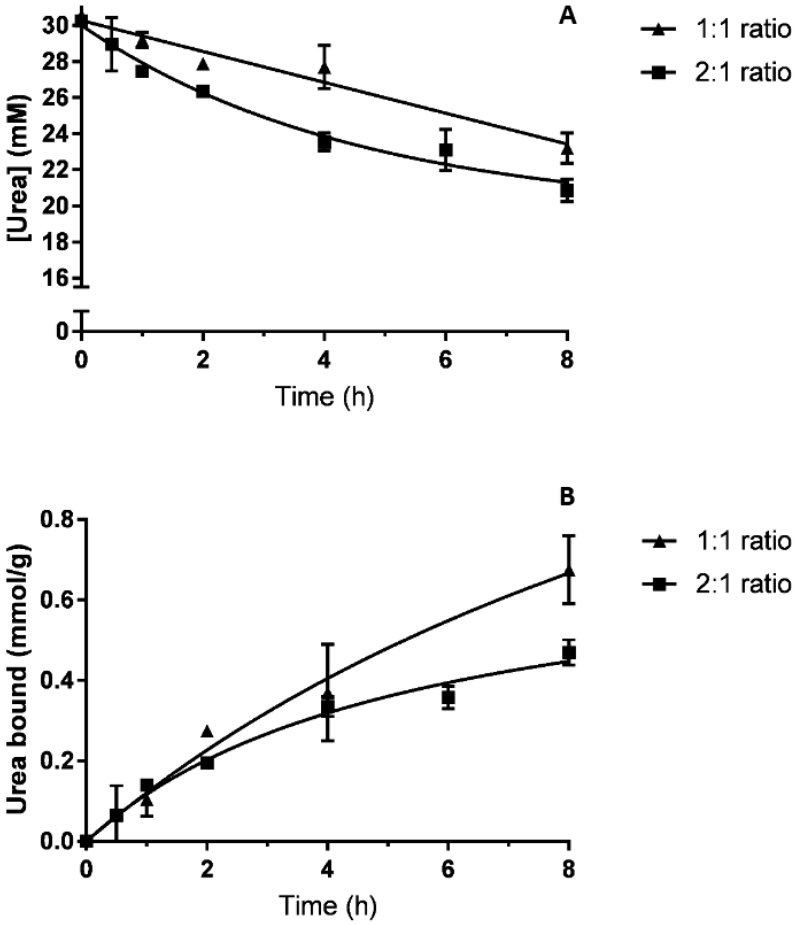

Figure 8: Urea removal of pVI-Ox beads at 37 °C at different ninhydrin : urea molar ratios. A) Plot of the urea concentration in time. B) Plot of the amount of urea bound per gram of sorbent in time.

2.7 Urea Binding of Urea on pVI-Ox Beads under Dynamic Conditions

To simulate the conditions of a dialysis session better than with static sorption, pVI-Ox beads were packed in a glass column and 30 mM urea in PBS, a concentration representative for dialysate,[35] was continuously pumped from a 37 °C reservoir in an Erlenmeyer through the sorbent column back into the Erlenmeyer (figure 9A). To compare with the binding under static conditions (figure 8A), the ninhydrin : urea molar ratio was 2 : 1. Figure 9B shows that the amount of urea that is bound (in mmol/g) under dynamic flow conditions was 0.6 mmol/g in 8 hours.

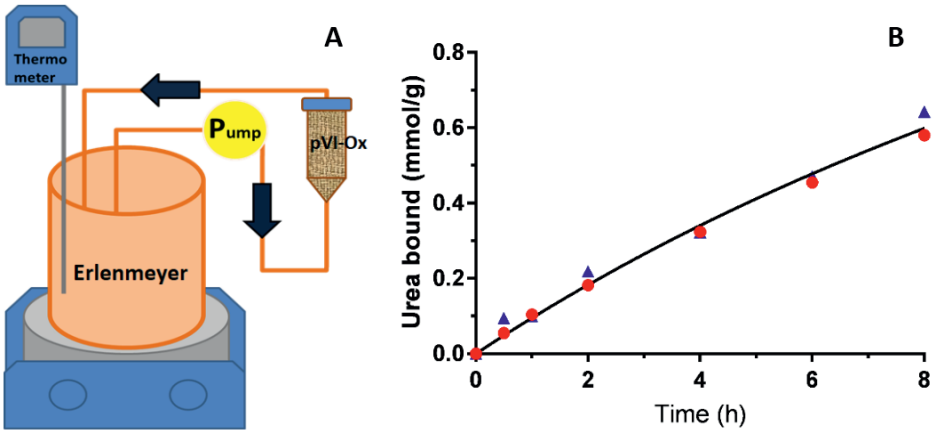

Figure 9: Binding of urea by pVI-Ox beads in time under dynamic conditions at 37 °C. A) Schematic representation of the experimental set up. B) Plot of the urea bound in time. The line shows a fit of the average amount of urea bound in time. Conditions: total volume 200 mL, 4.0 g pVI and a flow rate of 25 mL/min (N=2).

The total amount of urea removed from solution was (4 × 0.6 =) 2.4 mmol in 8 hours, thus 0.3 mmol/h. Therefore the clearance (*i.e.* the volume completely cleared of urea) was 10 mL/h. This clearance is relatively low as only 4 grams of sorbent was used, and it is expected that the clearance can be increased to clinically relevant values by increasing the amount of sorbent. Figure 10 shows the urea removal by pVI-Ox both under static conditions (from figure 8A) and dynamic conditions (from figure 9B) with the ninhydrin groups in the sorbent and urea in solution in a 2:1 molar ratio. The sorbent showed similar urea binding characteristics under static and dynamic conditions, especially during the first 4 hours. This can be explained by the fact that the flow rate (25 mL/min thus 1500 mL/h) was much higher than the clearance (10 mL/h) and thus did not limit the urea removal.

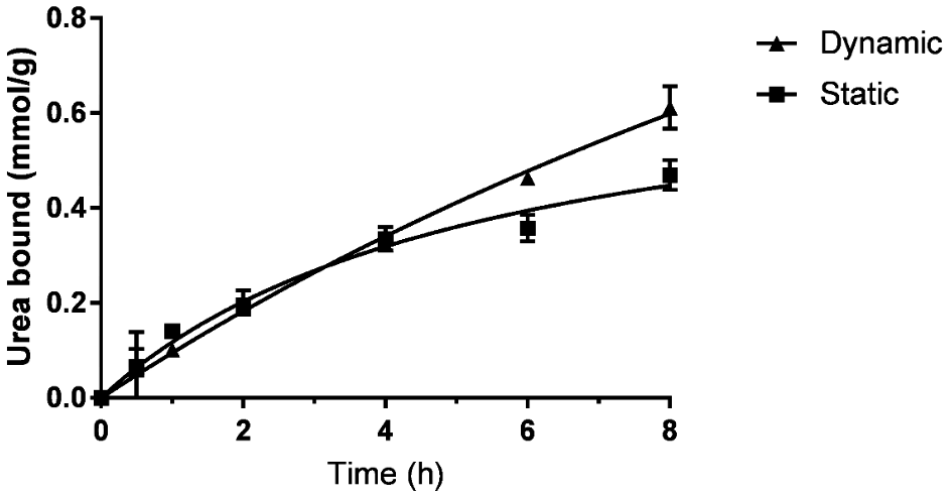

Figure 10: Urea bound by pVI-Ox from a 30 mM urea solution in time under static and dynamic conditions at 37 °C. Molar ratio ninhydrin : urea is 2 : 1.

3. Conclusion

This study reports an easy and scalable method to obtain a sorbent with high density of ninhydrin groups for urea removal from dialysate, which is crucial for realization of a wearable artificial kidney. The sorbent was obtained by suspension polymerization of 5-vinyl-1-indanone, followed by a single oxidation step, yielding a sorbent of which the backbone is 74% functionalized with ninhydrin groups (based on quantitative solid state ^{13}C-NMR). The beads have a maximum urea binding capacity of 3.2 mmol/g indicating that all ninhydrin groups are accessible for urea. It was found that the second order constant at 37 °C of the reaction of urea and ninhydrin groups of the beads was equal to that of the reaction in solution, with a reduced number of collisions compensated by a lower activation energy.

Static and dynamic binding studies suggest that ~600 grams of pVI-Ox beads are sufficient to remove the daily urea production of a patient (~400 mmol) within a 8 hour dialysis session, which brings the development of a wearable kidney a step closer to reality.

4. Materials and Methods

4.1 General

All materials were obtained from Sigma-Aldrich (Zwijndrecht, the Netherlands) and used as received unless stated otherwise. 5-Bromoindaone was obtained from CombiBlocks (San Diego, CA). Phosphate buffered saline (PBS, pH = 7.4, ion

composition: Na^+ 163.9 mM, Cl^- 140.3 mM, HPO_4^{2-} 8.7 mM, $H_2PO_4^-$ 1.8 mM) was obtained from B. Braun (Melsungen AG, Germany). Anhydrous dicalcium phosphate ($CaHPO_4$) was obtained from Chemtrade International (Bussum, the Netherlands). Polymethacrylic acid (Degalan® RG S mv) was obtained from Evonik Industries (Darmstadt, Germany). Flash chromatography was performed over silica gel (particle size 40-63 µm, VWR Chemicals, Leuven, Belgium) using the indicated eluent.

4.2 NMR and IR spectroscopy and TLC

^1H- and ^{13}C- liquid NMR spectra were recorded using an Agilent 400-MR DD2 equipped with a OneNMR probe at RT. Residual solvent signals were used as internal standard (^1H: δ 7.26 ppm, ^{13}C (^1H): δ 77.16 ppm for $CDCl_3$). Chemical shifts (δ) are given in ppm and coupling constants (J) are given in hertz (Hz). Resonances are described as s (singlet), d (doublet), t (triplet), q (quartet), bs (broad singlet) and m (multiplet) or combinations thereof. Infrared (IR) spectra were recorded neat using a Perkin Elkmer ATRU Spectrum 2 and reported in cm^{-1}. Thin Layer Chromatography (TLC) was performed using plates from Merck Darmstadt, Germany, (SiO_2, Kieselgel 60 F254 neutral, on aluminum with fluorescence indicator) and the compounds were visualized by UV detection (254 nm).

4.3 Determination of urea concentrations

Urea concentrations were determined with an AU 5800 routine chemistry analyzer (Beckman Coulter, Brea, CA) using a coupled enzyme reaction,[36] which results in a colorimetric (570 nm) product proportional to the urea concentration.

4.4 Synthesis of 5-vinyl-1-indanone (3-step route)

Synthesis of 2,3-dihydro-5-[2-(trimethylsilyl)ethynyl]inden-1-one.[24]

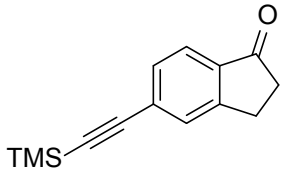

In a flame-dried 3-neck round bottom flask under nitrogen atmosphere, to a mixture of 5-bromo-1-indanone (44.3 g, 210 mmol, 1.0 eq.), $(Ph_3P)_2PdCl_2$ (1.4 g, 1 mol%,) and CuI (799 mg, 2 mol%) in 3:1 anhydrous Et_3N:DMF (350 mL) trimethylsilylacetylene (43.6 mL, 315 mmol, 1.5 eq.) was added slowly. The reaction mixture was then heated to 80 °C for 2 h and monitored by TLC until full conversion was observed. The reaction mixture was allowed to cool to room temperature (RT) and was transferred into a separation funnel. The mixture was extracted with CH_2Cl_2 and which phase was subsequently washed with water. The organic layer was furtheer washed with 10% HCl, 10% Na_2CO_3, and water and then dried over Na_2SO_4, filtrated and concentrated. The residue was purified by flash chromatography on silica gel (4:1 EtOAc:hexane gradient to 1:1 EtOAc:hexane), and 2,3-dihydro-5-[2-(trimethylsilyl)ethynyl]inden-

1-one was isolated as a solid (40.5 g, 84%). ^{1}H NMR (400 MHz, $CDCl_3$) δ 7.68 (d, *J* = 7.9 Hz, 1H), 7.57 (s, 1H), 7.44 (d, *J* = 7.9 Hz, 1H), 3.11 (t, *J* = 5.9 Hz, 2H), 2.71-2.68 (m, 2H), 0.26 (s, 9H). ^{13}C NMR (101 MHz, $CDCl_3$) δ 206.22 (C_q), 154.88 (C_q), 136.73 (C_q), 131.23 (CH), 130.18 (CH), 129.54 (C_q), 123.63 (C_q), 104.39 (C_q), 98.38 (CH_2), 36.44 (CH_2), 25.69 (CH_2), -0.04 (CH_3).

Synthesis of 5-ethynylindane-1-one.[24]

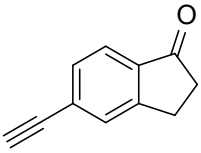

A mixture of 2,3-dihydro-5-[2-(trimethylsilyl)ethynyl]inden-1-one (40.0 g, 175 mmol, 1.0 eq.) and K_2CO_3 (12.0 g, 87.5 mmol, 0.5 eq.) in MeOH (200 mL) was stirred at RT for 2 h and monitored by TLC until full conversion was observed. The reaction mixture was concentrated and CH_2Cl_2 and water were added. The CH_2Cl_2 layer was washed with water (twice) and brine, and dried over Na_2SO_4. After filtration the mixture was concentrated under reduced pressure, and the crude product was purified by chromatography on silica gel (4:1 EtOAc/hexane) and 5-ethynylindane-1-one was isolated as a brown solid (25.0 g, 89%). ^{1}H NMR (400 MHz, $CDCl_3$) δ 7.71 (d, *J* = 7.9 Hz, 1H), 7.60 (s, 1H), 7.47 (d, *J* = 7.8 Hz, 1H), 3.25 (s, 1H), 3.13 (t, *J* = 6.0 Hz, 2H), 2.73-2.70 (m, 2H). ^{13}C NMR (101 MHz, $CDCl_3$) δ 206.17 (C_q), 154.91 (C_q), 137.12 (C_q), 131.39 (CH), 130.48 (CH), 128.50 (C_q), 123.75 (CH), 83.14 (C_q), 80.51 (CH), 36.43 (CH_2), 25.72 (CH_2).

Synthesis of 5-ethenylindane-1-one (vinylindanone):

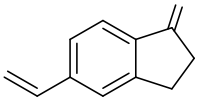

5-Ethynylindane-1-one (3.7 g, 23.6 mmol, 1.0 eq.) was suspended in EtOH (100 mL) and Lindlar's catalyst (110 mg, 3 weight%) was added. The reaction flask was capped with a septum and the air was replaced with H_2 (balloon), after which the reaction mixture was stirred vigorously for 2-16 hours. Importantly, to prevent over-reduction into the alkane, samples were frequently taken from the reaction mixture and, after evaporation of EtOH under reduced pressure, the conversion was determined by ^{1}H-NMR. After >90% conversion, the H_2-filled balloon was removed and the reaction mixture was concentrated under reduced pressure. The crude product was re-dissolved in CH_2Cl_2 and the catalyst was removed by filtration over Hyflo. The filtrate was concentrated under reduced pressure, giving 5-ethenylindane-1-one as a yellow solid (3.6 g, 97%). Melting point = 26°C, melting enthalpy = 22.9 J/g. ^{1}H NMR (400 MHz, $CDCl_3$) δ 7.71 (d, *J* = 8.0 Hz, 1H), 7.48 (s, 1H), 7.42 (d, *J* = 8.0 Hz, 1H), 6.78 (dd, *J* = 17.6 Hz, *J* = 10.9 Hz, 1H), 5.90 (d, *J* = 17.6 Hz, 1H), 5.42 (d, *J* = 10.9 Hz, 1H), 3.13 (t, *J* = 6.0 Hz, 2H), 2.72-2.69 (m, 2H). ^{13}C NMR (101 MHz, $CDCl_3$) δ 206.55 (C_q), 155.84 (C_q), 143.95 (C_q), 136.67 (C_q), 136.40 (CH), 125.72 (CH), 124.33 (CH), 124.04 (CH), 117.31 (CH_2), 36.63 (CH_2), 25.87 (CH_2).

4.5 Synthesis of 5-ethenylindane-1-one (1-step route)

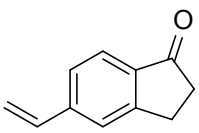

In a 10 L three necked round bottom flask 5-bromo-1-indanone (500 g, 2.37 mol, 1.0 eq.) and potassium trifluoro(vinyl)borate (381.0 g, 2.84 mol, 1.2 eq.) were dissolved in EtOH (5.0 L), and Et_3N (661 mL, 4.74 mol, 2 eq.) was added. The reaction mixture was flushed with nitrogen gas for 15 minutes and $Pd(dppf)Cl_2.CH_2Cl_2$ adduct (19.4 g, 23.7 mmol, 1 mol%) was added while nitrogen gas was flushed through the mixture continuously. The resulting mixture was heated to 80 °C under continuous magnetic stirring for 2-2.5 hours, after which clean and complete conversion was found with GC-MS (supporting information figure S1). The reaction mixture was cooled to RT and was concentrated to a thick paste under reduced pressure. Water (2.5 L) and EtOAc (2.5 L) were added to the paste to form a two-layered system. The solids present on the interface of the layers were removed by filtration through a P3 glass frit filter. The layers were separated and the organic layer was dried over Na_2SO_4 and concentrated under reduced pressure. The obtained oil was purified by filtration through a silica plug (using 4 weight volumes of silica) to yield 5-ethenylindane-1-one as a yellow-orange solid in good yield (318 g, 85% yield). Melting point = 42 °C, melting enthalpy = 92.8 J/g (supporting information figure S4).

4.6 Suspension polymerization of 5-vinyl-1-indanone and divinylbenzene (2 gram scale)

The aqueous phase was prepared by addition of NaCl (11 mg), polymethacrylic acid sodium salt solution (468 mg of a 10% solution in water (see Chapter 5, section 7.2)) and $CaHPO_4$ (81 mg) to water (15 mL) in a glass reactor equipped with Teflon blade stirrer (see Chapter 5, section 7.2). The aqueous phase was stirred for 30 minutes at RT. The organic phase was prepared by dissolving vinylindanone (2.0 g, 12.6 mmol) in a mixture of toluene and nitrobenzene (2.84 mL, different volume ratios) in a glass vial or beaker under gently heating. Next, 80% technical grade DVB (2.5 mol%) and a 50% benzoylperoxide blend with dicyclohexyl phthalate (61 mg, 0.13 mmol, 1.0 mol%) was added to the organic phase and stirred until a homogeneous solution was obtained. The organic phase was added to the aqueous phase in the glass reactor under continuous mechanical stirring at 330 rpm, yielding an o/w emulsion. The air was replaced by flushing with N_2 for 20 minutes and the stirring mixture was heated to 73 °C in an oil bath for 16 hours. Afterwards the suspension was allowed to cool to RT and poured over a filter (cut-off 200 µm). The residue was washed with acetone and water and dried over P_2O_5 under vacuum, resulting in polyvinylindanone (pVI, 1.5-1.9 grams, 75-95%).

4.7 Suspension copolymerization of vinylindanone and divinylbenzene (50 gram scale)

The same procedure was followed as for the suspension polymerization on a 2 gram scale synthesis, in which the reaction time was 20 instead of 16 hours. The amounts of the reagents were as follows: 242 mg NaCl, 11.7 g 10% polymethacrylic acid sodium salt solution, 2.025 g $CaHPO_4$, 375 mL water, 50.0 g vinylindanone, 64 mL toluene, 7.11 mL nitrobenzene and 1.531 g 50% benzoylperoxide blend with dicyclohexyl phthalate and 1.4 mL DVB. The yield was 91.6% (45.8 grams). The T_g of the product (pVI) was 189 °C (supporting information figure S5).

4.8 Halogenation and Kurnblum Oxidation of pVI to obtain pVI-Ox

In a glass reactor equipped with a Teflon blade stirrer, pVI beads (40.0 g, 253 mmol indanone groups) were swollen in dimethylsulfoxide (DMSO) (449 mL, 6.32 mol, 25 eq.) for 30 minutes under continuous stirring, after which iodine (64.2 g, 253 mmol, 1.0 eq.), aqueous 57% HI (28.9 mL, 253 mmol, 1.0 eq.) and aqueous 48% HBr (171 mL, 1.52 mol, 6.0 eq.) were added at RT. One of the outlets of the reactor was capped with a septum containing a needle, to allow escape of the formed Me_2S. The suspension was stirred for 24 hours at 90 °C, after which the reaction mixture was filtered (cut-off 200 µm). The residue was washed with DMSO and water until no iodine and acid were extracted from the residue (until pH of the filtrate > 5). The filtrate was dried over P_2O_5 under vacuum, resulting in pVI-Ox (49.2 grams). The T_g of the product (pVI-Ox) was not determined as it gradually decomposed >140 °C (supporting information figure S6).

4.9 Characterization of beads by SEM

The morphology of the different beads was analyzed by scanning electron microscopy (SEM, Phenom, FEI Company, the Netherlands). Dried beads were transferred onto 12-mm diameter aluminum specimen stubs (Agar Scientific Ltd., England) using double-sided adhesive tape. Prior to analysis, the beads were coated with platinum using an ion coater under vacuum. The samples were imaged using a 5 kV electron beam.

4.10 Determination of the size of the beads by light microscopy

The diameters of the beads were measured using optical microscopy, utilizing a size calibrated Nikon eclipse TE2000-U microscope equipped with a digital camera (Nikon DS-2Mv camera and Nikon DS-U1 digital adapter, with a 4× magnification) and the NIS-elements basic research software package. Images of the beads were taken in the dry state and for 30 arbitrary beads 3 points on the perimeter of the beads were identified to allow calculation of circular diameter by the program.[37] The average diameters and standard deviations are reported.

4.11 Thermogravimetric Analysis (TGA) of the beads

In a platinum pan the beads were heated at a rate of 10 °C/minute. The weight loss during the ramp heating (and thereby the decomposition temperature) was determined on a TAinstruments TGA Q50.

4.12 Differential Scanning Calorimetry (DSC) of monomer and beads

In an aluminum open pan the monomer or beads were first heated from -50 °C till 250 °C at a rate of 10°C/minute then cooled down to -50 °C and heated to 250 °C with rate of 10°C/minute. The heat flow was monitored. The T_g (or melting point) was determined with a TAinstruments Discovery DSC. Residual solvent evaporated during the first run and therefore the results of the second run are reported.

4.13 ^{13}C solid state NMR analysis of pVI and pVI-Ox beads

For solid-state ^{13}C NMR measurements, pVI and pVI-Ox beads were crushed and transferred into a 3.2 mm thin-wall rotor for the magic-angle spinning (MAS) solid-state NMR experiments. The cross-polarization (CP) experiments were performed on a Bruker 400 MHz, employing a spin rate of 17 kHz, 2000 µs contact time and a recycle delay of 2s for 3072 scans. The ^{13}C direct excitation spectrum was performed using a Bruker 500 MHz spectrometer at a spin rate of 12 kHz. 30˚ Pulses were applied with field strength of 55 kHz and 80 kHz SPINAL64.[38] The ^{13}C relaxation time (T_1) was measured to be 40 s with an inverse recovery and the recycle delay was set to 2*T1 (80 s). All measurements (CP and direct excitation) were conducted at 25 °C, applying 80 kHz ^{1}H decoupling during acquisition and MAS frequency of kHz chosen to minimize the overlap of the signal with spinning sidebands.

4.14 Nitrogen physisorption

N_2 physisorption isotherms were measured at -196 °C using a Micromeritics TriStar 3000 and TriStar II Plus apparatus. Prior to analysis, the samples were dried under vacuum at RT for 16 hours. Surface areas were determined using the Brunauer-Emmett-Teller (BET) method and the total pore volumes were derived from the amount of N_2 adsorbed at p/p_0 = 0.995.[39] A Barrett-Joyner-Halenda (BJH) analysis was employed to determine pore size/volume distributions of the samples with the use of a Harkins-Jura thickness curve.[40-41] Due to the shrinking of the polymeric beads with increasing pressure, and subsequent expansion with decreasing pressure, the correction of the dead volume is incorrect, as by default it assumes that the solid fraction of the sample does not change in volume with pressure. As the dead volume was determined at $p/p_0 \approx 0$ and assumed constant during the measurement, the default dead volume-corrected isotherms decreased slightly with increasing pressures, which is physically meaningless. The relative deviation is largest for

materials with low surface areas (< 5 m^2/g) and high materials volume fractions in the measurement tubes, such as for pVI-Ox. A correction for this deformation *i.e.* change in dead volume with pressure was applied to these isotherms by a linear swelling function ($V_{adjusted} = a \cdot (p/p_0) + V_{original}$), in which a represents the swelling factor relative to the material's volume at $p/p_0 \approx 0$, until $dV/d(p/p_0) > 0$ was achieved for all pressures. The S_{BET} surface areas of the pVI and pVI-Ox beads were calculated from the isotherms that were corrected for these volume changes as a function of pressure.

4.15 Urea binding of pVI-Ox beads under static conditions

The pVI-Ox beads (50 mg per glass vial, 0.16 mmol of ninhydrin groups) were incubated with urea solution (5.0 mL, 30 mM, 0.15 mmol urea) in PBS in 12 glass vials. The samples were placed in an oven at 37 °C on a rotating device or shaking water bath at 50 or 70 °C. After 1, 2, 4, 8, 16 and 24 hours, two glass vials per time point were taken and the beads were allowed to settle and the supernatant was removed (see supporting information section 7.7). To determine the maximum binding capacity of a sorbent, the sorbent beads (50 mg per vial, 0.16 mmol of ninhydrin groups) were incubated for 24 hours at 70 °C with a urea solution (5.0 mL, 50 mM, 0.25 mmol urea) in PBS in two glass vials, after which the beads were allowed to settle and the urea concentration in the supernatant was determined (see supporting information section 7.6).

4.16 Urea binding of pVI-Ox beads under dynamic conditions

In a glass column (for a picture see supporting information section 9) pVI-Ox sorbent beads (4.0 g) were pre-wetted with PBS (20 mL) and placed on a rotating device overnight. In an Erlenmeyer, PBS (180 mL) was heated to 37 °C and pumped with a peristaltic pump through the prewetted sorbent column (making the overall volume 200 mL) for 30 minutes at a flow of 25 mL/min, before returning to the Erlenmeyer (for a picture see supporting information section 9). Urea (360 mg, 6 mmol, 30 mM) was added to the Erlenmeyer and the urea concentration in the Erlenmeyer after 0, 0.5, 1, 2, 4, 6 and 8 hours by removing 0.5 mL of the volume.

5. Acknowledgement

The authors like to thank Carl C.L. Schuurmans for his help with the determination of the size of the beads, Lies A.L. Fliervoet for making figure 3 and Dr. Eelco Ruijter (VU Amsterdam) for the valuable discussions. This research was supported by the Dutch organization for Scientific Research (NWO-TTW, project 14433) and the Dutch Kidney Foundation. MB gratefully acknowledges NWO for funding the NMR infrastructure (Middle Groot program, grant number 700.58.102 and Groot program, grant number 175.010.2009.002). RD acknowledges the European Research Council (ERC) for funding (ERC-2014-CoG 648991).

6. References

1. Gura, V.; Rivara, M. B.; Bieber, S.; Munshi, R.; Smith, N. C.; Linke, L.; Kundzins, J.; Beizai, M.; Ezon, C.; Kessler, L.; Himmelfarb, J., A wearable artificial kidney for patients with end-stage renal disease. *JCI Insight* **2016,** *1* (8), 15.
2. Agar, J. W., Review: understanding sorbent dialysis systems. *Nephrology (Carlton)* **2010,** *15* (4), 406-11.
3. Davenport, A.; Gura, V.; Ronco, C.; Beizai, M.; Ezon, C.; Rambod, E., A wearable haemodialysis device for patients with end-stage renal failure: a pilot study. *Lancet* **2007,** *370* (9604), 2005-10.
4. Lehmann, H. D.; Marten, R.; Gullberg, C. A., How to catch urea? Considerations on urea removal f rom hemofiltrate. *Artif. Organs* **1981,** *5* (3), 278-85.
5. Weiner, I. D.; Mitch, W. E.; Sands, J. M., Urea and ammonia metabolism and the control of renal nitrogen excretion. *Clin. J. Am. Soc. Nephrol.* **2015,** *10* (8), 1444-58.
6. Shinaberger, C. S.; Kilpatrick, R. D.; Regidor, D. L.; McAllister, C. J.; Greenland, S.; Kopple, J. D.; Kalantar-Zadeh, K., Longitudinal associations between dietary protein intake and survival in hemodialysis patients. *Am. J. Kidney. Dis.* **2006,** *48* (1), 37-49.
7. Roberts, M., The regenerative dialysis (REDY) sorbent system. *Nephrology* **1998,** *4* (4), 275-278.
8. Blumenkrantz, M. J.; Gordon, A.; Roberts, M.; Lewin, A. J.; Pecker, E. A.; Moran, J. K.; Coburn, J. W.; Maxwell, M. H., Applications of the Redy sorbent system to hemodialysis and peritoneal dialysis. *Artif. Organs* **1979,** *3* (3), 230-6.
9. Urbanczyk, E.; Sowa, M.; Simka, W., Urea removal from aqueous solutions-a review. *J. Appl. Electrochem.* **2016,** *46* (10), 1011-1029.
10. Wernert, V.; Schaf, O.; Ghobarkar, H.; Denoyel, R., Adsorption properties of zeolites for artificial kidney applications. *Micropor. Mesopor. Mat.* **2005,** *83* (1-3), 101-113.
11. Poss, M. J.; Blom, H.; Odufu, A.; Smakman, R., Macromolecular ketoaldehydes. U.S. Patent 6,861,473 B2: **2005**.
12. Deepak, D., Evaluation of adsorbents for the removal of metabolic wastes from blood. *Med. Biol. Eng. Comput.* **1981,** *19* (6), 701-6.
13. Cheng, Y. C.; Fu, C. C.; Hsiao, Y. S.; Chien, C. C.; Juang, R. S., Clearance of low molecular-weight uremic toxins p-cresol, creatinine, and urea from simulated serum by adsorption. *J. Mol. Liq.* **2018,** *252*, 203-210.
14. Giordano, C.; Esposito, R.; Bello, P.; Quarto, E.; Gonzalez, F. M., Cold carbon apparatus for hemodialysis. *J. Dial.* **1976,** *1* (2), 165-79.
15. van Gelder, M. K.; Mihaila, S. M.; Jansen, J.; Wester, M.; Verhaar, M. C.; Joles, J. A.; Stamatialis, D.; Masereeuw, R.; Gerritsen, K. G. F., From portable dialysis to a bioengineered kidney. *Expert Rev. Med. Devices* **2018,** *15* (5), 323-336.
16. Abidin, M. N. Z.; Goh, P. S.; Ismail, A. F.; Said, N.; Othman, M. H. D.; Hasbullah, H.; Abdullah, M. S.; Ng, B. C.; Kadir, S.; Kamal, F., Highly adsorptive oxidized starch nanoparticles for efficient urea removal. *Carbohydr. Polym.* **2018,** *201*, 257-263.
17. Smakman, R.; van Doorn, A. W., Urea removal by means of direct binding. *Clin. Nephrol.* **1986,** *26 Suppl 1*, S58-62.
18. Shimizu, T.; Fujishige, S., A newly prepared surface-treated oxystarch for removal of urea. *J. Biomed. Mater. Res.* **1983,** *17* (4), 597-612.
19. Jong, J. A. W.; Smakman, R.; Moret, M.-E.; Verhaar, M. C.; Hennink, W. E.; Gerritsen, K. G. F.; Van Nostrum, C. F., Reactivity of (Vicinal) Carbonyl Compounds with Urea.

ACS Omega **2019,** *4* (7), 11928-11937.
20. Jong, J. A. W.; Moret, M. E.; Verhaar, M. C.; Hennink, W. E.; Gerritsen, K. G. F.; van Nostrum, C. F., Effect of substituents on the reactivity of ninhydrin with urea. *ChemistrySelect* **2018,** *3* (4), 1224-1229.
21. Smakman, R. Macromolecular carbonyl groups containing material suitable for use as sorbent for nitrogen compounds. U.S. Patent 4,897,200, **1990**.
22. Crouse, G.D.; Demeter, D.A.;Sparks, T.C.; Wang, N.X.; Dent, W.H.; De Amicis, C.; Niyaz, N.M.; Baum, E.W.; Fischer, L.G.; Giampietro, N.C., Pesticidal compositions and processes related thereto. U.S. Patent 9.440.964 B2, **2015**.
23. Bluchel, C. G.; Wang, Y.; Tan, K.C., Sorbent for a dialysis device., **2011**., U.S. Patent 0171713 A1.
24. Ortega, R.; Hubner, H.; Gmeiner, P.; Masaguer, C. F., Aromatic ring functionalization of benzolactam derivatives: new potent dopamine D3 receptor ligands. *Bioorg. Med. Chem. Lett.* **2011,** *21* (9), 2670-4.
25. Molander, G. A.; Brown, A. R., Suzuki-Miyaura cross-coupling reactions of potassium vinyltrifluoroborate with aryl and heteroaryl electrophiles. *J. Org. Chem.* **2006,** *71* (26), 9681-6.
26. Gokmen, M. T.; Du Prez, F. E., Porous polymer particles—A comprehensive guide to synthesis, characterization, functionalization and applications. *Prog. Polym. Sci.* **2012,** *37* (3), 365-405.
27. Van Krevelen, D. M., *Properties of Polymers*. Amsterdam, **1990**, 198-203.
28. Fedors, R. F., A method for estimating both the solubility parameters and molar volumes of liquids. *Polym. Eng. Sci.* **1974,** *14* (2), 147-154.
29. Matsukawa, H.; Yoda, S.; Okawa, Y.; Otake, K., Phase behavior of a carbon dioxide/methyl trimethoxy silane/polystyrene ternary system. *Polymers* **2019,** *11* (2), 11.
30. Cameron, N. R.; Barbetta, A., The influence of porogen type on the porosity, surface area and morphology of poly(divinylbenzene) PolyHIPE foams. *J. Mat. Chem.* **2000,** *10* (11), 2466-2471.
31. Hanssen, C. M., *The three dimensional solubility parameter and solvent diffusion coefficient, their Importance in surface coating formulation*. Danish Technical Press: Copenhagen, **1967**.
32. Cheah, W. K.; Sim, Y. L.; Yeoh, F. Y., Amine-functionalized mesoporous silica for urea adsorption. *Mater. Chem. Phys.* **2016,** *175*, 151-157.
33. Wilson, L. D.; Xue, C., Macromolecular sorbent materials for urea capture. *J. Appl. Polym. Sci.* **2013,** *128* (1), 667-675.
34. Also known as PENIS-NMR, see: Pines, A.; Gibby, M. G.; Waugh, J. S., Proton-enhanced nuclear induction spectroscopy ^{13}C chemical shielding anisotropy in some organic solids. *Chem. Phys. Lett.* **1972,** *15* (3), 373-376.
35. Vanholder, R.; Gryp, T.; Glorieux, G., Urea and chronic kidney disease: the comeback of the century? (in uraemia research). *Nephrol. Dial. Transplant.* **2018,** *33* (1), 4-12.
36. Talke, H.; Schubert, G. E., Enzymatic urea determination in the blood and serum in the warburg optical test. *Klin. Wochenschr.* **1965,** *43*, 174-5.
37. Schuurmans, C. C. L.; Abbadessa, A.; Bengtson, M. A.; Pletikapic, G.; Eral, H. B.; Koenderink, G.; Masereeuw, R.; Hennink, W. E.; Vermonden, T., Complex coacervation-based loading and tunable release of a cationic protein from monodisperse glycosaminoglycan microgels. *Soft Matter* **2018,** *14* (30), 6327-6341.
38. Fung, B. M.; Khitrin, A. K.; Ermolaev, K., An improved broadband decoupling

sequence for liquid crystals and solids. *J. Magn. Reson.* **2000,** *142* (1), 97-101.
39. Thommes, M.; Kaneko, K.; Neimark Alexander, V.; Olivier James, P.; Rodriguez-Reinoso, F.; Rouquerol, J.; Sing Kenneth, S. W., Physisorption of gases, with special reference to the evaluation of surface area and pore size distribution (IUPAC Technical Report). In *Pure and Applied Chemistry*, 2015; Vol. 87, p 1051.
40. Barrett, E. P.; Joyner, L. G.; Halenda, P. P., The determination of pore volume and area distributions in porous substances. I. Computations from nitrogen isotherms. *J. Am. Chem. Soc.* **1951,** *73* (1), 373-380.
41. Jura, G.; Harkins, W. D., Surfaces of Solids. XI. Determination of the decrease (π) of free surface energy of a solid by an adsorbed film. *J. Am. Chem. Soc.* **1944,** *66* (8), 1356-1362.

7. Supporting information

On request available are NMR spectra for the synthesized compounds.

7.1 Ninhydrin-type sorbents derived from polystyrene

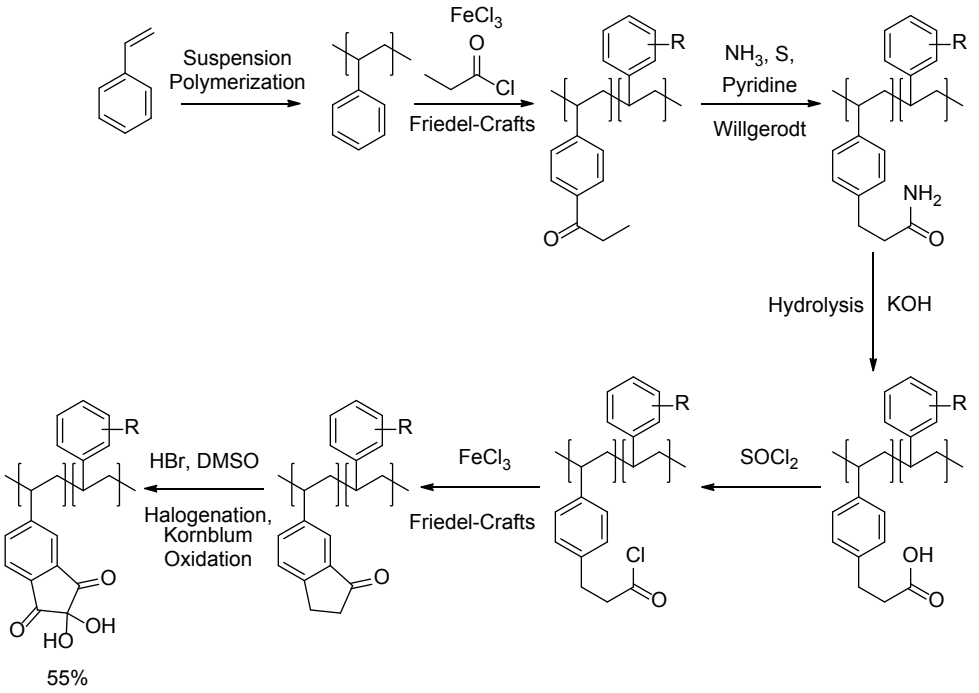

Scheme S1: Overview of the synthesis of ninhydrin-type sorbents starting from polystyrene.[21] R = side products.

7.2. Optimization of the reaction conditions of the Suzuki-Molander synthesis of vinylindanone.

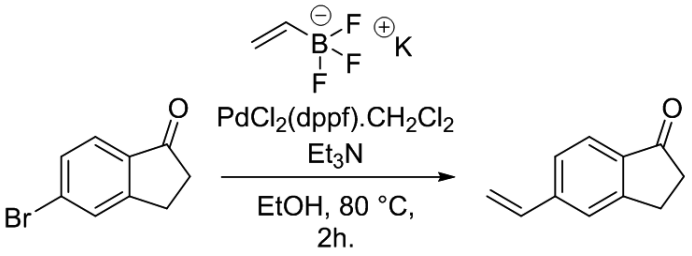

Scheme S2: One step synthesis of 5-vinylindan-1-one (vinylindanone).

Table S1: Optimization for the reaction conditions and scaling up of the synthesis of vinylindanone.

Entry	Vinylborate (eq.)	Pd Catalyst (mol%)	Yield (%)	Scale
1	1.5	10	n.d.	250
2	1.5	10	88	2.5 g
3	1.5	10	95.5	100 mg
4	1.5	5	98.5	100 mg
5	1.5	1	98.4	100 mg
6	1.5	0.5	98.2	100 mg
7	1.3	10	96.2	100 mg
8	1.3	5	97.7	100 mg
9	**1.3**	**1**	**99.0**	**100 mg**
10	1.3	0.5	89.5	100 mg
11	1.1	10	92.7	100 mg
12	1.1	5	95.9	100 mg
13	**1.1**	**1**	**99.1**	**100 mg**
14	1.1	0.5	86.9	100 mg
15	1.1	1	83	10.0 g
16	1.2	1	84	10.0 g
17	1.2	1	86	100 g
18	1.2	1	85	500 g

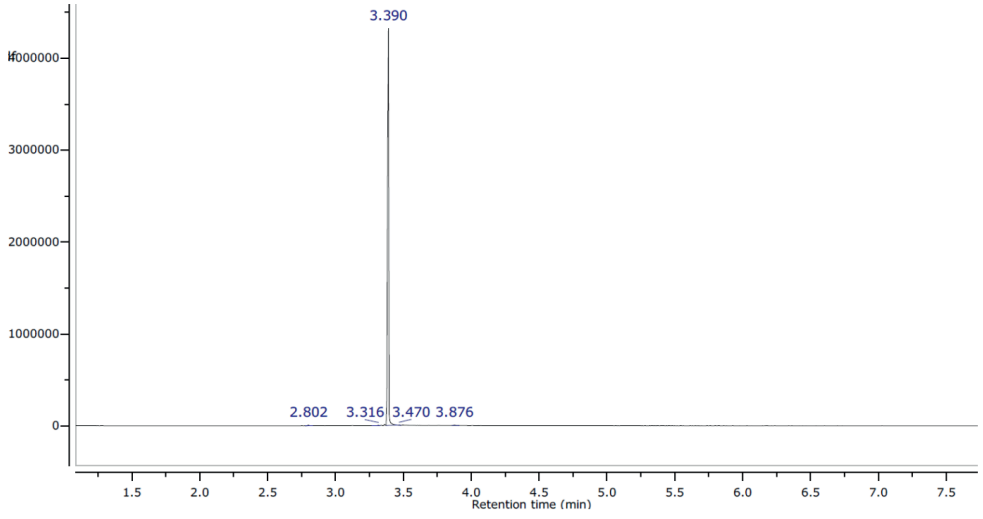

Figure S1: Gas chromatogram of vinylindanone. Carrier gas He (50 cm/s) in a RXi-5MS 20 m column (diameter 180 µm) with an injection volume of 1 µL. Initial temperature was 100 °C and was heated to 250 °C at a rate of 75 °C/min.

7. 3 Calculation of δ-values

The δ-value is calculated according to the following formula, in which Δe_i and Δv_i represent the group contributions to heat of evaporation and molar volume, respectively.

$$\delta = \sqrt{\frac{\Sigma \Delta e_i}{\Sigma \Delta v_i}}$$

Table S2: Calculated δ-value of vinylindanone.

Group	Δe_i (cal/mole)[28]	Δe_i (J/mole)	Δv_i (mL/mole)[28]
Ph (tri-substituted)	7630	31923.92	33.4
CH (vinyl)	1030	4309.52	13.5
CH2 (vinyl)	1030	4309.52	28.5
CO	1180	4937.12	10.8
CH_2	1180	4937.12	16.1
CH_2	1180	4937.12	16.1
Ring closure	250	1046	16.0
sum		56400.32	134.4

Table S3: Calculation of the δ-value of polyvinylindanone.

Group	Δe_i (cal/mole)	Δe_i (J/mol)	Δv_i (mL/mole)
Ph (tri-substituted)	7630	31923.92	33.4
CH (aliphatic)	820	3430.88	-1.0
CH_2 (aliphatic)	1180	4937.12	16.1
CO	1180	4937.12	10.8
CH_2	1180	4937.12	16.1
CH_2	1180	4937.12	16.1
Ring closure	250	1046	16.0
sum		56149.28	107.5

7.4 IR spectra of indanone, pVI, ninhydrin and pVI-Ox

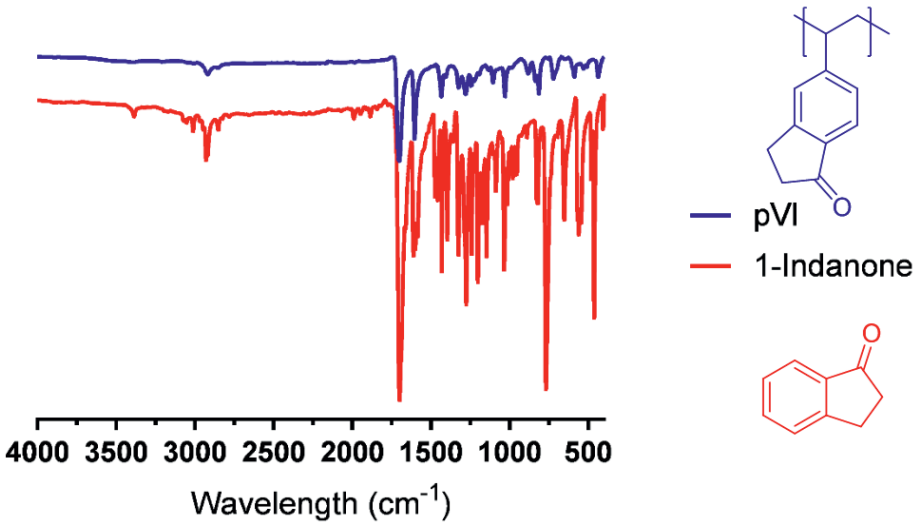

Figure S2: IR spectra of pVI and 1-Indanone.

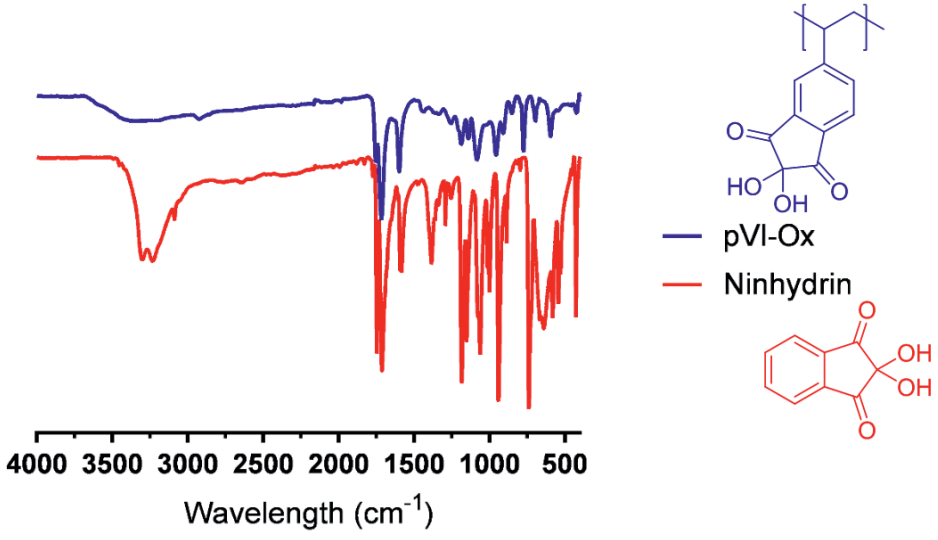

Figure S3: IR spectra of pVI-Ox and ninhydrin.

7.5 Thermal Analysis

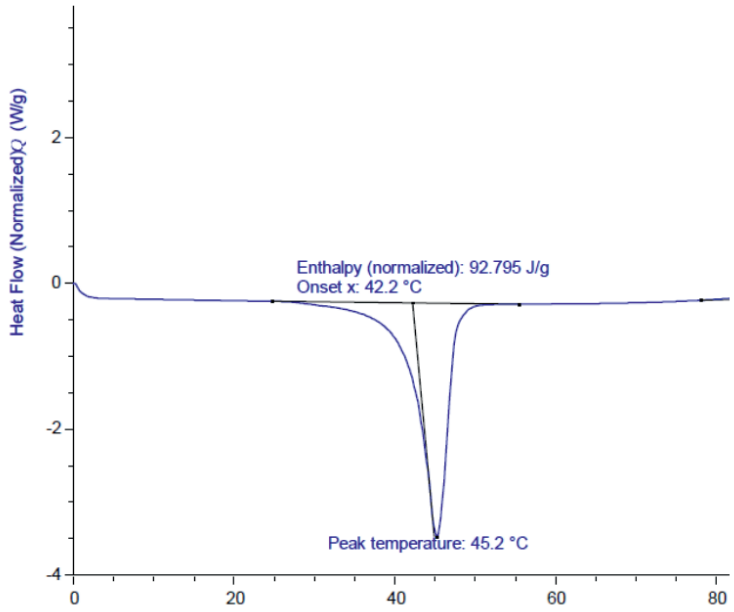

Figure S4: DSC thermogram of vinylindanone obtained in the 1-step Suzuki-Molander route. The endothermic peak at 42 °C (onset) shows the melting point of vinylindanone.

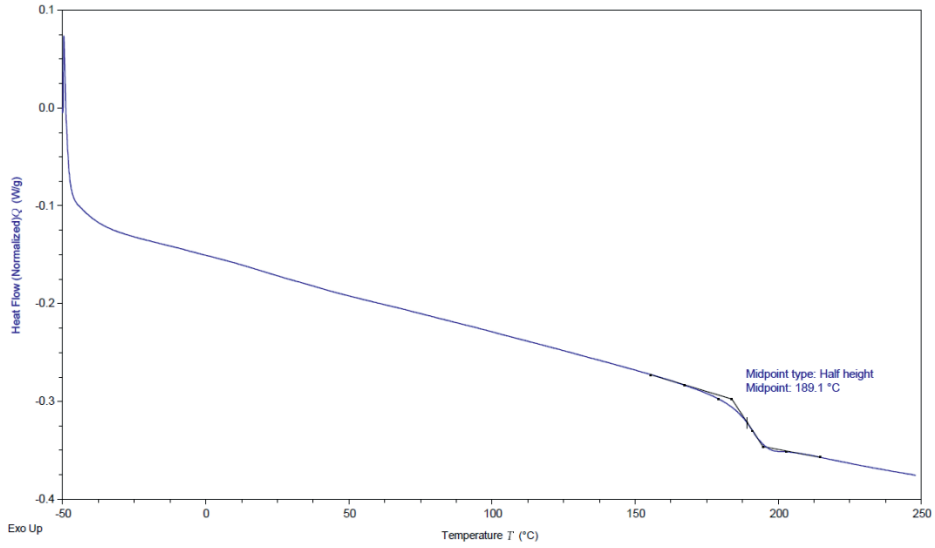

Figure S5: DSC analysis of polyvinylindanone (pVI). Glass transition temperature (T_g) is 189 °C.

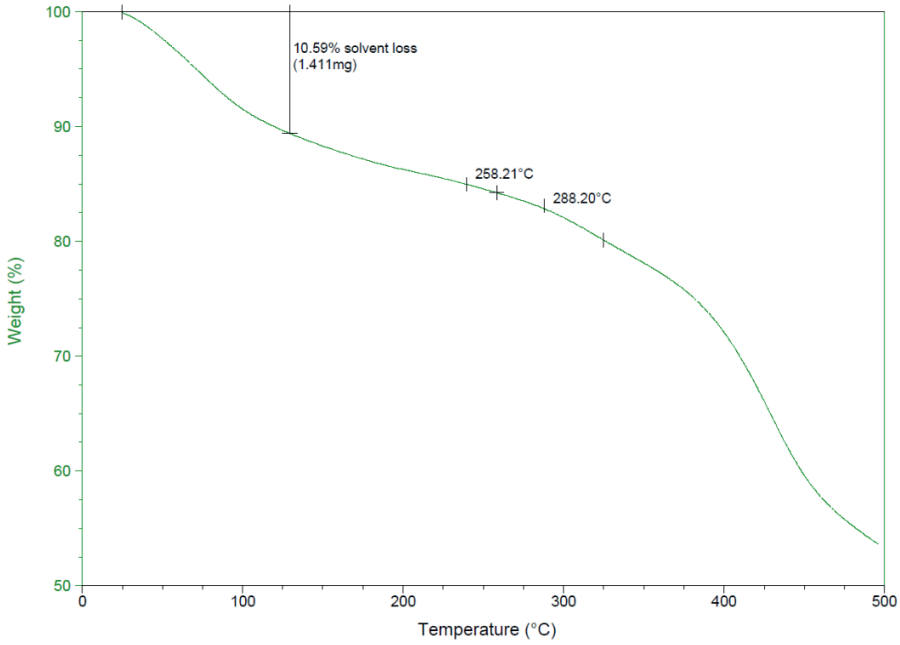

Figure S6: TGA of oxidized polyvinylindanone (pVI-Ox).

7.6 Determination of the maximum binding capacity

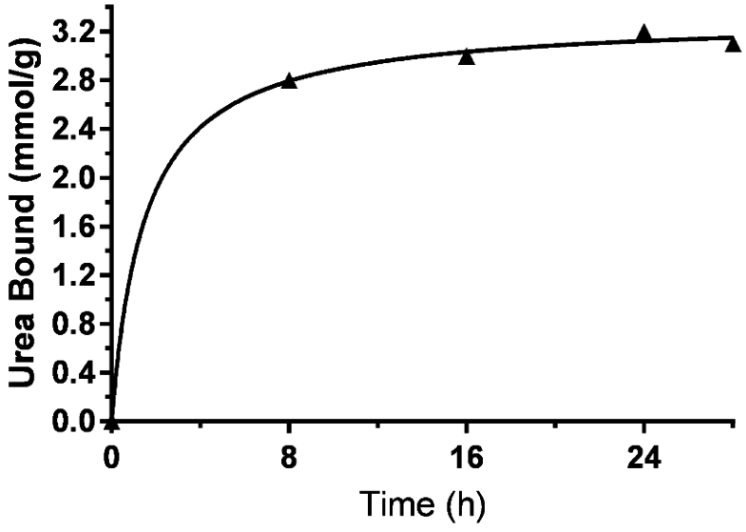

Figure S7: Determination of the maximum binding capacity of pVI-Ox beads. Conditions: beads (50 mg) were incubated in a 50 mM urea solution in PBS (5 mL) at 70 °C in an oven on a rotating device. The urea concentration in the supernatant was determined at different time points. It was found that the urea concentration did not decrease after 24 hours, therefore these conditions were considered sufficient to occupy all ninhydrin groups.

7.7 Urea binding of pVI-Ox beads under static and dynamic conditions.

Table S4: Urea concentration in the supernatant during the incubation of pVI-Ox beads (50 mg) in 30 mM urea in PBS (5 mL) at 37 °C (static conditions).

Time (h)	[Urea] (mM)		Urea bound(mmol/g)
	Duplicate #1	Duplicate #2	
0	30.6	30.5	0
1	29.2	29.8	0.11 ± 0.04
2	27.9	27.7	0.28 ± 0.01
4	27.7	26.0	0.37 ± 0.12
8	23.2	24.4	0.68 ± 0.08
16	18.4	20.3	1.12 ± 0.13
24	15.4	15.8	1.50 ± 0.03

Table S5: Urea concentration in the supernatant during the incubation of pVI-Ox (50 mg) in 30 mM urea in PBS (5 mL) at 50 °C (static conditions).

Time (h)	[Urea] (mM)		Urea bound (mmol/g)
	Duplicate #1	Duplicate #2	
0	29.9	29.4	0
1	28.4	28.6	0.12 ± 0.01
2	27.5	27.8	0.20 ± 0.02
4	24.3	24.1	0.55 ± 0.01
8	19.9	19.8	0.98 ± 0.01
16	15.7	15.7	1.40 ± 0.00
24	13.4	14.0	1.60 ± 0.04

Table S6: Urea concentration in the supernatant during the incubation of pVI-Ox beads (50 mg) in 30 mM urea in PBS (5 mL) at 70 °C (static conditions).

Time (h)	[Urea] (mM)		Urea Removed (mmol/g)
	Duplicate #1	Duplicate #2	
0	30.2	30.0	0
1	23.7	24.0	0.63 ± 0.02
2	20.6	20.1	0.98 ± 0.04
4	17.0	16.7	1.33 ± 0.02
8	12.2	11.8	1.81 ± 0.03
16	8.2	8.2	2.19 ± 0.00
24	6.6	6.9	2.34 ± 0.02

Table S7: Urea concentration in the supernatant during the incubation of pVI-Ox beads (50 mg) in 30 mM urea in PBS (2.5 mL) at 37 °C (static conditions).

Time (h)	[Urea] (mM)		Urea bound(mmol/g)
	Duplicate #1	Duplicate #2	
0	30.1	30.4	0
0.5	30.0	27.9	0.07 ± 0.07
1	27.5	27.4	0.14 ± 0.00
2	26.4	26.3	0.20 ± 0.00
4	23.9	23.2	0.34 ± 0.02
6	23.9	22.3	0.36 ± 0.03
8	21.3	20.4	0.47 ± 0.03

Table S8: Overview of the urea concentration at the different timepoints in the Erlenmeyer during dynamic binding of pVI-Ox beads in PBS at 37 °C. Conditions: 200 mL ~30 mM urea solution in PBS in an Erlenmeyer pumped through (25 mL/min) a sorbent cartridge containing pVI-Ox beads (4.0 g) back into the Erlenmeyer (set-up see figure S9).

Time (h)	[Urea] (mM)		Urea Removed (mmol/g)	
	Duplicate #1	Duplicate #2	Duplicate #1	Duplicate #2
0	31.4	30.6	0	0
0.25	n.d.	30.3	n.d.	0.02
0.5	29.5	29.5	0.09	0.05
1	29.4	28.5	0.10	0.10
2	27.0	26.9	0.22	0.18
4	24.9	24.0	0.32	0.32
6	21.9	21.3	0.47	0.45
8	18.4	18.7	0.64	0.58

7.8. Kinetics of urea binding

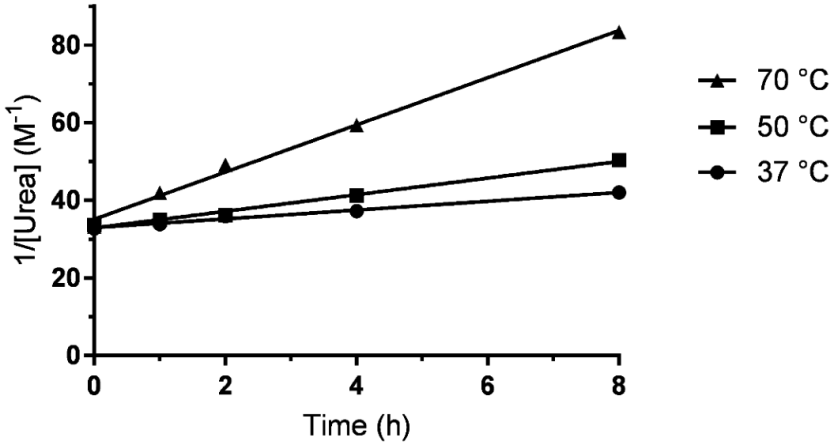

Figure S8: Plot of the inverse urea concentration in time during the reaction of pVI-Ox beads (50 mg) with urea (30 mM) in PBS (5 mL) at different temperatures.

Table S9: Rate constants (k_2) of the reaction of pVI-Ox beads (50 mg) with urea (30 mM) in PBS (5 mL) at different temperatures.

T (°C)	1/T (1/K)	k_2 ($M^{-1}h^{-1}$)	ln (k_2)
37	3.23×10^{-3}	1.1 ± 0.1	0.12
50	3.10×10^{-3}	2.1 ± 0.1	0.76
70	2.92×10^{-3}	6.1 ± 0.3	1.80

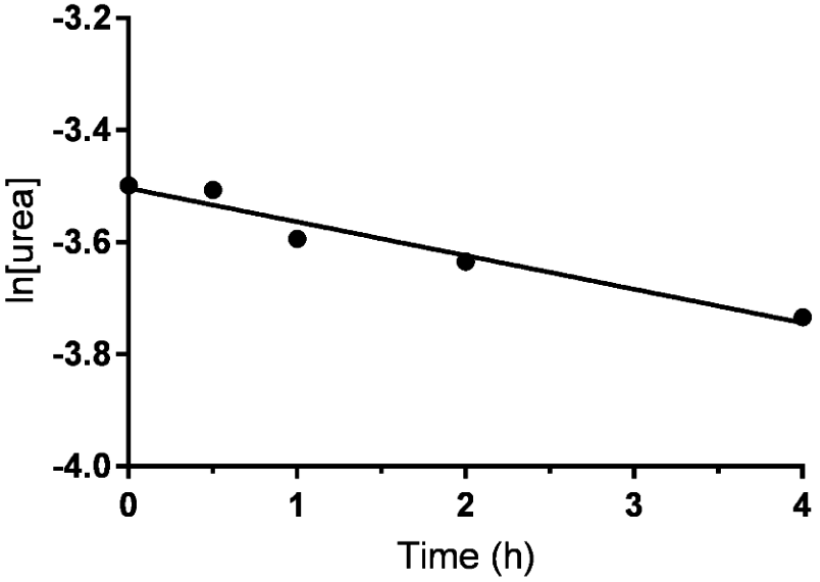

Figure S9: Plot of the natural logarithm of [urea] (M) in time during the reaction of pVI-Ox beads (50 mg, 0.16 mmol ninhydrin groups) with urea (30 mM) in PBS (2.5 mL, thus 0.075 mmol urea) of the first 4 hours at 37 °C. Linear regression gives y = -0.060x – 3.5. Assuming pseudo-first order (PFO) conditions $k_2 = k_{PFO}$/[ninhydrin groups] = 0.060/0.060 = 1.0 ± 0.1 $M^{-1}h^{-1}$.

7.9 Photograph of the set up used for determination of the urea binding by pVI-Ox sorbent beads from under dynamic conditions.

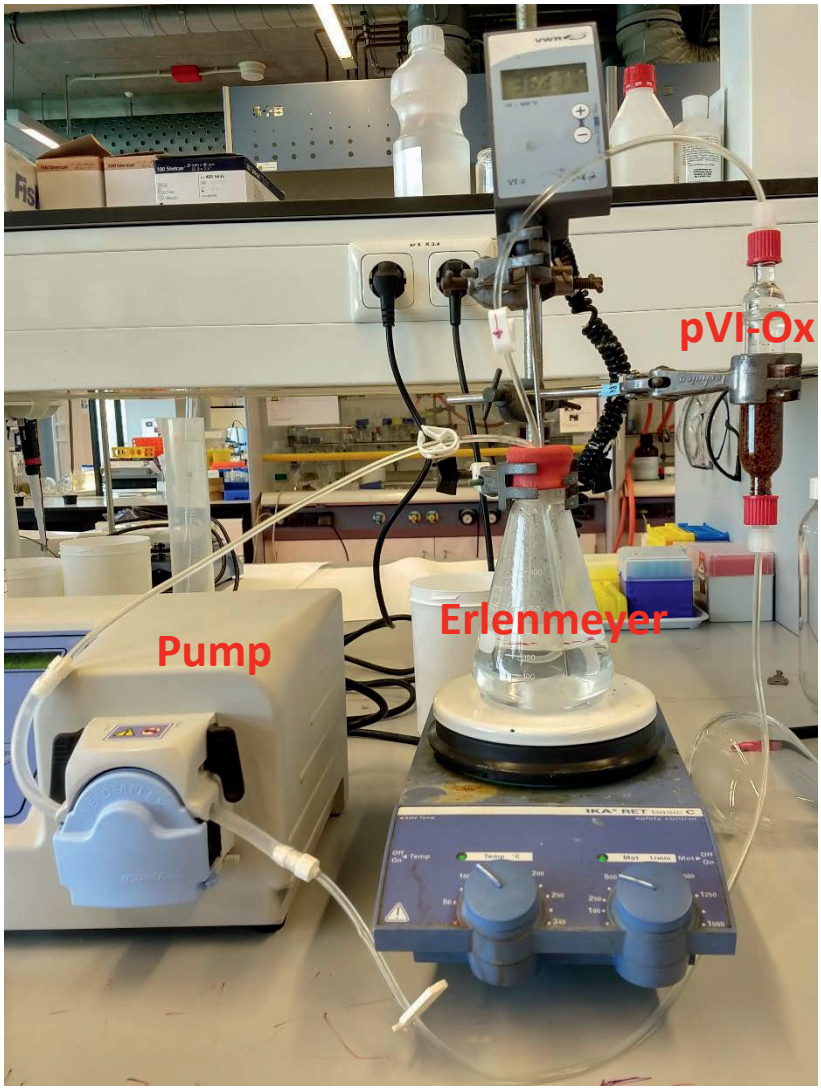

Figure S10: Picture of the experimental set-up determination of the urea binding by pVI-Ox sorbent beads under dynamic conditions with a urea solution in PBS.

7

Chapter 7

Summary and Perspectives

7.1 Summary

The majority of end-stage kidney disease (ESKD) patients is treated with hemodialysis (3 times per week; 4 hours per session) to support kidney function. This treatment has considerable shortcomings, such as inadequate removal of uremic toxins and accumulating fluid in the body, which leads to a poor quality of life and high mortality for ESKD-patients. In addition, because the hemodialysis machine is bulky and uses a large amount of dialysate per treatment (120 L/session), hemodialysis sessions usually take place in a hospital or dialysis center, thereby reducing patient's autonomy and flexibility. To improve autonomy and flexibility of life of ESKD patients, wearable artificial kidney devices are being developed which use a small volume of dialysate that is continuously regenerated by a purification unit and re-used in a closed loop system. It is aimed that patients potentially can use such a device at home (or elsewhere), thereby increasing the frequency and duration of the dialysis treatment. This leads to more adequate removal of uremic toxins and excess fluid. Most toxic solutes present in the dialysate can successfully be removed by physisorption to activated carbon, whereas the concentration of electrolytes can be controlled using ion-exchangers. However urea removal from dialysate is the major challenge in the realization of a wearable dialysis device.

Several strategies for urea removal from dialysate have been explored worldwide, namely enzymatic hydrolysis, electro-oxidation and adsorption or absorption of urea with sorbents. Ideally, the urea removal method for a wearable device 1) is selective, 2) does not generate toxic by-products, 3) is lightweight and 4) has fast urea removal kinetics. In **Chapter 2** the clinical and chemical aspects of the current urea removal strategies are discussed, including their drawbacks and possible solutions to enable application in a wearable dialysis device. The urea removal strategies and their favorable characteristics as well as drawbacks are summarized in table 1.

Table 1: Overview of pro's (+) and con's (-) of current urea removal strategies (from Chapter 2).

Method	*Selectivity*	*Avoidance of formation of toxic by-products*	*Urea removal capacity*	*Urea removal rate*
Enzymatic hydrolysis	+++	--- (ammonium)	+++	+++
Electrochemical decomposition	--	-- (oxidation products e.g. reactive chlorine species)	+	+
Physisorption	-	++	--	++
Chemisorption	-	++	+	--

The covalent binding of urea to sorbents (chemisorption) is a viable strategy to remove urea from dialysate as no toxic side products are formed. However, this method suffers from lack of selectivity and slow urea binding kinetics. This issue of selectivity can be overcome by placing activated carbon upstream of the urea sorbent, which reduces the concentration of competing solutes such as creatinine and amino acids. To overcome the issue of the slow urea removal kinetics, the aim of this thesis was to develop novel polymeric urea sorbents with fast urea removal kinetics, by introducing the highest possible density of highly reactive functional groups in a well-accessible matrix. In **Chapter 1** it is stated that an ideal urea sorbent has the following characteristics:

1) is stable in dialysate.
2) shows fast urea removal kinetics.
3) can be immobilized in a purification unit.
4) selectively reacts with urea.
5) is sterilizable.
6) The binding with urea is irreversible in dialysate and reversible under non-physiological conditions, meaning that the sorbent is regenerable.

For the structural design of a sorbent with these characteristics, we considered to develop polymers with a **carbon-carbon backbone**, because these bonds are very stable and easily obtained by free radical polymerization of monomers with a carbon-carbon double bond. Such double bonds should be introduced in the (precursor of) a urea reactive group to obtain the desired functional monomer, *e.g.* a vinyl substituted indanone (precursor for ninhydrin). To identify ninhydrin derivatives with a high reactivity for urea, the effect of electron withdrawing and donating substituents on ninhydrin on the kinetics of the reaction with urea was studied in **Chapter 3**. We found that ninhydrin without substituent has the highest reactivity with urea. Ninhydrin-derivatives bearing electron-withdrawing substituents showed very low reactivity towards urea. Free energy calculations on the intermediate reaction products of the reaction of ninhydrin-derivatives with urea showed that the dehydration of ninhydrin-derivatives is an essential step in the overall reaction, which is very sensitive to electronic effects of the substituent, and greatly influences the overall kinetics of the reaction of ninhydrin-derivatives with urea. Ninhydrin-derivatives bearing an **electron donating group** (EDG, such as an aliphatic group) on the aromatic ring showed intermediate reactivity. We observed that such EDG is best positioned on the **5-position** of the aromatic group (figure 1).

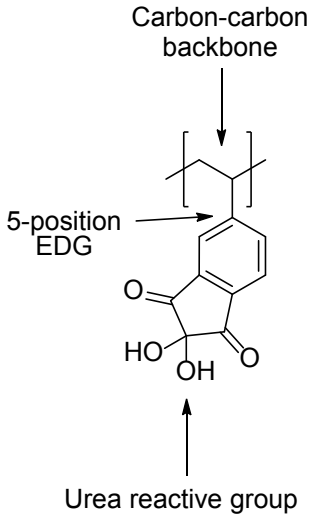

Figure 1: Structural design of a ninhydrin-type urea sorbent

In principle, besides ninhydrin, several other (hydrates of) carbonyl compounds could be candidates for the urea-reactive functional groups in a sorbent. Therefore, we systematically quantified the reactivity of urea with 31 different carbonyl compounds in **Chapter 4,** by determining the rate constant (*k*-value) of the reaction under conditions representative for dialysate regeneration. The (hydrates of) the carbonyl compounds triformylmethane, ninhydrin and phenylglyoxaldehyde were found to be the most reactive towards urea, and therefore these structures are suitable candidates for incorporation in a urea sorbent figure 2).

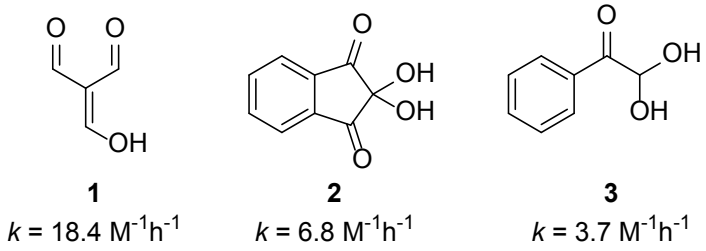

1 k = 18.4 $M^{-1}h^{-1}$ **2** k = 6.8 $M^{-1}h^{-1}$ **3** k = 3.7 $M^{-1}h^{-1}$

Figure 2: Structures of urea-reactive compounds: triformylmethane (**1**), ninhydrin (**2**) and phenylglyoxaldehyde (**3**).

To understand why these compounds show high reactivity towards urea whereas no reaction was observed for structurally related compounds, the free energies of the hydrated compounds, the dehydrated reactive compounds and the reaction intermediates were calculated. We found that the hydration and dehydration of the carbonyl groups are important for the overall reactivity towards urea.

With the optimal structures for the urea sorbent established, we synthesized two of the corresponding monomers that, after polymerization and an oxidation step, yield sorbents with phenylglyoxaldehyde (**Chapter 5**) and ninhydrin groups (**Chapter 6**),

respectively, in the highest possible density. The conditions for the polymerization reaction were selected such that spherical beads were obtained with particle size > 100 µm, which allows easy immobilization in a sorbent cartridge with minimal pressure building up in the dialysate circuit.

In **Chapter 5** we reproduced an existing method to obtain a phenylglyoxaldehyde-type sorbent from styrene in three steps; polymerization of styrene, acetylation of the aromatic ring in polystyrene and oxidation of the acetyl group. In addition, we explored a new route to obtain a phenylglyoxaldehyde-type sorbent from vinylphenylethanone in two steps; polymerization of vinylphenylethanone and oxidation of the acetyl groups (scheme 1). Because vinylphenylethanone already contains the acetyl group, polymerization of this monomer leads to an optimal acetyl content, eventually leading to a higher phenylglyoxaldehyde content.

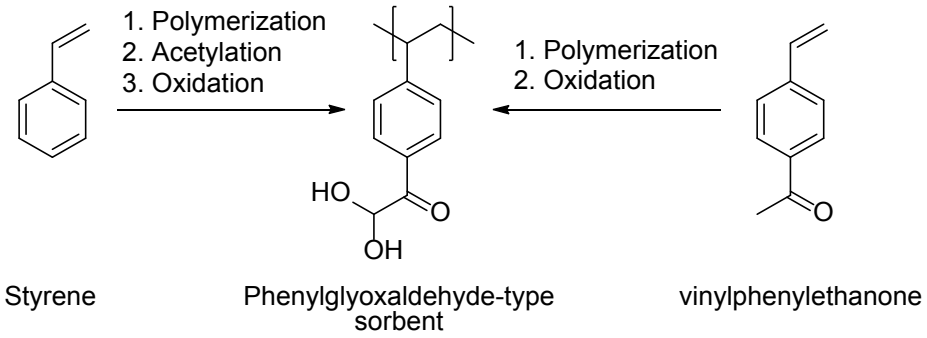

Scheme 1: Two routes to obtain phenylglyoxaldehyde-type sorbents as described in chapter 5.

Spherical polymeric beads (with average size of 0.54 ± 0.11 mm for styrene and 0.77 ± 0.20 mm for polyvinylphenylethanone) were obtained by performing a suspension polymerization. For both routes we established the structures of the side products formed during the post-polymerization modification steps, the phenylglyoxaldehyde content, and the maximum urea binding capacity. Solid-state ^{13}C NMR and IR analysis of the sorbents showed side-products of the oxidation, *i.e.* over-oxidation (PGOA formation) and crosslinking (aldol condensation of an acetyl group with a PGA-group) at high densities of acetyl groups. Theoretically, if these side reactions could be fully suppressed, this could lead to sorbents with a PGAH content of 5.5 mmol/g (including 2.5% crosslinker). However, it is unlikely to obtain quantitative conversion into PGAH due to these side reactions. In addition, the urea binding capacity of PGAH sorbents is lower than expected based on the PGAH content because PGAH and urea react both in a 1:1 (43%) and 2:1 (57%) ratio.

The urea sorption kinetics from simulated dialysate for both sorbents under static conditions were compared. It was observed that the sorbents based on vinylphenylethanone had higher urea binding capacities than the sorbents based on styrene (1.8-2.2 mmol/g *vs.* 1.4-1.8 mmol/g) due to the higher PGAH content

(~50% *vs.* ~40%) and thus removed more urea from simulated dialysate in 8 h (0.5-0.6 mmol/g *vs.* 0.4-0.5 mmol/g).

Chapter 6 describes a novel route to obtain a urea sorbent containing ninhydrin groups, by selecting vinylindanone as the monomer (scheme 2). Two synthetic routes were explored to obtain this monomer of which one route yielded this monomer on a 500 gram scale. The suspension polymerization of vinylindanone was optimized in terms of surface area and the synthesis was scaled up to 50 gram. The resulting beads with an average size of 0.74 ± 0.31 mm were oxidized to convert indanone into ninhydrin groups. According to quantitative solid state ^{13}C-NMR, 74% of the aromatic groups were converted into ninhydrin groups, resulting in sorbent beads with unprecedented high urea binding capacity of 3.2 mmol/g. The ninhydrin sorbent removed ~0.6-0.7 mmol/g urea in 8 hours at 37 °C from simulated dialysate under static conditions when urea and ninhydrin were in a 1:1 molar ratio. Under dynamic flow conditions in which the ninhydrin groups were in 2:1 excess as compared to urea, the ninhydrin-type sorbent removed a slightly lower amount of urea (~0.6 mmol/g) in 8 hours at 37 °C from simulated dialysate, which means that ~600-700 grams of ninhydrin-type sorbent is needed to remove the daily urea production of a dialysis patient.

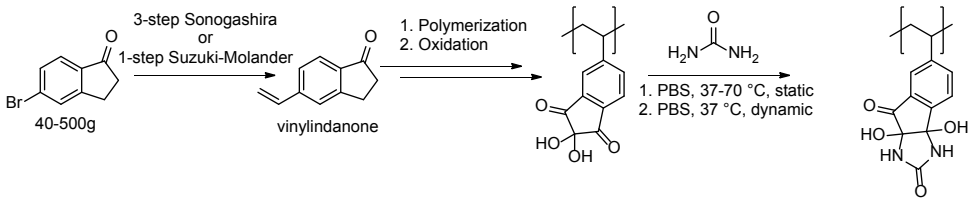

Scheme 2: The synthesis and evaluation of ninhydrin-type sorbents from 5-vinyl-1-indanone.

7.2 Perspectives

7.2.1. Evaluation of the sorbents presented in this thesis

In both section 1.4 and 7.1 it is stated that an ideal urea sorbent for regeneration of dialysate should apply to the six main criteria listed. In table 2 the sorbents described in **Chapter 5** and **Chapter 6** are assessed for these criteria that are further discussed below.

Table 2: Criteria of a urea sorbent.

#	Criteria	Phenylglyoxaldehyde-type sorbents (**Chapter 5**)	Ninhydrin-type sorbents (**Chapter 6**)
1	Stable in dialysate	Yes (assumed)	Yes (assumed)
2	Fast urea removal kinetics	~0.6 mmol/g (8h at 37 °C)	~0.6-0.7 mmol/g (8h at 37 °C)
3	Beads with size > 100 µm	Yes	Yes
4	Selective for urea	No	No
5	Sterilizable	Yes (assumed)	Yes (assumed)
6	Reversible reaction with urea under acidic or alkaline conditions	No	Yes

7.2.1.1. Stability

Both the phenylglyoxaldehyde- and the ninhydrin-type sorbents are synthesized via a free-radical polymerization of vinyl-group containing monomers and thus contain a carbon-carbon backbone which are generally very stable and are not expected to hydrolyze or decompose in dialysate. Assuming that the sorbents are properly washed, thereby removing residual initiator, solvents, monomers and other reagents, these sorbent should theoretically not leach toxic components into the dialysate. However this needs to be verified experimentally.

7.2.1.2. Urea removal kinetics

As for the urea removal kinetics, the aim was to develop a material that removes at least 2.0 mmol/g in 8 hours at 37 °C, to enable removing the daily urea production (400 mmol) of a dialysis patient by just 200 grams of material or less. We observed binding capacities of up to 2.2 mmol/g for the phenylglyoxaldehyde type sorbent and 3.2 mmol/g for the ninhydrin-type sorbents. Although we did not reach the theoretical maximum binding capacity of 5.6 and 4.9 mmol/g, respectively, both are superior to sorbents reported in literature. However, the problem is that only 20-30% of the binding capacity is reached in 8 hours at 37 °C. As a consequence, both the phenylglyoxaldehyde- and ninhydrin-type sorbents removed ~0.6 mmol/g at that time and temperature, which would mean that 600-700 gram of material is needed to remove the daily urea production of a dialysis patient. It can be argued that macroporous beads or beads that swell in aqueous solution increase the accessibility of the urea reactive groups, and would therefore solve this problem. However, we found similar binding capacities for a sorbent with surface area of 2.0 m^2/g, a sorbents with surface area <0.05 m^2/g (**Chapter 5**), which suggests that these sorbents swell to a minor extent in aqueous solution and that therefore the accessibility of the urea-reactive groups is not the limiting factor in the urea removal kinetics.

We recently found that beads that were ground to smaller size particles (500 nm - 63 µm) showed faster urea binding kinetics (2.0 mmol/g *vs.* 1.3 mmol/g in 4 hours

at 70 °C, respectively) but ultimately reached the same maximum binding capacity. As the kinetics of chemisorption are concentration dependent, an explanation for the slower urea removal kinetics of the unground beads is a lower local urea concentration inside the beads than outside because of the longer diffusion path. Although a decrease in bead size leads to faster urea removal kinetics, smaller particles increase the flow resistance across the packed bead column and lead to higher pressure drop across the column, which is unwanted. In future research it is recommended to investigate which bead size is optimal in terms of size and an acceptable pressure drop. In **Chapter 6** it is shown that an increase of the temperature substantially increases the rate of the urea removal. Therefore, a method to increase the urea binding kinetics is to heat the dialysate and sorbent, and cool it with a heat-exchanger before returning to the dialyzer. To what extent heating of the dialysate is feasible needs to be confirmed experimentally, as a higher temperature may lead to denaturation of (low molecular weight) proteins in the dialysate, which is highly unwanted.

7.2.1.3. Immobilization of the sorbent

We considered polymeric beads because of ease of immobilization in a sorbent cartridge by simply applying a filter which prevents the beads from leaving based on the pores of the filter. However, the flow of dialysate through a packed bed of sorbent beads leads to a pressure drop according to the Kozeny-Carman equation, depending on the size of the beads and the flowrate (see Chapter 1 equation 1). It was estimated that beads with size > 200 µm are needed to limit this pressure drop. The sorbent beads in this thesis are synthesized via a suspension polymerization, which usually yields beads with high polydispersity. For this reason we aimed for an average diameter of ~300 µm, thus giving only a relative small fraction of beads with a diameter < 100 µm, which was removed by sieving over a 100 µm sieve. Thereby a high yield of the polymerization reaction is maintained and the size of all sorbent particles presented in **Chapter 5** and **Chapter 6** have an average diameter >300 µm. However whether this indeed limits the pressure drop needs to be determined experimentally.

7.2.1.4. Selectivity

As discussed in **Chapter 2**, a drawback of carbonyl-hydrate sorbents is that they are not selective. Because urea is a very weak nucleophile, other nucleophiles such as creatinine and amino acids could compete for the ninhydrin groups, effectively reducing the binding sites for urea. In a preliminary experiment there are indications that creatinine can be removed from dialysate by activated carbon, therefore placing activated carbon upstream would avoid competition from this solute. However, preliminary results also showed that a portion of the amino acids passes the activated carbon filter and reacts with the ninhydrin groups in the urea

sorbent column, indicated by a change in color of the sorbent from brown to purple (figure 3A-C), characteristic for the reaction between ninhydrin and amino acids as shown in **Chapter 3**. Using larger amounts of activated carbon may completely remove these competing solutes, but further experiments are needed. It can be argued whether loss of urea binding sites due to reaction with amino acids will be an issue in clinical reality because the concentration of these competing solutes is much lower than the urea concentration ([creatinine] = ~1 mM, [amino acids] = ~5 mM). Further, the amount of urea removed in 8 hours at 37 °C was not significantly reduced due to this competition as the ninhydrin groups are in present large excess.

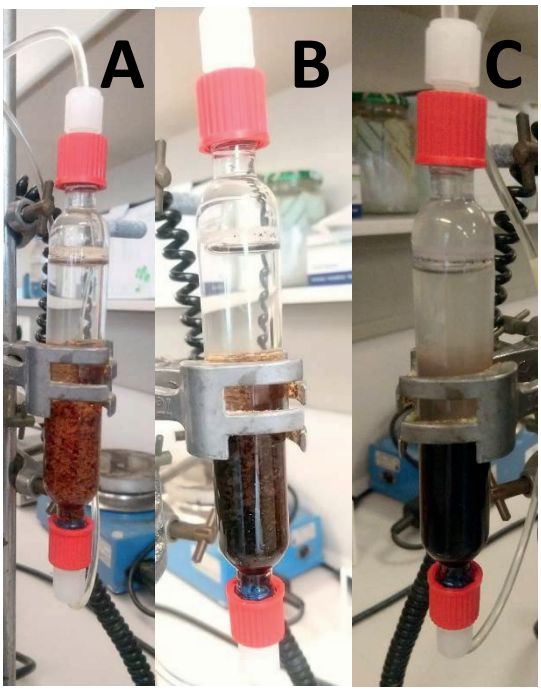

Figure 3: A) Urea sorbent (brown) before reaction with amino acids. B) Urea sorbent (brown/purple) during reaction with amino acids. C) Urea sorbent (purple/black) after reaction with amino acids.

As discussed in **Chapter 2**, one potential method to obtain selective urea sorbents is molecular imprinting. In unpublished work (manuscript in preparation) we attempted to obtain selective molecular imprinted polymers able to adsorb urea based on hydrogen-bonds, dipole interactions and shape recognition. We found that these sorbents were able to adsorb urea from non-aqueous solution (acetonitrile) but unable to remove urea from aqueous solution most likely due to the competition with water. Further, we attempted to molecularly imprint ninhydrin-type sorbents able to recognize and bind urea via covalent bonds instead of hydrogen bonds. Therefore, we synthesized vinyl-ninhydrin and its isomeric reaction products with urea (figure 4), and polymerized these monomers to obtain the non-molecular imprinted polymer (NIP) and the corresponding molecular imprinted polymer (MIP),

respectively. The idea was that the MIP, after removal of the urea template (see section 7.2.1.6.), contains a specific reactive cavity for urea in the polymeric matrix and thereby reacts more selectively with urea than the NIP. However, preliminary results indicated that the imprinting was unsuccessful.

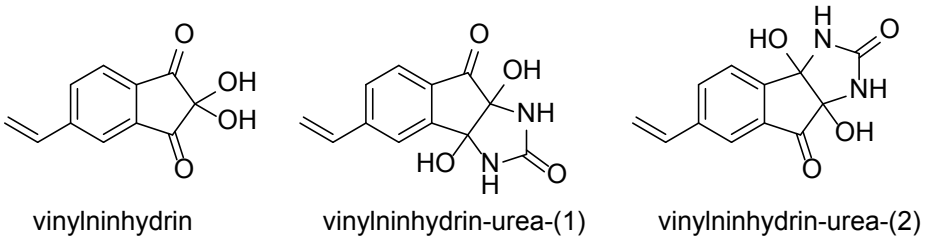

Figure 4: Structures of vinylninhydrin and the corresponding reaction products with urea.

7.2.1.5. Sterilizable

Although the sterilization of the sorbents described in **Chapter 5** and **Chapter 6** of this thesis was not been investigated, it is reported that ninhydrin-type sorbents based on polystyrene have been successfully sterilized by gamma-radiation without loss of their function. Because these reported sorbents are, in structure and morphology, very similar to the sorbents described in **Chapter 5** and **Chapter 6**, we assume that these sorbents can be sterilized as well via gamma-radiation, however this needs to be confirmed experimentally. In addition, other sterilization processes can be explored such steam sterilization or dry heating.

7.2.1.6. Regeneration

Ideally the reaction of urea with the sorbents can be reversed and thus the sorbents can, after use, be regenerated which potentially reduces the cost of production. In **Chapter 4,** the mechanism of the reaction of phenylglyoxaldehyde and urea was elucidated. Elimination of water after the 1:1 reaction yielded a tautomeric equilibrium product of which one is aromatic, therefore this reaction is most likely irreversible. Moreover, as determined in **Chapter 4** and **Chapter 5**, phenylglyoxaldehyde and urea can react also in a 2:1 ratio within the beads, and since a carbon-carbon bond is formed in the formation of the 2:1 adduct, this reaction is also most likely irreversible and limiting the possibilities for regeneration.

In principle, the reaction between ninhydrin and urea is an equilibrium, which lies predominantly at the ninhydrin-urea adduct side at physiological pH and temperature. In unpublished work (manuscript in preparation) we found that this equilibrium is shifted to the ninhydrin and urea side by very strong acids that hydrolyze the acid-labile hemi-aminal bonds in the ninhydrin-urea adduct. We were able to regenerate ninhydrin-type sorbents to up to 93% of the original binding capacity by washing with 6 M perchloric acid at 70 °C for 4×2 hours. This means that

regeneration of ninhydrin-based sorbent beads is in principle possible.

As discussed in section 7.2.1.4, the ninhydrin-type sorbents are not selective and we found that these sorbents also react with amino acids present in spent dialysate (visible as the sorbent turned purple in time). Since the reaction of amino acid with urea includes a decarboxylation step (see scheme 1 in **Chapter 3**), it is highly unlikely that this reaction is reversible and the binding capacity will be (if amino acids are not completely removed by activated carbon) further reduced after each use and regeneration cycle, which makes the regeneration of the ninhydrin sorbent less attractive.

7.2.1.7. Final Evaluation

As shown in table 2 and discussed above, the two types of sorbents described in this thesis have similar characteristics in terms of stability, urea removal kinetics, morphology, selectivity and can very likely be sterilized. Because the reaction of ninhydrin-type sorbents with urea can be reversed under strong acidic conditions, in theory this material could be re-used and would therefore be more cost-effective. However, as strong acid and high temperature (6M perchloric acid and 70 °C) are needed to (partially) regenerate this sorbent the logistics of the regeneration seem troublesome. To explain, the sorbents need to be transferred to a laboratory, undergo the regeneration process followed by washing and sterilization and finally be transferred back to the patient before they can be re-used again. Therefore this advantage is probably not more cost-effective than the use of a disposable sorbent cartridge. From this point of view, the phenylglyoxaldehyde-type sorbents are probably the most cost-effective as reasonable binding capacities and urea removal kinetics are obtained with the phenylglyoxaldehyde-type sorbents based on styrene, which is very cheap starting material. In addition, phenylglyoxaldehyde-type sorbents based on styrene still have room for improvement as the conditions for the Friedel-Crafts acetylation and Kornblum oxidation can probably be optimized, which might lead to a higher PGA densities and thus higher urea binding capacity. As the maximum binding capacity of phenylglyoxaldehyde-type sorbents are ~4 mmol/g (when side reactions would be fully suppressed) and ~30% of the maximum binding capacity is reached in 8 hours at 37 °C (**Chapter 5**), phenylglyoxaldehyde type sorbents can theoretically remove up to 1.2 mmol/g in 8 hours, thereby reducing the amount of sorbent needed to remove the daily urea production to 300-350 g.

7.2.2. Future urea sorbents with increased urea removal kinetics and high binding capacities

7.2.2.1 Triformylmethane-type sorbents

One of the findings in **Chapter 4** was that triformylmethane (TFM) is the carbonyl

compound with the highest reactivity towards urea among the carbonyl compounds that were tested. In addition, we found that TFM not only reacts very efficiently with urea, but also with water and with itself. The reaction between TFM and urea finally yields an enamine, therefore the keto-enol equilibrium between the aldehyde and the central carbon is most likely necessary for its reactivity towards urea (scheme 3). Therefore, in order to incorporate TFM-structure in a sorbent, only an aldehyde group would be available for functionalization to a polymeric backbone. We have tried several approaches to obtain the (methyl acetal protected) TFM-structure in a monomer or polymer by functionalizing the aldehyde group into a ketone or amide. Unfortunately so far we were not able to isolate a stable monomer or a polymer containing the TFM structure and further investigation is needed how/whether TFM-type sorbents can be obtained.

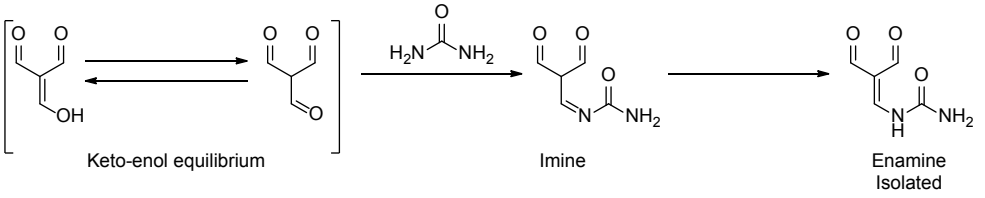

Scheme 3: Reaction of triformylmethane with urea.

7.2.3. Are covalent sorbents suitable for urea removal in a wearable artificial kidney?

The results presented in thesis show that covalent sorbents are promising as only 600-700 grams are needed to remove the daily urea production of a patient at 37 °C in 8 hours. However, to assess whether these urea removal kinetics are sufficient for regeneration of dialysate we encounter the following challenge: Ideally, the urea concentration in the dialysate is reduced to a large extent by a single pass through the urea sorbent column (*e.g.* ≥ 75% at a dialysate flow of 100 mL/min), thus obtaining a urea reduction ratio of a dialysis session (*i.e.* ($[urea]_{before}$-$[urea]_{after}$)/$[urea]_{before}$) of ≥ 0.65 . The urea reduction across the column is dependent on many factors (*e.g.* the amount of sorbent present in the column and the flow rate of the dialysate passing though the column). We found very low urea reduction across the sorbent column ((~0-5%) in our dynamic experiments in **Chapter 6** in our down-scaled set-up (4.0 grams sorbent, dialysate flow 25 mL/min, urea concentration ~30 mM upstream of the sorbent), but this may be due to the relatively low amount of sorbent as compared to the urea supply to the sorbent. We do not know how this translates to a more representative scale for regeneration of dialysate (700 gram sorbent, 100-300 mL/min (for a miniature dialysis device), dialysate [urea] decreasing from ~20-30 mM to ~5-10 mM during a dialysis session). Therefore the influence of dialysate flow rate, the urea supply to the sorbent and the amount of sorbent needs to be further investigated in order to determine the potential of these sorbents in the regeneration of dialysate.

The work in this thesis describes the bottom-up development of urea sorbent based on phenylglyoxaldehyde and ninhydrin, in which first the kinetics of the reaction of urea with compounds with carbonyl groups as well as the structures of formed adducts were studied. Subsequently, the obtained insights were used for the rationale design of urea sorbents. Although phenylglyoxaldehyde- and ninhydrin-type sorbents for urea removal from dialysate were reported in literature, the kinetics of the urea removal were considered too slow. In the present thesis, the fundamental principles of the urea removal exploiting covalent sorbents were investigated, and thus the obstacles that should be overcome to improve the urea removal kinetics and binding capacities have been identified. The sorbents presented in this thesis show improvements in terms of kinetics and maximum binding capacity over the sorbents reported in literature and it is established that the kinetics can be further increased by decreasing the diameter of the beads or by increasing the density of urea-reactive groups or the temperature of the dialysate. This offers more than sufficient opportunities to further optimize the sorbents identified in this thesis for application in a wearable artificial kidney which will contribute to the quality of life of ESKD patients.

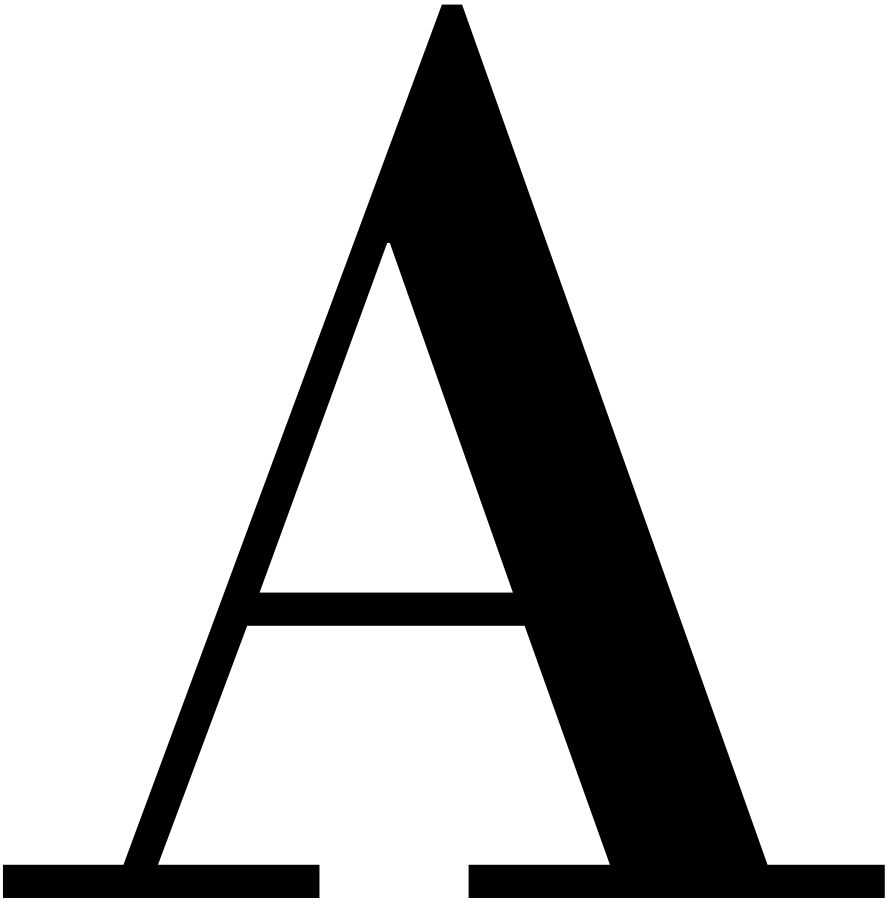

Appendices

Nederlandse Samenvatting
Curriculum Vitae
List of publications
Acknowledgements

Nederlandse Samenvatting

Veel patiënten met chronisch nierfalen wordt behandeld met hemodialyse (3 keer per week; 4 uur per sessie) om de nierfunctie te ondersteunen. Deze behandeling heeft aanzienlijke tekortkomingen, zoals beperkte verwijdering van uremische toxines en overtollige vloeistof in het lichaam, wat leidt tot een slechte kwaliteit van leven en hoge mortaliteit voor nierpatiënten. Omdat de hemodialysemachine omvangrijk is en een grote hoeveelheid dialysaat per behandeling gebruikt (120 L / sessie), vinden hemodialysesessies meestal plaats in een ziekenhuis of dialysecentrum, wat de autonomie en flexibiliteit van de patiënt vermindert. Om de autonomie en flexibiliteit van het leven van nierpatiënten te verbeteren, wordt er gewerkt aan de ontwikkeling van draagbare dialyseapparatuur die een relatief kleine hoeveelheid dialysaat gebruikt dat continu wordt geregenereerd door een zuiveringseenheid en opnieuw wordt gebruikt binnen een gesloten systeem. Het doel is dat patiënten een dergelijk apparaat thuis (of elders) kunnen gebruiken, waardoor zowel de frequentie als de duur van de dialysebehandeling toeneemt. Dit leidt tot een adequatere verwijdering van uremische toxines en overtollig vocht. De meeste stoffen die aanwezig zijn in het dialysaat kunnen met succes worden verwijderd door fysisorptie aan actieve kool, en de concentratie van elektrolyten kan worden gereguleerd met behulp van ionenwisselaars. De verwijdering van ureum uit dialysaat is echter de grootste uitdaging bij het realiseren van een draagbaar dialyseapparaat.

Er zijn verschillende strategieën voor ureumverwijdering uit dialysaat onderzocht: enzymatische hydrolyse, elektro-oxidatie en adsorptie of absorptie van ureum met absorbentia. Ideaal gezien is de ureumverwijderingsmethode voor een draagbaar apparaat 1) selectief, 2) zonder vorming van toxische bijproducten, 3) licht in gewicht en 4) snel in kinetiek. In **Hoofdstuk 2** worden de klinische en chemische aspecten, voor- en nadelen van de huidige ureumverwijderingsstrategieën besproken, en mogelijke oplossingen gegeven om deze methoden toepasbaar te maken in een draagbaar dialyse-apparaat.

Het voordeel van covalente binding van ureum aan absorbentia (chemisorptie) voor ureumverwijdering uit dialysaat is dat er geen toxische bijproducten worden gevormd. Deze strategie heeft als nadeel dat de verwijdering van ureum langzaam en niet selectief is. Deze kwestie van selectiviteit kan vermoedelijk worden opgelost door actieve kool stroomopwaarts van het absorbens te plaatsen, wat de concentratie van concurrerende opgeloste stoffen zoals creatinine en aminozuren vermindert. Om het probleem van de langzame ureumverwijderingskinetiek op te lossen, was het doel van het werk beschreven in dit proefschrift om nieuwe polymere absorbentia met snelle ureumverwijderingskinetiek te ontwikkelen, door ureum-reactieve groepen in een hoge dichtheid in een goed toegankelijke matrix te plaatsen. In **Hoofdstuk 1** wordt vermeld dat een ideaal absorbens voor ureum de

volgende kenmerken heeft:

1) is stabiel in dialysaat.
2) heeft een snelle ureumverwijderingskinetiek.
3) kan worden geïmmobiliseerd in een zuiveringseenheid.
4) reageert selectief met ureum.
5) is steriliseerbaar.
6) De binding met ureum is onomkeerbaar in dialysaat en omkeerbaar onder niet-fysiologische omstandigheden, wat betekent dat het sorptiemiddel regenereerbaar is.

Voor het structurele ontwerp van een absorbens voor ureum met deze kenmerken hebben we besloten polymeren te ontwikkelen met een koolstof-koolstofketen, omdat deze bindingen zeer stabiel zijn en gemakkelijk worden verkregen door vrije radicaalpolymerisatie van monomeren met een dubbele koolstof-koolstofbinding. Het gewenste functionele monomeer bevat een dergelijke dubbele binding en (de voorloper van) een ureumreactieve groep, bijvoorbeeld een vinylgesubstitueerde indanon (voorloper van ninhydrine). Om ninhydrine-derivaten met een hoge reactiviteit voor ureum te identificeren, werd het effect van elektronen-zuigende en -donerende substituenten op ninhydrine op de kinetiek van de reactie van ninhydrine met ureum onderzocht in **Hoofdstuk 3**. We vonden dat ninhydrine zonder substituent de hoogste reactiviteit heeft met ureum. Ninhydrine-derivaten met elektronenzuigende substituenten vertoonden een zeer lage reactiviteit ten opzichte van ureum.

Vrije-energie berekeningen aan de startmaterialen en (tussen)reactieproducten van de reactie van ninhydrine-derivaten met ureum hebben aangetoond dat de dehydratatie van ninhydrine-derivaten een essentiële stap is in de algehele reactie. Ook bleek deze dehydratatiestap zeer gevoelig voor elektronische effecten van de substituent, en dat deze stap de algehele kinetiek sterk beïnvloedt. Ninhydrine-derivaten die een elektrondonerende groep (EDG, bijvoorbeeld een alifatische groep) bevatten vertoonden een minder verlaagde reactiviteit dan ninhydrine-derivaten met een electronzuigende groep. We hebben vastgesteld dat een dergelijke EDG het best op de 5-positie van de aromatische groep wordt geplaatst (figuur 1).

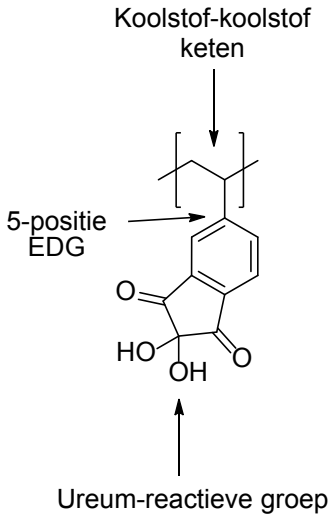

Figuur 1: Het structurele ontwerp van een ninhydrine-type ureum absorbens.

In principe zijn naast ninhydrine ook andere (hydraten van) carbonylverbindingen potentiele ureum-reactieve functionele groepen die kunnen dienen als ureum binders in ureum absorbentia. Daarom kwantificeerden we systematisch de reactiviteit van ureum met 31 verschillende carbonylverbindingen in **Hoofdstuk 4**, door de snelheidsconstante (*k*-waarde) van de reactie te bepalen onder omstandigheden die representatief zijn voor dialysaatregeneratie. De (hydraten van) de carbonylverbindingen triformylmethaan, ninhydrine en fenylglyoxaldehyde bleken het meest reactief met ureum, en daarom zijn deze structuren geschikte kandidaten als functionele groepen in ureum absorbentia (figuur 2).

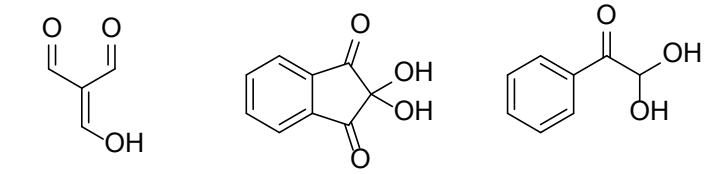

1 k = 18.4 $M^{-1}h^{-1}$ **2** k = 6.8 $M^{-1}h^{-1}$ **3** k = 3.7 $M^{-1}h^{-1}$

Figuur 2: De structuren en snelheidsconstantes van de ureum-reactieve verbindingen: triformylmethaan (**1**), ninhydrine (**2**) en fenylglyoxaldehyde (**3**).

Om te begrijpen waarom deze verbindingen een hoge reactiviteit vertonen met ureum, terwijl er geen reactie werd waargenomen voor structureel verwante verbindingen, werden de vrije energieën berekend van de gehydrateerde verbindingen, de niet-gehydrateerde carbonylverbindingen en de tussenproducten berekend. We vonden dat de hydratatie en dehydratatie van de carbonylgroepen

belangrijk zijn voor de algehele reactiviteit ten opzichte van ureum.
Met de meest reactieve carbonylverbindingen met ureum vastgesteld, was de volgende stap de synthese van twee van de overeenkomstige monomeren die, na polymerisatie en een oxidatiestap, ureum-adsorbentia opleveren met respectievelijk fenylglyoxaldehyde (**Hoofdstuk 5**) en ninhydrine-groepen (**Hoofdstuk 6**). De omstandigheden voor de polymerisatiereactie werden zodanig gekozen dat bolvormige parels werden verkregen met een deeltjesgrootte > 100 µm, hetgeen gemakkelijke immobilisatie mogelijk maakt in een zuiveringseenheid met minimale drukopbouw in het dialysaatcircuit.

In **Hoofdstuk 5** hebben we een bestaande methode gereproduceerd om een fenylglyoxaldehyde-type absorbens uit styreen te verkrijgen in drie stappen; polymerisatie van styreen, acetylering van de aromatische groep in polystyreen en oxidatie van de acetylgroep. Daarnaast hebben we een nieuwe twee-stapsroute vanuit vinylfenylethanon onderzocht om een fenylglyoxaldehyde-type absorbens te verkrijgen; polymerisatie van vinylfenylethanon en oxidatie van de acetylgroep (schema 1). Omdat vinylfenylethanon al de acetylgroep bevat, leidt polymerisatie van dit monomeer tot een optimaal acetylgehalte, wat uiteindelijk leidt tot een hoger fenylglyoxaldehydegehalte.

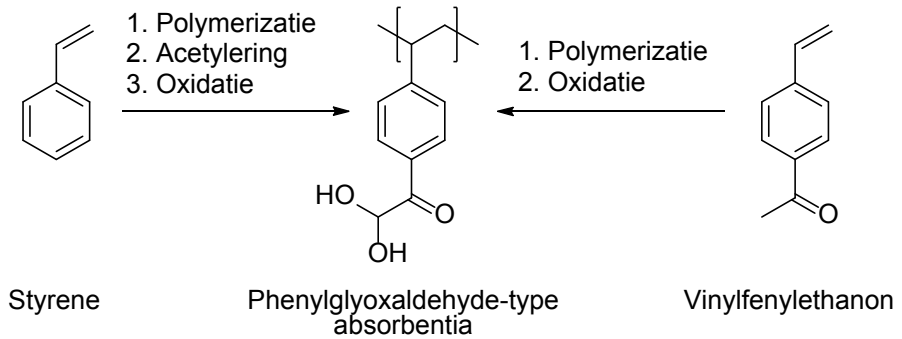

Schema 1: Twee routes om fenylglyoxaldehyde-type absorbentia te verkrijgen zoals beschreven in **Hoofdstuk 5**.

Sferische polymere parels (met een gemiddelde grootte van 0,54 ± 0,11 mm voor styreen en 0,77 ± 0,20 mm voor polyvinylfenylethanon) werden verkregen door een suspensiepolymerisatie uit te voeren. Voor beide routes hebben we de structuren van de bijproducten (die gevormd worden tijdens de post-polymerisatie modificatiestappen), het fenylglyoxaldehydegehalte en de maximale ureumbindingscapaciteit vastgesteld. Analyse van de absorbentia met behulp van ^{13}C NMR- en IR-analyse vertoonden bijproducten van de oxidatie (d.w.z. overoxidatie van het aldehyde naar het carbonzuur, en aldolcondensatie van een acetylgroep met een PGA-groep bij hoge dichtheden van acetylgroepen). Theoretisch zou dit, als deze nevenreacties volledig zouden kunnen worden onderdrukt, kunnen leiden tot absorbentia met een PGAH-gehalte van 5,5 mmol/g (inclusief 2,5% crosslinker). Vanwege deze nevenreacties is het echter onwaarschijnlijk dat kwantitatieve

conversie in PGAH wordt verkregen. Bovendien was de ureumbindingscapaciteit van PGAH-absorbentia lager dan verwacht op basis van het PGAH-gehalte omdat PGAH en ureum kunnen reageren in zowel een 1: 1 verhouding (43%) als een 2: 1 verhouding (57%).
De kinetiek van de ureumverwijdering uit gesimuleerd dialysaat voor PGAH-absorbentia op basis van styreen en vinylfenylethanon werd onder statische omstandigheden met elkaar vergeleken. De absorbentia op basis van vinylfenylethanon vertoonden een hogere ureumbindingscapaciteit dan de absorbentia op basis van styreen (1,8-2,2 mmol/g versus 1,4-1,8 mmol/g) vanwege het hogere PGAH-gehalte (~50% versus ~40 %) en verwijderde aldus meer ureum uit gesimuleerd dialysaat in het beoogde tijdsbestek van 8 uur (0,5-0,6 mmol/g versus 0,4-0,5 mmol/g).

Hoofdstuk 6 beschrijft een nieuwe route om een ninhydrin-type absorbens te synthetiseren, door 5-vinyl-1-indanon als het monomeer te selecteren (schema 2). Twee synthetische routes werden onderzocht om dit monomeer te verkrijgen, waarvan één route dit monomeer op 500 gram schaal opleverde. De suspensiepolymerisatie van vinylindanon werd geoptimaliseerd en de synthese werd opgeschaald tot 50 gram. De resulterende parels met een gemiddelde grootte van 0,74 ± 0,31 mm werden geoxideerd om de indanon-groepen om te zetten in ninhydrine-groepen. Van de aanwezige indanon-groepen werden 74% omgezet in ninhydrine-groepen, resulterende in een absorbens met een ongeëvenaard hoog ureumbindingscapaciteit van 3,2 mmol/g. Het absorbens verwijderde ~ 0,6-0,7 mmol/g ureum in 8 uur bij 37 °C uit gesimuleerd dialysaat onder statische condities wanneer ureum en ninhydrine in molaire verhouding van 1:1 aanwezig waren. Onder dynamische condities, waarin de ninhydrine-groepen in een overmaat van 2: 1 aanwezig waren ten opzichte van ureum, verwijderde het ninhydrin-type absorbens een iets lagere hoeveelheid ureum (~ 0,6 mmol/g) in 8 uur bij 37 ° C uit gesimuleerd dialysaat. Dit betekent dat ~600-700 gram ninhydrin-type absorbens nodig is om de dagelijkse ureumproductie van een dialysepatiënt (400 mmol) te verwijderen.

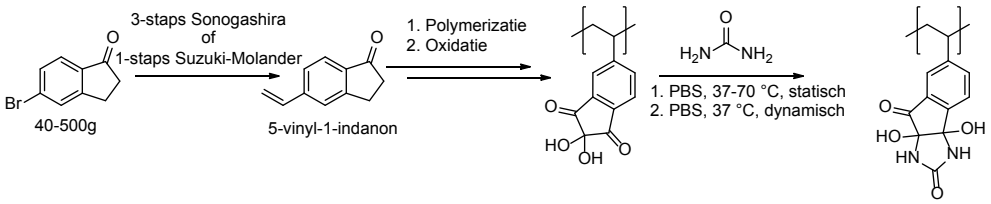

Schema 2: De synthese en evaluatie van ninhydrine-type absorbens op basis van 5-vinyl-1-indanone.

Curriculum Vitae

Jacobus Adrianus Wilhelmus (Sjaak) Jong was born on July 14th, 1992 in Alkmaar, the Netherlands. In 2010 he obtained his high school diploma (VWO Natuur en Techniek & Natuur en Gezondheid) at the Petrus Canisius College (PCC) in Alkmaar. From 2010 to 2013 he studied the Bachelor program Chemistry with a minor in Organic Chemistry at the Vrije Universiteit (VU) in Amsterdam. After obtaining his Bachelor degree he pursued the Master program in Chemistry, track Molecular Design, Synthesis and Catalysis at the University of Amsterdam (UvA) and the VU. During the Master program he conducted internships in the Synthetic Bio-Organic Chemistry (SyBOrCh) group of the Vrije University in Amsterdam and at Laboratory of Synthesis and Natural Products (LSPN) at the Swiss Federal Institute of Technology in Lausanne (EPFL) and finished his studies in 2015. In October 2015 he started his PhD in the Drug Innovation program at Utrecht University in the Pharmaceutics group, of which the results of his work are presented in this PhD thesis entitled "Bottom-up Development of Urea Sorbents for Dialysate Regeneration".

List of publications

This thesis

M.K. van Gelder*, J.A.W. Jong*, L. Folkertsma, Y. Guo, C. Blüchel, M.C. Verhaar, M. Odijk, C.F. van Nostrum, W.E. Hennink, K.G.F. Gerritsen, Urea removal strategies for dialysate regeneration in a wearable artificial kidney, *submitted*.

J.A.W. Jong, M.E. Moret, M.C. Verhaar, W.E. Hennink, K.G.F. Gerritsen, C.F. van Nostrum, Effect of substituents on the reactivity of ninhydrin with urea, *ChemistrySelect*, 2018, 3, 4, 1224–1229.

J.A.W. Jong, R. Smakman, M.E. Moret, M.C. Verhaar, W.E. Hennink, K.G.F. Gerritsen, C.F. Van Nostrum, Reactivity of (vicinal) carbonyl compounds with urea, *ACS Omega*, 2019, 4, 7, 11928-11937.

J.A.W. Jong, Y. Guo, C. Veenhoven, M.E. Moret, J. van der Zwan, A. Lucini Paioni, M. Baldus, K.C. Scheiner, R. Dalebout, M.J. van Steenbergen, M.C. Verhaar, R. Smakman, W.E. Hennink, K.G.F. Gerritsen, C.F. van Nostrum, Phenylglyoxaldehyde-functionalized polymeric sorbents for urea removal from aqueous solutions, *submitted*.

J.A.W. Jong*, Y. Guo*, D. Hazenbrink, S. Douka, D. Verdijk, J. van der Zwan, K. Houben, M. Baldus, K.C. Scheiner, R. Dalebout, M.C. Verhaar, R. Smakman, W.E. Hennink, K.G.F. Gerritsen, C.F. van Nostrum, A ninhydrin-type urea sorbent for the development of a wearable artificial kidney, *submitted*.

Other publications:

G. van der Heijden, J.A.W. Jong, E. Ruijter, R.V.A. Orru, 2-Bromo-6-isocyanopyridine as a universal convertible isocyanide for multicomponent chemistry, *Organic Letters*, 2016, 18, 984-987.

J.A.W. Jong, X. Bao, Q. Wang, J. Zhu, Formal [4+1] cycloaddition of *o*-aminobenzyl chlorides with isocyanides: Synthesis of 2-amino-3-substituted indoles, *Helvetica Chimica Acta*, 2019, 102, No. e1900002.

R. Smakman, W.E. Hennink, K.G.F. Gerritsen, J.A.W. Jong, C.F. van Nostrum, Macromolecular compositions comprising indene-derivatives, preparation thereof, and use thereof, *WO/2019/110557*, 2019.

Y. Guo*, J.A.W. Jong*, M.C. Verhaar, R. Smakman, W.E. Hennink, K.G.F. Gerritsen, C.F. van Nostrum, Regeneration of ninhydrin-type sorbents for urea removal from dialysate, *in preparation*.

Acknowledgements

Toen ik aan mijn promotietraject begon (maar ook een jaar geleden) had ik nooit gedacht dat ik het afronden van mijn proefschrift en dus ook het schrijven van het dankwoord vanuit mijn nieuwe woning in Singapore zou doen. Als ik door de hoofdstukken heen ga besef ik dat sommige projecten inderdaad als lang geleden voelen, en dat de (voornamelijk leuke) tijd voorbij is gevlogen. Tijdens dit promotietraject heb ik veel geleerd over het doen van onderzoek en heb ik veel samengewerkt, wat ook blijkt uit de vele coauteurs die op de manuscripten staan. Daarom wil ik graag de mensen bedanken met wie ik dit onderzoek heb uitgevoerd en mij hebben geholpen tijdens mijn PhD.

Allereerst wil ik Rene bedanken. Ik vond de 2 à 3-wekelijkse meetings waarin met een verse en optimistische blik naar de resultaten werd gekeken altijd erg nuttig. Daarbij stond je deur altijd open als ik er even niet uit kwam of om mijn enthousiasme mee te delen als er nieuwe opmerkelijke resultaten binnen waren gekomen. Ook was de feedback op mijn manuscripten altijd erg snel, wat er toe heeft geleid dat alle manuscripten nu ingediend/geaccepteerd zijn. Karin, ik bewonder je inzet en toewijding aan de realisatie van de draagbare kunstnier, en hoe je overal bovenop zit naast al je andere lopende projecten en werkzaamheden. Tijdens de meetings dwaalden Rene en ik vaak af in mogelijk interessante zij-projecten, terwijl jij dan benadrukte dat de patiënt echt niks heeft aan het reactie mechanisme of welk isomeer nou energetisch gunstiger is, waardoor we naar de applicatie zijn blijven toewerken. Wim, tijdens de meetings en het schrijven van de manuscripten heb ik veel geleerd van je fundamentele kijk op onderzoek en heb me verbaast over hoe jij uit dezelfde dataset toch weer extra conclusies weet te trekken. Ook bedankt dat je in de laatste periode het afronden van mijn proefschrift flink versneld hebt. Rob jouw expertise in de synthese en karakterisering van macroporeuze ureum sorbents was onmisbaar en ik ben erg dankbaar voor al je tips, trucs en advies de afgelopen jaren. Marianne, bedankt voor de meetings waarin we de globale onderzoekslijn bespraken en je me tijdig liet nadenken over hoe ik verder wil na mijn promotie. Ik hoor mezelf nog zeggen dat ik niet verder wil met onderzoek binnen de universiteit, en eigenlijk graag terug wil naar Noord-Holland. Dat laatste is (nog) niet helemaal gelukt. Yong, I am very happy that you joined the team for the past 2 years. Thanks for your expertise in the characterization of the beads, your help finishing the PGA- and ninhydrin-sorbent projects and the support during the meetings. It is a pity the USA-trip did not go as planned but I happily look back to the concert of the Dubliners and the tour-de-Gruyere trip we did together.

I would also like to thank the students who helped me in the projects; Cosimo, Mark, Toorya, Cas, Stefania and Fréderique and Herre who helped with the supervision of the students. The efforts of Cas and Stefania on the PGA- and the ninhydrin-type sorbents lay the groundwork for the Chapters 5 and 6. Mies, naast de uitvoering

en analyse van de TGA en DSC experimenten, wil ik je ook bedanken voor de overwegend positieve manier waarop je het synthese lab draaiende houdt en hoe je altijd een snelle manier vindt om een probleem op te lossen. Diënty bedankt voor je hulp in de alledaagse UMC-gerelateerde zaken en het opzetten/uitvoeren van de dynamische experimenten. Het is fijn dat je zo creatief bent in het bedenken van oplossingen want er ging nog wel eens wat mis en de plannen werden vaak op het laatste moment omgegooid. Maaike bedankt voor de samenwerking m.b.t. de review, ik vond dat we een goed team waren al was het een hele bevalling om deze uiteindelijk de deur uit te krijgen. Laura, jij was de expert op het gebied van de electro-oxidatie en het maken van de illustraties, bedankt voor jouw bijdrage aan de review. Ook bedankt dat ik jouw illustraties mocht gebruiken in Hoofdstuk 1. Marc-Etienne, thanks for your help and input on the physical-organic and theoretical chemistry parts of Chapters 3, 4 and 5. After 1.5 years of my PhD I had a set of data with somewhat surprising results and a vague explanation for this, but I had no idea how to prove this. With your help we were able to support this theory, which quickly led to my first publication. Karina, bedankt voor het uitvoeren van de SEM experimenten en de bijbehorende voorbereiding van de samples met de “Scheiner-methode”. Niet alleen zijn daar mooie figuren uitgekomen, de tripjes naar het Kruyt-gebouw vond ik ook altijd erg gezellig. Thanks to Johan, Klaartje, Alessandra, and Marc for performing the ^{13}C-solid state NMR experiments and their help in the quantification of the functional groups present in the sorbent materials. Dick en Jantien, bedankt voor jullie expertise en input tijdens de vergaderingen van de gebruikerscommissie, het uitvoeren van de stikstof fysisorptie experimenten en de geactiveerde kool die we van jullie gekregen hebben. Remco, bedankt voor het uitvoeren van de stikstof fysisorptie experimenten op de uiteindelijke sorbents en de analyse van de resultaten. Ook bedankt voor je kritische kijk op mijn manuscripten: ik dacht dat ik goed was in het spotten van kleine “inconsistency-errors”, maar jij bent heer en meester. Verder wil ik de SyBOrCh-groep en mijn scheikunde-vrienden bedanken; niet alleen de kennis van de organische chemie die ik bij de VU heb opgedaan heeft als goede basis gediend voor mijn promotietraject, de borrel-besprekingen en de korte lijntjes met Shell en MercaChem waren ook erg nuttig in de voortgang van mijn onderzoek. Ook wil ik Jasper bedanken voor het ontwerpen van de cover, en Barbara voor de hulp met alle administratieve rompslomp. Further, I would like to thank everybody who helped me out in the lab and I had valuable discussions with during the synthesis-, nephrology- and user committee meetings, Tuesday morning colloquia, borrels and conferences.

The years in Utrecht have passed so fast, primarily because I really enjoyed working and spending my time with my friends and colleagues in the Pharmaceutics group. Lies en Carl met jullie heb ik veel tijd doorgebracht zowel in het David de Wiedgebouw als daarbuiten en ik vond het altijd bar gezellig. Omdat we in dezelfde periode begonnen en veel gedeeld hebben heb ik het gevoel dat ik dit traject samen met jullie heb afgelegd, en het is een eer dat jullie mijn paranimfen willen zijn.

Bedankt! Also thanks my friends and colleagues from the “Lunch Group” and the “VU-lunch group”, it was good to get some fresh air every day to clear your mind and have a nice coffee. I would like to thank “Synthesis Gamma” and the other members of the synthesis lab for the great time inside the lab. The practical work in the laboratory is often boring and repetitive, however the work became a lot of fun with you around. Thanks to the Pharmaceutics group, it has been great to spend time with friends and colleagues and to learn about your cultures during the (hotpot) dinners, drinks, bowling, barbecues, Mexican Halloween, indoor soccer, ping-pong, running, boardgames and D&D.

Tot slot wil ik mijn lieve vrienden en familie bedanken voor de steun, nodige afleiding en omdat ik altijd bij jullie terecht kon en kan. Ondanks dat ik nu aan de andere kant van de wereld woon voel ik me niet alleen als ik aan jullie denk.